New bioactive metabolites from the marine-derived fungus *Dichotomomyces cejpii* and their pharmacological relevance

Dissertation

zur

Erlangung des Doktorgrades (Dr. rer. nat.)

der

Mathematisch-Naturwissenschaftlichen Fakultät

der

Rheinischen Friedrich-Wilhelms-Universität Bonn

vorgelegt von

Henrik Harms

aus

Köln

Bonn 2014

Angefertigt mit Genehmigung der Mathematisch-Naturwissenschaftlichen Fakultät
der Rheinischen Friedrich-Wilhelms-Universität Bonn

1. Gutachterin	:	Prof. Dr. G. M. König
2. Gutachterin	:	Prof. Dr. E. Kostenis

Tag der Promotion	:	16.10.2014
Erscheinungsjahr	:	2015

Vorveröffentlichungen der Dissertation/In Advance Publications of the Dissertation

Teilergebnisse aus dieser Arbeit wurden mit Genehmigung der Mathematisch-Naturwissenschaftlichen Fakultät, vertreten durch die Mentorin/Betreuerin der Arbeit, in folgenden Beiträgen vorab veröffentlicht:

Parts of this study have been published in advance by permission of the Mathematisch-Naturwissenschaftlichen Fakultät, represented by the supervisor of this study:

Publikationen/Research Papers

Harms, H.; Rempel, V.; Kehraus, S.; Kaiser, M.; Hufendiek, P.; Müller, C. E. Müller; König, G. M.: Indoloditerpenes from the a marine-derived fungus strain of *Dichotomomyces cejpii* with antagonistic activity at GPR18 and cannabinoid receptors. *J. Nat. Prod.* **2014**, *77*, 673–677.

Harms, H.; Kehraus, S.; Mosaferan, N. D.; Hufendieck, P.; Meijer, L., König, G. M.: Aβ-42 lowering agents from the marine-derived fungus *Dichotomomyces cejpii.* (*In preparation*).

Harms, H.; Orlikova, B.; Kehraus, S; Mosaferan, N. D.; Diederich, M; König, G. M.: New epimonothiodiketopiperazines from the marine derived fungus *Dichotomomyces cejpii* with NF-κB lowering activity. *(In preparation).*

Tagungsbeiträge/Research Presentations

Harms, H.; Rempel, V.; Kehraus, S.; Kaiser, M.; Müller, E. C.; König, G. M. :Novel indoles from the marine-derived fungus *Dichotomomyces cejpii* with antagonistic activity at GPR18 and cannabinoid receptors, Poster presentation for Marine Natural Products Conference, September, 2013, La Toja Island, Spain

Harms, H., Rempel, V.; Kehraus, S.; Müller E. C..; König, G. M. :
The marine-derived fungus *Dichotomomyces cejpii* as a source for novel antibiotics and selective cannabinoid receptor ligands, Poster presentation and oral communication for Deutsche Pharmazeutische Gesellschaft Doktorandentagung, November, 2012 Weimar, Germany

Acknowledgements

I wish to express my sincere and cordial gratitude to my supervisor Prof. Dr. G. M. König for the expert guidance, encouragement and kind support during my doctorate. I would like to thank her that she provided constructive freedom on the one hand while at the same time always had an open door for dialogue and advice, especially in times of uncertainty about the project. Special thanks also for the absolute friendly atmosphere throughout the whole period of this project which made the work very motivating and pleasant.

Special thanks go to Prof. Dr. E. Kostenis for officiating as second referee.

My appreciation goes to Prof. Dr. Christa E. Müller and Prof. Dr. Heike Wägele for participating in the examination committee.

Many specific tasks involved in this study were performed in cooperation with other research groups. For this work thanks go to:
Viktor Rempel and Clara Schoeder (Institute of Pharmaceutical Chemistry, University of Bonn, Germany) for performing cannabinoid receptor bioassays.
Michaele Josten, Tanja Schneider and Ina Berthold (Pharmaceutical Microbiology, University of Bonn, Germany) for performing agar diffusion tests and MIC assays.
Dr. L. Meijer (Protein Phosphorylation & Disease, CNRS, Roscoff, France) for performing the protein kinases assays and Aß-42 production assay.
Dr. Marc Diederich and Ph.D. Barbora Orlikova, (LBMCC, Luxembourg) for performing the NF-κB activity and cytotoxicity assays.
Dr. Steinar Paulsen (University of Tromsø, MabCent, Tromsø, Norway) for performing the nuclear type II receptor activity assays and Dr. Thomas Sæther from the University of Oslo, who has done all the cloning and sequencing of the inserts for the Nuclear receptor assays.
Dr. Marcel Kaiser (Swiss Tropical and Public Health Institute, Basel, Swiss) for performing the antiparasitic activity assays.
Manuel Grundmann (Institute for Pharmaceutical Biology, University of Bonn) for performing the fatty acid receptor assay.
Prof. Dr. M. Gütschow (Institute for Pharmaceutical Chemistry, University of Bonn, Germany) for performing the panel of proteases inhibition assays.

Dr. Markus Helfer (Institute for Virology, Helmholtz Zentrum Munich, Germany) for performing the HIV antiviral assay.
Isabell Zech (Institute for Biochemistry and Molecularbiology, University of Bonn, Germany) for performing the cerebrosid-sulfotransferase assay.
Anna Spindler (Pharmaceutical Chemistry, University of Bonn, Germany) for providing some useful advices for chemical synthesis of an indoloditerpene derivative.

Many specific tasks involved in this study were performed in cooperation with other members of the Institute for Pharmaceutical Biology, University of Bonn. For this work cordial thanks go to:
Dr. S. Kehraus for providing professional laboratory support during all phases of this study, for proofreading manuscripts and for indispensable help concerning the implementation and interpretation of NMR experiments, for which he has my great admiration and gratitude.
Ekaterina Eguereva for introducing me to the work with marine-derived fungi, cultivation methods and for recording LC-MS spectra.
Edith Neu for conducting agar diffusion assays and the generously given ‘Füllhorn der Nächstenliebe’.
Dr. Till Schäberle for proofreading parts of my dissertation.
Dr. M. Koch for her help in administrative questions and her no small efforts to provide an electric kettle for tea which kept me awake during so many strenuous hours.
Thomas Koegler for his support in all technical matters, regarding computer, software and equipment.
Irene Loef for assistance and conducting of cultivation experiments.
Damun Nesaei Mosaferan for his applied great efforts during his master's thesis.
Special thanks go to Dr. Alexander Schmitz for sharing both, good and hard times in the laboratory, and for being such a wonderful optimistic pessimist. The discussions with you made the laboratory work much easier.
I would like to thank also all other members of the Institute for Pharmaceutical Biology, University of Bonn, present or past for cooperation and friendship.

I would like to express my deepest gratitude to my family, in particular my mother, father, and my two sisters, who have always supported me and enabled this study by their limitless love, trust and encouragement.

Abbreviations

°C	degrees Celsius
1D	one dimensional
2D	two dimensional
$[\alpha]^{T}_{D}$	specific rotary power, sodium D-line (589 nm); T: temperature
δ	NMR chemical shift [ppm]
λ	wavelength [nm]
µ	micro (10^{-6})
µg	10^{-6} gram
µl	10^{-6} liter
µM	10^{-6} molar, micromolar (= 10^{-6} mol/L)
ν	wave number [cm^{-1}]
AβP	amyloid β peptide
AC	adenylate cyclase
AD	Alzheimer disease
ADP	adenosine-5´-diphosphate
APP	Aβ precursor protein
ASW	artificial seawater
ATP	adenosine-5´-triphosphate
AU	absorbance units
BACE	β-secretase
BMS	biomalt salt medium
br	broad (in connection with NMR data)
c	concentration
C_{18}	C-18 modified silica gel
calcd	calculated
cAMP	cyclic 3´-5´-adenosine monophosphate
CB	cannabinoid
CB_1	cannabinoid subtype 1
CB_2	cannabinoid subtype 2
$CDCl_3$	chloroform-*d*
CD_3CN	acetonitrile-d_3
CD_3OD	methanol-d_4
CH_2Cl_2	dichloromethane (DCM)

CH_3CN	acetonitrile
CO_2	carbon dioxide
CoA	coenzyme A
conc.	concentration
COSY	correlated spectroscopy
cm	10^{-2} meter
d	doublet (in connection with NMR data)
Da	Dalton
DAD	diode array detector
DC	dendritic cells
DEPT	distortionless enhancement by polarization transfer
dm	10^{-1} meter
dmol	10^{-1} mol
DNA	deoxyribonucleic acid
EC	endcapped (in connection with HPLC columns)
EC_{50}	half maximal effective concentration (drug concentration causing 50% of maximal effect)
EDTA	ethylenediamine-tetra-acetic acid
e.g.	exempli gratia [lat.]or example given (for example)
EI	electron ionization
ESI	electron spray ionization
et al.	et alii [lat.]: and others
EtOAc	ethyl acetate
EtOH	ethanol
g	gram
GGPP	geranylgeranyldiphosphat
GI	growth inhibition
GPCR	G protein-coupled receptor
G protein	guanine nucleotide-binding protein
GTP	guanosine-5´-triphosphate
G_i	adenylate cyclase inhibitory G protein
G_q	phospholipase C activating G protein
G_s	adenylate cyclase stimulating G protein
GSI	γ-secretase inhibitor

GSM	γ-secretase modulator
h	hour
H_3BO_3	boric acid
HMBC	heteronuclear multiple-bond correlation
HPLC	high performance liquid chromatography
HR	high resolution
HSQC	heteronuclear single quantum correlation
HTS	high-throughput screening
Hz	Hertz
H_2O	water
H_2SO_4	sulfuric acid
IC_{50}	half maximal inhibitory concentration (drug concentration causing 50% inhibition)
i.e.	id est [lat.] or that is
IGP	indole-3-glycerolphosphate
IP_3	inositol-triphosphate
IR	infrared
J	spin-spin coupling constant [Hz]
L	liter
laeA	global regulator gene in *Aspergillus* spp.
LBD	ligand binding domain
LC	liquid chromatography
LXR	liver X receptor
m	meter
m	multiplet (in connection with NMR data)
m/z	mass-to-charge ratio (in connection with mass spectrometry)
Me	methyl
PEP	phosphoenolpyruvat
MeOH	methanol
MeOD	methanol-d_4
mg	10^{-3} gram
MHz	megahertz
min	minute
mL	10^{-3} liters

mm	10^{-3} meters
mM	10^{-3} molar, millimolar (= 10^{-3} mol/L)
mol. wt.	molecular weight [g/mol]
MS	mass spectrometry
NADPH	nicotinamide adenine dinucleotide phosphate
NaOH	sodium hydroxide
NCEs	new chemical entities
n.d.	not detectable
NF-κB	Nuclear factor-κB
ng	10^{-9} gram
NH_4Ac	ammonium acetate
nm	10^{-9} meter
NMR	nuclear magnetic resonance
no	number
NOE	nuclear Overhauser effect
NOESY	nuclear Overhauser effect spectroscopy
NP	natural product
NP	normal phase (in connection with chromatography)
NR	nuclear receptor
NRPS	non-ribosomal peptide synthetase
OSMAC	one strain many compounds
p	pentet (in connection with NMR data)
p53	tumor suppressor protein 53
PPAR	peroxisome proliferator-activated receptor
PDA	photodiode-array
PE	petroleum ether
pH	potentia hydrogenii
PKS	polyketide synthase
PLC	phospholipase C
ppm	parts per million
PFT	protein fold topology
q	quartet (in connection with NMR data)
qC	quaternary carbon
RNA	ribonucleic acid

RP	reversed phase
RT	room temperature
RXR	retinoid X receptor
s	singlet (in connection with NMR data)
SAR	structure activity relationship
SCUBA	self contained underwater breathing apparatus
sec	second
SEM	standard error of the mean
Si	silica gel
sp.	species
spp.	species (plural)
SPPARγMS	selective PPARγ modulators
sxt	sextet (in connection with NMR data)
t	triplet (in connection with NMR data)
T	total inhibition
TLC	thin layer chromatography
TM	transmembrane domain
UV	ultraviolet
VIS	visible
VLC	vacuum-liquid chromatography
WG	working group
X-ray	roentgen-ray

Table of contents Page

1 Introduction

1.1 Natural products as lead structures for therapeutical drug development

Today high-throughput screening (HTS) of substance libraries has become an integral part of pharmaceutical research in order to identify hits for drug research.[1] The majority of commercially available molecules and by extension also the majority of screening libraries, lack typical structural motifs and ring scaffolds which can be found in Natural Products (NPs).[2] Therefore it is interesting to note that natural products nevertheless still play a major role in the successful research for novel drug candidates. From January 1981 through December 2010 over 50% of 1073 small-molecules, which were so called new chemical entities (NCEs) and introduced as drugs in Western medicine were natural product derived. That means over 50% were NPs, derivatives of NPs or synthetic compounds with NP derived pharmacophore and only 36% of the NCEs were truly devoid of natural inspiration.[3]

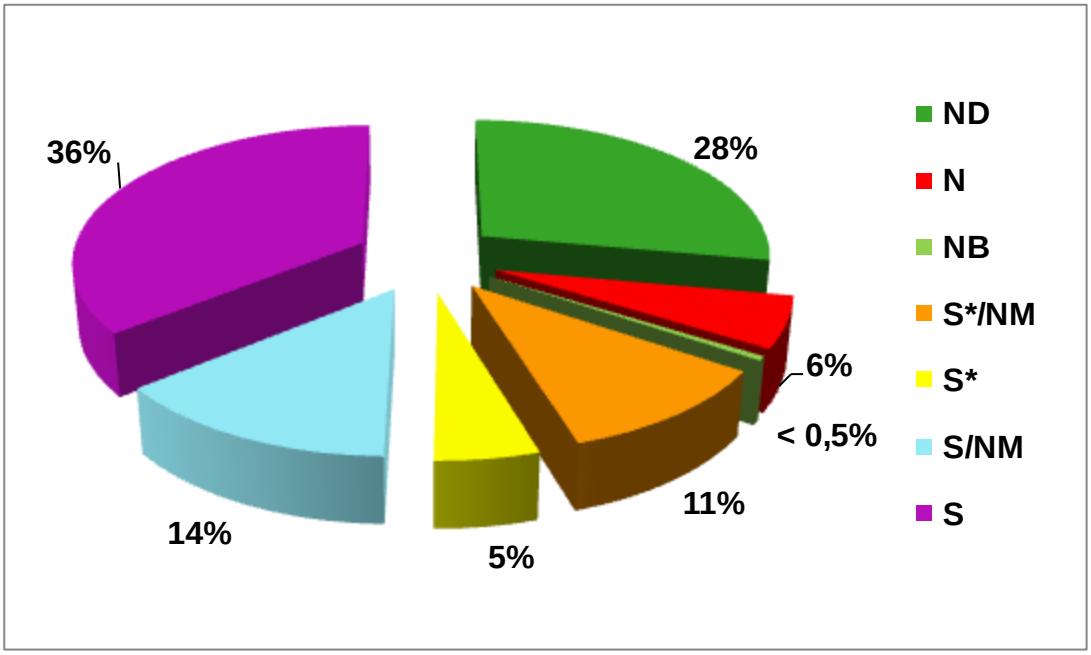

Figure 1.1: Source of small molecules approved drugs in the time frame 1981 - 2010

N: Natural product; **NB**: Natural product botanical; **ND**: Derived from a natural product (e.g. semisynthetic modification); **S***: Made by total synthesis, but the pharmacophore is/was from a natural product; **S*/NM**: Natural product mimic (direct inhibitor/antagonists of the natural substrate) made by total synthesis with natural product pharmacophore; **S/NM**: Natural product mimic (direct inhibitor/antagonists of the natural substrate) made by total synthesis; **S**: Synthetic compound completely devoid of natural inspiration

An advantage of NPs is that they are more complementary to biological three-dimensional structure space, which comprises the protein binding sites for potential ligands. Natural products, as well as their biological targets, e. g. receptor/proteins are produced by interaction with biosynthetic enzymes. This constitutes the concept of 'biosynthetic imprint' or shared 'protein fold topology' (PFT), which explains a closer relationship of NPs to biological space that facilitates interactions with biological therapeutic targets via common 'natural product binding motifs'.[4,5] The deep knowledge on PFT which implies identification of PFT and natural product binding motifs, can also be used as drug discovery tool to identify potential drug targets and possible ligands in drug research.[4] But also classical HTS drug discovery is supposed to benefit from the enhanced inclusion of NP scaffolds which are typically neglected by common screening libraries.[2]

In this regard it has to be taken into account, that nature does not manufacture drugs for humans. Hits derived from NP drug discovery, as well as hits from HTS screening of synthesized compounds, usually require extensive optimization to obtain therapeutically useable drugs. Natural products therefore rather provide lead structures as starting points for drug optimization than being directly therapeutically usable drugs. Once an active skeleton has been identified as lead, combinatorial chemistry with its superior development capability proves its strength and can reveal the complete potential of natural products.[3,6]
The following two chapters will focus on natural products obtained from fungal sources.

1.2 Fungal metabolites as drugs or lead structures for therapeutical drug development

Classical sources for bioactive NPs are derived from plants, bacteria, fungi and animals.[7] The fungal kingdom includes many species which have demonstrated to be a fruitful source of structurally highly diverse bioactive metabolites.[8] It is assumed that production of fungal secondary metabolites depends on environmental conditions and interaction with competitors or hosts. Therefore production of such compounds are considered to allow occupation of special ecological niches or rather provide competitive advantages against competitors.[9] In some cases these metabolites have been implicated with diseases like aspergillosis where they are considered as virulence factors. Especially filamentous fungi like different *Aspergillus* species are known to interact with human immune system. Fungal secondary metabolites like the immunosuppressive gliotoxin produced by several Ascomycota play an important role as

virulence factor.[10] As the innate immune response is the primary line of defense against fungal respiratory infections, immunosuppressive acting agents may assist the fungi to evade immune clearance, and to increase their pathogenicity in order to colonize new niches.[10]

In contrast many of these secondary metabolites have been used in medicine, due to their prominent bioactivities, helpful for a range of indications.[7] Immunosupressive compounds like the cyclopeptid cyclosporin A, first time isolated from the fungus *Tolypocladium inflatum (*originally misidentified as *Trichoderma polysporum)*[11,12] and derivatives of mycophenolic acid, first time isolated from the fungus *Penicillium glaucum*[13], have become very valuable therapeutics for organ transplant recipients to prevent transplant rejection.[11]

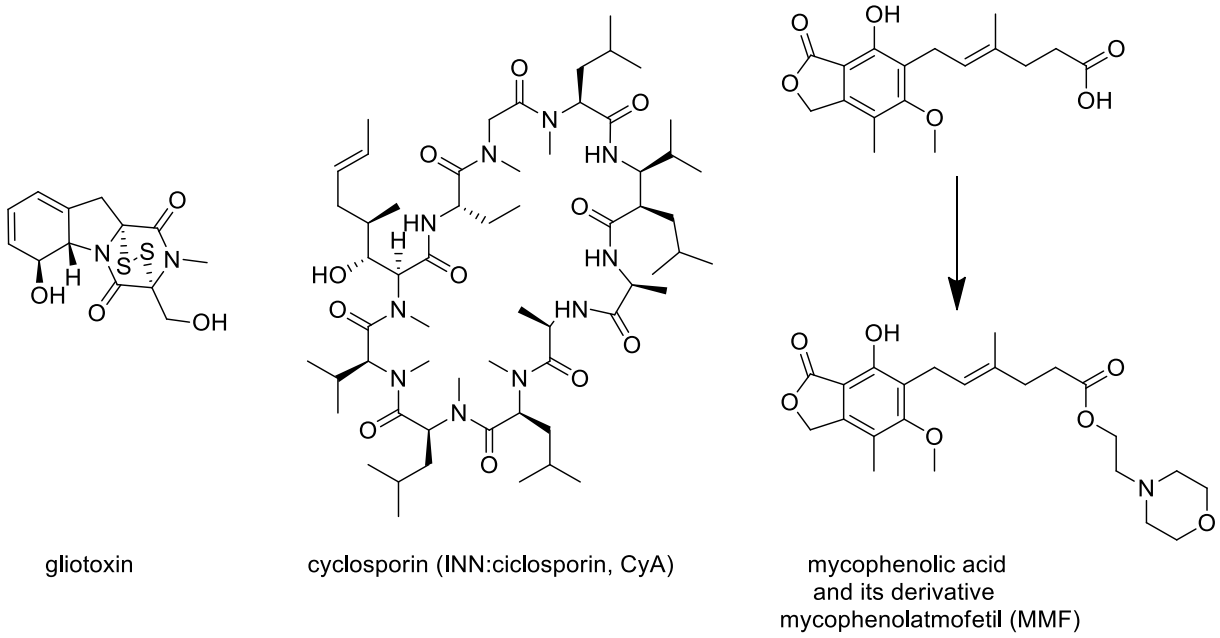

Figure 1-2: Immunosuppressive compounds isolated from fungi or derived from fungal metabolites.

More recently fingolimod (FTY720) was introduced as the first orally active immunomodulatory drug for the treatment of multiple sclerosis, a neurodegenerative chronic autoimmune disorder.[14] Fingolimod itself is derived of myriocin (ISP-1), first time isolated from the fungus *Myriococcum albomyces.*[15]

It is interesting to note that most of these immunosuppressive fungal compounds also display antibiotic or antifungal activities which open up speculations about their real physiological role in fungal colonies.

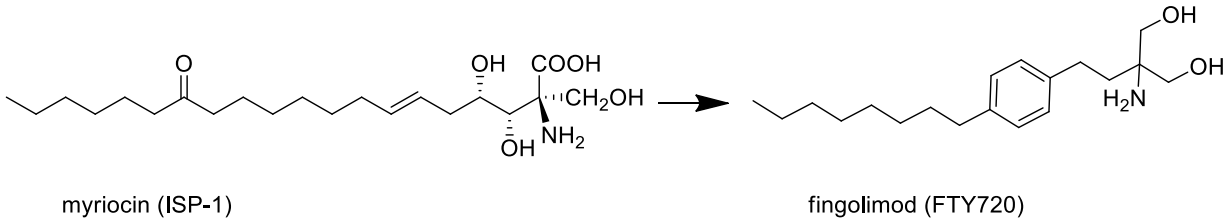

Figure 1-3: Approved immunomodulatory compound fingolimod and its parent lead structure.

The progress in organ transplantation, possible also due to the availability of advanced immunosuppressives, and the growing population of AIDS patients led to increased numbers of immunocompromised patients. These patients are threatened by infections with opportunistic fungi like *Candida* spp. or *Aspergillus* spp. Antimycotics, which are ironically derived from fungal secondary metabolites, are an important contribution to encounter these life threatening infections.

The isolation of the cyclic lipopeptides echinocandin B from *Aspergillus* species[16] and pneumocandin B_0 from *Glarea lozoyensis*[17] led to the development of β-1,3-D-glucan synthase inhibitors like anidulafungin (LY303366) and caspofungin (MK-0991) [17,18] These have become very important antifungal agents because they demonstrated excellent clinical efficacy and more favourable adverse event profiles than traditional antifungal agents.[18] Other β-1,3-D-glucan synthase inhibitors derived from papulacandin B isolated from *Papularia sphaerosperma* are currently under development[19,20]

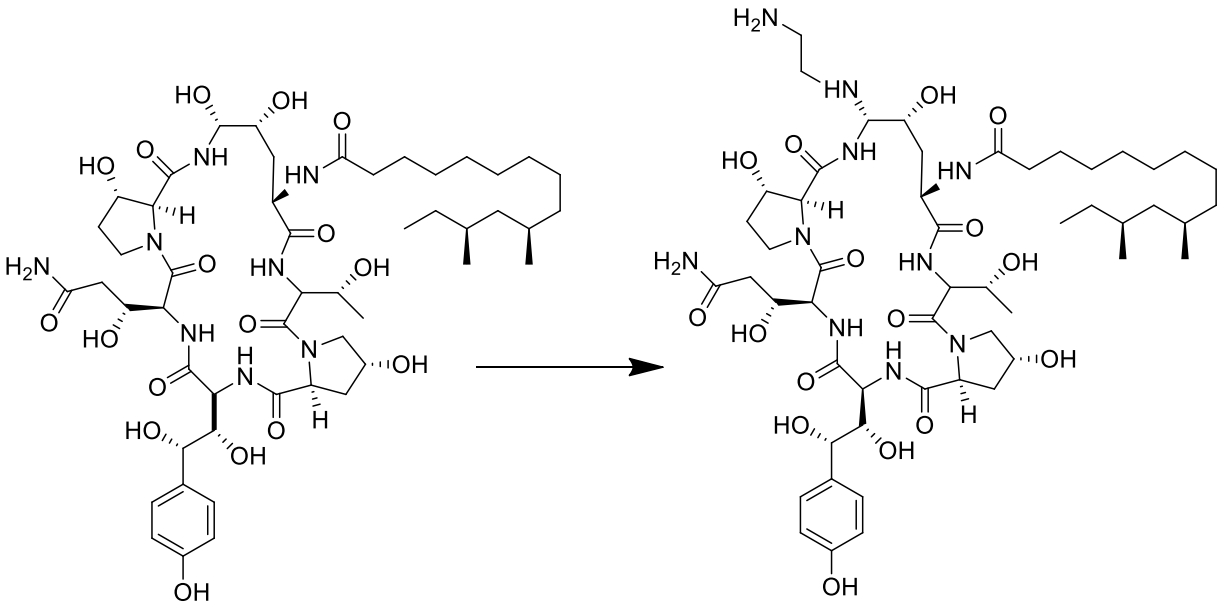

Figure 1-4: Approved antifungal compounds and their parent lead structures.

Their mode of action as inhibitors of fungal cell wall synthesis has given this group of antimycotic agents the informal name ‘fungal penicillins’. This name is based on the famous bacterial cell wall inhibitors derived from the tripeptid penicillin, which had been isolated from a fungal strain as well, *Penicillium chrysogenum (*formaly known as *Penicillium notatum).*[21,22]

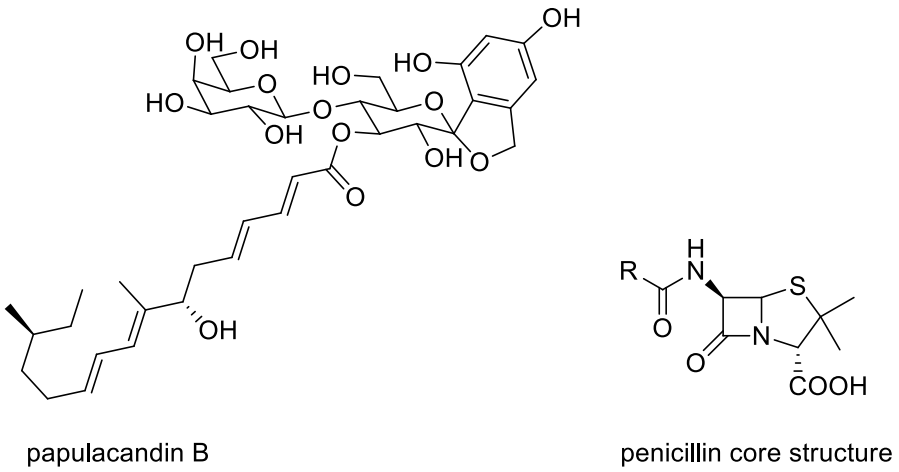

Figure 1-5: Potential lead structure for new antifungal compounds and core structure for β-lactam antibiotics.

Beside antibiotics and immunomodulatory compounds, fungal metabolites have been developed for many other indications. In some cases commercially very successful, like the cholesterol lowering agent lovastatin (monacolin K, mevinolin) and its derivatives. Lovastatin has originally been isolated from *Monascus ruber* and *Penicillium citrinum* and led to the development of the drug class of statins, which are used to prevent atherosclerosis and related coronary heart diseases. [23–25]

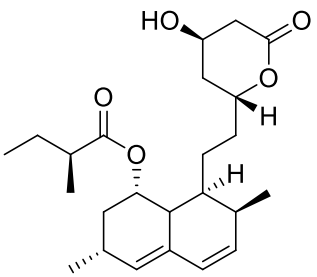

lovastatin (monacolin K, mevinolin)

Figure 1-6: Lead structure and first approved cholesterol lowering agents of the drug class of statins.

1.3 Potential of natural products derived from microorganisms from extraordinary habitats

Terrestrial sources for natural products have been investigated intensively. Although they still bear an enormous potential, (e.g. only 15% of higher plants have been phytochemically investigated so far) the increased endeavour to investigate more uncommon less investigated habitats appears to be promising when trying to discover novel bioactive chemotypes.[7] The marine environment has gained a lot of attraction to natural product researchers. The enormous marine biodiversity equates to chemical diversity and lead to the isolation of an impressive number of complex bioactive compounds. Some of these have gained access to clinical trials or are even already used as drugs, like the antitumor agent trabectidin (ET743), isolated from the tunicate *Ecteinascidia turbinata*.[26–28]

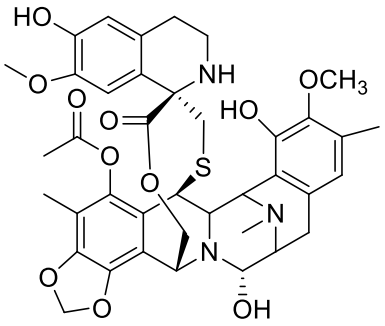

trabectedin(ET-743)

Figure 1-7: The marine natural product trabectidin (Yondelis®) is an approved anti-cancer drug

One reason for the plenty of highly bioactive compounds might be the circumstance that secondary metabolites play an important role as chemical defense for marine organisms, especially for vulnerable macroorganisms like soft corals, sponges or slugs.[29–31] Further prominent features of marine ecosystems are the associations between micro- and macroorganisms. Thereby associated microbes are considered to contribute eventually to the chemical defence of their hosts.[32]

Marine derived fungi are found in marine animals like sponges, and algae as epi- or endobionts.[26] Most of these isolated fungi are not obligate marine and do not appear to contribute directly to the biosynthesis of natural products found in marine organisms. However many of these fungi seem to be adapted to the marine habitat and there are reports which describe genetically and biochemically differences between marine derived and terrestrial fungi from the same genus, which makes them interesting for natural product researchers.[26]

Other interesting approaches target for extremophilic microbes found in ‘extreme habitats’. Those habitats are normally hostile for life e.g. because of pH value, temperature or salt/metal content. This include acidophile microbes from acidic sulphurous hot springs or rather alkalophiles from alkaline lakes. Hyperthermophile microbes from deep sea vents are also barophile, while cryophile microbes have been isolated from arctic and antartic waters. Halophile microbes occupy environments with a concentration of salt five times greater than the salt concentration of the ocean and there are microbes known, that live in metal rich and in some cases also very acidic polluted environments for example found in derelict mine sites.[7,33]

2 Scope of the present study

Natural products from fungal sources provide an astonishing diversity of bioactive molecules. These compounds have a high potential for drug discovery in a wide array of therapeutic indications and there are many successful stories of approved drugs so far. Thereby marine-derived fungi are considered as a very promising source.

The main goal of this study is the isolation, identification and biological evaluation of secondary metabolites from the marine-derived fungus *Dichotomomyces cejpii*. This fungus was chosen for intensive investigation on the basis of promising results from spectroscopic analysis and positive antibiotic agar diffusion tests of fungal crude extracts. Furthermore analysis of available literature had shown that this fungus had been scarcely chemically investigated so far.

In order to achieve this goal a classical approach for natural product research is envisaged, which is in case of antbiotic activity, supported by bioactivity guided fractionation.

An array of cultivation experiments on different culture media shall examine suitable conditions for large scale cultivation. On the basis of the chemical and biological results, the most promising cultivation conditions shall be selected for large scale cultivation. Therefore biological tests in form of agar diffusion assays for antibacterial and antifungal activity and ^{1}H NMR spectroscopy and LC-MS analyses for chemical characterization are available.

The obtained extracts of these large scale cultivations, shall be further processed by separation, using diverse chromatographic methods. It is intended to use the interpretation of experimental spectroscopic (NMR, UV, IR, OR) and mass spectrometric data for chemical investigation and structure elucidation of isolated pure compounds.

In addition to *in vitro* antibiotic activity tests, the collaboration with several work groups allows further bioactivity tests of pure isolated compounds, with an emphasis on activities toward cannabinoid and type II nuclear receptors and for Aβ-42 lowering activity.

3 Materials and methods

3.1 Origin and taxonomy of sponge samples

Marine sponge samples had been collected by Dr. Ullrich Höller via snorkelling and SCUBA diving at the coral reef surrounding Bare Island, New South Wales Australia in depth between 3-15 m. Taxonomical identification of the sponge sample was performed by Dr. R. Desqueroux-Faundez, Musée d'Histoire Naturelle Genève.

The collected marine sample of *Callyspongia* spec. cf *C. flammea*, Desqueyroux-Faundez 1984 (CT 293 K), which is relevant for the context of the present study, served as substrates for the isolation of associated microbes.

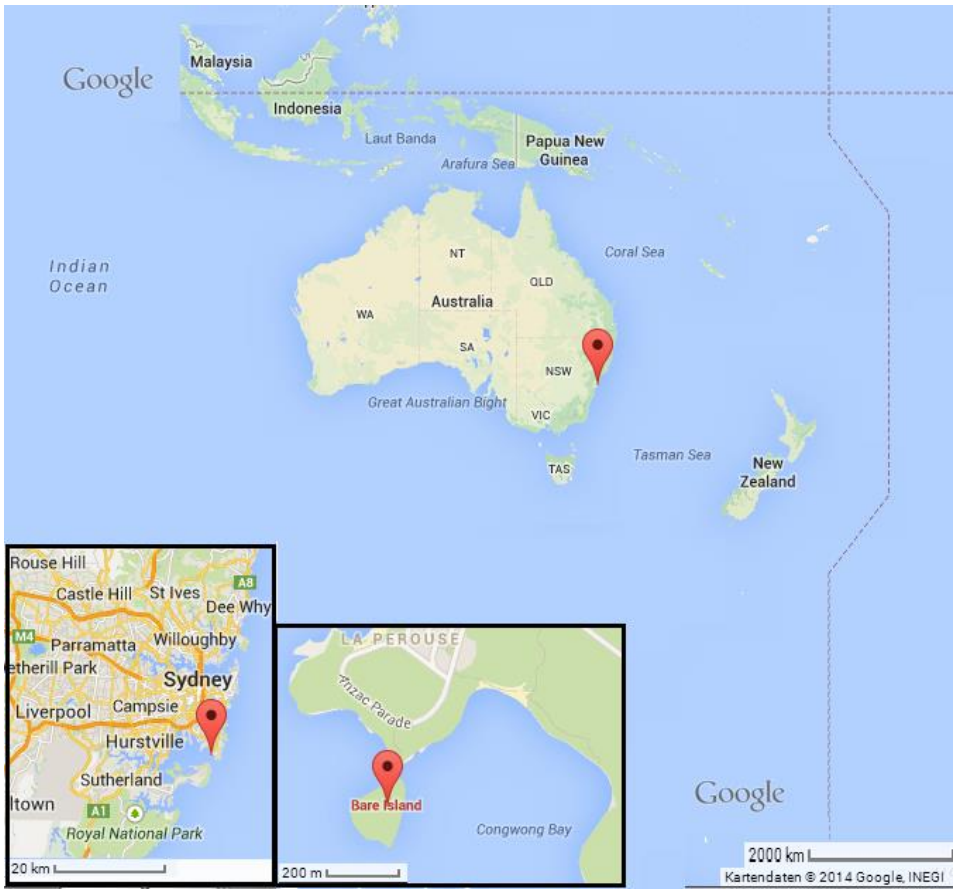

Figure 3-1: Sample collection at Bare Island, marked with a red arrow on the maps. (The map is taken from: https://www.google.de/maps/place/Bare+Island)

3.2 Fungal material

3.2.1 Origin, isolation and taxonomy of fungal sample

The marine-derived fungus *Dichotomomyces cejpeii* was isolated from a sample of the sponge *Callyspongia* sp. cf. *C. flammea*. The isolation of the fungus was carried out using an indirect isolation method. Sponge samples were rinsed three times with sterile H_2O. After surface sterilization with 70% EtOH for 15 s the sponge was rinsed in sterile artificial seawater (ASW). Subsequently, the sponge material was aseptically cut into small pieces and placed on agar plates containing isolation medium: agar 15 g/L, ASW 800 mL/L, glucose 1 g/L, peptone from soymeal 0.5 g/L, yeast extract 0.1 g/L, benzylpenicillin 250 mg/L, and streptomycin sulfate 250 mg/L. The fungus growing out of the spongeal tissue was separated on biomalt medium (biomalt 20 g/L, agar 10 g/L, ASW 800 mL/L) until the culture was pure. The isolated fungus was identified by P. Massart and C. Decock, BCCM/MUCL, Catholic University of Louvain, Belgium. A specimen is deposited at the Institute for Pharmaceutical Biology, University of Bonn, isolation number "293K09", strain number 225.

3.2.2 Cultivation and extraction of selected fungal strain for prescreening

The fungal isolate (293K09) was cultivated in a small scale (5 x 100 mL Petri dishes) for screening purposes by Ekaterina Eguereva, Irene Loef and Henrik Harms (Institute for Pharmaceutical Biology, University of Bonn, Germany), utilizing four different solid media (BMS, MPY, REA, Tennelin). All four media were autoclaved prior to use. After one month of cultivation at room temperature, the fungal biomasses, including the medium were homogenized using an Ultra-Turrax apparatus and the mixtures were extracted with EtOAc (3 x 100 mL). The solvents were subsequently removed at reduced pressure at 37 °C until dryness of the residues. These residues will be referred to as "screening extracts" in this study and were used to evaluate the qualification of the individual culture medium for large cultivation. Therefore biological activity and spectroscopical properties of the screening extracts were analysed.

- **BMS** medium: 15 g/L agar, 20 g/L biomalt extract, ad 1 L ASW (artificial sea water: 0.1 g/L KBr, 23.48 g/L NaCl, 10.61 g/L $MgCl_2$ x 6 H_2O, 1.47 g/L $CaCl_2$ x 2 H_2O, 0.66 g/L KCl, 0.04 g/L $SrCl_2$ x 6 H_2O, 3.92 g/L Na_2SO_4, 0.19 g/L $NaHCO_3$,and 0.1 g/L H_3BO_3).
- **MPY** medium: 15 g/L agar, malt extract 20 g/L, peptone 2.5 g/L, yeast extract 2.5 g/L) ad 1 L demineralized water.
- **REA** medium (without polysorbate 80): 20 g/L agar 20g/L rice for rice extract, ad 1 L demineralized water.
- **Tennelin** medium: agar 15g/L, mannitol 50 g/L, 5 g KNO_3 , 1g KH_2PO_4, 0.5g $MgSO_4$ x 7 H_2O, 0.1g NaCl, 0.2 g $CaCl_2$, 20 mg $FeSO_4$ x 7 H_2O, 10 ml Liquid 2: [$ZnSO_4$x 7 H_2O 880 mg/L, $CuSO_4$ x 5 H_2O, 40 mg/L $MnSO_4$ x 4 H_2O, 7.5 mg/L, Boracid, 6 mg/L, 4 mg/L $(NH_4)_6Mo_7O_4$ x H_2O ad 1 L Aqua dem.], ad 1 L demineralized water.

3.2.3 Cultivation and extraction of selected fungal strain for detailed chemical investigations

Upscaled cultivations (10 L solid medium) were generated for detailed chemical investigations of the fungal strain with the two most promising culture media. Therefore the nutrient rich MPY medium and the minimal medium Tennelin were selected.

The fungal sample was cultivated in Fernbach flasks at room temperature for 30 or 40 days, respectively, using the same media as for screening purposes. The homogenized fungal biomass and cultivation medium was extracted with EtOAc exhaustively and the solvent was subsequently removed at reduced pressure and 37 °C. Specific cultivation conditions were as follows:

- **Cultivation medium 1**: 10 L solid MPY medium in 40 Fernbach flasks for 30 days. (see Figure 3-2a)
- **Cultivation medium 2**: 10 L solid Tennelin medium in 40 Fernbach flasks for 40 days (see Figure 3-2b)

a) *Dichotomomyces cejpii* preculture and large scale cultivation on MPY medium

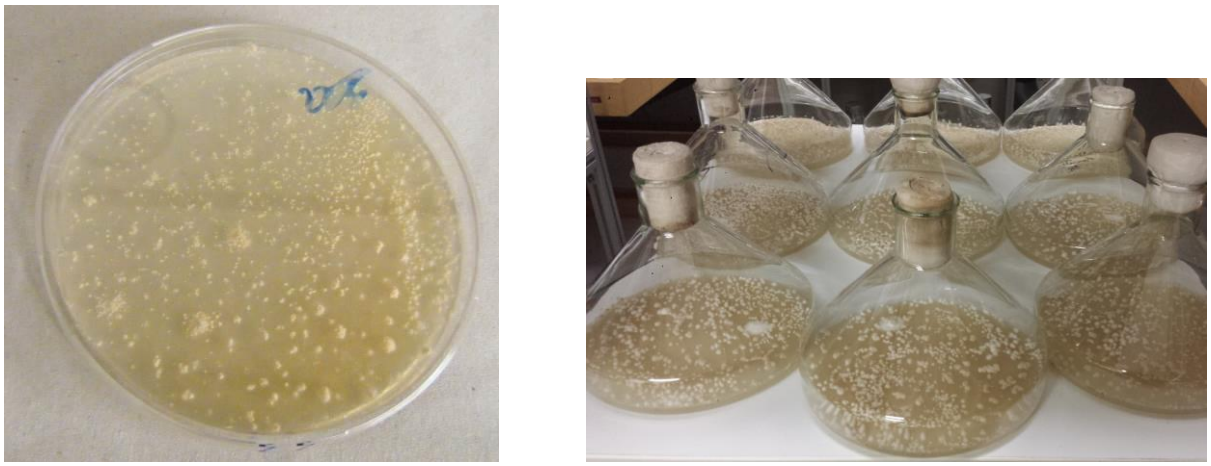

b) *Dichotomomyces cejpii* preculture and large scale cultivation on Tennelin medium

Figure 3-2: *Dichotomomyces cejpii* growing on two different culture media a) and b)

3.3 Chromatography

3.3.1 Thin layer chromatoraphy (TLC)

TLC was performed using either TLC aluminum sheets silica gel 60 F_{254} (Merck) or TLC aluminum sheets RP_{18} F_{254} (Merck) as stationary phase. Standard chromatograms of extracts and fractions were developed on silica gel using PE-acetone in different mixtures (standard: 70-30), or on RP_{18} TLC plates with MeOH/H_2O mixtures (standard: 70-30), both under saturated conditions at room temperature. Chromatograms were detected under UV light (254 and 366 nm), vanillin-H_2SO_4 reagent (0.5 g vanillin dissolved in a mixture of 85 ml methanol,

10 mL acetic acid and 5 mL H_2SO_4, TLC plate heated at 100°C after spraying) and with van Urk reagent reagent (50 mg 4-(Dimethylamino)-benzaldehyd dissolved in 1 ml H_2SO_4 conc, ad 100ml EtOH 95%) if compounds with indole moiety were suspected.

3.3.2 Vacuum liquid chromatography (VLC)

Sorbents for VLC were silica gel 60 (0.063–0.200 mm, Merck), silica gel 60 (0.040–0.063 mm, Merck) or Polygoprep 60 C_{18} (0.05 mm, Macherey-Nagel). Columns were wet-packed under vacuum, using PE or dichloromethane for normal-phase, and MeOH for reversed-phase conditions. Glass wool layer above the sorbent material was used to protect the sorbent material against disturbance. Before applying the sample solution, the columns were equilibrated with the first designated eluent.

3.3.3 High performance liquid chromatography (HPLC)

Preparative HPLC was carried out using four different systems: A: Waters system, controlled by Waters Millenium software, consisting of a 600E pump, a 996 PDA, and a 717 plus autosampler; B: HPLC system controlled by Merck Hitachi Model D-7000 Chromatography Data Station Software HPLC System Manager Version 4.0 software, consisting of L6200 A intelligent pump; D 6000 interface and an L4500 PDA; C: controlled by HP ChemStation for LC Rev.A.06.03[909] software, consisting of a L-7100 Merck Hitachi pump and a HP-series 1050 detector; D: HPLC composed of a Waters 515 pump together with a Knauer K-2300 differential refractometer.

3.4 Structure elucidation

The chemical structures of the isolated compounds were elucidated using one and two dimensional NMR techniques in combination with MS methods. ACD/Labs-software NMR-calculations were utilized to support the NMR-based structure elucidation (ACD/Labs-software, 2006). If necessary, optical rotation was determined and further spectroscopic methods, such as UV and IR spectroscopy provided additional structural information. The determination of the absolute configuration of sugar moieties was performed using chiral

stereoselective HPLC columns via retention times comparison. Identity of isolated compounds in comparison to previously published structures was judged due to the ^{1}H and ^{13}C NMR data, and specific optical rotation. Database and literature searches were carried out using the MarinLit database (MarinLit database®, AntiBase database® and the SciFinder® database. Chemical structures were designated as new, if they could not be found in any of these databases**.**

3.4.1 NMR spectroscopy

All NMR spectra were recorded using either a Bruker Avance 300 DPX operating at 300 MHz (^{1}H) and 75 MHz (^{13}C) or a Bruker Avance 500 DRX spectrometer operating at 500 MHz for (^{1}H) and 125 MHz for (^{13}C) respectively. NMR Spectra were processed using Bruker 1D WIN-NMR, 2D WIN-NMR or XWIN-NMR Version 2.6, 3.1 and 3.5 software, or Bruker TopSpin software package Version 1.3. Spectra were recorded in $CDCl_3$, acetone-d_6 or CD_3OD and were referenced to residual solvent signals with resonances at $\delta_{H/C}$ 7.26/77.0 ($CDCl_3$), 1.93/117.7 (acetone-d_6), 3.35/49.0 (CD_3OD) and 2.04/29.8 (acetone-d_6). Multiplicity of carbons was deduced by ^{13}C and DEPT experiments. Structural assignments were based on spectra resulting from one or more of the following NMR experiments: ^{1}H, ^{13}C, DEPT135, ^{1}H-^{1}H COSY, ^{1}H-^{13}C direct correlation (HSQC), ^{1}H-^{13}C long range correlation (HMBC), ^{1}H-^{1}H NOESY. Two dimensional NMR measurements were guided by Dr. Stefan Kehraus (Institute for Pharmaceutical Biology, University of Bonn, Germany).

3.4.2 Mass spectrometry (MS)

HPLC-ESIMS (referred to as LC-MS or HPLC-MS) measurements were performed by Ekaterina Eguereva (Institute for Pharmaceutical Biology, University of Bonn, Germany) employing an Agilent 1100 Series HPLC including DAD, with RP C 18 column (Macherey-Nagel Nucleodur 100, 125 mm x 2 mm, 5 µm) and gradient elution (0.25 mL/min, NH_4Ac buffer 2 mmol, from MeOH 10: H_2O 90 in 20 min to 100% MeOH, then isocratic for 10 min), coupled with an API 2000, Triple Quadrupole LC/MS/MS, Applied Biosystems/MDS Sciex and ESI source. All samples for LC-MS (extracts, fractions, and pure compounds) were solved in MeOH (1 mg/mL) for injection into the HPLC-ESIMS system.

LREIMS and HREIMS were recorded on a Finnigan MAT 95 spectrometer, and HRESIMS on a Bruker Daltonik micrOTOF-Q Time-of-Flight mass spectrometer with ESI source, all carried out by C. Sondag (Department of Chemistry, University of Bonn, Germany). HRESI FT/ICR MS was conducted by H. Hamacher (Bayer Industry Services, Leverkusen, Germany) via applying a Bruker Daltonics APEX–III FT-ICR-MS spectrometer.

3.4.3 UV measurements

UV spectra were recorded on a Perkin-Elmer Lambda 40 with UV WinLab Version 2.80.03 software, using 1.0 cm quartz cells. The molar absorption coefficient ε was determined in accordance with the Lambert-Beer-Law:

$$A = \varepsilon \times c \times b \;\Leftrightarrow\; \varepsilon\left[\frac{L}{mol \times cm}\right] = \frac{A}{c\left[\frac{mol}{L}\right] \times b\,[cm]}$$

ε = molar absorption coefficient

A = absorption at peak maximum

c = concentration

b = layer thickness of solution

3.4.4 IR spectroscopy

IR spectra were recorded as film, using a Perkin-Elmer FT-IR Spectrum BX spectrometer. Analysis and reporting were performed with Spectrum v3.01 software.

3.4.5 Optical rotation

Optical rotation measurements were conducted on a Jasco model DIP-140 polarimeter (1 dm, 1 cm^3 cell) operating at the wavelength λ=589 nm corresponding to the sodium D line at room temperature. The specific optical rotation $[\alpha]_D^T$ was calculated pursuant to:

$$[\alpha]_D^T = \frac{100 \times \alpha}{c \times l}$$

T = temperature [ºC]
D = sodium D line at λ=589 nm
c = concentration [g/100 mL]
l = cell length [dm]

The compounds were dissolved in an appropriate organic solvent (e.g., MeOH). The rotation angles α were determined as an average value based on at least 10 measurements.

3.5 Chemical derivatizations

3.5.1 Carbamat formation of compound 4

The carbarmat formation of compounds **4** was conducted in accordance with the procedure utilized by Stock and Brückner et al, 2010.[34] Emindole SB (**4**) (7.6 mg) was stirred with 3.5 µL propylisocyanat (ρ 0.908 g/ml) and 0.58 mg MoO_2Cl_2 in 1 ml CH_2Cl_2 at room temperature for 96 h. Every 12 hours additional 3.5 µl propylisocyanat were added. The reaction was quenched with 15.7 µl diethylamin after 96 hours. The solvent was removed under vacuum to

give a brown residue, which was suspended in 2 ml CH_2Cl_2 and 3 ml H_2O. Liquid-liquid extraction was utilized 5 times. The obtained CH_2Cl_2 phase was removed under vacuum again and further purified using RP_{18}-HPLC system B (Nucleodur 100-S 250mm x 4.6 mm) with H_2O-ACN (82:180), 1.5 mL/min as the eluent system gave 3.5 mg of the desired emindole SB-N-propylcarbamate, analysed via ^{1}H and ^{13}C NMR as well as HRMS.

3.6 Evaluation of biological activity

3.6.1 Agar Diffusion Assay in Working Group König

Antimicrobial tests of extracts and isolated pure compounds were performed by Edith Neu (Institute for Pharmaceutical Biology, University of Bonn) following the method described by Schulz et al. (Schulz et al., 1995). The bacteria Bacillus megaterium de Bary (Gram positive) and Escherichia coli (Migula) Castellani & Chambers (gram negative), the fungi Microbotryum violaceum (Pers.) Roussel (Ustomycetes), Eurotium rubrum (formerly E. repens) König, Spieckermann & Bremer (Ascomycetes) (all from DSMZ; Braunschweig, Germany), and Mycotypha microspora Fenner (Zygomycetes kindly provided by B. Schulz, Institute of Microbiology, University of Braunschweig, Germany) were used as test organisms. Sample solutions contained 1 mg/mL per test sample. 50 µL (equivalent to 50 µg) of each solution were pipetted onto a sterile antibiotic filter disk (Schleicher & Schuell 2668), which was then placed onto the appropriate agar medium and sprayed with a suspension of the test organism. Growth media, preparation of spraying suspensions, and conditions of incubation were carried out according to Schulz et al. (Schulz et al., 1995). Growth inhibition was defined as follows: growth of the appropriate test organism was significantly inhibited compared to a negative control; total inhibition: no growth at all in the appropriate zone. Benzyl penicillin (1 mg/mL MeOH), streptomycin (1 mg/mL MeOH) and miconazole (1 mg/2 mL DCM) were used as positive controls.

3.6.2 Agar Diffusion Assay in Working Group Sahl

Antimicrobial tests of extracts and isolated pure compounds were performed by Michaele Josten (Institute for medical microbiology, University of Bonn).

Culture plates (5% sheep blood Columbia agar, BD) were overlaid with 3 ml Tryptic soy soft agar, inoculated with TSB (Tryptic soy broth, Oxoid) growth suspension of the bacteria to be tested. Compounds were diluted to a concentration of 1mg/ml (Syringomycin 0,5mg/ml) with DMSO and 3 µl of this dilution were placed on the surface of the agar. Compounds diffuse into the agar and the size of the inhibition zone was measured after 24 hours incubation at 37 °C.

MIC determinations

MIC determinations were carried out in microtiter plates. Strains were grown in half-concentrated Mueller-Hinton broth (Oxoid). MICs with serial twofold dilution steps were performed (1:2). Bacteria were added to give a final inoculum of 10^5 CFU/ml in a volume of 0.2 ml. After incubation for 24 h at 37 °C the MIC was read as the lowest compound concentration causing inhibition of visible growth.

3.6.3 Radioligand Binding Studies at CB_1 and CB_2 Receptors

Assays were performed by Viktor Rempel and Clara Schoeder (Institute for Pharmaceutical Chemistry, University of Bonn). Competition binding assays were performed versus the cannabinoid receptor agonist radioligand [^{3}H](-)-cis-3-[2-hydroxy-4-(1,1-dimethylheptyl)phenyl]-trans-4-(3-hydroxy-propyl)-cyclohexanol (CP55,940) as described before.[35] Stock solutions of test compounds were prepared in DMSO. The final DMSO concentration in the assay was 2.5%. Data were obtained from three independent experiments, performed in duplicate.

3.6.4 cAMP Accumulation Assays

Assays were performed by Viktor Rempel and Clara Schoeder (Institute for Pharmaceutical Chemistry, University of Bonn). The measurement of intracellular cAMP concentration was performed as described before.[36] Inhibition of adenylate cyclase activity was determined in CHO cells stably expressing the CB_1 or CB_2 receptor subtype using a competition binding assay for cAMP quantification. Data were obtained from three independent experiments, performed in duplicate.

3.6.5 β-Arrestin-Recruitment Assays

Assays were performed by Viktor Rempel and Clara Schoeder (Institute for Pharmaceutical Chemistry, University of Bonn). Recruitment of β-arrestin to the respective GPCR was detected by using the β-galactosidase enzyme fragment complementation technology (β-arrestin PathHunter assay, DiscoverX) as previously described.[35] CHO cells stably expressing the respective receptor were seeded in a volume of 90 µL into a 96-well plate and were incubated at a density of 20.000 cells/well in assay medium (Opti-MEM, 2% FCS, 100 U-mL^{-1} penicillin, 100 µg mL^{-1} streptomycin, 800 µg mL^{-1} geneticin and 300 µg mL^{-1} hygromycin) for 24 h at 37°C. Test compounds were diluted in PBS buffer containing 10% DMSO and 0.1% BSA and 10 µL were added to 90 µL of the cell culture, followed by incubation for 90 min at 37°C. For determination of β-arrestin recruitment to GPR18, the commercial detection reagent was used, according to the suppliers protocol (DiscoverX). The detection reagent for GPR55 was prepared by mixing the chemiluminescent substrate Galacton-Star (2 mM), with the luminescence enhancer Emerald-II and a lysis buffer (10 mM TRIS, 1 mM EDTA, 100 mM NaCl, 5 mM $MgCl_2$, 1% Triton-X; pH 8) in a ratio of 1:5:19. After the addition of 50 µL/well of detection reagent to the cells, the plate was incubated for further 60 min at RT. Finally luminescence was determined in a luminometer (TopCount NXT, Packard / Perkin-Elmer). Screening for antagonism of test compounds was performed in the presence of 10 µM Δ^9-THC (GPR18), or 1 µM of LPI (GPR55), respectively. IC_{50} values of compounds were determined in the presence of a constant concentration of 7.5 µM Δ^9-THC (GPR18), or 1 µM LPI (GPR55), respectively. Data were obtained from three independent experiments, performed in duplicate.

3.6.6 Acid Hydrolysis and Chiral-phase HPLC

To 0.5-2.0 mg of test substance 2 mL 2 M HCl was added and the resulting solution was heated at 80 °C for 5 h under reflux. The residual solvent was removed under reduced pressure and the residue was solved in 1 mL EtOH. This solution was used for chiral-phase HPLC analysis using the Merck HPLC system B with the ELSD detector under following conditions: Compounds **1**: Merck HPLC system B with ELSD detector was employed applying the conditions: column 1, Diacel CHIRALPAK IA column Nr 1 (250 mm x 4.6 mm, 5 µm); mobile phase, hexane-EtOH (70-30); flow, 0.5 mL min-1. Using these conditions the α-D-mannose had a retention time of 11.2 min, β-D-mannose of 17.0 min, α-L-mannose of 13.1 min, and β-L-mannose of 22.4 min, respectively.
Compounds **10** and **11:** Merck HPLC system B with ELSD detector was employed applying the conditions: column 2, Diacel CHIRALPAK IA column Nr 2 (250 mm x 4.6 mm, 5 µm); mobile phase, hexane-EtOH (75-25); flow, 0.5 mL min-1. Using these conditions the α-D-mannose had a retention time of 12.5 min and α-L-mannose of 13.1 min

3.6.7 Cell viability/cytotoxicity tests

3.6.7.1 In vitro Cytotoxicity with L-6 Cells

Assay was performed by Dr. Marcel Kaiser (Swiss Tropical and Public Health Institute, Basel) Assays were performed in 96-well microtiter plates, each well containing 100 µL of RPMI 1640 medium supplemented with 1% L-glutamine (200 mM) and 10% fetal bovine serum, and 4000 L-6 cells (a primary cell line derived from rat skeletal myoblasts).[37] Serial drug dilutions of 11 threefold dilution steps covering a range from 100 to 0.002 µg mL^{-1} were prepared. After 70 hours of incubation the plates were inspected under an inverted microscope to assure growth of the controls and sterile conditions. 10 µL of Alamar Blue was then added to each well and the plates incubated for another 2 h. Then the plates were read with a Spectramax Gemini XS microplate fluorometer (Molecular Devices Cooperation using an excitation wave length of 536 nm and an emission wave length of 588 nm. The IC_{50} values were calculated by linear regression from the sigmoidal dose inhibition curves using SoftmaxPro software (Molecular Devices Cooperation, Sunnyvale). Podophyllotoxin (Sigma P4405) was used as the control.[38]

3.6.7.2 MTS survival assay

N2a cells stably transfected with human APP695 were maintained in Dulbecco's modified Eagle's medium (DMEM/optiMEM), supplemented with 5% fetal bovine serum, 1% penicillin-streptomycin solution and G418 (Sigma, St. Louis, MO, USA) (0.1 mg/mL) in a humidified atmosphere at 37°C with 5% CO_2. N2a-APP695 cells were plated at a density of approximately 10,000 cells per well on 96-well plates in Dulbecco's modified Eagle's medium (DMEM/optiMEM), supplemented with 0.5% fetal bovine serum. After 24 h incubation, the conditioned media were replaced by new media containing compounds at the final concentrations indicated. Viability of cells was measured by MTS-formazan reduction using CellTiter 96 Aqueous One Solution Cell Proliferation Assay (Promega, Madison, WI, USA) at 18 h post treatment. Incubation was pursued for 1h30 (37°C, 5% CO_2 and 95% humidity). Optical density (OD) was measured at 490 Δ 630 nm using a microELISA reader. 10 μM was used as final compound concentration. Blanks without cells and untreated cells were used as control. Cell viability was calculated as Cell viability (%) = (OD of treated cell – OD of blanks) / (OD of controls (vehicle treated cells) – OD of blanks) x 100.

3.6.7.3 Viability and proliferation assessment by trypan blue exclusion test

Assay performed by Barbora Orlikova (Department of Pharmacy, Seoul National University) to assess percentage of viable cells within sample and to determinate the proliferation trypan blue exclusion test was used. Trypan blue is a vital stain that belongs to the family of azo compounds. As selective dye trypan blue stains only dead cells, passing through their plasma membrane. Viable cells chamber. In order to assess the cell viability, the percentage of unstained cells (K562) to the total amount of cells within the sample was calculated and normalized to 100% of control cells viability. In order to assess cell proliferation the concentration of unstained cells was determined and normalized to 100% of control cells concentration.

3.6.8 Amyloid β-42 production induction assay

Assay performed by WG *Meijer* (ManRos Therapeutics, Roscoff). N2a cells stably transfected with human APP695 were maintained in Dulbecco's modified Eagle's media

(DMEM/optiMEM) as described above. After 18 h incubation, the conditioned media were replaced by new media containing compounds at the indicated final concentrations. After 18 h incubation, the cultured media were harvested for Amyloid β-42 determination by ELISA assay. Aβ-42 levels were measured in a double antibody sandwich ELISA using a combination of monoclonal antibody (mAb) 6E10 (SIG-39320, Covance, Eurogentec, Seraing, Belgium) and biotinylated polyclonal Aβ-42[39] antibody (provided by Dr. P.D. Mehta, Institute for Basic Research in Developmental Disabilities, Staten Island, USA).[39] Briefly, wells of microtiter plates (Maxisorp, Nunc, ThermoFisher Scientific, Illkirch, France) were coated 100 µL mAb 6E10 diluted in carbonate-bicarbonate buffer (buffer (0.015 M Na_2CO_3 + 0.035 M $NaHCO_3$) pH 9.6) at a 1.5 µg/mL final concentration, and plates were incubated overnight at 4°C. The plates were then washed with PBST (PBS containing 0.05% Tween-20) and blocked for 1 h with 1% BSA in PBST to avoid non-specific binding. Following a washing step, 100 µL of cell supernatant was added and incubated for 2 h at room temperature (RT) on a shaking device. Plates were then washed with PBST and 100 µL of biotinylated antibodies (diluted to 1 µL/mL in PBST containing 0.5% BSA) were added and incubation was carried out for 75 min at RT under constant shaking. After a washing step, streptavidin-Poly-HRP (horseradish peroxidase) conjugate (Pierce, ThermoFisher Scientific, Illkirch, France), diluted in PBS + 1% BSA, was added and incubation was carried out for 45 min at RT under continuous shaking. After washing, 100 µL of OPD (o-Phenylenediamine Dihydrochloride, Pierce, ThermoFisher Scientific, Illkirch, France) in pH 5.0 citrate buffer (0.049M citric acid monohydrate + 0.1M $Na_2HPO_4*2H_2O$ + 1 mL H_2O_2 30%/L) were added as a substrate and after 15 min incubation at room temperature, the reaction was stopped by addition of 100 µL 1 N sulfuric acid. OD was measured at 490 nm using a plate reader (BioTek Instrument, El 800, Gen 5 software). 10 µM of the compounds were used as a final concentration. Blank without cells, vehicle treated cells and cells + 100 µM Aftin-5, the reference activator of extracellular Aβ-42 production[40] were used as control. Aftin-5 was produced by *ManRos Reagents* and is available from Adipogen International, San Diego. Aβ-42 were calculated as (x=x0-b.ln(a/(DO-y0)-1) with x = amount of Aβ-42, x0 = $-5.06.10^{-10}$, y0 = -11.4656, a = 14.8527and b = $4.15.10^{-10}$. Fold change in Aβ-42 levels was calculated as Fold change = Amount of Aβ-42 in sample treated cells / amount of Aβ-42 in control (vehicle treated cells)

3.6.9 Amyloid β Quantification

Assay performed by WG *Meijer* (ManRos Therapeutics, Roscoff). Standard curves were prepared with synthetic Aβ-42 HFIP treated (JPT Peptide Technologies) and Aβ-42 specific polyclonal antibody. Curve fitting was performed using a 4 parameters sigmoid equation (SigmaPlot, Systat). Results are expressed as fold change ± s.d. The fold change was calculated by dividing the amount of Aβ peptides produced by treated cells by the of Aβ peptides produced by untreated cells. All experiments were performed in triplicate.

3.6.10 Effects on inhibition of Amyloid β-42 production induced by Aftin-5

Assay performed by WG *Meijer* (ManRos Therapeutics, Roscoff). N2a cells stably transfected with human APP695 were maintained in Dulbecco's modified Eagle's media (DMEM/optiMEM), as described above. After 18 h incubation, the conditioned media were replaced by new media containing respective sample at the indicated final concentrations. After 1 h incubation, Aftin-5 is added (100 μM 1% DMSO final). After 18 h incubation, the cultured media were harvested for Amyloid β-42 determination by ELISA assay. Compounds were tested in concentrations 0.1, 0.33, 1.0, 3.3, 10 μM. Blanks without cells, vehicle treated cells, cells + 100 μM Aftin-5 and cells + 10 μM DAPT (N-[(3,5-difluorophenyl)acetyl]-Lalanyl-2-phenyl]glycine-1,1-dimethylethyl ester) were used as controls.

3.6.11 Protein kinase assays

Assay performed by WG *Meijer* (ManRos Therapeutics, Roscoff). Protein kinase assay buffer Buffer A : 10 mM MgCl2, 1 mM EGTA (MW 380.4), 1 mM DTT (MW 154.2), 25 mM Tris/HCl (MW 121.1) and 50 μg/ml Heparin.
Buffer C: 20 mM ß-glycerophosphate, 10 mM p-nitrophenylphosphate, 25 mM MOPS, 5 mM EGTA, 15 mM MgCl2, 1 mM DTT and 0.1 mM sodium vanadate.
Preparation and assay of protein: [41]
Kinase activities were assayed in buffer A or C, with their corresponding substrates, in the presence of 15 μM [γ-33P] ATP (3,000 Ci/mmol; 10 mCi/mL, PerkinElmer, Courtaboeuf, France) in a final volume of 30 μL. After 30 min incubation at 30°C, the reaction was stopped by harvesting on a FilterMate harvester (Packard) onto P81 phosphocellulose papers (GE

Healthcare). Filters were washed in 1% phosphoric acid. 20 µL of scintillation fluid were added and the incorporated radioactivity was measured in a Packard counter. Blank values were subtracted and activities calculated as pmoles of phosphate incorporated during the 30 min incubation. The activities were expressed in % of the maximal activity, i.e. in the absence of inhibitors. Controls were performed with appropriate dilutions of DMSO.

CDK1/cyclin B (M phase starfish oocytes, native) was prepared as previously described .[42] Kinase activity was assayed in buffer A, with 1 mg histone H1/mL.

CDK2/cyclin A (human, recombinant, expressed in insect cells) was assayed as described for CDK1/cyclin B. **CDK5/p25** (mammalian, recombinant, expressed in *E. coli*) was assayed as described for CDK1/cyclin B. **CDK9/cyclin T** (human, recombinant, expressed in insect cells) was assayed as for CDK1/cyclin B using the Tide 7/9 substrate (YSPTSPSYSPTSPSYSPTSPSKKKK, Proteogenix, Oberhausbergen, France) (500 µM). **CK1δ/ε** (porcine brain, native, affinity purified on axin-2 beads [6]) was assayed as described for CDK1 but in buffer C and using the CK1-specific peptide substrate (CKs: RRKHAAIGSpAYSITA, Proteogenix, Oberhausbergen, France) (1 mM). **CLK1** (Human, recombinant, expressed in E. coli as GST fusion protein) was assayed in buffer A (+ 0.15 mg BSA/ml) with RS peptide (GRSRSRSRSRSR, Proteogenix, Oberhausbergen, France) (1 µg/assay). **DYRK1A** (human, recombinant expressed in Escherichia coli as a glutathione S-transferase fusion protein) were purified by affinity chromatography on glutathione-agarose and assay as described for CDK1/cyclin B using Woodtide (KKISGRLSPIMTEQ, Proteogenix, Oberhausbergen, France) (1.5 µg/assay) as a substrate, a residue of transcription factor FKHR. **GSK-3α/β** (porcine brain, native, affinity purified on axin-1 beads [7]) was assayed as described for CDK1 using a GSK-3–specific substrate (GS-1: YRRAAVPPSPSLSRHSSPHQSpEDEEE; Sp stands for phosphorylated serine, Proteogenix, Oberhausbergen, France) (250 µM).

3.6.12 Luciferase-based reporter system to detect agonism toward NR

Tests were performed by Dr. Paulsen Steinar (The Norwegian Structural Biology Centre and Department of Chemistry, University of Tromsø) following the method described by Ciocoiu et al.,2010 and Tzameli et al., 2004[43,44]: Cos-1 cells (ATCC no. CRL-1650) were maintained in DMEM (Invitrogen, Carlsbad, CA) containing gentamicin (10 µg/ml) and fetus bovine serum (10%), at 37°C in a humidified atmosphere of 5% CO_2. Cell confluence never reached

above 80% before sub-culturing or transfection. The pSG5-Gal4-hPPAR-LBD (α, γ and β/δ isotypes) and the pSG5-Gal4-hLXR-LBD (α and β/δ isotypes) expression constructs were generous gifts from Dr. Hilde Nebb, University of Oslo, Norway. The pGL3-5XUAS-SV40 luciferase reporter construct was purchased from Promega Corporation, Madison, WI. Cos-1 cells were transiently transfected with 1.7 µg of the expression plasmids and 8.5 µg of the reporter construct per 1 x 10^7 cells. Transient transfection was achieved using the Neon electroporation system (Invitrogen). Cells were seeded (2 x 10^4/well) in 96-plates (white F96 microwell, Nalge Nunc Int., Rochester, NY) and allowed to attach (5 hrs) before test compounds was added. Test compound dissolved in DMSO was tested in dilution series made prepared in cell medium. Following incubation for 19 hrs cell media was a sucked of by a multi-canal vacuum pipette and cells washed in PBS, at room temperature.Results were developed by adding D-luciferin K-salt (0.12 mg/ml) dissolved in 30 mM HEPES supplemented with 1 mM MgSO4 and 0.5 mM in a volume of 50 µl per well. Following 10 min of incubation at room temperature the light signal was read on an Envision instrument, PerkinElmer, Turku, Finland.

Assay	**Positive control**	**AC uM**	**DMSO %**	**WS mM**	**AS in DMEM/FCS**
PPARγ	Rosiglitazone	5	0.05	10	5 µl of 10 mM in 5 ml = 10 uM
PPARβ/δ	GW501516	1	0.01	10	2 µl of 10 mM in 10 ml = 2 uM
PPARα	Bezafibrate	100	0.072	138	7.2 µl of 138 mM in 5 ml = 200 µM
LXRα	T0901317	1	0.02	5	2 µl of WS in 5 ml = 2 µM
LXRβ	T0901317	1	0.02	5	2 µl of WS in 5 ml = 2 µM

AC: Assay concentration; WS: working stock; AS: assay stock DMEM/FCS: cell growth medium. All dissolved in DMSO (100 %) to make up the working stocks. As negative controls, cell medium supplemented with DMSO equivalent to the positive control was used.

3.6.13 Enzyme inhibitory activity

Tests were performed by Working group Guetschow (Pharmaceutical Institute University of Bonn) Inhibitory activity was tested toward Cathepsin L, Cathepsin B, Cathepsin K following the method described by Frizler et al., 2011 [45]

Inhibitory activity was tested toward human leukocyte elastase following the modified method described by Gütschow et al. [46] (Enzo, 250 ng/mL, [MeOSuc-Ala-Ala-Pro-Val-pNA] = 100 µM, 1.5% DMSO, 25 °C;Inhibitory activity was tested toward bovine chymotrypsin, bovine trypsin and porcine cholesterol esterase following the method described by Pietsch und Gütschow, 2005 [47]

3.6.14 Label-Free Dynamic Mass Redistribution (DMR) Assay for FFA receptor expressing cells

Cell based dynamic mass redistribution assays were performed by Manuel Grundmann (Institute for Pharmaceutical Biology, University of Bonn) as described previously in detail[48,49], using the Enspire® benchtop optical label-free system in conjunction with the Mini Janus liquid handing station (Perkin Elmer, Hamburg, Germany). Briefly refractive waveguide grating optical biosensors, integrated in 384-well microplates, allow extremely sensitive measurements of changes in local optical density in a detecting zone up to 150 nm above the surface of the sensor. Cellular mass movements induced upon GPCR activation can be detected by illuminating the underside of the biosensor with polychromatic light and measurement of changes in wavelength of the reflected monochromatic light that is a sensitive function of the index of refraction. The magnitude of this wavelength shift (in picometers) is directly proportional to the amount of DMR. Cells were seeded at a density of 18,000 cells/well (FFA1-HEK, FFA2-HEK, FFA3-HEK, Flp-In T-Rex293) on fibronectin-coated biosensor plates and were cultivated for 20-24 h (37 °C, 5 % CO_2) to obtain confluent monolayers. Cells were treated with 1µg/mL Doxycycline for 5 h to induce the expression of the respective receptor protein. Before the assay, cells were washed twice with Hank's buffered salt solution (HBSS) containing 20 mM HEPES and incubated for 1 h in the Enspire® reader at 37 °C. The sensor plate was then scanned and a baseline optical signature was recorded. Hereafter, compound solutions were transferred into the biosensor plate and DMR was monitored for at least 4,000 s. Quantification of DMR signals for concentration effect curves was performed by calculation of the area under the curve (AUC) in DMR between 0 and 4,000 s. All optical DMR recordings were buffer and solvent corrected. For data normalization, indicated as relative response (%), DMR induced by 100µM ATP were set 100 % and bottom levels 0 %. Data calculation and EC_{50} value determination by nonlinear regression was performed using GraphPad Prism 5.04 (GraphPad Software).

3.6.15 Cerebrosid-Sulfotransferase Assay

Assay was performed by Isabell Zech (Institute for Biochemie and Molekularbiologie, University Bonn) following the modified procedure of Jungalwala et al. [50]

Modified volumina and concentrations:

1 µg Galactosylceramid (Avanti Polar Lipids, 860544P, solved in $CHCl_3$/MeOH 1:1)

0.5 µl 10 % Triton X-100-solution ($CHCl_3$/MeOH 2:1)

3 µl of tested compounds (1 mM in 10 % DMSO) or 3 µl 10%-DMSO-solution.

30 µl Reaction buffer

1 µl CST-sample to start reaction

Tris-HCl pH 7,1 (concentration: 100 mM, final concentration: 100 mM)

$MgCl_2$ (concentration: 20 mM, final concentration: 16 mM)

PAP[35S] (Perkin Elmer, 250 µCi, Lot 0813) (concentration 0.33 nmol/µl, final concentration: 1.1µM)

3.6.16 HIV Assay

Assay was performed by Dr. Markus Helfer (Institute of Virology, Helmholtz Zentrum München) following the procedure of Kremb et al. [51]

3.6.17 Antiparasitic Assay

Anti-parasitic activities were assessed by Dr. Marcel Kaiser (Swiss Tropical and Public Health Institute,Basel)

3.6.17.1 In Vitro Antimalarial Activity Assay

Plasmodium strain was cultured according to Trager and Jensen et al., 1976 [52] and is described at mr4.org (sensitive strains: NF54). IC_{50} values were determined in vitro by measuring incorporation of the nucleic acid precursor [^{3}H]hypoxanthine [53]. In vitro time-, stage-, and concentration-dependent effects were assessed using pyrimethamine as a stage-specific and slow acting control, as described elsewhere.[54]

3.6.17.2 Activity Against Other Parasitic Protozoa

In vitro activity against *T. brucei rhodesiense*, T. cruzi, *Leishmania donovani* and was determined as described by Regalado et al., 2010[55]

3.6.17.3 *L. donovani* Macrophage Assay:

Mouse peritoneal macrophages (4 x 104 in 100 µL RPMI 1640 medium with 10% heat–inactivated FBS) were seeded into wells of Lab–tek 16–chamber slides. After 24 h 1.2 x 105 amastigote *L. donovani* in 100 µL were added. The amastigotes were taken from an axenic amastigote culture grown at pH 5.4. 4 h later the medium containing free amastigote forms was removed and replaced by fresh medium. Next day the medium was replaced by medium containing different compound dilutions. Parasite growth in the presence of the drug was compared to control wells. After 96 hours of incubation the medium was removed and the slides fixed with MeOH for 10 min followed by a staining with a 10% Giemsa solution. Infected and non–infected macrophages were counted for the control cultures and the ones exposed to the serial drug dilutions. The infection rates were determined. The results were expressed as % reduction in parasite burden compared to control wells, and the IC_{50} calculated by linear regression analysis. [56]

4 Results

4.1 Preparations and screening of fungal extracts and fractions to examine ideal culture conditions

4.1.1 Screening of fungal extracts to examine ideal culture conditions for further investigations

For screening purposes four different solid media (BMS, MPY, REA and Tennelin) were chosen for the cultivation of a marine-derived strain of *Dichotomomyces cejpii*. This strategy follows the idea of the so-called OSMAC approach (One Strain Many Compounds), which was developed by Zeeck and co-workers to achieve different secondary metabolite profiles from one organism.[57] In contrast to the complex, nutrient rich media BMS (biomalt agar medium containing artificial seawater [ASW]) and MPY (malt, peptone, yeast agar medium), the REA (rice extract agar medium) and Tennelin media are minimal media, providing only a reduced amount and composition of nutrients. The Tennelin medium contains furthermore only exclusively selected ingredients, such as inorganic nitrate as sole nitrogen source. The fungal strain of *Dichotomomyces cejpii* was cultivated on each media as described before (3.2.2) and the four obtained crude extracts were further investigated. These "screening extracts" were screened for their antibiotic activities against different bacteria and fungi species. NMR spectroscopic and mass spectroscopic analysis was used to evaluate the crude extracts to judge the qualification of each media for a scaled up cultivation. As shown in Table 4-1, all extracts showed antibiotic activities. The media of the two extracts with the most prominent antibiotic activities were identified (MPY and Tennelin) and due to their likewise interesting spectroscopic data and sufficient biomass production selected for large scale cultivation

Table 4-1: Antimicrobial activity of "screening extracts" obtained from Dichotomomyces cejpii cultivated on four different culture media

	sample concentration: 1 mg/mL (at 50 µg/disk level)[1]					
	growth inhibition (GI) and total inhibition (T) zones against test organisms [mm]					
medium	*Escherichia coli*	*Bacillus megaterium*	*Microbotryum violaceum*	*Eurotium rubrum*	*Mycotypha microspora*	*Chlorella fusca*
BMS	0	3.0 (T)	0	0	2.5 (GI)	0
MPY	0	4.0 (T)	2.5 (GI)	0	2.5 (GI)	0
REA	3.0 (GI)	0	/	/	/	/
Tennelin	2 .0 (GI)	3.0 (T)	/	/	/	/

[1] 50 µL (equivalent to 50 µg) of each sample solution (1 mg/mL) were pipetted onto a sterile filter disk.

4.1.2 Screening of fungal extracts and fractions for antibiotic activity

The obtained material of large scale cultivation medium 1 (MPY) was tested for antibiotic activity and then fractionated by normal-phase (NP) vacuum liquid chromatography (VLC) using a stepwise gradient solvent system of increasing polarity starting with 100% CH_2CL_2 to 100% EtOAc and to 100% MeOH which yielded 10 fractions.

The obtained material of large scale cultivation medium 2 (Tennelin) was tested for antibiotic activities and then further fractionated as well, by NP VLC using a stepwise gradient solvent system of increasing polarity starting with 100% CH_2CL_2 to 100% EtOAc, to 100% MeOH and H_2O-MeOH (50-50) which yielded 11 fractions. Crude extracts and VLC fractions were tested for antibacterial activities in WG König. Crude extracts were additionally tested for anbiotic activities in WG Sahl. Agar diffusion tests of the fractions obtained from Tennelin medium revealed an increased antibiotic activitiy for some of the hydrophilic VLC fractions in comparison to the fractions of MPY medium.

Table 4-2: Antimicrobial activity of fungal extracts and fractions obtained from two different media (3.6.1).

sample concentration: 1 mg/mL (at 50 µg/disk level)[1]						
growth inhibition (GI) and total inhibition (T) zones against test organisms [mm]						
	medium	***Escherichia coli***	***Bacillus megaterium***	***Microbotryum violaceum***	***Eurotium rubrum***	***Mycotypha microspora***
large scale cultivation	MPY	3.0 (T)	9.0 (T)	5.0 (GI)	3.5 (GI)	10.0 (T)
	Tennelin	2.5 (T)	7.0 (T)	8.0 (T)	5.0 (T)	8.0 (T)
Fraction 1	MPY	2.5 (T)	9.0 (T)	6.0 (GI)	2.5 (GI)	10.0 (T)
Fraction 2	MPY	2.0 (T)	10.0 (T)	15.0 (T)	2.5 (T)	10.0 (T)
Fraction 3	MPY	0	10.0 (T)	10.0 (T)	0	10.0 (T)
Fraction 4	MPY	0	10.0 (T)	0	0	10.0 (T)
Fraction 5	MPY	0	10.0 (T)	0	0	2.0 (T)
Fraction 6	MPY	0	3.5 (GI)	0	0	0
Fraction 7	MPY	0	3.0 (GI)	0	0	0
Fraction 8	MPY	0	0	0	0	0
Fraction 9	MPY	0	0	0	0	0
Fraction 10	MPY	0	0	0	0	0
Fraction 1	Tennelin	0	0	0	0	0
Fraction 2	Tennelin	0	6.0 (T)	14.0 (T)	3.0 GI)	4.0 (T)
Fraction 3	Tennelin	5.0 (T)	11.0 (T)	6.0 (T)	5.0 (T)	8.0 (T)
Fraction 4	Tennelin	0	0	3.5 (T)	0	0
Fraction 5	Tennelin	0	2.0 (T)	3.0 (T)	3.5 (GI)	2.5 (T)
Fraction 6	Tennelin	0	3.0 (T)	0	0	0
Fraction 7	Tennelin	0	3.5 (T)	0	0	0
Fraction 8	Tennelin	0	3.0 (T)	3.5 (GI)	3.0 (GI)	0
Fraction 9	Tennelin	0	5.0 (T)	5.0 T)	4.0 (GI)	2.5 (GI)
Fraction 10	Tennelin	0	5.5 (T)	5.0 (T)	3 .0 (T)	2.0 (GI)
Fraction 11	Tennelin	0	5.5 (T)	5.0 (T)	2.5 (GI)	0

[1] 50 µL (equivalent to 50 µg) of each sample solution (1 mg/mL) were pipetted onto a sterile filter disk.

Table 4-3: Antimicrobial activity of crude extracts obtained from three different media, monitored by agar diffusion assays in AG Sahl (3.6.2).

sample concentration: 1 mg/mL (at 3 µg[1] or 5 µg[2] / spot			
growth inhibition (GI) and total inhibition (T) zones against test organisms [mm]			
test organism	**MPY[1] large scale**	**Tennelin[1] large scale**	**REA[2] screening**
Staphylococcus aureus (MSSA)	6 (T)	6 (T)	/
Staphylococcus aureus (MRSA)	9 (T)	8 (T)	0
Staphylococcus simulans	8 (T)	6 (T)	/
Staphylococcus epidermidis (MRSE)	12 (T)	6 (T)	0
Enterococcus faecium	0	0	0
Bacillus subtilis	13 (T)	10 (T)	0
Bacillus megaterium	12 (T)	4 (T)	0
Listeria welchimeri	7 (T)	4 (T)	0
Corynebacterium xerosis	16 (T)	20 (T)	0
Mycobacterium smegmatis	12 (T)	5 (T)	0
Echerichia coli	11 (T)	5 (T)	3 (GI)
Citrobacter freundii	7 (T)	4 (T)	0
Klebsiella pneumoniae subsp. Ozeanae	0	0	/
Arthrobacter crystallopoietes	16 (T)	8 (T)	4 (GI)
Candida albicans	9 (T)	0	/
Candida glabrata	/	5 (T)	/

3-5 µL (equivalent to 3-5 µg) of each sample solution (1 mg/mL) were pipetted onto the agar (3.6.1).

4.2 Isolation and evaluation of compounds with antagonistic activity at GPR18 and cannabinoid receptors

4.2.1 Introduction to the examined cannabinoid and related receptors

Cannabinoid (CB) receptors belong to the G protein-coupled receptor (GPCR) superfamily[58] and are divided into two distinct subtypes, designated CB_1 and CB_2. Both receptors are coupled to $G_{i/0}$ proteins mediating adenylate cyclase inhibition, which results in reduced intracellular cAMP levels.[59,60] The CB_1 receptor is highly expressed in the central nervous system, but is also present in peripheral tissues, including heart, liver, lungs and kidneys.[61,62] CB_1 activation mediates a variety of physiological responses including analgesia, stimulation of appetite, and psychoactive effects, *e.g.* euphoria. The CB_2 receptor is mainly present in organs and cells of the immune system including, spleen, tonsils, thymus, T-lymphocytes, macrophages and B-cells, and its activation results in analgesic and immunomodulatory effects.[61–63]

Non-selective CB_1/CB_2 agonists like dronabinol (Marinol®) and nabilone (Cesamet®) are therapeutically used for the suppression of chemotherapy-induced nausea and vomiting,[64] for the treatment of neuropathic pain, and for the therapy of anorexia in patients suffering from AIDS.[61] Furthermore, beneficial effects for patients with fibromyalgia and multiple sclerosis have been reported.[61] CB_1-selective antagonists have gained much attraction, due to their suppressing effects on appetite and food intake.[65] In addition, blockade of CB_1 receptors was shown to ameliorate several metabolic parameters including triglyceride levels.[65,66] Thus CB_1-selective antagonists are regarded as promising drugs for the treatment of obesity and metabolic disorders, such as diabetes and dyslipidemia.[67] However, the first approved CB_1-antagonist, rimonabant, has meanwhile been withdrawn from the market due to its side-effects, which included anxiety, depression and suicidality.[68] These are attributed to an interaction with central CB_1 receptors.[69,70] Therefore current strategies focus on the development of CB_1 antagonists that do not penetrate into the brain.[68–72] This may be achieved by increasing the compounds' polarity.[72] Besides their potential use in patients with obesity and metabolic disorders, peripherally acting CB_1 antagonists are regarded as promising drugs for the treatment of coronary artery disease, inflammatory bowel disorders

and arthritis.[67] CB_2-selective antagonists/inverse agonists are of interest as potential drugs for the therapy of osteoporosis, and for the treatment of dermatitis provoked by allergic skin inflammation.[64,73–75]

Meanwhile, several reports have indicated the existence of further CB receptors, and the orphan receptors GPR18 and GPR55 have been proposed as potential candidates.[76–78] Several cannabinoids including the nonselective agonist Δ^9-tetrahydrocannabinol (Δ^9-THC), as well as the selective CB_1 inverse agonist rimonabant were shown to interact with GPR18 and GPR55.[35,79–82] GPR18 is coupled to G_i proteins and is highly expressed in spleen, thymus, leukocytes, testis and endometrium.[79,83,84] As an endogenous agonist for GPR18 *N*-arachidonoylglycine (NAGly) was proposed by several groups.[84–87] However, this could not be confirmed by other laboratories, including ours, in various assay systems.[88,89] The physiological role of GPR18 is poorly understood. Studies indicate an involvement of the receptor in endometriosis, regulation of intraocular pressure, and microglial activation.[79,87,90,91] Potent and selective GPR18 agonists and antagonists are urgently needed as pharmacological tools to further explore the physiological effects of this putative novel CB receptor subtype, which has potential as a novel drug target.

The primarily $G_{12,13}$-coupled GPR55 is mainly expressed in the brain, as well as in osteoclasts and osteoblasts.[77,92–94] In addition, the receptor was shown to be highly expressed in several cancer cell lines, such as glioblastoma, astrocytoma, breast cancer, prostate and ovarian carcinomas.[95,96] GPR55 antagonists are considered as potential drugs for the treatment of cancer and neuropathic pain.[80,95,96] Besides its interaction with cannabinoids, the receptor is activated by 1-lysophosphatidylinositol (LSI), an endogenous lipid that does not interact with the established CB receptors.[35,97,98]

Here we report on novel indole derivatives derived from a marine fungal source. Our study shows that compounds of fungal origin have the potential to serve as lead structures for the development of novel ligands for GPCRs – for CB receptors and the related orphan receptor GPR18.

4.2.2 Isolation of compounds 1–6 from *Dichotomomyces cejpii*

Bioassay- and chemical (LC-MS and ^{1}H NMR)-guided fractionation of the crude extracts, obtained from the marine derived fungus *Dichotomomyces cejpii* on two different media, yielded 6 indoloditerpenes in total (**1–6**, compound **7** is a semisynthetic derivative of **5**; Figure 4-13). The investigated fungal strain was cultivated on cultivation medium 1 as described before (3.2.2–3.2.3).

Fungal biomass and media were homogenized using an Ultra-Turrax apparatus and extracted with 5 L EtOAc to yield 4.1 g of extract. This material was fractionated by NP vacuum liquid chromatography (VLC) using a stepwise gradient solvent system of increasing polarity starting with 100% CH_2Cl_2 to 100% EtOAc and to 100% MeOH which yielded 10 fractions. Compound **1** (emindole SB beta-mannoside) was isolated from VLC fraction 7, while compounds **2**, **3** and **4** were found in VLC fraction 2. Fraction 7 was separated via reversed phase C18 ($RP_{18)}$-VLC using stepwise elution with MeOH-H_2O (70-30) to 100% MeOH which yielded 7 fractions. Subfraction 7.6 was further purified by RP C_{18}-HPLC system D (Nucleodur 100-S 250 mm x 8 mm) using MeOH-H_2O (95-5), 2.0 mL min^{-1}. Compound **1** was isolated as a white powder in subfraction 7.6, t_R: 10 min (6.5 mg).

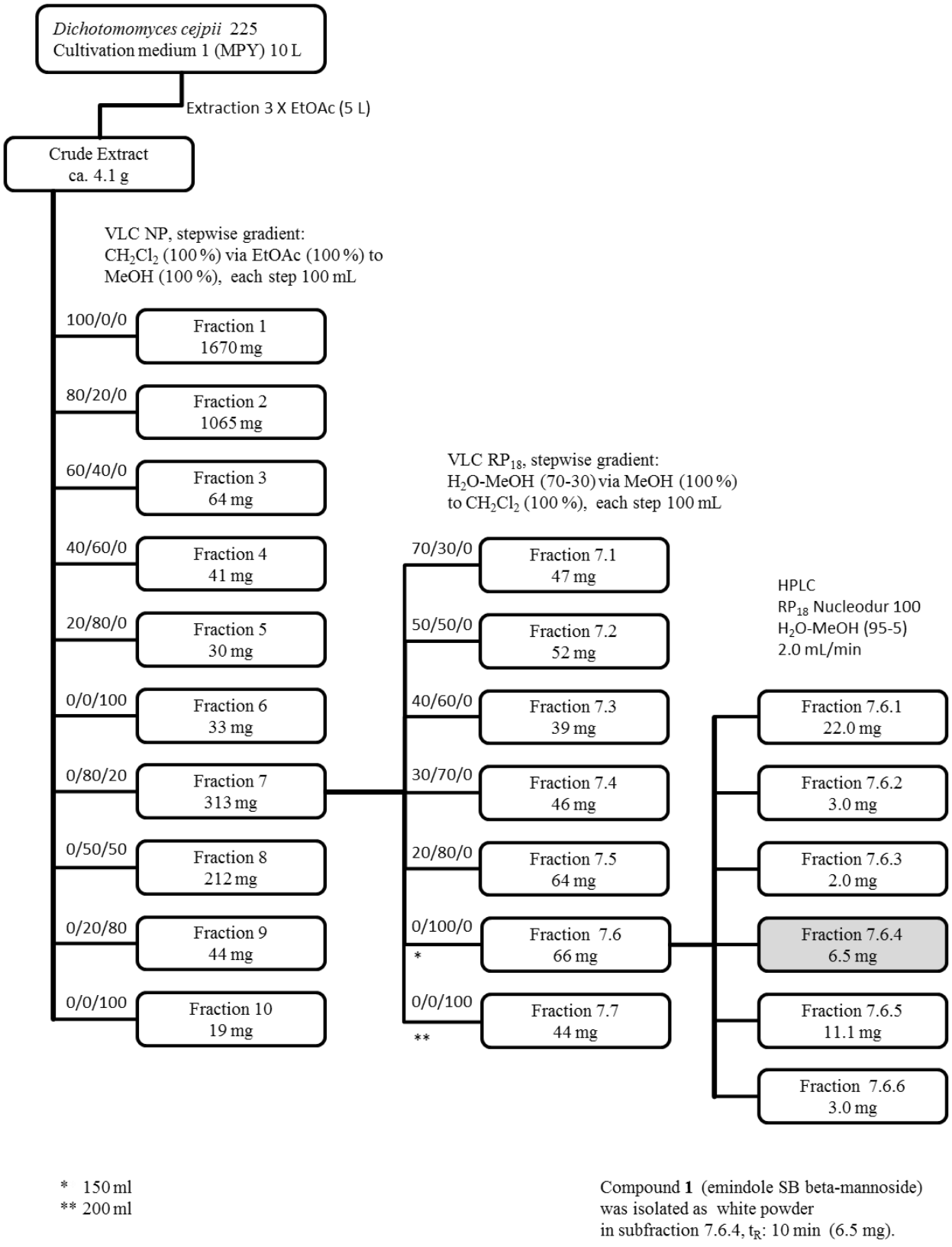

Figure 4-1: Isolation scheme for compound **1**. For reasons of clarity only the most important fractions are listed.

VLC fraction 2 was separated with a NP VLC, eluted stepwise with CH_2Cl_2-petroleum ether (50-50), up to 100% CH_2Cl_2, and 100% MeOH which yielded 15 fractions. Subfraction 2.1 and VLC fraction 1 were separated three times with a solvent/solvent extraction with hexane (100%) and MeOH-H_2O (60-40) using a separation funnel. The combined hexane phases were further separated with a NP VLC column and eluted stepwise with CH_2Cl_2-petroleum ether (20-80), up to 100% CH_2Cl_2, 100% acetone, and 100% MeOH which yielded 16 fractions. Subfraction 2.1.7 was further separated with a RP_{18}-solid phase extraction (SPE) cartridge, eluted stepwise with MeOH-H_2O (50-50), MeOH, acetone, and CH_2Cl_2 which yielded eight fractions. Subfraction 2.1.7.4 contained compound **2**, while compounds **4** and **5** were found in subfraction 2.1.7.5. Compound **2** (27-O-methylasporyzin C) was isolated via RP_{18}-HPLC (Nucleodur 100-S 250 mm x 4.6 mm) with MeOH-H_2O (82-18), 1.2 mL-min^{-1} as a white powder, t_R: 12 min (2.0 mg) . Subfraction 2.1.7.5 was further purified via RP_{18}-HPLC system C (Nucleodur 100-S 250 mm x 4.6 mm) with MeOH-H_2O (87.5-12.5), 1.3 mL-min^{-1}. Compound **4** (JBIR-03) was isolated as a yellowish white powder [t_R: 23 min] (30.0 mg) and compound **5** (emindole SB) as a white powder [t_R: 21 min] (7.2 mg).

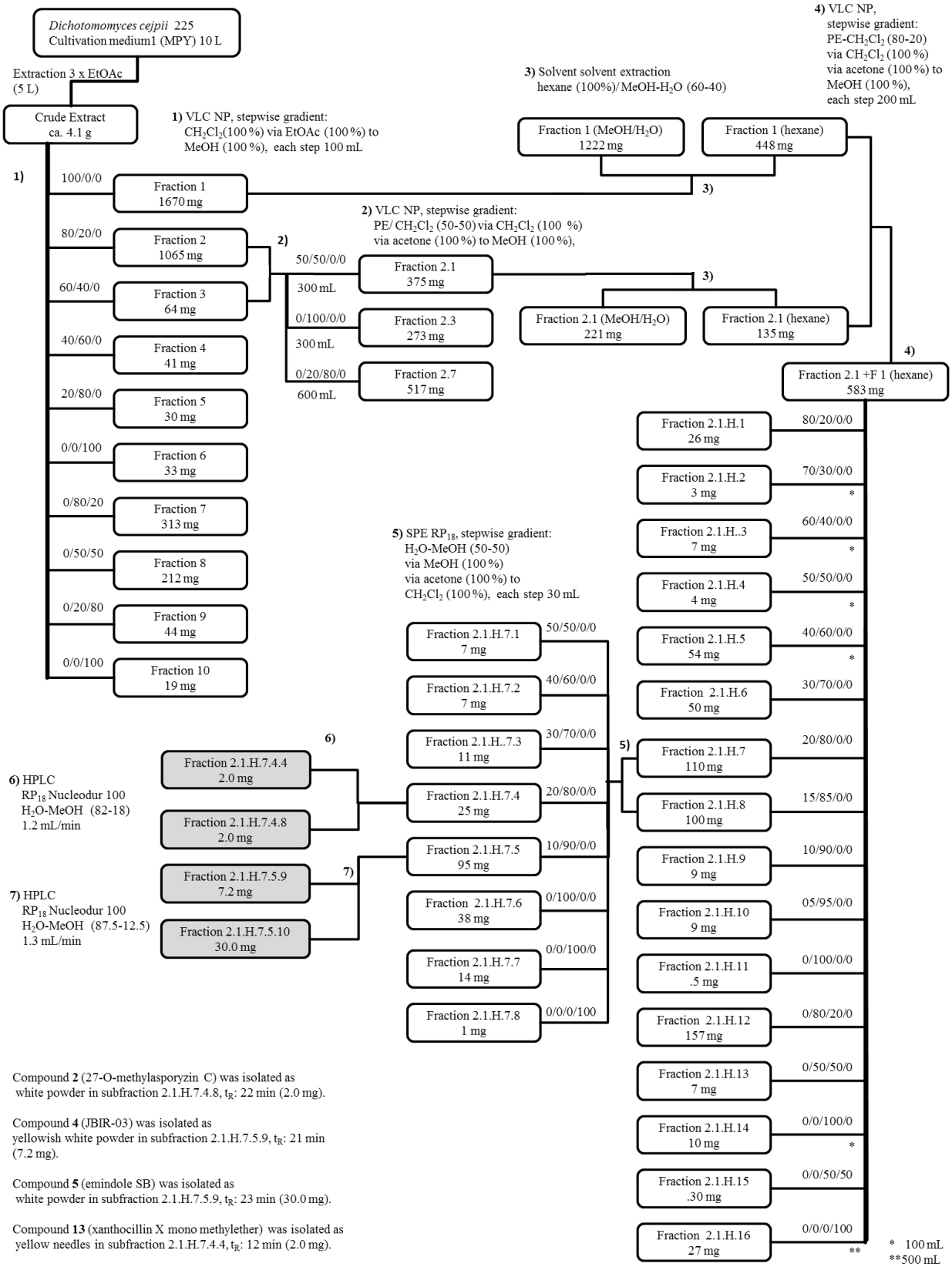

Compound **2** (27-O-methylasporyzin C) was isolated as white powder in subfraction 2.1.H.7.4.8, t_R: 22 min (2.0 mg).

Compound **4** (JBIR-03) was isolated as yellowish white powder in subfraction 2.1.H.7.5.9, t_R: 21 min (7.2 mg).

Compound **5** (emindole SB) was isolated as white powder in subfraction 2.1.H.7.5.9, t_R: 23 min (30.0 mg).

Compound **13** (xanthocillin X mono methylether) was isolated as yellow needles in subfraction 2.1.H.7.4.4, t_R: 12 min (2.0 mg).

Figure 4-2: Isolation scheme for compounds **2**, **4, 5** and **13**. For reasons of clarity only the most important fractions are listed.

VLC fraction 1 contained compounds **3** and was distributed between hexane (100%) and MeOH-H_2O (60-40) using a solvent/solvent extraction three times. The methanolic phase was further separated using a RP_{18} VLC column and eluted stepwise with H_2O-MeOH (80-20) to 100% MeOH, 100% CH_2CL_2 which yielded 8 fractions. Subfraction 1.4 was further separated with a second NP VLC column, eluted stepwise with petrolether-CH_2CL_2 (80-20), to 100% CH_2CL_2, 100% acetone, and to 100% MeOH which yielded 6 fractions. Compound **3** (emindole SB-formate) was isolated from subfraction 1.4.1 via RP_{18}-HPLC system C (Nucleodur 100-S 250 mm x 4.6 mm) with MeOH-H_2O (90-20), 1.7 mL-min^{-1} as a white powder, t_R: 46 min (1.0 mg).

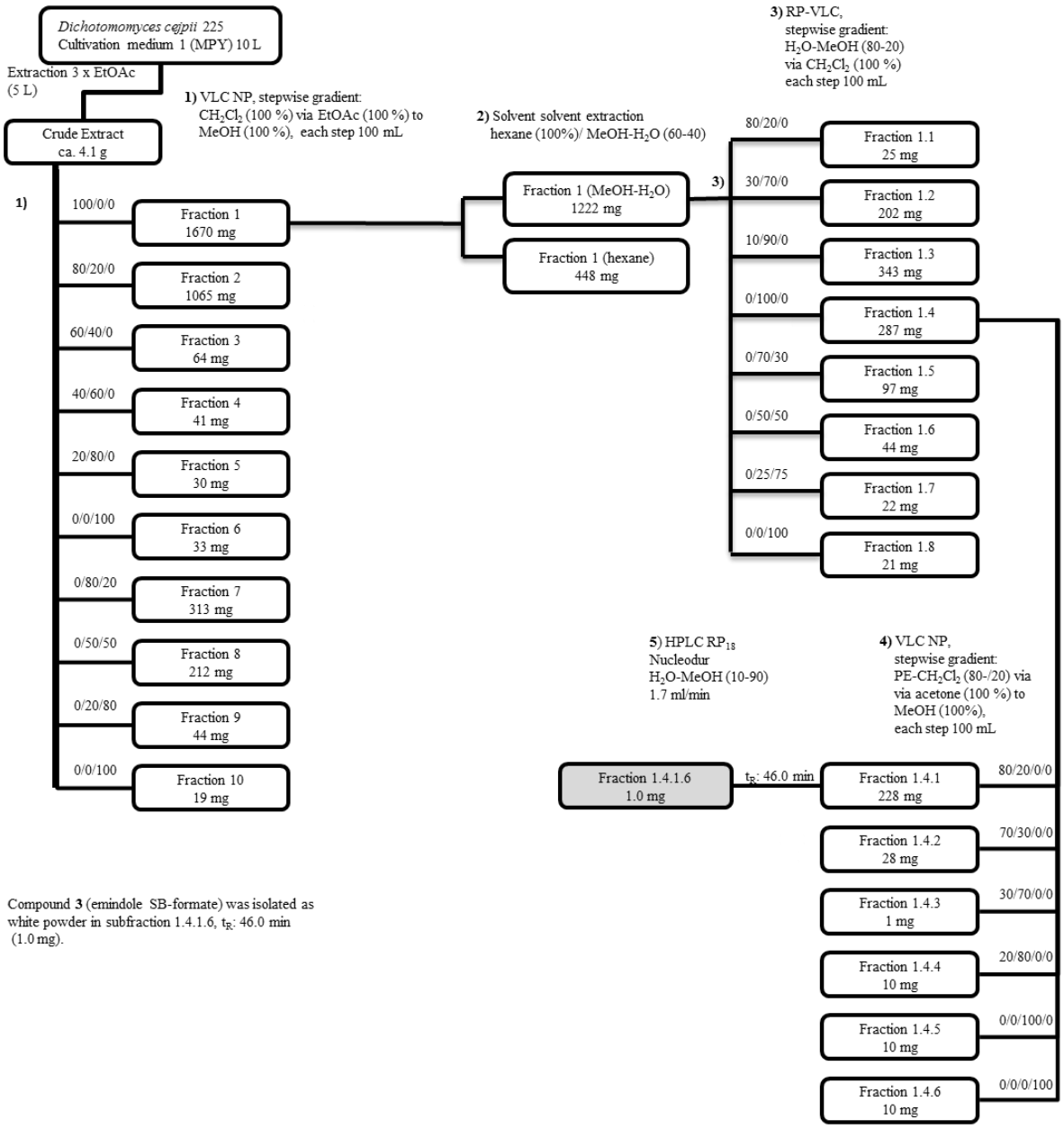

Figure **4-3**: Isolation scheme for compounds **3.** For reasons of clarity only the most important fractions are listed.

The investigated fungal strain was cultivated on cultivation medium 2 as described before (3.2.2–3.2.3)

Fungal biomass and media were homogenized using an Ultra-Turrax apparatus and extracted with 5 L EtOAc to yield 1.2 g of crude extract. This material was fractionated by normal-phase (NP) vacuum liquid chromatography (VLC) using a stepwise gradient solvent system of increasing polarity starting with 100% CH_2CL_2 to 100% EtOAc, to 100% MeOH and H_2O-MeOH (50-50) which yielded 11 fractions. Compound **6** was isolated from VLC fraction 8 and 9. The combined fractions were separated via reversed-phase C18 (RP_{18})-VLC, eluted stepwise with H_2O-MeOH (70-30), to 100% MeOH, and 100% CH_2CL_2, which yielded 8 fractions. Subfraction 8.6 contained both compounds. Subfraction 8.6.3 was further purified using RP_{18} Xterra^{TM} 250 x 4.6 mm) with H_2O-MeOH (60-40), 1.2 mL/min to obtain compound **6 (**asporyzin C) as a white powder, t_R: 10.0 min (1.0 mg).

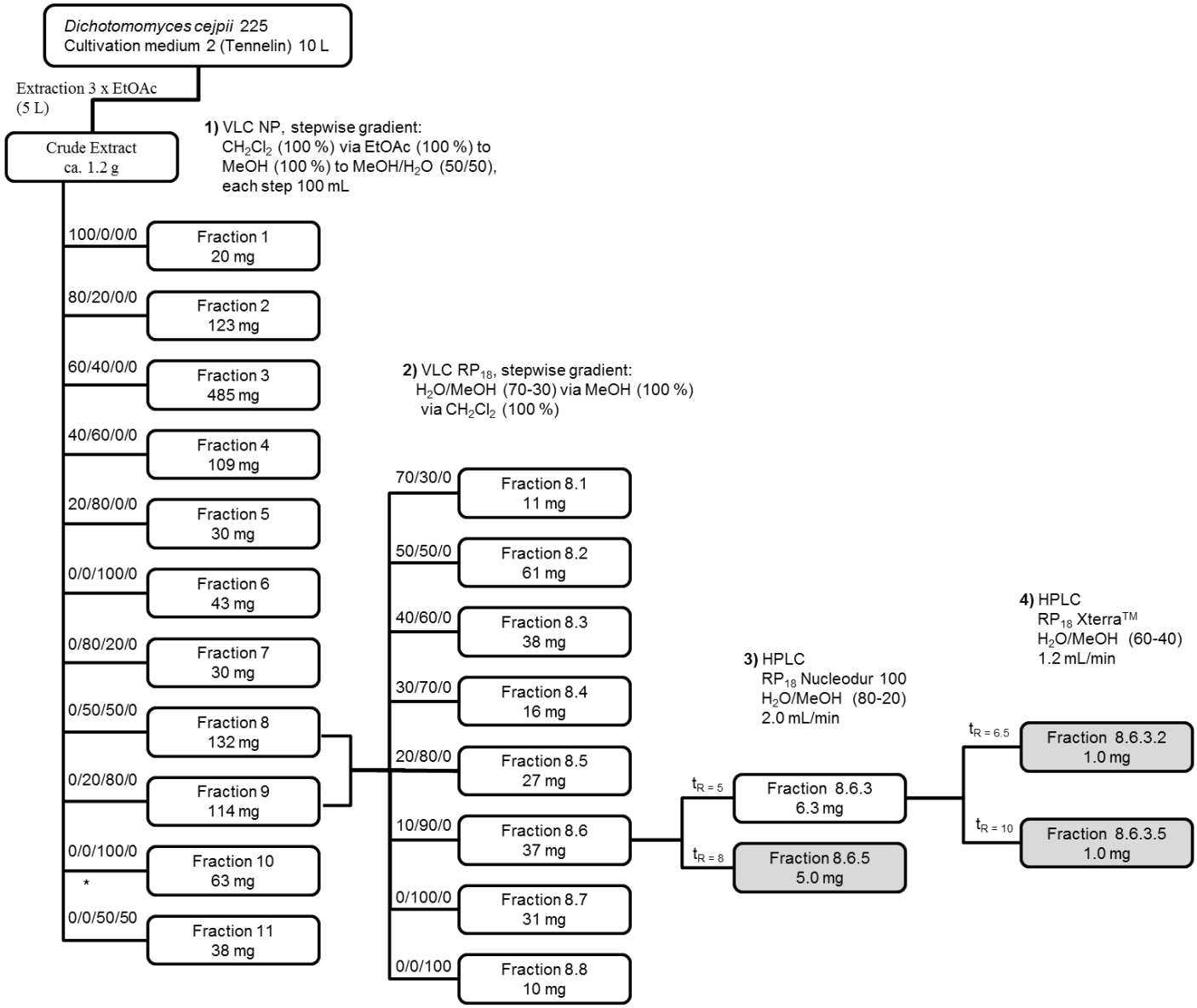

Figure 4-4: Isolation scheme for compound **6, 9** and **10.** For reasons of clarity only the most important fractions are listed.

4.2.3 Structure elucidation of isolated indoloditerpenes

The structure of the fungal metabolite **1** was deduced via analysis of spectroscopic data. The UV maximum at 281 nm indicated the presence of an aromatic moiety.[99] An IR absorption at 3347 cm^{-1} and 1651 cm^{-1} pointed toward several hydroxyl groups and a heterocyclic bound nitrogen, respectively. The molecular formula of compound **1** was deduced from the results of an accurate mass measurement (HRESIMS, *m/z* = 590.3440 $(M+Na)^+$ to be $C_{34}H_{49}NO_6$, and was supported by ^1H and ^{13}C NMR data (Table 4-1). The ^{13}C NMR and DEPT135 spectra denote the presence of 34 resonances for five methyl groups, eight sp^3 methylene groups, five sp^2 methine, eight sp^3 methine, and eight quaternary carbons in the molecule.

The four aromatic methine carbons CH-16 to CH-19 form one ^1H-^1H spin system and are all connected as evidenced by mutual cross peak correlations in both, the COSY and HMBC spectra. They are also bound to the quaternary aromatic carbons C-15 and C-20, as confirmed by HMBC correlations, *e.g.* from H-16 and H-18 to C-20, and from H-17 and H-19 to C-15. The ^{13}C NMR resonance frequencies of the quaternary carbon atoms C-2 and C-14 are characteristic for an indole ring system,[100–102] which is additionally evident from HMBC correlations between H-16 and C-14 and the UV maximum of **1**. A second spin system was deciphered from COSY correlations from H_2-24 through to H_3-28 and H_3-29 and revealed a 4-methylpent-3-ene, *i.e.* part of a terpene moiety. Two further substructures were also deduced from COSY correlations, *i.e.* mutual ^1H couplings from H-7 to H_2-6 and H_2-5 on one side, and from H-9 to H_2-10, H_2-11, H-12 and H_2-13 on the other side. HMBC correlations arising from the resonances of the three methyl groups CH_3-21, CH_3-22 and CH_3-23 allowed to connect and extend these substructures, revealing the three central rings of **1,** apart of the indole. The latter was mainly accomplished by taking into account HMBC correlations between the resonances for the methyl group CH_3-21 and C-2, C-3, C-4 and C-12, and between the methyl group resonance CH_3-22 and C-3, C-4, C-5, and C-9 as well as between the methyl group CH_3-23 and C-7, C-8, C-9 and C-24. Additionally, further diagnostic heteronuclear couplings, *e.g.* between H_2-10 and C-8 and between H_2-13 and C-14 clearly allowed to deduce the complete structure of the aglycone part of the molecule. The relative configuration of the aglycone was assigned on the basis of a NOESY experiment (Table 4-1). NOESY correlations between H-12, H_3-22 and H_3-23 indicated that these protons are located on the same side of the molecule, whereas NOESY correlations between H-7, H-9 and H_3-21 proved the opposite orientation of these substituents. Further proof for the trans-anellated ring system came from

NOESY correlations between H-12/H-13a and between H-21/H-13b. Comparison with literature ^{1}H and ^{13}C NMR data of related compounds like emindole SB[100] and JBIR-03[101] confirmed the structure of the aglycone of **1**. The absolute configuration of the indoloditerpene scaffold was assumed to be identical to that of the co-occurring compound emindole SB for which the absolute configuration had been determined.[101,103] Additional ^{1}H and ^{13}C NMR resonance frequencies pointed toward a sugar moiety in the molecule. Thus, the methine groups CH-7, CH-1', CH-2', CH-3', CH-4', CH-5 and the methylene group CH_2-6' resonate in the range of δ_H 3.2 to 4.6 and δ_C 63 to 104, respectively. The COSY spectrum showed correlations for a spin system from H-1' through to H_2-6' and established a pyranose moiety. Analysis of the coupling constants and NOEs revealed a mannopyranose.[104] The anomeric configuration of the mannose was considered as β because of the magnitude of the heteronuclear coupling constant between the anomeric carbon and the respective proton ($^{1}J_{CH}$ = 155 Hz).[105] Hydrolysis and HPLC-ELSD analysis using a chiral-phase column revealed the sugar to have the D-configuration (Figure 4-6–4.9). The mannose is attached via the CH-7 methine group to the indoloditerpene nucleus, due to a heteronulear long range coupling from H-1' to C-7. The absolute configuration of the indoloditerpene scaffold of **1** is considered to be to the same as that of the co-occurring compound emindole SB for which the absolute configuration had been determined recently.[11,13] The fungal metabolite **1** is thus an indoloditerpene, substituted with a dimethylallyl containing side chain and a mannose moiety, for which we suggest the trivial name emindole SB beta-mannoside .

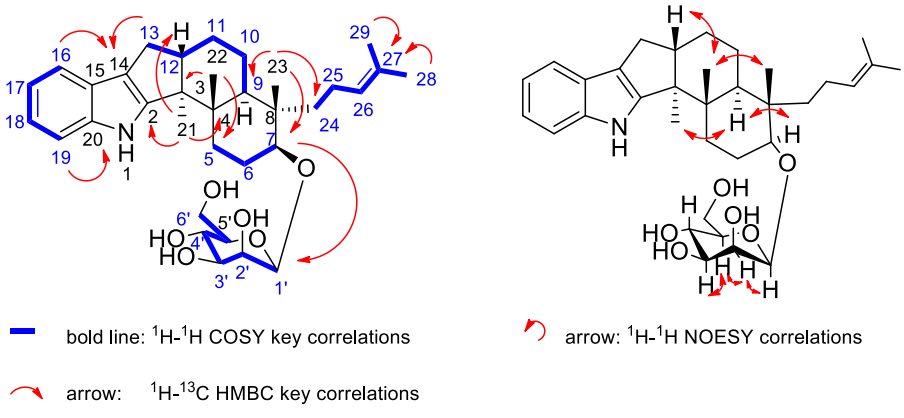

Figure **4-5**: NMR key correlations of compound **1**

Carbohydrate analysis of compound 1

Measurement conducted as described in 3.6.6

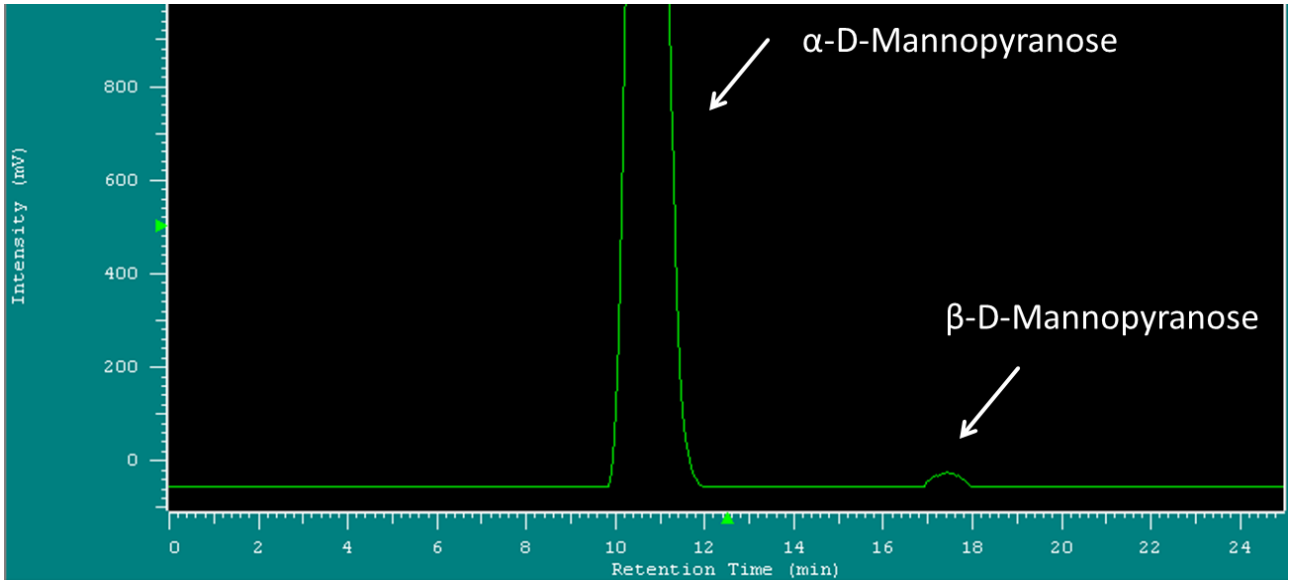

Figure **4-6**: HPLC chromatogram of D-Mannose

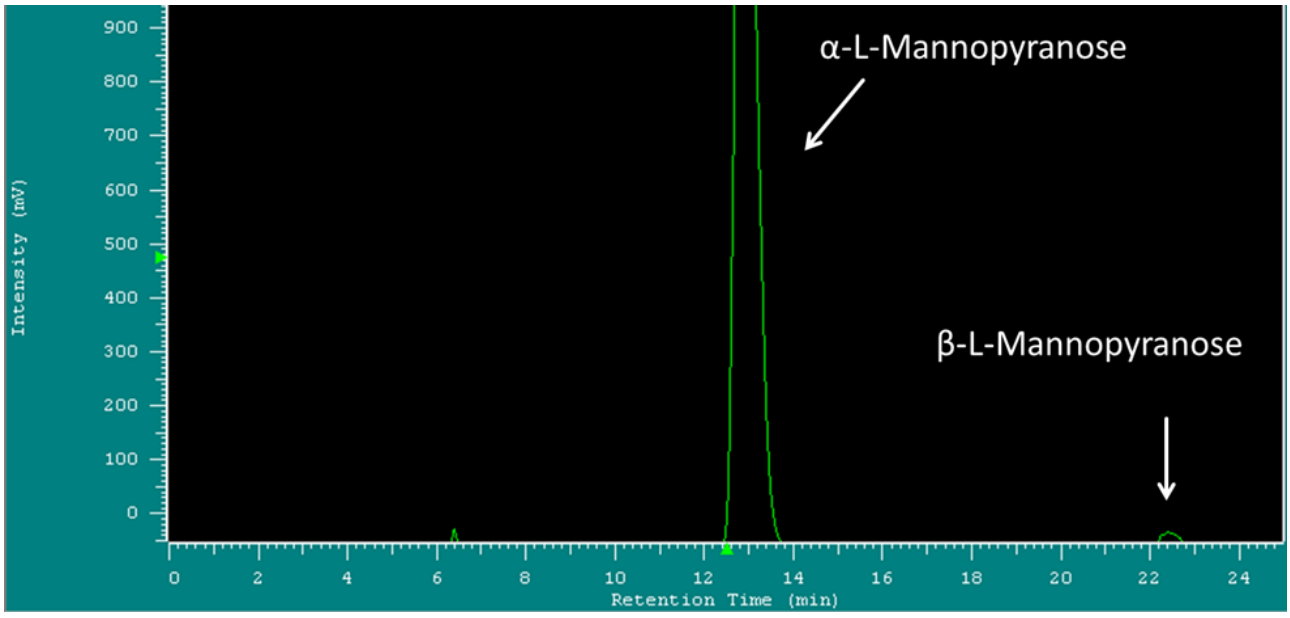

Figure **4-7**: HPLC chromatogram of L-Mannose

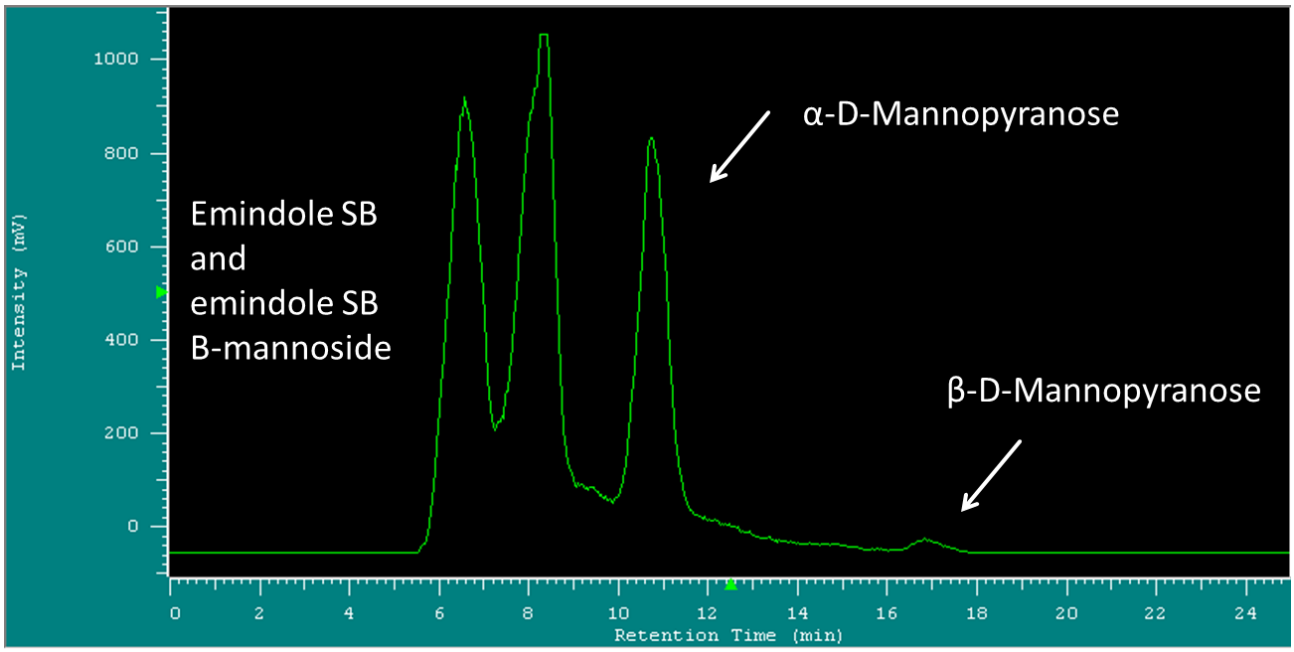

Figure **4-8**: HPLC chromatogram of hydrolysis mixture

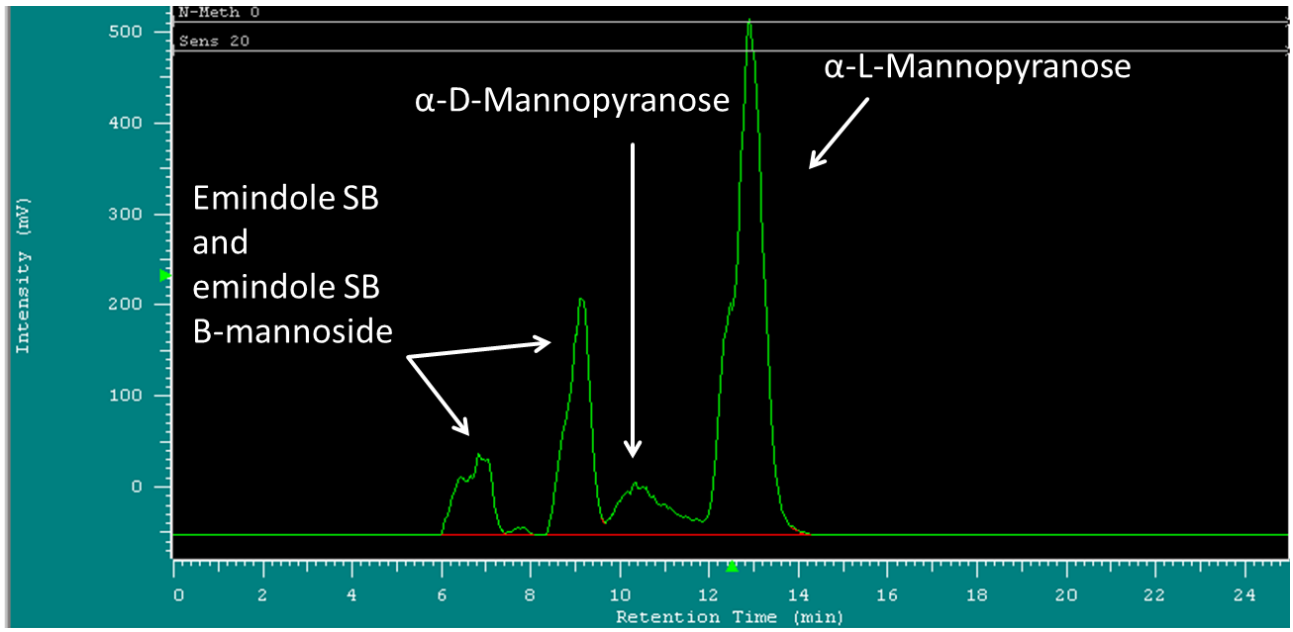

Figure **4-9**: HPLC chromatogram of hydrolysis mixture + L-Mannose

The structure of the fungal metabolite **2** was found to be closely related to that of **1**. The molecular formula of **2** was deduced as $C_{29}H_{41}NO_2Na$ from the results of an accurate mass measurement (HRESIMS, *m/z* = 458.3043 $[(M+Na)]^+$).

The structure of compound **2** differs from that of compound **1** solely by the missing sugar moiety at C-7 and some structural changes in the terpene side chain. The ^{13}C NMR resonance frequency at δ_C 72.9 for the methine group CH-7 was shifted upfield by 11 ppm as compared

to **1** and thus, verified the presence of an unsubstituted hydroxyl group at that position.[100] The structure of the terpenoid chain was elucidated by COSY correlations from H_2-24 through to H-26 and HMBC correlations between the methyl groups CH_3-28 and CH_3-29 and CH-26. The configuration of the double bound between CH-25 and CH-26 was determined as *E*, based on a coupling constant of $J_{H\text{-}25/H\text{-}26}$ = 15.7 Hz. Since C-27 was quaternary in **2** and resonated at δ_C 75.2, the methoxy group in the molecule, which was evident from ^1H and ^{13}C NMR resonance frequencies at δ_H 3.12 and δ_C 50.3, was clearly located at C-27. Furthermore, the NMR chemical shifts of the terpenoid moiety were identical with those of the 4 methoxy-4-methylpent-2-enyl unit in momordicosides K.[106] The configuration of **2** was assigned in the same manner as described for **1**. For the fungal metabolite **2** we suggest the name 27-O-methylasporyzin C.

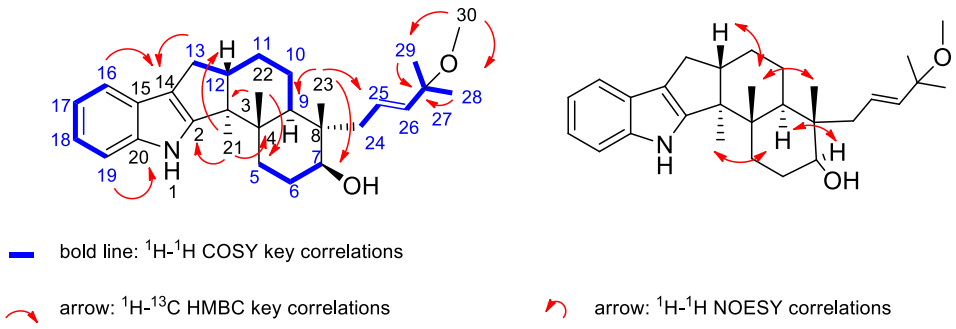

Figure **4-10**: NMR key correlations of compound **2**

The structure of the fungal metabolite **3** was found to be closely related to that of **1**. The molecular formula of **3** was deduced as $C_{29}H_{39}NO_2$ from the results of an accurate mass measurement (HRESIMS, *m/z* = 433.29840). The structure of compound **3** differs from that of compound **1** solely by the missing sugar moiety at C-7 which was replaced by a carbonyl substituent. The ^{13}C NMR resonance frequency at δ_C 76.8 for the methine group CH-7 was shifted upfield by 7 ppm as compared to **1** and verfied a different substitution pattern**.** The ^{13}C NMR resonance frequency at δ_C 162.8 and the typical ^1H NMR resonance frequency at δ_H 8.15, indicated the presence of an aldehyde moiety which could be linkend to C-7, due to HMBC correlations between the resonances for the methin group CH-7 and carbon atom C-30. Furthermore, the NMR chemical shifts of the aldehyde moiety and methin CH-7 were almost identical with those of the corresponding aldehyde unit in the fungal compound

colletotrichin B.[107] The configuration of **3** was assigned in the same manner as described for **1**. For the fungal metabolite **3** we suggest the name emindole SB-formate.

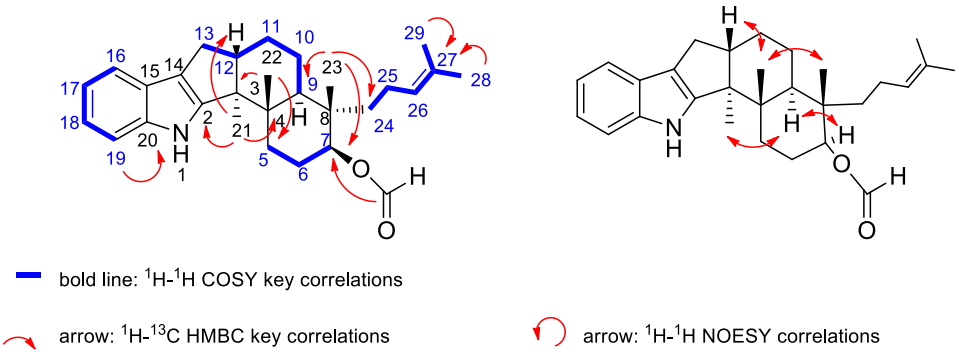

Figure **4-11**: NMR key correlations of compound **3**

Comparison of data from NMR and mass spectroscopy with literature data, lead to the identification of compounds **4**–**6.** The fungal metabolites **3**–**6** were identified as the indoloditerpene JBIR-03, emindole SB and asporyzin C, respectively.[100,101,103,108]

It is remarkable that the optic rotation values of JBIR-03 could not be reliably measured in methanol, due to the low solubility of JBIR-03 in the solvent. Repeated measurement of JBIR-03 in CH_3CN, showed negative optic rotation values, similar to other indoloditerpenes.

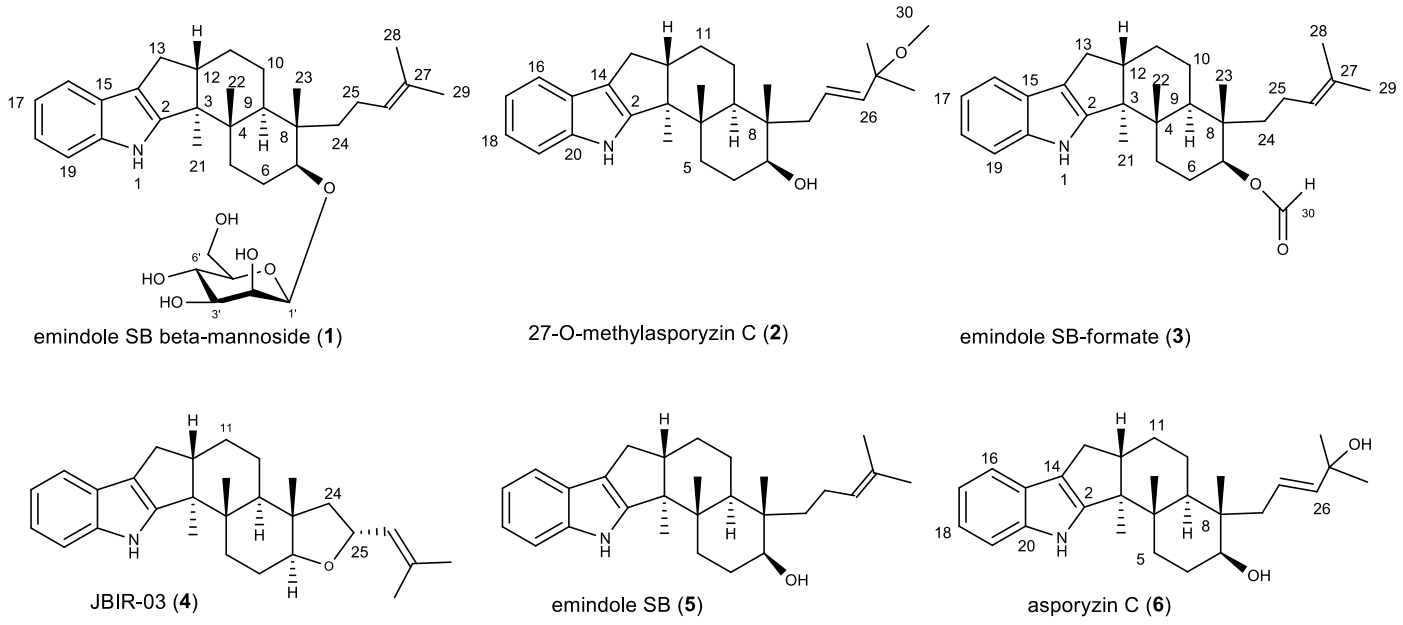

Figure **4-12**: Structures of isolated indoloditerpenes.

Table **4-4**: NMR spectroscopic data (300 MHz, acetone-d_6) for emindole SB beta-mannoside (**1**)

position	δ_C , mult.	δ_H (*J* in Hz)	^1H -^1H COSY	^1H-^{13}C HMBC	^1H-^1H NOESY
1	NH	9.80, brs	-	-	-
2	152.0, C	-	-	-	-
3	53.8, C	-	-	-	-
4	39.7, C	-	-	-	-
5	33.3, CH_2	1.81, m	6a,6b	9,22	-
6	26.8, CH_2	6a: 2.10, m	5,6b,7	7,8	-
		6b: 1.86, m	5,6a,7	7,8	-
7	83.9, CH	3.62, m	6a,6b	1’	9
8	42.0, C	-	-	-	-
9	40.7, CH	1.81, m	10a,10b	4,7,8	7,21
10	23.3, CH_2	10a: 1.63, m	9,10b,11a,11b	-	-
		10b: 1.45, m	9,10a,11a,11b	-	-
11	25.9, CH_2	11a: 1.75, m	10a,10b,11b,12	-	-
		11b: 1.65, m	10a,10b,11a,12	-	-
12	49.7, CH	2.75, m	11a,11b,13a,13b	-	13a,22
13	28.0, CH_2	13a: 2.62, dd (6.2, 13.2)	12,13b	2,3,12,14	12,13b
		13b: 2.29, dd (10.6, 13.2)	12,13a	2,12,14	13a,21
14	117.7, C	-	-	-	-
15	126.0, C	-	-	-	-
16	118.6, CH	7.31, dd (1.8, 7.6)	17	14,18,20	17
17	119.6, CH	6.92, td (7.6, 1.8)	16,18	15,16,19	16
18	120.5, CH	6.96, td (7.6, 1.8)	17,19	16,19,20	19
19	112.5, CH	7.28, dd (1.8, 7.6)	18	15,17,20	18
20	141.5, C	-	-	-	-
21	15.0, CH_3	1.03, s	-	2, 3, 4, 12	9,13b
22	19.4, CH_3	1.11, s	-	3,4,5,9	12,23
23	17.9, CH_3	0.83, s	-	7,8,9,24	22
24	38.2, CH_2	24a: 1.50, m	24b,25a,25b	-	-
		24b: 1.27, m	24a,25a,25b	-	-
25	22.2, CH_2	25a: 2.03, m	24a,24b,25b,26	26,27	-
		25b: 1.93, m	24a,24b,25a,26	26,27	-
26	125.8, CH	5.13, t (7.0)	25a,25b,28,29	28,29	28
27	131.1, C	-	-	-	-
28	25.9, CH_3	1.66, s	26 29	26,27,29	26
29	17.8, CH_3	1.64, s	26,28	26,27,28	-

1´	103.5, CH	4.63, s	2’	7,2´,5’	2´,3´,4’,5’
2´	72.2, CH	3.89, brd (3.3)	1´,3´	3’,4’	1’,3’
3´	75.5, CH	3.42, brdd, (3.3, 9.2)	2´,4´	4’	1’,2’
4´	69.2, CH	3.64, m	3´,5´	3’,5’	1’
5´	77.6, CH	3.25, ddd (3.3, 5.9, 9.2)	4´,6´	3’	1´,3´
6´	63.2, CH_2	6´a: 3.82, dd (3.3, 12.1)	5´,6´b	-	6’b
		6´b: 3.69, dd (5.9, 12.1)	5´,6´a	5’	6’a

Table **4-5**: NMR spectroscopic data (300 MHz, acetone-d_6) for 27-O-methylasporyzin C (**2**)

Position	δ_C , mult.	δ_H (*J* in Hz)	^{1}H-^{1}H COSY	^{1}H-^{13}C HMBC	^{1}H-^{1}H NOESY
1	NH	9.77, brs	-	-	-
2	151.9, C	-	-	-	-
3	53.7, C	-	-	-	-
4	39.9, C	-	-	-	-
5	33.3, CH_2	1.80, m	6a,6b	9	-
6	28.3, CH_2	6a: 1.80, m	5,6b,7	7,8	-
		6b: 1.68, m	5,6a,7	7,8	
7	72.9, CH	3.52, m	6a, 6b	-	9
8	43.1, C	-	-	-	-
9	41.1, CH	1.69, m	10a,10b	4	7,25
10	23.2, CH_2	10a: 1.75, m	9,10b,11b	-	-
		10b: 1.46, m	9,10a,11b	-	-
11	25.9, CH_2	11a: 1.74, m	11b,12	-	-
		11b: 1.59, m	10a,10b,11a,12	-	-
12	49.7, CH	2.75, m	11a,11b,13a,13b,	-	13a,22
13	27.9, CH_2	13a: 2.61, dd (6.2, 13.2)	12,13b	2,3,12,14,	13b,12
		13b: 2.28, dd (10.6, 13.2)	12,13a	2,12,14	13a
14	117.7, C	-	-	-	-
15	125.9, C	-	-	-	-
16	118.6, CH	7.30, dd, (1.8, 7.7)	17	14,18,20	17
17	119.5, CH	6.90, td, (1.8, 7.7)	16,18	15,16,19	16
18	120.5, CH	6.95, td, (1.8, 7.7)	17,19	16,19,20	19
19	112.5, CH	7.28, dd (1.8, 7.7)	18	15,17,20	18
20	141.5, C	-	-	-	-
21	14.8, CH_3	0.98, s	-	2,3,4,12	5,9,13b
22	19.1, CH_3	1.10, s	-	3,4,5,9	5,12,23
23	16.8, CH_3	0.84, s	-	7,8,9,25	22,24a
24	40.6, CH_2	24a: 2.45, dd (6.2, 13.9)	24b,25	8,25,26	24b,23
		24b: 1.95, dd (8.8, 13.9)	24a,25	8,25,26	24a
25	126.6, CH	5.66, ddd (6.2, 8.8, 15.7)	24a,24b,26	24,26,27	28,29,30
26	139.2, CH	5.50, d (15.7)	25	24,25,27,28	28,29,30
27	75.2, C	-	-	-	-
28	26.9, CH_3	1.22, s	-	26,27,29	25,26,30
29	26.3, CH_3	1.22, s	-	26,27,28	25,26,30
30	50.3, CH_3	3.12, s	-	27	25,28,29

Table **4-6**: NMR spectroscopic data (300 MHz, acetone-d_6) for emindole SB-formate (**3**)

position	δ_C , mult.	δ_H (*J* in Hz)	^1H -^1H COSY	^1H-^{13}C HMBC	^1H-^1H NOESY
1	NH	9.82, brs	-	-	-
2	151.9, C	-	-	-	-
3	54.3, C	-	-	-	-
4	40.3, C	-	-	-	-
5	33.1, CH_2	1.90, br m	6	9	-
6	22.4, CH_2	1.92, br m	5, 7	-	-
7	76.8, CH	4.99, br m	6	-	9
8	41.4, C	-	-	-	-
9	41.3, CH	1.86, m	10a,10b	10	7,21
10	23.6, CH_2	10a: 1.60, m	9,10b,11a,11b	-	-
		10b: 1.50, m	9,10a,11a,11b	-	-
11	25.2, CH_2	11a: 1.86, m	10a,10b,11b	-	-
		11b: 1.67, m	10a,10b,11a,12	-	-
12	50.2, CH	2.76, m	11b,13a,13b	-	11a,22
13	28.3, CH_2	13a: 2.62, dd (6.2, 13.2)	12,13b	2,3,12,14,16,	12,13b
		13b: 2.29, dd (7.7, 13.2)	12,13a	2,12,14,	13a,22
14	118.0, C	-	-	-	-
15	126.2, C	-	-	-	-
16	118.7, CH	7.28, dd (6.6)	17	17, 18	17,18
17	119.7, CH	6.91, td (6.6)	16,18	16,19	16,19
18	120.8, CH	6.94, td (6.6)	17,19	16,19	16,19
19	112.6, CH	7.26, dd (6.6)	18	15,17,20	17,18
20	142.1, C	-	-	-	-
21	14.9, CH_3	1.03, s	-	2, 3, 4, 12	9,13b
22	19.4, CH_3	1.14, s	-	3,5,8,9,23	12,23
23	18.2, CH_3	0.93, s	-	7,8,9,22,24	22
24	38.6, CH_2	1.22, m	25	-	-
25	22.2, CH_2	1.93, m	24,26	-	-
26	125.5, CH	5.05, m	25,28,29	-	-
27	132.2, C	-	-	-	-
28	26.0, CH_3	1.67, s	26, 29	26,27,29	26
29	17.7, CH_3	1.60, s	26, 28	26,27,28	-
30	162.8, C	8.15, s	-	7	-

Table **4-7**: NMR spectroscopic data (300 MHz) for compounds **4**–**6**

	JBIR-03 (**4**) (methanol-d_4)		**emindole SB** (**5**) (acetone-d_6)		**asporyzin C** (**6**) (acetone-*d6*)	
Pos.	δ_C , mult.	δ_H (*J* in Hz)	δ_C, mult.	δ_H (*J* in Hz)	δC, mult.	δH (J in Hz)
1	-	9.78 brs	-	9.76, brs	NH	-
2	152.0, C	-	152.0, C	-	150.7, C	-
3	54.1, C	-	53.9, C	-	52.6, C	-
4	41.5, C	-	40.0, C	-	39.4, C	-
5	34.5, CH_2	1.95, m	33.4, CH_2	1.81, m	33.9, CH_2	1.80, m
6	23.6, CH_2	10a: 1.90, m	28.4, CH_2	1.81, m	28.4, CH_2	6a: 1.85, m
		10b: 1.70, m		1.71, m		6b: 1.78, m
7	87.5, CH	3.31, m	72.9, CH	3.53, m	72.3, CH	3.55, m
8	46.2, C	-	42.0, C	-	42.0, C	-
9	47.8, CH	1.79, m	40.6, CH	1.79, m	40.0, CH	1.65, m
10	26.5, CH_2	1.58, m	23.5, CH_2	10a: 1.66, m	22.2, CH_2	10a: 1.76, m
				10b: 1.46, m		10b: 1.49, m
11	26.4, CH_2	11a: 1.70, m	26.0, CH_2	11a: 1.74, m	24.8, CH_2	11a: 1.75, m
		11b: 1.57, m		11b: 1.66, m		11b: 1.50, m
12	50.3, CH	2.80, m	49.8, CH	2.76, m	48.8, CH	2.80, m
13	28.4, CH_2	13a: 2.66, dd (6.6, 13.2)	28.0, CH_2	13a: 2.62, dd (6.6, 13.2)	27.6, CH_2	13a: 2.65, dd (6.3, 13.2)
		13b: 2.33, dd (10.6, 13.2)		13b: 2.30, dd (10.6, 13.2)		13b: 2.31, m
14	117.9, C	-	117.7, C	-	116.7, C	-
15	126.3, C	-	125.4, C	-	126.3, C	-
16	118.7, CH	7.33, m	118.6, CH	7.31, dd (1.8, 7.6)	117.2, CH	7.32, m
17	119.7, CH	6.97, brtd (7.6, 1.8)	119.5, CH	6.92, td (7.6, 1.8)	119.1, CH	6.95, m
18	120.7, CH	6.99, brtd (7.6, 1.8)	120.5, CH	6.95, td (7.6, 1.8)	121.9, CH	6.98, m
19	112.6, CH	7.33, m	112.5, CH	7.28, dd (1.8, 7.6)	111.1, CH	7.30, m
20	142.1, C	-	141.6, C	-	141.0, C	-
21	15.0, CH_3	1.07, s	15.0, CH_3	1.03, s	13.5, CH_3	0.94, s
22	21.0, CH_3	1.14, s	19.4, CH_3	1.11, s	17.8, CH_3	1.16, s
23	15.4, CH_3	0.94, s	17.3, CH_3	0.83,s	15.3, CH_3	0.88, s
24	49.5, CH_2	24a: 2.01, m	38.2, CH_2	24a: 1.68, m	38.9, CH_2	24a: 2.36, m
		24a: 1.29, m		24b: 1.21, m		24b: 2.00, m
25	75.3, CH	4.89, m	22.1, CH_2	25a: 2.00, m	121.8, CH	5.75, m
				25b: 1.91, m		
26	127.9, CH	5.38, brd (8.8)	126.1, CH	5.11, brt (6.7)	138.5, CH	5.40, m
27	135.6, C	-	131.0, C	-	73.0, C	-
28	26.0, CH_3	1.78, s	25.9, CH_3	1.66, s	28.5, CH_3	1.31, s
29	18.0, CH_3	1.74, s	17.7, CH_3	1.61, s	28.8, CH_3	1.36, s

*extracted from HMBC meassurement

4.2.4 Semisynthetic preparation of compound 7

Compound **7** was prepared as described in 3.5.1 to yield 3.5 mg.
Proposed structure of the semisynthetical product was confirmed by NMR and MS measurements (Table 4-8). The structure of the fungal metabolite **7** was found to be closely related to that of **1**. The molecular formula of **7** was deduced as $C_{32}H_{46}N_2O_2$ from the results of an accurate mass measurement (HRESI-MS *m/z* 513.3442 $[(M+Na)]^+$). We suggest the trivial name emindole SB-N-propylcarbamate for compound **7.**

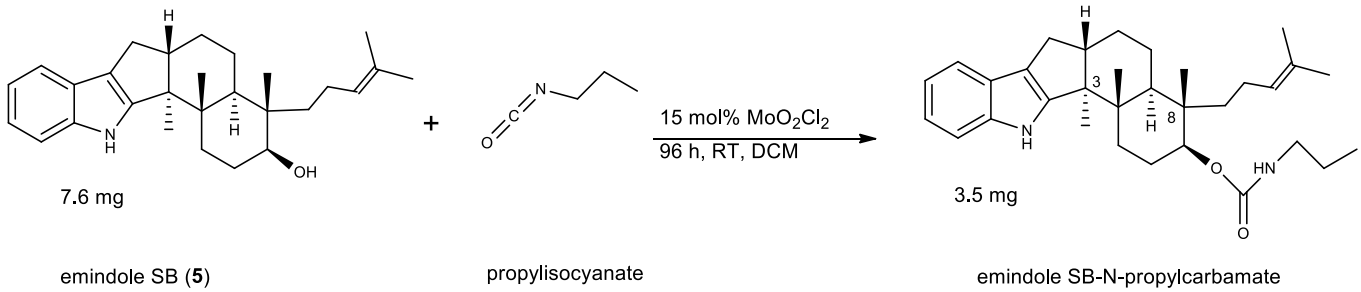

Figure **4-13**: Carbamoylation of emindole SB with propylisocyanate

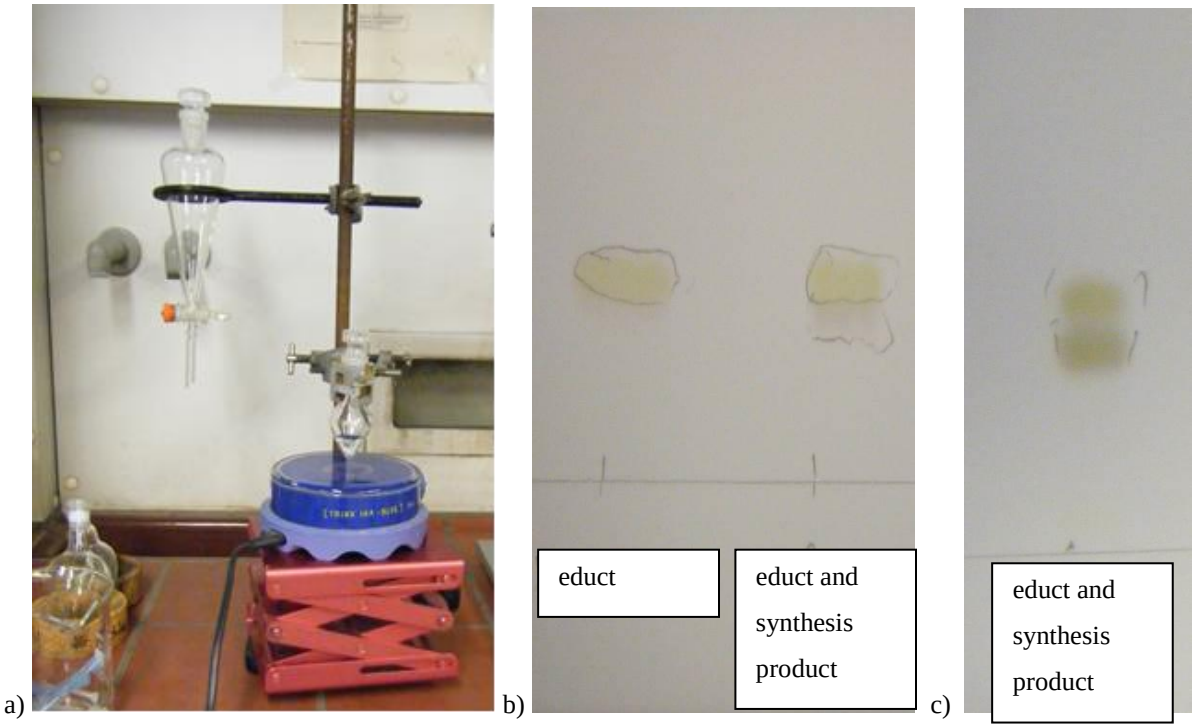

Figure **4-14**: a) Experimental setup; RP_{18} TLC, MeOH-H_2O (90-10) of b) synthesis product and educt, detected with vanillin-H_2SO_4-reagent after 24h; c) synthesis product, detected with vanillin-H_2SO_4-reagent after 96h.

Table **4-8**: NMR spectroscopic data (300 MHz, acetone-d_6) for emindole SB-N-propylcarbamate (**7**)

Position	δ_C , mult.	δ_H (*J* in Hz)	^1H -^1H COSY	^1H-^{13}C HMBC
1	NH	6.2	-	-
2	151.9, C	-	-	-
3	53.9, C	-	-	-
4	39.7, C	-		-
5	33.1, CH_2	1.85	6a,6b,7	6,7,9
6	25.9, CH_2	6a 1.86	5,6b,7	-
		6b 1.70	5,6a,7	4,5,7,8
7	75.6, CH	4.69, dd (4.4, 9.9)	5,6a,6b	-
8	41.0, C	-	-	-
9	41.3, CH	1.81, br m	10a,10b,11a,11b	6,8
10	23.3, CH_2	10a 1.65, m	9, 11a,11b	-
		10b 1.47, m	9, 10a,11a,11b	
11	25.2, CH_2	11a 1.75, m	9,10a,10b,11b	3
		11b 1.64, m	9,10a,10b,11a, 12	
12	49.8, CH	2.76, m	11b,13a,13b	-
13	27.9, CH_2	13a 2.63, dd (6.6, 13.2)	13b,12	2, 3, 12, 14
		13b 2.31 (10.6, 13.2)	13a,12	2, 12, 14
14	117.8, C	-	-	-
15	125.9, C	-	-	-
16	118.7, CH	7.31, dd (1.1, 3.7, 7.3)	17,18	15, 17, 18
17	120.6, CH	6.93, dd (1.8, 7.3, 12.8)	16,19	15, 19, 20
18	119.6, CH	6.96, dd (1.8, 7.3, 12.8)	17,19	15, 19, 20
19	112.5, CH	7.28, dd (1.1, 3.7)	17,18	15, 17, 18
20	141.7, C	-	-	-
21	15.0, CH_3	1.06 (s)	-	2,3, 4,12
22	19.4, CH_3	1.13 (s)	-	3 ,4, 5
23	18.0, CH_3	0.85 (s)	-	7,4, 8, 9,24
24	38.5, CH_2	1.25, dd (8.4, 16.1)	25a,25b	-
25	22.1, CH_2	25a 2.06, m	24,26	-
		25b 1.84 m		
26	125.6, CH	5.06, t (7.3)	25a,25b,28,29	-
27	131.4 , C	-	-	-
28	25.9, CH_3	1.64, s	26	26,27,29
29	17.6, CH_3	1,58, s	26	26,27,28
30	157.0, C	-	-	-
31	NH	6.2, s	-	-
32	43.2, CH_2	3.08, m (6.6, 13.2, 19.4)	31,33	30
33	23.9, CH_2	1.50, dd (7.3,14.6)	32,34	32,34
34	11.5, CH_3	0.89	32,33	32,33

Emindole SB beta-mannoside (**1**): white amorphous compound (6.5 mg; 0.65 mg L^{-1}). $[\alpha]_D^{25}$ + 33.1 (c 0.36, MeOH); UV (MeOH) λ_{max} (log ε) 229 (4.27), 281 (3.67) nm; IR (ATR) ν_{max} 3347, 2924, 1651, 1454, 1375, 1303, 1254, 1072, 1025, 740 cm^{-1}; ^{1}H and ^{13}C NMR data (Table 4-4); ESI-MS *m/z* 568 $[M+H]^+$, 586 $[M+NH_4]^+$; HRESI-MS *m/z* 590.3440 $[M+Na]^+$ (calcd for $C_{34}H_{49}NO_6Na$, *m/z* 590.3452).

27-O-methylasporyzin C (**2**): white amorphous compound (2.0 mg; 0.2 mg L^{-1}); $[\alpha]_D^{25}$ - 27.6 (c 0.17, MeOH); UV (MeOH) λ_{max} (log ε) 229 (5.31), 280 (4.76) nm; IR (ATR) ν_{max} 3361, 2924, 1642, 1585, 1376, 1202, 1072, 1376, 1202, 668, 631 cm^{-1}; ^{1}H and ^{13}C NMR data (Table 4-5); ESI-MS *m/z* 436 $[M+H]^+$; HRESI-MS *m/z* 458.3043 $[M+Na]^+$ (calcd for $C_{29}H_{41}NO_2Na$, *m/z* 458.3030).

Emindole SB beta-formate (**3**): white amorphous compound (1.0 mg; 0.1 mg L^{-1}). $[\alpha]_D^{25}$ - 5.7 (c 0.23, MeOH); UV (MeOH) λ_{max} (log ε) 228 (3.56), 280 (3.06) nm; IR (ATR) ν_{max} 3385, 2924, 2850, 1720, 1512, 1248, 1180, 1032, 668, 630cm^{-1}; ^{1}H and ^{13}C NMR data (see Table 4-6); ESI-MS *m/z* 434 $[M+H]^+$, 432 $[M-H]^-$, HRESI-MS *m/z* 433.2984 $[M+Na]^+$ (calcd for $C_{29}H_{39}N_2O_2$, *m/z* 433.2981).

JBIR-03 (**4**): white amorphous compound (30.0 mg, 3.0 mg L^{-1}); $[\alpha]_D^{25}$ - 18.1 (c 1.10, CH_3CN) [lit: $[\alpha]_D^{24.5}$ +46.2 (*c* 0.05, MeOH)[101]]; ^{1}H and ^{13}C NMR data (Table 4-7); ESI-MS *m/z* 404 $[M+H]^+$.

Emindole SB (**5**): white amorphous compound (7.2 mg, 0.72 mg L^{-1}); $[\alpha]_D^{25}$ - 24.2 (c 0.12, acetone), [lit: $[\alpha]_D^{25}$ -19 (c 0.2, $CHCl_3$)[103]]; ^{1}H and ^{13}C NMR data (Table 4-7); ESI-MS *m/z* 406 $[M+H]^+$.

Asporyzin C (**6):** white amorphous compound (1.0 mg; 0.1 mg L^{-1}); ^{1}H and ^{13}C NMR data (Table 4-7); ESI-MS *m/z* 422 $[M+H]^+$; 480 $[M+HAc-H]^-$.

Emindole SB-N-propylcarbamate (7): white amorphous compound (3.5 mg); $[\alpha]_D^{25}$ + 6.1 (c 0.14, CH_3CN); UV (MeOH) λ_{max} (log ε) 228 (3.95), 280 (3.32) nm; IR (ATR) ν_{max} 3385, 2924, 2850, 1720, 1512, 1248, 1180, 1032, 668, 630cm^{-1}; ^{1}H and ^{13}C NMR data (Table 4-8); ESI-MS *m/z* 491 $[M+H]^+$; 489 [M-H]; HRESI-MS *m/z* 513.3442 $[M+Na]^+$ (calcd for $C_{32}H_{46}N_2O_2Na$, *m/z* 513.3451).

4.2.5 Biological activity of indoloditerpenes

Synthetic CB receptor ligands based on an indole scaffold have been described, *e.g.* the CB_1/CB_2 agonist (*R*)-[2,3-dihydro-5-methyl-3-(4-morpholinylmethyl)-pyrrolo[1,2,3-de]-1,4-benzoxazin-6-yl]-1-naphthalenylmethanone (WIN55,212-2), and the CB_2 antagonist/inverse agonist6-iodo-2-methyl-1-[2-(4-morpholinyl)ethyl]-1H-indol-3-yl](4-methoxy-phenyl) methanone (AM630).[73,109,110] Recently, we identified amauromine (**8**, Figure 4-16), an indole derivative derived from the marine fungus *Auxarthron reticulatum*, as a novel lead structure for CB_1-selective antagonists.[111] Due to structural similarities between the here reported indoloditerpenes (**1**–**7**) and amauromine we investigated **1**–**2, 4**–**5** and **7** in radioligand binding and functional assays (inhibition of forskolin-stimulated cAMP accumulation) at human CB_1 and CB_2 receptors. In addition we studied indole derivatives for their interaction with the CB receptor-like orphan GPCRs GPR18 and GPR55 using β-arrestin translocation assays.[35,112] (see 3.6.3–3.6.5)

All isolated examined indole derivatives interacted with one or more of the four investigated receptors (Table 4-9). Examples for concentration-inhibition curves are shown in Figure 4-15 and Figure 4-16. None of the compounds showed any significant effect on GPR55 at the highest test concentration of 10 µM. All of the active compounds were characterized as receptor antagonists in functional assays at CB_1 and/or CB_2 receptors and/or GPR18 (see Table 4-10).

The new fungal metabolite emindole SB beta-mannoside (**1**), a pentacyclic indole derivative, displayed preferenced binding to the CB_2 receptor with a K_i value of 10.6 µM. cAMP accumulation assays showed that it was a CB_2 antagonist since it did not lead to receptor activation (see Table 4-10). It is surprising that the CB_2 receptor accepted the polar sugar moiety attached to the lipophilic core structure in compound **1**. One explanation may be that the sugar moiety points towards the extracellular aqueous space of the receptor. In contrast to the majority of known CB receptor ligands indole derivative **1** shows high water-

solubility due to the attached mannose. Thus, compound **1** may be a starting point for the development of water-soluble CB_2 receptor antagonists with increased affinity.

Its aglycon-derivative emindole SB (compound **5**) was about 5-fold more potent at the CB_2 receptor (K_i 2.24 µM) than mannoside **1**, and displayed additional affinity for the CB_1 receptor (K_i 7.05 µM).

The new pentacyclic indole derivative 27-O-methylasporyzin C (**2**), which is lacking the sugar moiety of **1** and features a different side-chain , was found to be an antagonist at the CB-like receptor GPR18 with an IC_{50} value of 13.4 µM measured in a functional assay versus 7.5 µM THC (corresponding to its EC_{80}) (Table 4-9 and 4-10, Figure 4-15). Compound **2** showed some selectivity versus all of the other investigated receptors, CB_1, CB_2 and GPR55. So far, selective GPR18 antagonists are unknown. Therefore **2** may be used as a tool to study GPR18, and as a lead structure for further optimization.

Compound **4**, a hexacyclic indole derivative, was almost equipotent at CB_1 (K_i 4.40 µM) and CB_2 (K_i 4.76 µM) receptors, and similarly active at GPR18 (IC_{50} 9.91 µM). At GPR18, the inhibition curves for compounds **2** and **4** went down below basal values (Figures 4-15 C and D) indicating an inverse agonistic mode of action for these two compounds.

We additionally investigated the recently published selective CB_1 antagonist amauromine (**8**)[111] for an interaction with the CB-like receptors GPR18 and GPR55. Like **2** and **4**, amauromine showed no significant interaction with GPR55, but it exhibited a remarkable inhibition of GPR18 (IC_{50} 3.74 µM, Figure 4-12). Our results show that the binding pocket of GPR18 appears to be closely related to those of the CB receptors, while GPR55 has clearly different structural requirements.

Due to our results we endeavoured the synthesis of an emindole SB derivative with a substitution at the hydroxylgroup at C-7 similar to compound **1**, following the hypothesis that a substitution at this position might shift compound properties toward more selective CB_2 receptor activities. Unfortunetly the N-propylcarbamate (**7**) failed to interact with one of these receptors indicating that other substitution patterns with maybe more hydrophilic moieties should be tested.

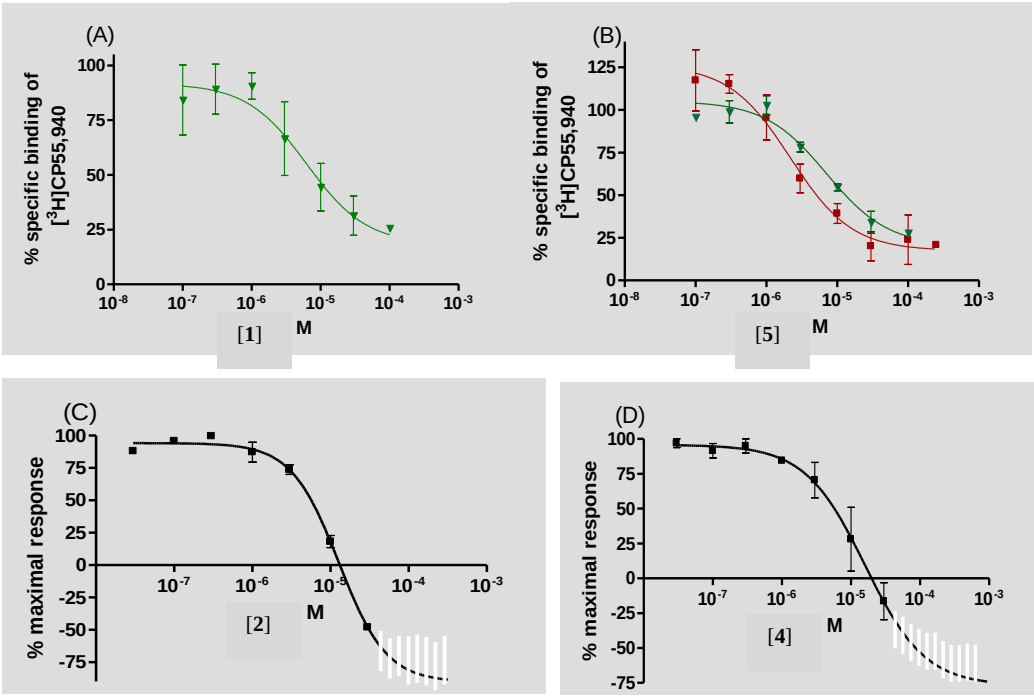

Figure **4-15**: Concentration-inhibition curves. (A) Inhibition of specific [^{3}H]CP55,940 binding by compound **1** at CB_2 receptors (K_i CB_2 10.6 µM); (B) inhibition of specific [^{3}H]CP55,940 binding by compound **5** at CB_1 (▼, K_i 7.05 µM) and CB_2 receptors (■, K_i 2.24 µM); (C, D) inhibition of Δ^9-THC (7.5 µM)-induced β-arrestin recruitment by **2** (C, IC_{50} 13.4 µM), and **4** (D, IC_{50} 9.91 µM), respectively. Data points represent means ± SEM of three independent experiments, performed in duplicates.

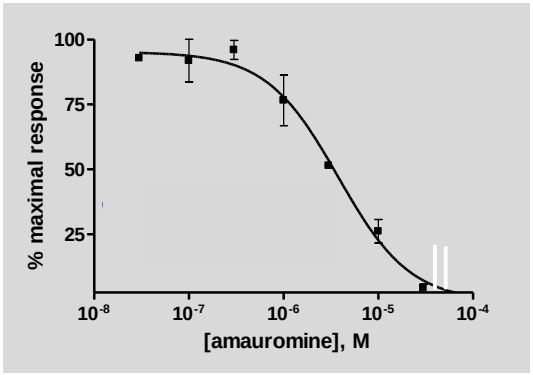

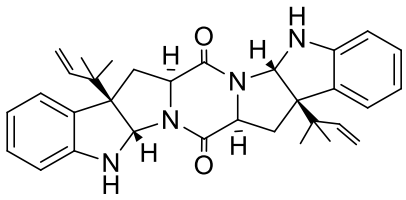

amauromine (**8**)

Figure **4-16**: Structure of auromine (**8**) and **i**nhibition of Δ^9-THC (7.5 µM)-induced β-arrestin recruitment by **8** at GPR18 (IC_{50} 3.74 µM). Data points represent means ± SEM of three independent experiments, performed in duplicates.

Table 4-9: Biological evaluation of compounds **1**–**2, 4**–**5** and **7–8** at human CB receptors and orphan receptors GPR18 and GPR55.

Compound	Radioligand binding vs. [^{3}H]CP55,940 K_i ± SEM (μM)		β-Arrestin assays IC_{50} (μM)	
	CB_1	CB_2	GPR18	GPR55
Emindole SB beta-mannoside (**1**)	**>10** (30%)[d]	**10.6** ± 1.8	**>10** (15%)[b]	**>10** (13%)[c]
27-O-methylasporyzin C (**2**)	**>10** (39%)[d]	**>10** (33%)[d]	**13.4** ± 1.3	**>10** (31%)[c]
JBIR-03 (**4**)	**4.40** ± 1.07	**4.76** ± 1.39	**9.91** ± 2.59	**>10** (0%)[c]
Emindole SB (**5**)	**7.05** ± 1.04	**2.24** ± 0.30	**>10** (37%)[b]	**>10** (12%)[c]
Emindole SB-N-propylcarbamate (**7**)	**>10** (31%)[d]	**>10** (26%)[d]	**>10** (15%)[b]	**>10** (19%)[c]
Amauromine (**8**)	**0.178**[111]	**>10**[111]	**3.74** ± 0.52	**>10** (17%)[c]

[a] Efficacy related to the maximum effect of the full agonist CP55,940 (1 μM = 100%).

[b] %Inhibition of THC (10 μM)-mediated β-arrestin recruitment.

[c] %Inhibition of LPI (1 μM)-mediated β-arrestin recruitment.

[d] %Inhibition of [^{3}H]CP55,940 binding.

Table **4-10**: Intrinsic activities of compounds **1-2, 4-5** and **7–8** at CB receptors and GPR18 and GPR55

Compound.	cAMP Assays % inhibition of forskolin(10 µM)-induced cAMP production		β-Arrestin assays EC_{50} (µM)	
	CB_1	CB_2	GPR18	GPR55
Emindole SB beta-mannoside (**1**)	n.d.	(0%)	>**10** (0%)[a]	>**10** (0%)[b]
27-O-methylasporyzin C (**2**)	n.d.	n.d.	>**10** (0%)[a]	>**10** (0%)[b]
JBIR-03 (**4**)	(0%)	(0%)	>**10** (0%)[a]	>**10** (0%)[b]
Emindole SB (**5**)	(12%)	(0%)	>**10** (0%)[a]	>**10** (0%)[b]
Emindole SB-N-propylcarbamate (**7**)	n.d	n.d	>**10** (0%)[a]	>**10** (0%)[b]
Amauromine (**8**)	(6%) KB 66.6 nM	n.d.	>**10** (0%)a	>**10** (36%)b

[a]% activation of β-arrestin recruitment related to the effect of THC (10 µM, set at 100%).[b]% activation of β-arrestin recruitment related to the effect of LPI (1 µM, set at 100%), n.d: not detectable.

4.2.6 Discussion of indoloditerpenes and their biological activities

Biological activity

Due to increasing knowledge on the pathophysiological roles of the endocannabinoid signaling system, ligands for CB receptors and related GPCRs, such as GPR18 and GPR55, are currently in the focus of interest in drug research.

Natural products are known to be an excellent source for the identification of novel lead compounds.[4,7] It is interesting to note that CB receptor ligands from natural sources like plants and fungi have been isolated before. Non-selective CB receptor ligands have been obtained most prominently from *Cannabis sativa*,[113,114] but also from *Magnolia officinalis*,[112] a medicinal plant used in Chinese traditional medicine, and from the fungus *Eurotium repens*.[115] *M. officinalis* contains magnolol, which is an agonist at both CB receptor subtypes, however with a preference for CB_2 (K_i CB_1 3.15 µM; K_i CB_2 1.44 µM). The same plant also contains honokiol which behaves as a CB_1 agonist and a CB_2 antagonist (K_i CB_1 6.46 µM; K_i CB_2 5.61 µM).[112] Selective CB_1 antagonists have also been isolated from plants and fungi. From the plant *Voacanga africana* the CB_1-selective iboga-type bis-indole voacamine, and

two iboga-type monomeric alkaloids have been described,[116] while the CB_1-selective diketopiperazine amauromine was found in the fungus *Auxarthron reticulatum*.[111]

Recently a group of structurally related indoloditerpenes, *e.g.* lolitrem B, have been reported to decrease immune responses associated with cytokine production in spleen and macrophages. These effects have up to now only been correlated with the observed inhibition of potassium channel function.[117,118] However, reduction of cytokine production has also been noted for CB receptor antagonists.[119] Due to our results an additional role of the CB receptor system for the observed immunosuppressive effects should be considered and further investigated.

The herein described emindole SB beta-mannoside (**1**) is the first CB receptor antagonist from a fungal source with a preference for the CB_2 receptor subtype. Compound **1** was examined for cytotoxic activity toward an L6 rat skeletal muscle cell line. In comparison to the cytotoxic reference compound podophyllotoxin with an IC_{50} of 0.007 µg/mL, compound **1** was shown to hardly display any cytotoxic activity (IC_{50} 32.8 µg/mL).[37,38,120]

In addition we identified **2**, **4** and **8** as the first ligands of fungal origin for the orphan receptor GPR18. Selective GPR18 antagonists are urgently needed as pharmacological tools to further elucidate the physiological role of this poorly characterized receptor. So far, no selective antagonists for the GPR18 have been described. GPR18 antagonists are regarded as potential drugs for the treatment of cancer and endometriosis.[79,121] The structurally novel antagonists **1** and **2** may serve as important leads for the development of more potent and selective ligands for this therapeutically interesting CB receptor-related drug target.

4.3 Isolation and evaluation of uncommon sterols and xanthocillin derivatives with Aβ-42 lowering activity

4.3.1 Introduction to the role of Aβ-42 lowering agents in Alzheimer disease

Alzheimer disease (AD) causes dementia in many elderly people and is an increasing problem, especially in aging western societies.[122] The neurodegenerative AD is defined by two pathological features, amyloid plaques and aggregates of mis-folded tau proteins.

Accumulation of neurotoxic amyloid β peptides (AβP) like Aβ-42 within the brain plays an important role in the pathology of Alzheimer disease.[122,123] Aβ precursor proteins (APPs) are cleaved by β- and γ-secretases and release several species of Aβ-peptides with different properties, depending on the cleavage site.[122,123] Compounds influencing this cascade, i.e. inhibitors of β-secretases (BACE), γ-secretase (GSIs) and γ-secretase modulators (GSMs), are needed as research tools and investigated as potential therapeutical agents.[123–126,125,126] Aftin-5 an activator of extracellular Aβ-42 production, can be used to simulate essential aspects of AD in cell cultures and facilitates the identification of Aβ-lowering agents.[40,123]

The therapeutic use of secretase inhibitors is regarded as critical, since they cause severe side effects. One well known reason for the latter is inhibition of the cleavage of substrates other than APP, like neuregulin-1 or Notch.[124,125] To avoid this problem, the identification of secretase inhibitors which display increased substrate selectivity is desired. In order to achieve this, optimization of assays and biomarkers, allowing a more comprehensive assessment of secretase inhibitors is necessary.[124,125] Another approach is the development of γ-secretase modulators. GSMs partially shift the preferred cleavage site of γ-secretase to various extents. Consequently the production ratio of AβP subspecies is influenced, without inhibiting the γ-secretase cleavage, completely.

Here we report on novel, untypical sterol derivatives from a marine fungal source (**9**–**11**), as well as on two aromatic isonitrile containing xanthocillin X derivatives (**12** and **13**). 16-O-desmethylasporyergosterol-ß-D-mannoside (**9**) and xanthocillin X dimethylether (**12**) reduced Aβ-42 production, in Aftin-5 treated cells.

4.3.2 Isolation of compounds 9–13 from *Dichotomomyces cejpii*

Bioassay- and chemical (LC-MS and ^{1}H NMR)-guided fractionation of the crude extracts, obtained from the marine derived fungus *Dichotomomyces cejpii* on two different media was conducted. Cultivation medium 2 yielded two sterols (**9**–**10**) while cultivation medium 1 yielded one sterol (11) and two xanthocillin derivatives (12 and 13). The investigated fungal strain was cultivated on cultivation medium 2 as described before (3.2.2–3.2.3)

Fungal biomass and media of cultivation medium 2 (Tennelin) were homogenized using an Ultra-Turrax apparatus and extracted with 5 L EtOAc to yield 1.2 g of crude extract. This material was fractionated by normal-phase (NP) vacuum liquid chromatography (VLC) using a stepwise gradient solvent system of increasing polarity starting with 100% CH_2CL_2 to 100%

EtOAc, to 100% MeOH and H_2O-MeOH (50-50) which yielded 10 fractions. Compound **9** and **10** were isolated from VLC fraction 8 and 9. The combined fractions were separated via reversed-phase C_{18} (RP_{18})-VLC, eluted stepwise with H_2O-MeOH (70-30), to 100% MeOH, and 100% CH_2CL_2, which yielded 8 fractions. Subfraction 8.6 contained both compounds. Using RP_{18}-HPLC system C (Nucleodur 100-S 250mm x 4.6 mm) with H_2O-MeOH (80-20), 2.0 mL/min compound **9** (16-O-desmethylasporyergosterol-ß-D-mannoside) was isolated directly in subfraction 8.6.5 as a white powder, t_R: 8 min (5.0 mg).

Subfraction 8.6.3 was further purified using RP_{18}-HPLC system B (Xterra™ 250 x 4.6 mm) with H_2O-MeOH (60-40), 1.2 mL/min to obtain compound **10** (16-O-desmethylasporyergosterol-3-one-mannoside) as a yellowish white powder, t_R: 6.5 min (1.0 mg). (see Figure 4-4 for isolation schema)

For the isolation of compound **10**–**13** investigated fungal strain was cultivated on cultivation medium 1 (MPY) as described before (3.2.2–3.2.3). Fungal biomass and media were homogenized using an Ultra-Turrax apparatus and extracted with 5 L EtOAc to yield 4.1 g of crude extract. This material was fractionated by NP vacuum liquid chromatography (VLC) using a stepwise gradient solvent system of increasing polarity starting with 100% CH_2CL_2 to 100% EtOAc and to 100% MeOH which yielded 10 fractions. Fraction 2 was separated via NP VLC, using stepwise elution with CH_2CL_2-petroleum ether (50-50) to 100% CH_2CL_2, and 100% MeOH which yielded 15 fractions. VLC fraction 1 and subfraction 2.1 contained compound **12** xanthocillin X dimethylether, while subfraction 2.7 contained compound **11** (16-O-desmethylasporyergosterol).

Subfraction 2.7 was further separated using a second NP VLC column and eluted stepwise with petroleum ether-CH_2CL_2 (50-50) to 100% CH_2CL_2, 100% acetone, 100% EtOAc and finally to EtOAc-MeOH (25-75) which yielded 15 fractions. Subfraction 2.7.4 and 2.7.5 were combined and further separated with a RP_{18}-solid phase extraction (SPE) cartridge, eluted stepwise with H_2O-MeOH (65-35), to 100% MeOH, and 100% CH_2CL_2 which yielded 6 fractions. Subfraction 2.7.4.4 contained compound **11**. Compound **11** (16-O-desmethylasporyergosterol) was isolated via Diol-HPLC system D (Eurosphere Diol 100-S 250 mm x 4.6 mm) with petroleum ether-acetone (75-25), 1.5 mL/min as a yellowish powder, t_R: 17 min (2.0 mg).

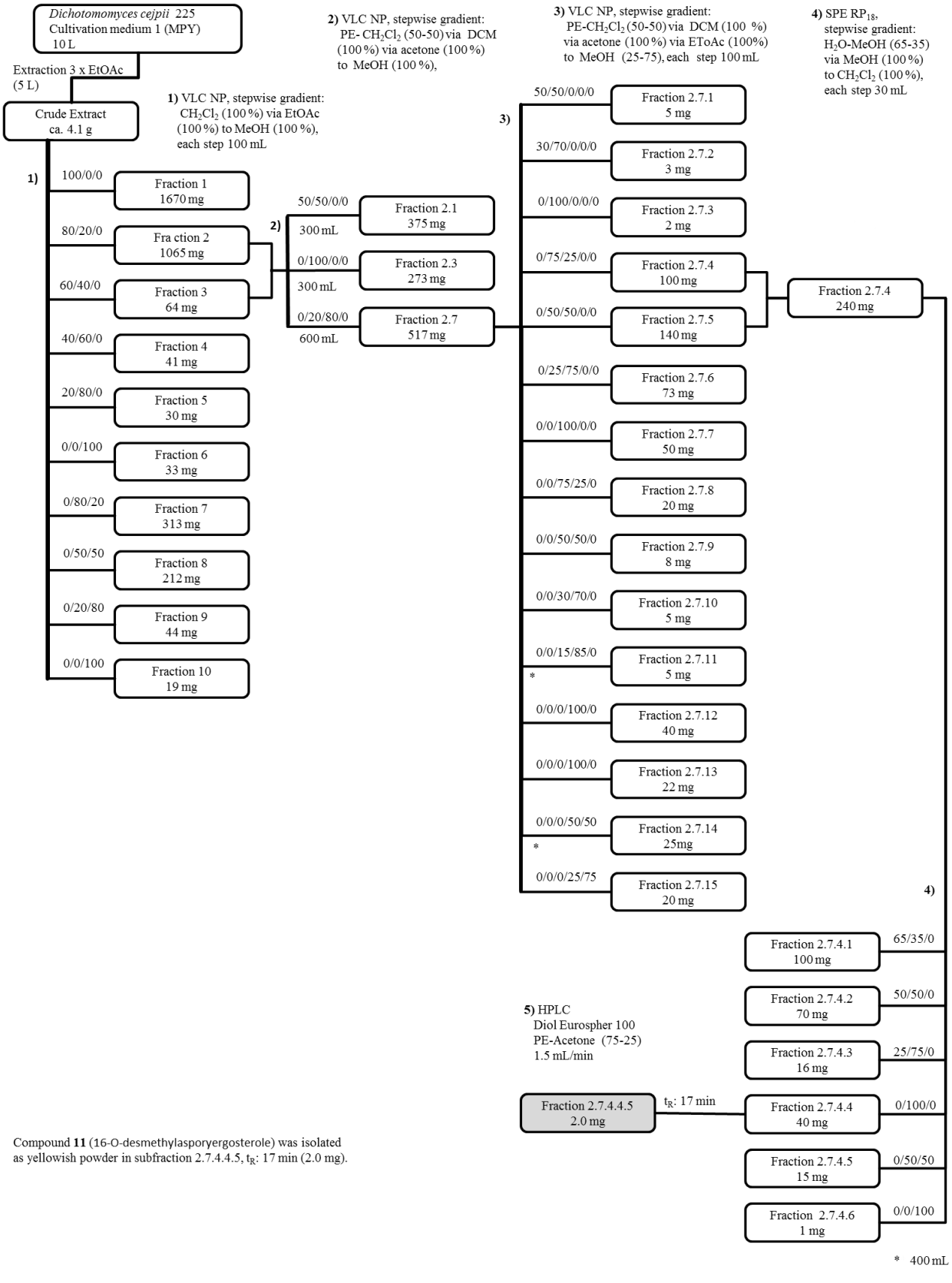

*

Figure 4-17: Isolation scheme for compound **11**. For reasons of clarity only the most important fractions are listed.

VLC fraction 1 and subfraction 2.1 contained xanthocillin X dimethylether (**12**) and xanthocillin X monomethylether (**13**). These fractions were separated three times with a solvent/solvent extraction with hexane (100%) and MeOH-H_2O (60-40) using a separation funnel. The combined hexane phases were further separated with a NP VLC column and eluted stepwise with petroleum ether-CH_2Cl_2 (80-20), up to 100% CH_2Cl_2, 100% acetone, and 100% MeOH which yielded 16 fractions. Subfraction 2.1.5 contained compound **12** and was further separated with a NP-HPLC system D (Eurospher II Si 250 x 8 mm) with petroleum ether-CH_2CL_2 (50-50), 1.2 mL/min. Subfraction 2.1.5.2 was further purified using NP-HPLC system D (Eurospher II Si 250 x 4 mm) with petroleum ether-CH_2CL_2 (80-20) to obtain compound **12** (xanthocillin X dimethylether) as yellow needles, t_R: 5 min (20.0 mg).

Subfraction 2.1.7 contained compound **13** and was further separated with a RP_{18}-SPE cartridge, eluted stepwise with MeOH-H_2O (50-50), MeOH, acetone, and CH_2Cl_2 which yielded eight fractions. Subfraction 2.1.7.4 contained compound **13** and was further purified. Xanthocillin X monomethylether (**13**) was isolated via RP_{18}-HPLC (Nucleodur 100-S 250 mm x 4.6 mm) with MeOH-H_2O (82-18), 1.2 mL-min^{-1} as yellow needles, [t_R: 12 min] (1.0 mg). (see Figure 4-2 for isolation schema)

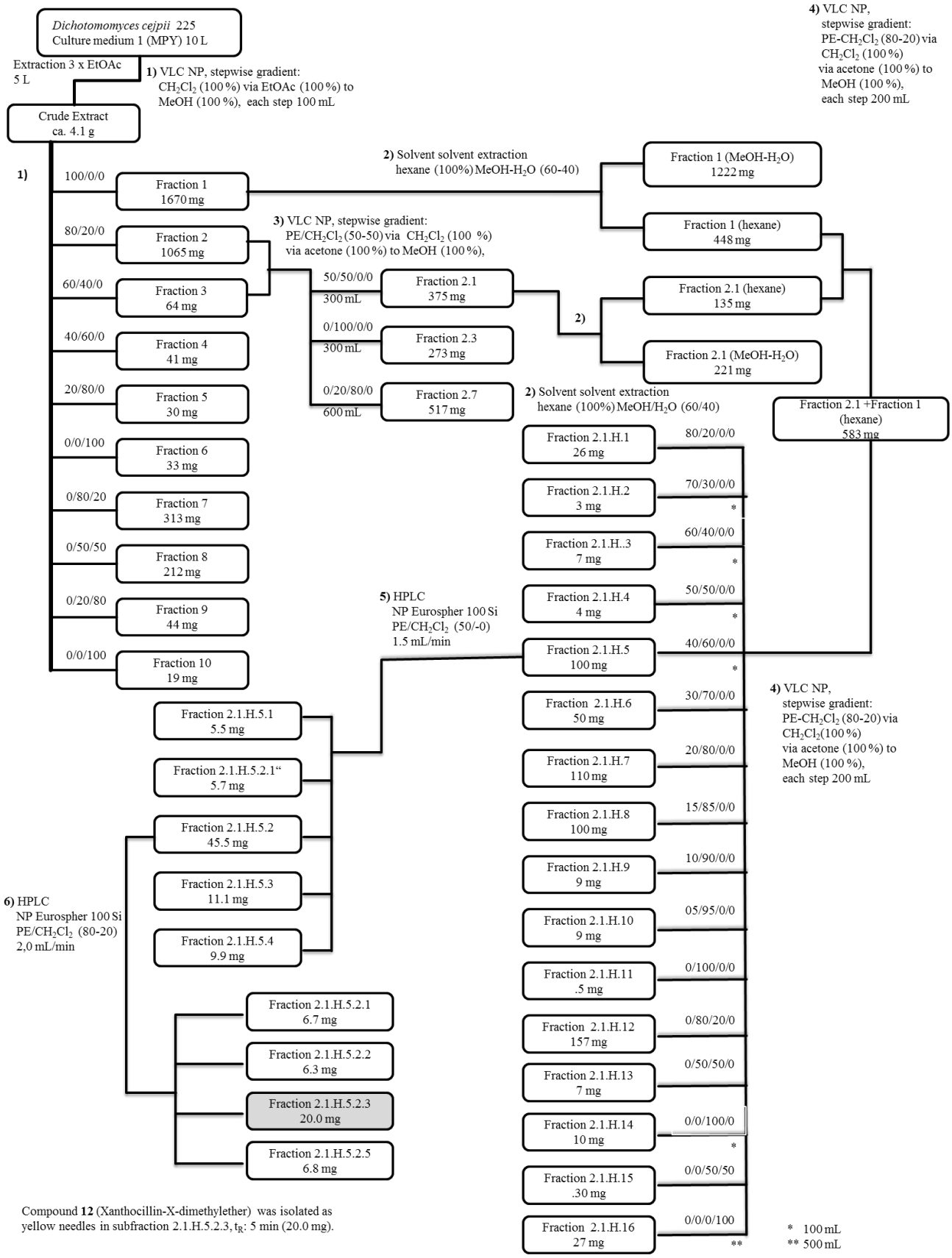

Figure 4-18: Isolation scheme for compound **12.** For reasons of clarity only the most important fractions are listed.

4.3.3 Structure elucidation of isolated sterols and xanthocillin X derivatives

Compound **9** was obtained from the marine sponge-derived fungus *Dichotomomyces cejpii* and its structure was elucidated via analysis of spectroscopic data and chemical degradation. A UV maximum at 252 nm indicated the presence of a conjugated $\pi \rightarrow \pi^*$ system, whereas a broad IR absorption at 3389 cm^{-1} pointed toward hydroxy groups. The molecular formula of compound **9** was deduced from the results of an accurate mass measurement (HRESIMS, *m/z* =595.3603 $(M+Na)^+$ as $C_{34}H_{52}O_7$, indicating nine degrees of unsaturation. The ^{13}C NMR and DEPT135 spectra denoted the presence of 34 resonances for six methyl groups, seven sp^3 methylene groups, four sp^2 methine, eleven sp^3 methine, and six quaternary carbons in the molecule (Table 4-11)

The first substructure, an unsaturated decalin system, was deciphered from ^1H-^1H COSY correlations from H_2-1 through to H-7, and HMBC cross peaks between the resonances for the methyl group CH_3-19 and C-1, C-5, C-9 and C-10, as well as of H-7 to C-8 and C-9. Another partial structure was deduced from ^1H-^1H COSY correlations from H-9 to H_2-11 and H_2-12, extending the decalin ring by two methylene groups attached to C-9. A third ^1H-^1H spin system comprised solely H_2-15 to H-16. HMBC correlations arising from the resonance of CH_2-15 to C-14, as well as of the methyl group CH_3-18 to CH_2-12, C-13, C-14 and C-17, and of the methine group CH-16 to C-17 defined the C-13 to C-18 part of the molecule as a methyl substituted cyclopentane ring. Further heteronuclear couplings between CH-7 and C-14, in addition to the above mentioned H-7/C-8 coupling allowed to connect the substructures, revealing the four characteristic rings of a sterol scaffold. The protons and carbon atoms of the methine groups CH-3 and CH-16 resonated at δ_H 3.56 and 5.08, and at δ_C 71.6 and 79.4, respectively, proving a substitution with oxygen at these sites. The structure of the side chain was revealed from ^1H-^1H COSY correlations from H-22 through to H_3-26/27 and H_3-28. This moiety could be extended and finally attached to the sterol scaffold due to HMBC correlations between the resonances for the methyl group CH_3-21 and C-17, C-20 and C-22. Altogether, the molecule had four carbon-carbon double bounds, i.e. $\Delta^{6,7}$, $\Delta^{8,14}$,$\Delta^{17,20}$ $\Delta^{22,23}$, which could be located due to the ^{13}C NMR chemical shifts of the respective carbon atoms in a range of 125 to 147 ppm. At this point of the structure elucidation, eight of the nine degrees of unsaturation as suggested by the molecular formula were accounted for.

Additional ^1H and ^{13}C NMR resonances pointed toward a sugar moiety in the molecule. The methine groups CH-1', CH-2', CH-3', CH-4', CH-5' and the methylene group CH_2-6'

resonated in the range of δ_H 3.1 to 4.6 and δ_C 62 to 99, respectively. The ^{1}H-^{1}H COSY spectra showed correlations for a spin system from H-1' through to CH_2-6' and allowed to established a pyranose ring. Analysis of the coupling constants and NOEs revealed mannopyranose.[104] Hydrolysis and HPLC-LSD analysis using a chiral column revealed the sugar to possess the D-configuration. The anomeric configuration of the mannose was considered as β, because of the magnitude of the heteronuclear coupling constant between the anomeric carbon and respective proton ($^1J_{CH}$ = 154 Hz).[105] The mannose is attached via the CH-16 methine group to the sterole nucleus, due to a heteronuclear long range coupling from H-1' to C-16.

The relative configuration of the sterol scaffold was assigned on the basis of a NOESY experiment and the magnitude of significant ^{1}H-^{1}H coupling constants. NOESY correlations between H-3, H-5 and H-9 indicated that these protons are located on the same side, i.e. α, of the molecule, whereas NOESY correlations between H-16 and H_3-18 proved the opposite orientation, i.e. β. The configuration of $\Delta^{6,7}$ ($J_{H\text{-}6/H\text{-}7}$ = 9.9 Hz) and $\Delta^{8,14}$ had to be *Z* and *E*, respectively to allow the ring closures of the steroid nucleus. $\Delta^{22,23}$ was determined as *E* based on a coupling constant of $J_{H\text{-}22/H\text{-}23}$ = 15.7 Hz. The double bound $\Delta^{17,20}$ was also assigned as *E* configured due to NOESY correlations between H-16 and H_3-21. The relative configurations (C-3, C-5, C-9, C-10, C-13, C-16) were thus assigned to be the same as those of the closely related asporyergosterol.[108,127] The configuration at C-24 could not be determined.

The fungal metabolite **9** is thus an ergostane steroid with an untypical number and location of double bounds and a mannose moiety, for which we suggest the trivial name 16-O-desmethylasporyergosterol-ß-D-mannoside.

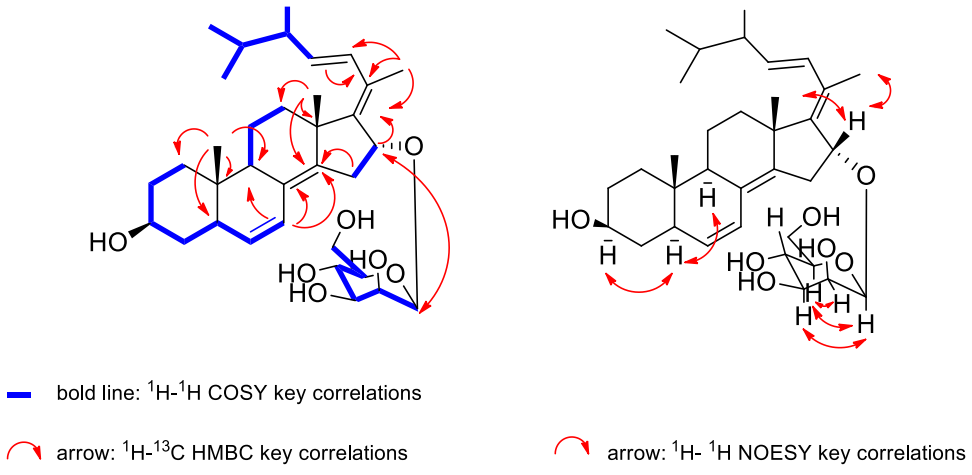

Figure **4-19**: NMR key correlations of compound **9**

Carbohydrate analysis of compound 9

Measurement conducted as described in 3.6.6.

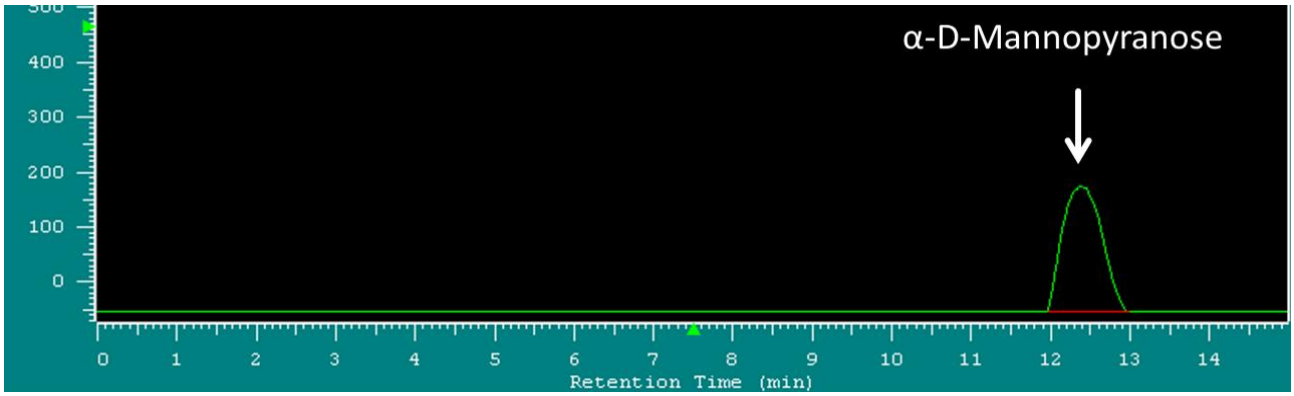

Figure **4-20**: HPLC chromatogram of D-mannose

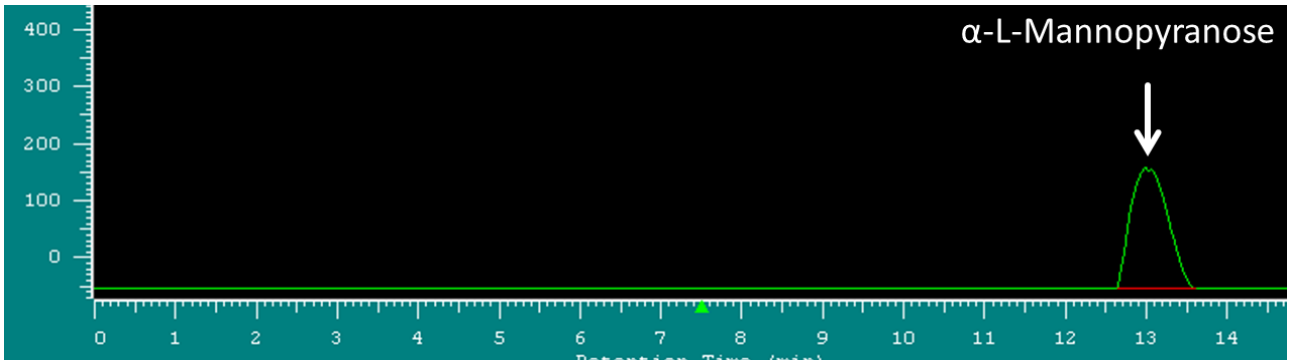

Figure **4-21**: HPLC chromatogram of L-mannose

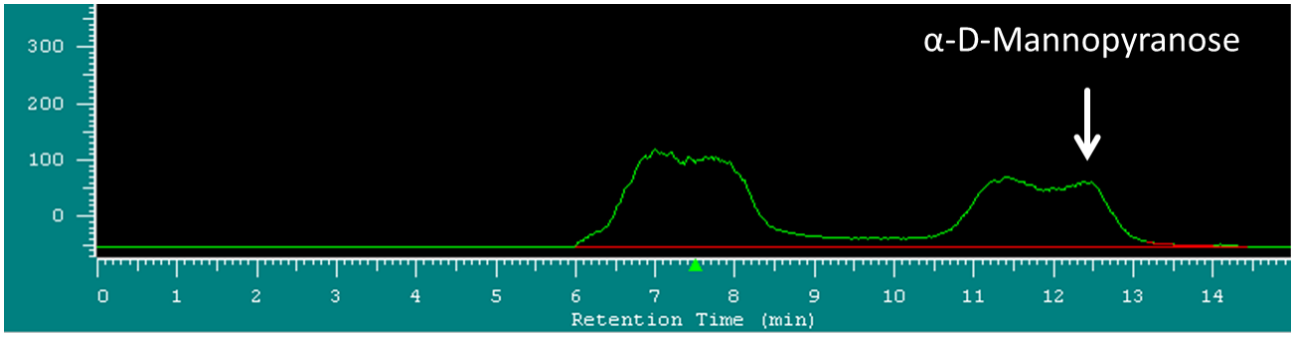

Figure **4-22**: HPLC chromatogram of the hydrolysis mixture of 16-O-desmethylasporyergosterol-ß-D-mannoside

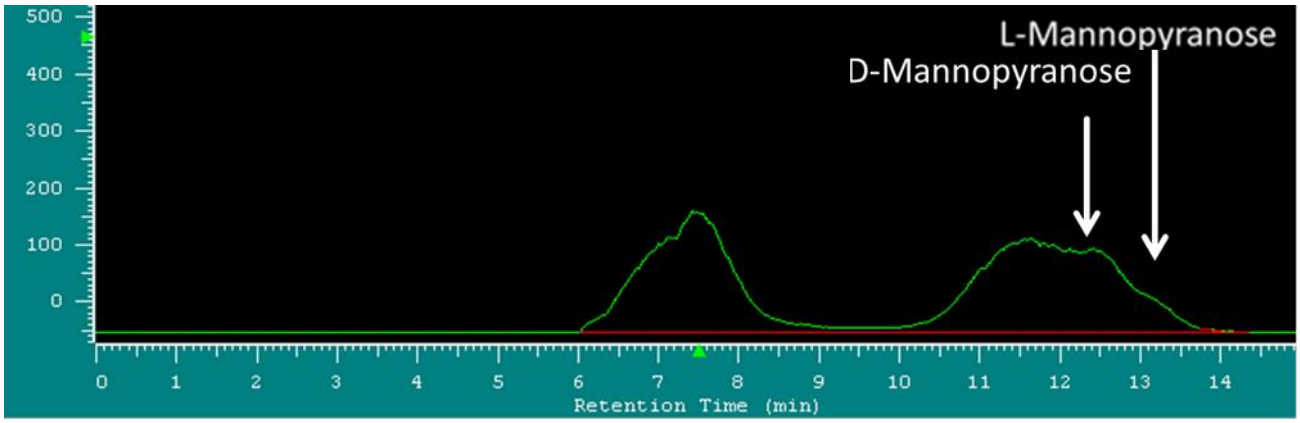

Figure **4-23**: HPLC chromatogram of hydrolysis mixture of 16-O-desmethylasporyergosterol-ß-D-mannoside + L-mannose

The structure of the fungal metabolite **10** was found to be closely related to that of **9**. The molecular formula of **10** was deduced as $C_{34}H_{48}O_7$ from the results of an accurate mass measurement (HRESIMS, *m/z* = 591.3293 $[(M+Na)]^+$). The UV spectrum showed an additional UV maximum at 344 nm and thus indicated a more extended conjugated system. The ^{13}C NMR resonance at δ_C 71.6 for the CH-3 methine group in **9** was missing in the case of **10**, instead a resonance at 202.2 ppm, as expected for a ketone moiety, appeared in the respective spectra for **10**. Additionally, the presence of a double bound between CH-4 and C-5 was indicated by the downfield shifted resonance frequencies for these two carbon atoms (δ_C 123.4 and δ_C 167.5), respectively. Altogether, this resulted in the assumed extended conjugated system, ranging from the carbonyl group at C-3 via $\Delta^{4,5}$, $\Delta^{6,7}$ and $\Delta^{8,14}$. ^1H- and ^{13}C NMR chemical shift values of ring A and B of the steroid scaffold were similar to the related compound ergosta-4,6,8(14),22-tetraen-3-one and confirmed the proposed structure.[128] The relative configuration of **10** was assigned on the basis of a NOESY experiment and significant ^1H-^1H coupling constants (Table 4-12). NOESY correlations between H-16 and H_3-18 indicated that these protons are located on the same side of the molecule, whereas H-9, whose ^1H NMR signal at δ_H 2.26, m, showed similar ^1H NMR couplings at the respective resonance of **9**, did not display any NOEs and was therefore orientated opposite to these substituents, as in compound **9**. The double bound $\Delta^{17,20}$ was assigned as *E* configured due to NOESY correlations between H-16 and H_3-21. The configuration of the ß-D-mannose was determinated in the same manner as described for **9** (4-23 and 4-24). The structure of compound **10** thus differs from that of compound **9** in that the hydroxyl group at C-3 of **9** is replaced by a carbonyl function, and by an additional double bound between C-4 and C-5. For

the fungal metabolite **10** (Figure 4-23), we suggest the name 16-O-desmethylasporyergosteron-β-D-mannoside.

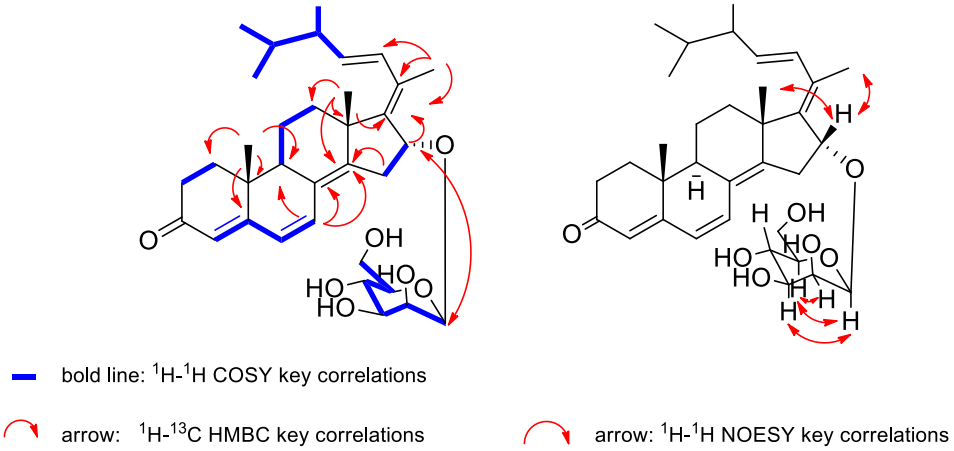

Figure **4-24**: NMR key correlations of compound **9**

Carbohydrate analysis of compound 10

Measurement conducted as described in 3.6.6.

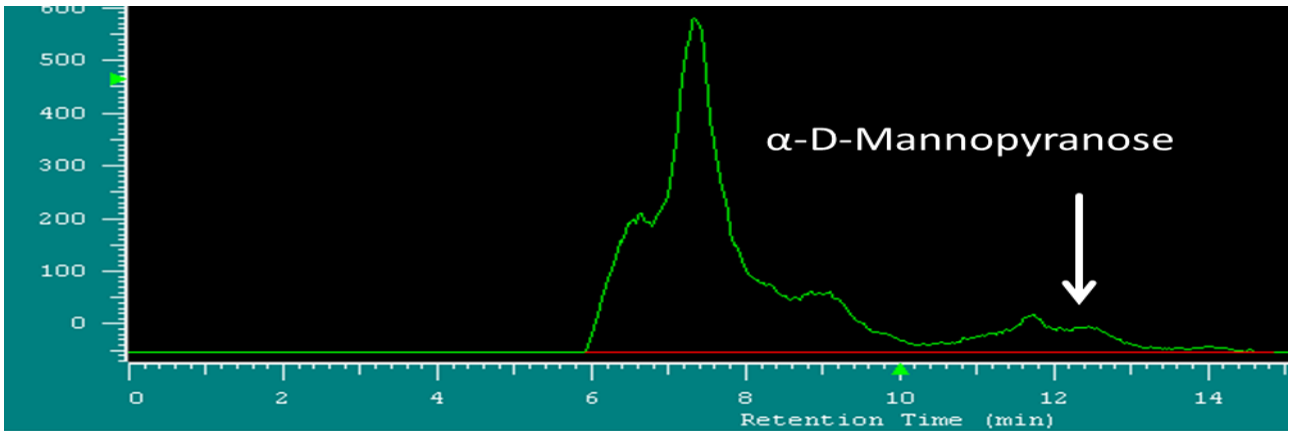

Figure **4-26**: HPLC chromatogram of hydrolysis mixture of 16-O-desmethylasporyergosteron-ß-D-mannoside (**10**)

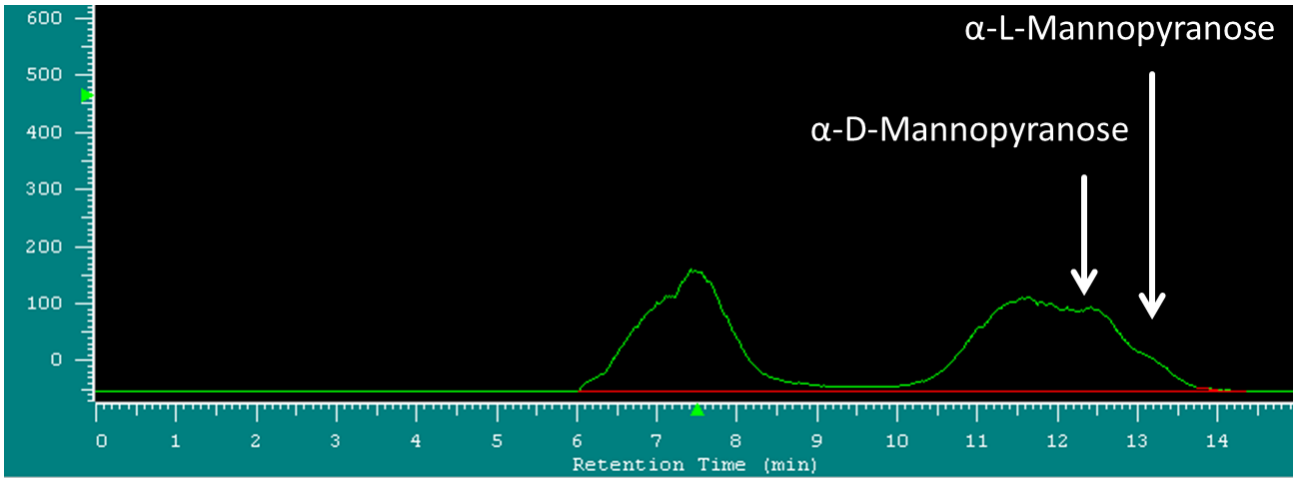

Figure **4-27**: HPLC chromatogram of hydrolysis mixture of 16-O-desmethylasporyergosterol-ß-D-mannoside + L mannose

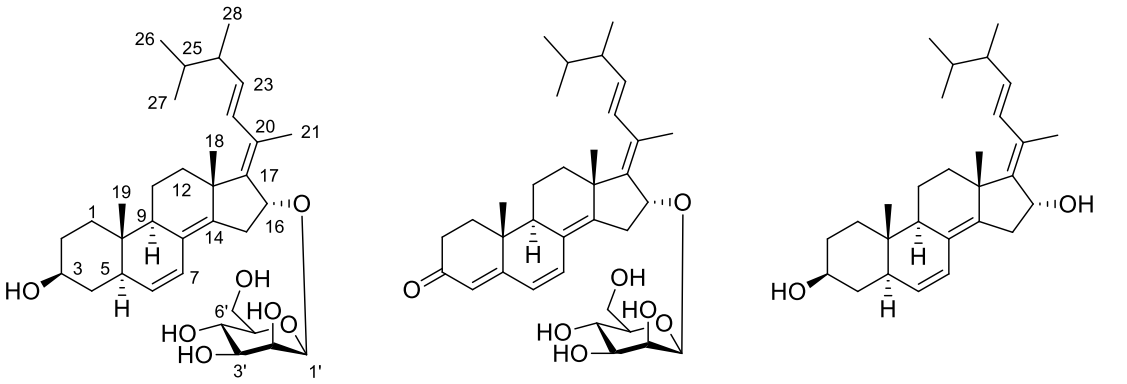

Figure **4-25**: Structure of isolated sterols.

The molecular formula of **11** was deduced as $C_{28}H_{49}O_2$ (HRESIMS, *m/z* =433.3077 $(M+Na)^+$. The structure of compound **11** differs from that of compound **9** solely by the missing sugar moiety at C-16. The ^{13}C NMR resonance frequency at δ_C 72.6 for the methine group CH-16 was shifted upfield by 8 ppm as compared to **9** and thus, verified the presence of an unsubstituted hydroxy group at this position. The configuration of **9** was assigned in the same manner as described for **9** (Figure 1). The fungal metabolite **9** is thus an ergostane steroid, for which we suggest the trivial name 16-O-desmethylasporyergosterole (4-23).

Table **4-11**: NMR spectroscopic data (300 MHz, methanol-d_4) of 16-O-desmethylasporyergosterol-ß-D-mannoside (**9**)

Position	δ_C , mult	δ_H (*J* in Hz)	^{1}H -^{1}H COSY	^{1}H-^{13}C HMBC	^{1}H -^{1}H NOESY
1	34.7, CH_2	1a: 1.91, m	1b,2a,2b	-	-
		1b: 1.23, m	1a,2a,2b	-	-
2	31.5, CH_2	2a: 1.74, m	1a,1b,2b, 3,4	-	-
		2b: 1.32, m	1a,1b,2a,3,4	-	-
3	71.6, CH	3.56, m	2a,2b,4a,4b	-	5
4	39.9, CH_2	4a: 1.92, m	2a,2b,3,4b,5	-	6,19
		4b: 1.25, m	2a,2b,3,4a,5	-	-
5	45.7, CH	1.88, m	4a,4b,6,7	-	9
6	131.3, CH	5.63, dd (5.1, 9.9)	5,7	5, 10	5,7
7	125.5, CH	6.30, d (9.9)	5,6	5, 8, 9, 14	6, 15a
8	127.7, C	-	-	-	-
9	36.0, CH	2.58, m	11a,11b,12a	-	5
10	35.3, C	-	-	-	-
11	20.5, CH_2	11a: 1.69, m	9,12a,12b	-	-
		11b: 1.63, m	9,12a,12b	-	-
12	36.3, CH_2	12a: 2.49, m	9,11a,11b,12b	-	-
		12b: 1.70, m	9,11a,11b,12a	-	-
13	45.3, C	-	-	-	-
14	144.9, C	-	-	-	-
15	33.3, CH_2	15a: 3.03, d (15.7)	15b,16,1’	13, 14, 16, 17	7,15b,1’
		15b: 2.40, m	15a,16	-	15a,16
16	79.4, CH	5.08, d (5.5)	15a,15b,21	13,14,17,20,1’	15b,18(w), 21,1‘
17	146.4, C	-	-	-	-
18	27.1, CH_3	1.33, s	-	12,13,14,17,	16(w),22
19	23.1, CH_3	0.80, s	-	1,5,9,10	-
20	133.8, C	-	-	-	-
21	16.8, CH_3	2.01, s	-	17,20,22	16,23
22	130.0, CH	6.69, d (15.7)	23,24	17,20,21,24	18,24
23	136.2, CH	5.72, dd (8.4, 15.7)	22,24	20,24,28	21,24,25,28
24	45.2, CH	2.10, m	22,23,25,28	-	22,23,26,28
25	34.6, CH	1.62, m	24,26,27	-	26,27,28
26	20.5, CH_3	0.94, d (7.0)	25	24,25,27	25,28
27	20.1, CH_3	0.91, d (7.0)	25	24,25,26	25
28	18.1, CH_3	1.07, d (7.0)	24	23,24,25	23,24,26
1´	99.4, CH	4.57, s	2’	16,2’	15,16, 2’,3’,5’
2´	73.3, CH	3.66, m	1’,3’,4’,5’	3’,5’	1’,3’
3´	75.5, CH	3.46, dd (3.3, 9.5)	2’,4’	2’,4’	1’,5’

4´	68.2, CH	3.65, t (9.5)	2',3',5'	3'	-
5´	78.3, CH	3.17, ddd (2.2, 4.8, 9.5)	4', 6'a, 6'b	-	1', 3', 6'a,6'b
6´	62.7, CH_2	6'a: 3.93, dd (2.2, 11.7)	5',6'b	2'	6'b
		6'b: 3.77, dd (4.8, 11.7)	5',6'a	-	6'a

w: weak

Table **4-12**: NMR spectroscopic data (300 MHz) of 16-O-desmethylasporyergosteron-ß-D-mannoside (**10**)

Position	δ_C , mult	δ_H (*J* in Hz)	^1H -^1H COSY	^1H-^{13}C HMBC	^1H -^1H NOESY
1	35.1, CH_2	1a: 2.14, m	1b,2a,2b	-	-
		1b: 1.88, m	1a,2a,2b	-	-
2	35.0, CH_2	2a: 2.51, m	1a,1b,2b	-	-
		2b: 2.42, m	1a,1b,2a	-	-
3	202.2, C	-	-	-	-
4	123.4, CH	5.78, s	2b,6	6,10	6
5	167.5, C	-	-	-	-
6	126.3, CH	6.21, d (9.9)	4,7	5,8,10	4
7	136.1, CH	6.97, d (9.9)	6	5	-
8	126.9, C	-	-	-	-
9	45.2, CH	2.26, m	11a,11b,12a	-	-
10	38.1, C	-	-	-	-
11	20.3, CH_2	11a: 1.87, m	9,12a,12b	-	-
		11b: 1.80, m	9,12a,12b	-	-
12	34.8, CH_2	12a: 2.54, m	11a,11b,12b	-	-
		12b: 1.63, m	11a,11b,12a	-	-
13	45.6, C	-	-	-	-
14	154.7, C	-	-	-	-
15	33.8, CH_2	15a: 3.19, d (15.7)	15b	13	6
		15b: 2.59, m	15a,16	-	-
16	79.0, CH	5.15, d (5.5)	15b	13,14,17,1'	18 (w),21
17	145.1, C	-	-	-	-
18	26.9, CH_3	1.40, s	-	12,13,14,17	16 (w)
19	17.0, CH_3	1.10, s	-	1,5,9,10	-
20	134.4, C	-	-	-	-
21	16.8, CH_3	2.03, s	-	17,20,22	16
22	129.8, CH	6.69, d (15.7)	23	17,20,24	-
23	136.7, CH	5.76, dd (8.4, 15.7)	22,24	20,24,28	-
24	45.3, CH	2.10, m	23,28	-	-

25	34.6, CH	1.58, m (6.6, 13.2)	26,27	-	-
26	20.5, CH_3	0.94, d (7.0)	25	24,25,27	25,27
27	20.2, CH_3	0.92, d (7.0)	25	24,25,26	25,26
28	18.0, CH_3	1.07, d (7.0)	24	23,24,25	-
1´	98.4, CH	4.61, s	2’	16, 2’	-
2´	73.3, CH	3.66, m	1’,3’,4’,5’	-	-
3´	75.5, CH	3.48, dd (3.3, 9.5)	2’,4’	-	-
4´	68.4, CH	3.62, t (9.5)	2’,3’,5’	5’	-
5´	78.4, CH	3.22, m	4’,6’a,6’b	-	-
6´	62.8, CH_2	6’a: 3.91, dd (2.2, 11.7)	5’,6’b	2’	6b
		6’b: 3.77, dd (4.8, 11.7)	5’,6’a	-	6a

Table **4-13**: NMR spectroscopic data (300 MHz, acetone-d_6) of 16-O-desmethylasporyergosterol (**11**)

Position	$\delta_{C,}$ mult	δ_H (*J* in Hz)	^{1}H -^{1}H COSY	^{1}H-^{13}C HMBC	^{1}H -^{1}H NOESY
1	34.4, CH_2	1a: 1.82, m	1b,2a,2b	-	-
		1b: 1.16, m	1a,2a,2b	-	-
2	31.7, CH_2	2a: 1.66, m	1a,1b,2b,3	-	-
		2b: 1.26, m	1a,1b,2a,3	-	-
3	70.8, CH	3.51, m	2a,2b,4a,4b	-	5
4	40.2, CH_2	4a: 1.88, m	3,4b,5	-	-
		4b: 1.23, m	3,4a,5	-	-
5	45.2, CH	1.83, m	3,4a,4b,6,7	-	3
6	130.5, CH	5.54, dd (5.1, 9.9)	5,7	5,8,10	5,7
7	125.3,CH	6.20, d (9.9)	5,6	5,8,9,14	6,15a
8	127.4, C	-	-	-	-
9	35.4, CH	2.55, m	11a,11b,12a	-	5
10	34.8, C	-	-	-	-
11	20.1, CH_2	11a: 1.62, m	9,12a,12b	-	-
		11b: 1.58, m	9,12a,12b	-	-
12	36.2, CH_2	12a: 2.43, m	9,11a,11b,12b	-	12b
		12b: 1.70, m	9,11a,11b,12a	-	12a
13	44.4, C	-	-	-	-
14	145.1, C	-	-	-	-
15	37.5, CH_2	15a: 2.65, d (15.7)	15b,16	8,14,16,17	7,15b,16
		15b: 2.40, m	15a,16	8,14,16	15a,16
16	72.6, CH	4.70, d (5.1)	15a,15b	13,14,17,20	15b,18,21
17	150.1, C	-	-	-	-
18	26.8, CH_3	1.26, s	-	12,13,14,17	16,22
19	23.0, CH_3	0.74, s	-	1,5,9,10	-
20	130.2, C	-	-	-	-
21	16.5, CH_3	1.92, s	-	17,20,22	16,23
22	129.8, CH	6.65, d (15.7)	23	17,20,21,24	18,24
23	134.6, CH	5.62, dd (8.4, 15.7)	22,24	22, 24, 28	21,28
24	44.6, CH	2,07, m	22,23,28	22,23, 25	22,23,26,28
25	34.1, CH	1.57, m	24,26,27	24,26,27,28	26,27,28
26	20.3, CH_3	0.88, d (7.0)	25	24,25,27	25,28
27	20.0, CH_3	0.86, d (7.0)	25	24,25,26	25
28	18.0, CH_3	1.01, d (7.0)	24	23,24,25	23,24,26

Aside from the sterols, two isocyanide containing xanthocillin derivatives, xanthocillin X dimethylether (**12**) and xanthocillin X monomethylether (**13**) formerly obtained from strains of *Aspergillus sp.*[129] and *Dichotomomyces cejpii* (formely known as Dichotomomyces albus)[130], respectively, could be re-islolated by us. The structure of both compounds were elucidated on the basis of detailed ^{1}H and ^{13}C NMR data comparison with literature values.[131–133]

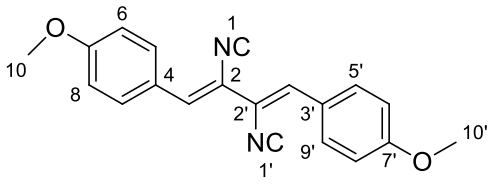

xanthocillin X dimethylether (**12**)

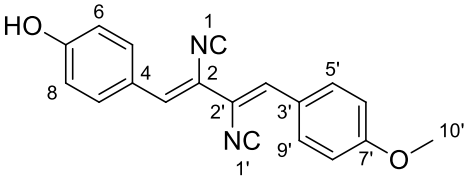

xanthocillin X monomethylether (**13**)

Figure **4-28**: Structure of isolated xanthocillin X derivatives.

Table **4-14**: NMR spectroscopic data (300 MHz) for compound **12** and **13**.

	Xanthocillin X dimethylether (12) (chloroform-*d*)		**Xanthocillin X monomethylether (13)** (acetone-*d6*)	
position	δ_C , mult.	δ_H (*J* in Hz)	δ_C , mult.	δ_H (*J* in Hz)
1	173.1, C	-	175.2, C	-
1’	173.1, C	-	175.0, C	-
2	127.4, CH	-	116.1, C	-
2’	127.4, CH	-	116.1, C	-
3	124.7, C	7.01, s	128.1, CH	7.11, s
3’	124.7, C	7.01, s	128.7, CH	7.10, s
4	125.8, C	-	125.8, C	-
4’	125.8, C	-	125.8, C	-
5	131.7, CH	7.78, d (8.8)	132.9, CH	7.82, d (8.8)
5’	131.7, CH	7.78, d (8.8)	132.6, CH	7.89, d (8.8)
6	114.4, CH	6.98, d (8.8)	114.4, CH	7.00, d (8.8)
6’	114.4, CH	6.98, d (8.8)	114.4, CH	7.09, d (8.8)
7	161.0, C	6.98, d (8.8)	116.8, C	7.00, d (8.8)
7’	161.0, C	6.98, d (8.8)	115.3, C	7.09, d (8.8)
8	114.4, CH	7.78, d (8.8)	116.8, CH	7.00, d (8.8)
8’	114.4, CH	7.78, d (8.8)	115.3, CH	7.09, d (8.8)
9	131.7, CH	7.78, d (8.8)	132.9, CH	7.82, d (8.8)
9’	131.7, CH	7.78, d (8.8)	132.6, CH	7.89, d (8.8)
10	55.4, CH_3	3.87, s	-	-
10’	55.4, CH_3	3.87, s	55.8, CH3	3.89, s

16-O-desmethylasporyergosterol-ß-D-mannoside (**9**): white amorphous compound (5.0 mg; 0.5 mg/L); $[\alpha]_D^{25}$ + 40.8 (c 0.34, MeOH); UV (MeOH) λ_{max} (log ε) 252 (3.65) nm; IR (ATR) ν_{max} 3389, 2938, 1681, 1366, 1305, 1136, 1053, 1021, 844, 668 cm^{-1}; ^{1}H and ^{13}C NMR data (see Table 4-11); ESI-MS *m/z* 590 $[M+NH_4]^+$, 631 $[M+HAc-H]^-$; HRESI-MS *m/z* 595.3603 $[M+Na]^+$ (calcd. for $C_{34}H_{52}O_7Na$, *m/z* 595.3611).

16-O-desmethylasporyergosteron-ß-D-mannoside (**10)**: yellowish white amorphous compound (2.0 mg; 0.2 mg/L); $[\alpha]_D^{25}$ + 26.5 (c 0.17, MeOH); UV (MeOH) λ_{max} (log ε) 246 (3.77), 344 (3.73) nm; IR (ATR) ν_{max} 3361, 2959, 1642, 1584, 1376, 1202, 1072, 668, 631 cm-1; ^{1}H and ^{13}C NMR data (see Table 4-12); ESI-MS m/z 569 $[M+H]^+$, 627 [M+HAc-H]-; HRESI-MS *m/z* 591.3293 [M+Na]+ (calcd. for $C_{34}H_{48}NO_7Na$, m/z 591.7305).

16-O-desmethylasporyergosterol (**11**): yellowish amorphous compound (3.0 mg; 0.3 mg/L). $[\alpha]_D^{25}$ + 145.4 (c 0.25, MeOH); UV (MeOH) λ_{max} (log ε) 252 (3.90) nm; IR (ATR) ν_{max} 3426, 2923, 1735, 1655, 1418, 1386, 1237, 1180, 1051, 979, 878 cm^{-1}; ^{1}H and ^{13}C NMR data (see Table 4-13); ESI-MS *m/z* 411 $[M+H]^+$, 469 $[M+HAc-H]^-$; HRESI-MS *m/z* 433.3070 $[M+Na]^+$ (calcd. for $C_{28}H_{42}O_2Na$, 433.3083).

Xanthocillin X dimethylether (12): yellow needles (20.0 mg 2 mg/L). UV (MeOH) λ_{max} (log ε) 242 (3.27) 366 (3.80) nm; IR (ATR) ν_{max} 2931, 2117, 1599, 1508, 1462, 1355, 1177, 1025, 876, 825, 779 cm-1; ^{13}CNMR data (see Table 4-14); ESI- MS *m/z* 317 $[M+H]^+$, 334 $[M+NH_4]^+$, 349 $[M+CH_3OH]^+$.

Xanthocillin X monomethylether (13): yellow needles (1 mg 0.1 mg/L). ^{11}H and ^{13}C NMR data (see Table 4-14); ESI- MS *m/z* 303 $[M+H]^+$, 301 $[M-H]^-$.

4.3.4 Biological activities of isolated sterols and xanthocillin X derivatives

We evaluated the steroid glycosid 16-O-desmethylasporyergosterol-ß-D-mannoside (**9**) and the isonitrile xanthocillin X dimethylether (**12**) in an Alzheimer's disease cellular assay. Neither compound **9** nor **12** displayed relevant cytotoxic effects at a concentration of 10 µM (Figure 4-29) in N2a cells, which were transfected with human APP695. Then, the compounds were tested for their ability to induce amyloid β-42 production in N2a-APP695 cells in comparison to the known amyloid β-42 production inducer Aftin-5. Neither compound **9** nor **12** induced amyloid β-42 production (±0.75 and ±0.8 fold change, respectively) in comparison to cells treated solely with Aftin-5 (±6.3 fold change) (Figure 4-30). In a further experiment 100 µM Aftin-5 was used to induce amyloid β-42 production in N2a-APP695, and whether a pretreatment with compound **9** or **12** could inhibit this amyloid β-42 production.

Both, 16-O-desmethylasporyergosterol-ß-D-mannoside (**1**) and xanthocillin X dimethylether (**12**) reduced Aβ-42 production in Aftin-5 treated cells (Figure 4-31). This activity was further confirmed in dose-response (0.1, 0.33, 1, 3.3 and 10 µM) experiments. (Figure 4-28) This effect was compared to that of N-[N-(3,5-difluorophenylacetyl)-l-alanyl-]-(S)-phe-nylglycine-t-butylester (DAPT), a known inhibitor of Aβ-42 production. Cells solely treated with 100 µM Aftin-5 displayed a fold change (i.e. amount of Aβ peptides produced by treated cells compared to the Aβ peptides produced by untreated cells) about ±9.4 while a pretreatment with 10 µM of compound **9** , **12** and DAPT reduced fold change to ±3.8, ±2.9, ±0.3, respectively. Compound **9** and **12** therefore displayed a moderate Aβ-42 lowering activity, but the effect was rapidly lost upon dilution of the compound.

Further characterizations of compound **9** and **12** are advised to assess the potential of these compounds as Aβ-42 lowering agents. Such studies should investigate in which way these compounds interact with β- or γ-secretases, and if they belong to the group of secretase inhibitors or modulators. If they act as secretase inhibitors it would be important to know, if substrate selectivity is provided by one of these compounds.

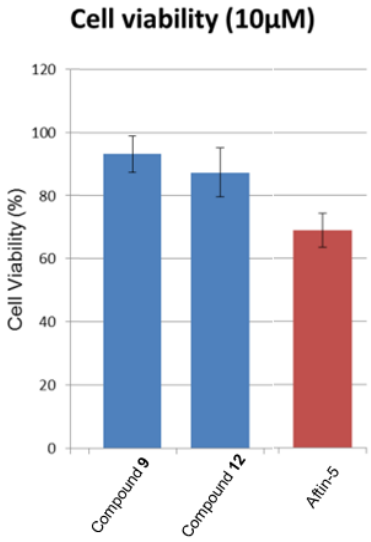

Figure **4-29**: MTS cell survival assay

Effects of compound **9**, **12** and Aftin-5 on N2a-APP695 cell viability

Compounds (in blue) were tested at 10 µM. As control, Aftin-5 (in red) was tested at 100 µM**.**

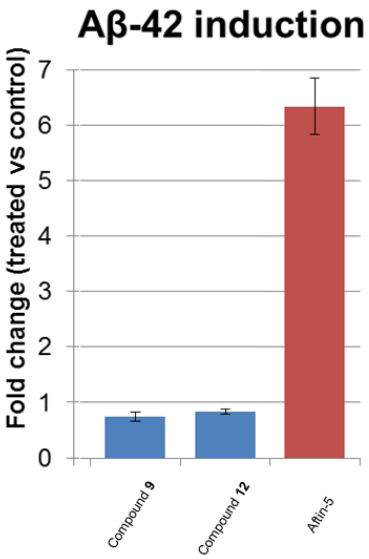

Figure **4-30**: Inducing of Aβ-42 production

Amyloid β-42 inducing activity of compound **9** and **12**, compared to 100 µM of the reference compound Aftin 5. Compounds (in blue) were tested at 10 µM. Results are expressed as fold change ± s.d. The fold change was calculated by dividing the amount of Aβ peptides produced by treated cells by the of Aβ peptides produced by untreated cells. All experiments were performed in triplicate.

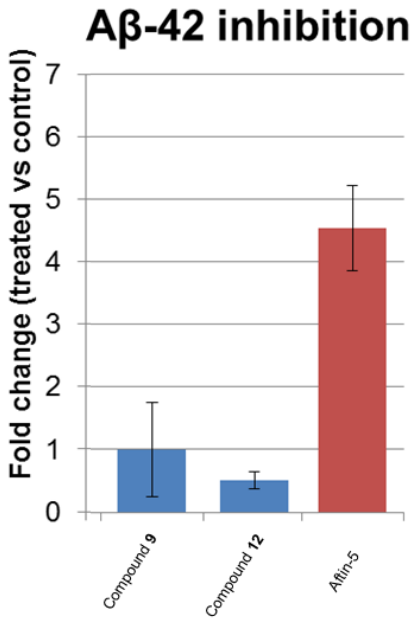

Figure **4-31**: Initial screening; Influence of samples on Aβ-42 production

Reduction of Aβ-42 production, induced by a treatment with 100 µM of Aftin-5, in the presence of compound **9** and **12** at 10 µM**.** Results are expressed as fold change ± s.d. The fold change was calculated by dividing the amount of Aβ peptides produced by treated cells by the of Aβ peptides produced by untreated cells. All experiments were performed in triplicate.

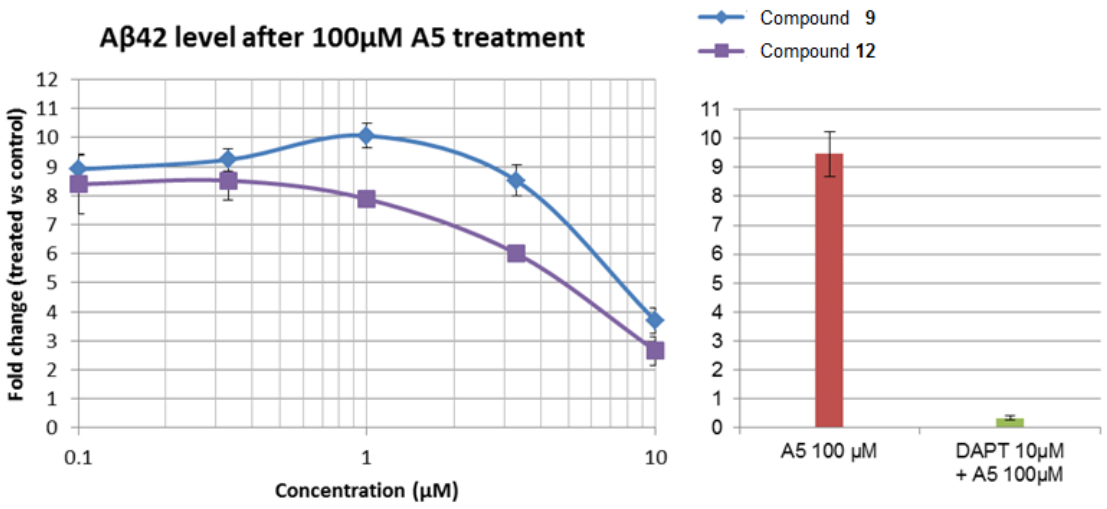

Figure **4-32**: Reduction of Aβ-42 production: Dose response

Reduction of Aβ-42 production, induced by treatment with 100 µM of Aftin-5. Compound **9** (blue line) and **12** (violet line) were tested and activity was confirmed in dose-response. Control with 100 µM Aftin-5 (red bar), an activator of Aβ-42 production and 10 µM DAPT (green bar), an inhibitor of Aβ-42 production. Results are expressed as fold change ± s.d. The fold change was calculated by dividing the amount of Aβ peptides produced by treated cells by the of Aβ peptides produced by untreated cells. All experiments were performed in triplicate.

4.3.5 Discussion of isolated sterols and xanthocillin X derivatives and their biological activities

Biological activity

Recently, the natural product derived triterpenoid glycoside 24-O-acetylhydroshengmanol 3-O-β-D-xylopyranoside-Δ16,17-enol ether (IC_{50} of 0.1 μM towards Aβ42) and its further developed derivatives like SPI-1865 (IC_{50} of 0.1 μM towards Aβ42) have been identified as GSMs.[134,135] This triterpene-based γ-secretase modulators gained a lot of interest, because they possess an unusual profile, when compared to other GSMs, in that they raise Aβ37 and Aβ39 and lower Aβ37 and Aβ42 levels. In contrast to that, common GSMs usually solely reduce Aβ42 and increase Aβ37 and Aβ38 production.[135]

Subtle differences between GSMs, regarding the modulation of AβP-subspecies production, are considered to be maybe therapeutically important and could display different biological activity profiles.[125] Aside from Alzheimer disease, Aβ-42 lowering agents are also considered as therapeutics for further indications, e.g. various cancers or macular degeneration.[125] The potential of Aβ-42 lowering agents is immense and for the diverse indications, different anti Aβ agents with distinct properties could be beneficial.

Therefore, the improved characterization of existing, and the identification of further Aβ-42 lowering agents can be very valuable for future drug development. The development of triterpenoid GSMs illustrates the potential of natural products as lead structures and our results confirm that screening of natural compounds, like **9** and **12,** is a valuable strategy to find new active compounds, which could be used for further investigation of the pathophysiology of Aβ42 related diseases and drug development.[134]

4.4 Isolation of thiodiketopiperazines and evaluation for activities toward nuclear receptors

4.4.1 Introduction to the role of nuclear type II receptors

Nuclear receptors (NRs) are a family of ligand-regulated transcription factors.[136] Their ligands can cross plasma membranes, and their subsequent interaction with NRs then alters the transcription of a spectrum of genes. The latter control a wide range of biological processes, like reproduction or metabolism.[136,137]

Nuclear receptors share a common basic structure and are composed of 6 domains. The well conserved E domain contributes to ligand binding and is also called ligand binding domain (LBD). There are four types of nuclear receptors, i.e. type I-IV. Among these, type II receptors reside bound in the nucleus and generally form heterodimers with the retinoid X receptor (RXR). Without ligand interaction they induce repressive functions via bound co-repressor complexes. Whereas binding of ligands to the LBD replaces co-repressors by co-activator complexes and induce individual receptor functions. Because they bind to small molecules, NRs represent promising therapeutic targets for a range of disorders, for which selective agonists and antagonist can be engineered. [138,137]

Peroxisome proliferator-activated receptors (PPAR) or Liver X receptors (LXR) are prominent, well investigated representatives of type II NRs. There are three known PPAR subtypes (PPARα, PPARβ/δ and PPARγ). A multitude of divers endogenous PPAR ligands, derived from fatty acid and lipid metabolism, have been identified.[139]

PPARα plays an important role in the hepatic lipid metabolism.[140] PPARα agonists like fibrates are already used as hypolipidemic agents. However, the use of PPARα agonist is challenged by safety concerns regarding potential side effects like renal dysfunction or rhabdomyolysis and unsatisfactory clinical outcome and health benefits. It is uncertain if these effects are derived from specific toxicity of the individual investigated compound or a general adverse effect of PPARα activation.[140,141] More potent and selective PPARα agonist are therefore investigated for the treatment of hyperlipidaemia in the hope to achieve more robust benefits with less unwanted side effects.[140–142]

PPARsβ/δ are almost ubiquitously expressed, but show particular high levels inter alia in adipocytes, skeletal muscles and heart.[143] PPARβ/δ activation has demonstrated anti-inflammatory effects which are connected to increased insulin sensitivity of adipose tissues.

Anti-obese effects are correlated to PPARβ/δ activity as well. Therefore a potential use of PPARβ/δ agonists for the treatment of metabolic syndrome is supposed.[143] Furthermore PPARβ/δ plays an important role in muscle fatty acid metabolism and muscle development. PPARβ/δ agonists are therefore suggested as potential therapeutical treatment in muscle degenerative diseases and heart failures, which are often associated with reduced myocardial fatty acid oxidation.[143] However controversial results of pro-tumorigenic effects in different cancer cell lines induced by PPARβ/δ activation, raise safety concerns which have to be clarified.[143]

PPARγ plays an important role for the insulin sensitivity in numerous tissues.[136] These effects are already therapeutically addressed by thiazolidones, like pioglitazone in the treatment of type II diabetes, where insulin sensitivity is usually reduced. Due to side effects of the known PPARγ agonists, like increased risk for heart failures and bone fractures, their therapeutically use is restricted and safer PPARγ agonists are desired.[136] Therefore selective PPARγ modulators (SPPARγMS) like SR1664 are supposed to have improved side effect profiles and are considered to have the chance to revival the role of PPARγ ligands in the therapeutical treatment of type 2 Diabetes.[136,138]

Liver X receptors LXRα and LXRβ are inter alia important regulators of cholesterol, lipid and glucose metabolism.[144,145] LXRα is highly expressed in liver, adipose tissue and macrophages, whereas LXRβ is expressed more widespread in distinct tissues.[144] Endogenous ligands are oxidized cholesterol derivatives (oxysterols), like e 22(R)-hydroxycholesterol.[136] Targeting LXR has demonstrated to possess therapeutic potential in the treatment of atherosclerosis, diabetes, cancer, cardiovascular disease, autoimmune disorders, and Alzheimer disease[136,146–151] However, synthetic unselective LXR ligands have shown to have problematic side effects, like hypertriglyceridemia induced by activation of SREBP1 expression, which limit their application.[136] To avoid these problems, further development of LXR agonist, which display selectivity for the LXRα or LXRβ subtype or act as LXR modulators is desired.

We evaluated a group of nontoxic gliotoxin derivatives and one nonadride for agonistic effects toward several type II nuclear receptors (PPAR subtype α, β/δ and γ and LXR subtype α and β).

4.4.2 Isolation of compounds 14–17 from *Dichotomomyces cejpii*

Bioassay- and chemical (LC-MS and ^{1}H NMR)-guided fractionation of the crude extracts, obtained from the marine derived fungus *Dichotomomyces cejpii* on cultivation medium 1 yielded four thiodiketopiperazines (**14–16**) and the nonadride heveadride (**17**)**.** The investigated fungal strain was cultivated on cultivation medium 1 as described before (3.2.2–3.2.3) Fungal biomass and media were homogenized using an Ultra-Turrax apparatus and extracted with 5 L EtOAc to yield 4.1 g of crude extract. This material was fractionated by NP vacuum liquid chromatography (VLC) using a stepwise gradient solvent system of increasing polarity starting with 100% CH_2CL_2 to 100% EtOAc and to 100% MeOH which yielded 10 fractions. Fraction 2 was separated via NP VLC, using stepwise elution with CH_2Cl_2-petroleum ether (50-50) to 100% CH_2Cl_2, and 100% MeOH which yielded 15 fractions. VLC fraction 1 contained compounds **14–17** and was distributed between hexane (100%) and MeOH-H_2O (60-40) using a solvent/solvent extraction three times. The methanolic phase was further separated using a RP_{18} VLC column and eluted stepwise with H_2O-MeOH (80-20) to 100% MeOH, 100% CH_2CL_2 which yielded 8 fractions. Subfraction 1.3 was further separated with a second NP VLC column, eluted stepwise with petrolether-acetone (95-5), to 100% acetone, and acetone-MeOH (50-50) which yielded 8 fractions. Subfraction 1.3.3 contained compound **14**–**17**.

Compound **14** (6-acetylmonodethiogliotoxin) was isolated from subfraction 1.3.3 via NP-HPLC system D (Eurosphere II, 250mm x 4.6 mm) with petroleum ether-acetone (85-15), 1.0 mL/min as a yellowish white powder, t_R: 22 min (19.5 mg).

Compound **15** was found in VLC fraction 4 and subfraction 1.3.3. Subfraction 1.3.3 was separated as described above and compound **15** (6-acetylbisdethiobis(methylthio)gliotoxin) was obtained as yellowish white powder, t_R: 30.2 min (98.9 mg). Minor amounts were isolated from VLC fraction 4 via RP_8-HPLC system D (Eurosphere II, 250mm x 8mm) with H_2O-MeOH (50-50), 1.5 ml/min, t_R: 15.5 min (4.5 mg).

Compound **16** was obtained from subfraction 1.3.3, as well, which was in a first round separated as described above. From this separation, subfraction 1.3.3.3 (t_R:18.2 min) resultated, and was further purified using NP-HPLC system D (Eurosphere II, 250mm x 4.6 mm) with petroleum ether-acetone (90-10), 1.0 mL/min and compound **16** (5a,6-anhydrobisdethiobis(methylthio)gliotoxin) was isolated as yellowish white powder, t_R: 33.5 min (4.6 mg).

Compound **17** was found in subfractions 1.3.1, 1.3.2 and 1.3.3. Subfraction 1.3.1 was separated with NP-HPLC system D (Eurosphere Si, 250mm x 8mm) using petrolether-acetone (90-10), flow 1.0. The resulting subfraction 1.3.1.3, t_R: 8.0 min was further purified via RP_{18}-HPLC system B with (Nucleodur 250 x 4.6mm) H_2O-CH_3CN (43-57), flow: 1.7 ml/min, t_R: 8.0 min to obtain heveadride (**17**) (30.0 mg). Subfraction 1.3.2 was purified via NP-HPLC system D (Eurosphere Si, 250mm x 8mm) with petrolether-acetone (90-10), flow 1.0, t_R: 8.0 min and heveadride (**17**) was isolated as white powder (35.0 mg). Subfraction 1.3.3 was separated via NP-HPLC system D (Eurosphere II, 250mm x 4.6 mm) with petroleum ether-acetone (85-15), 1.0 mL/min and heveadride (**17**) was isolated as white powder, t_R: 6.0 min (12.9 mg).

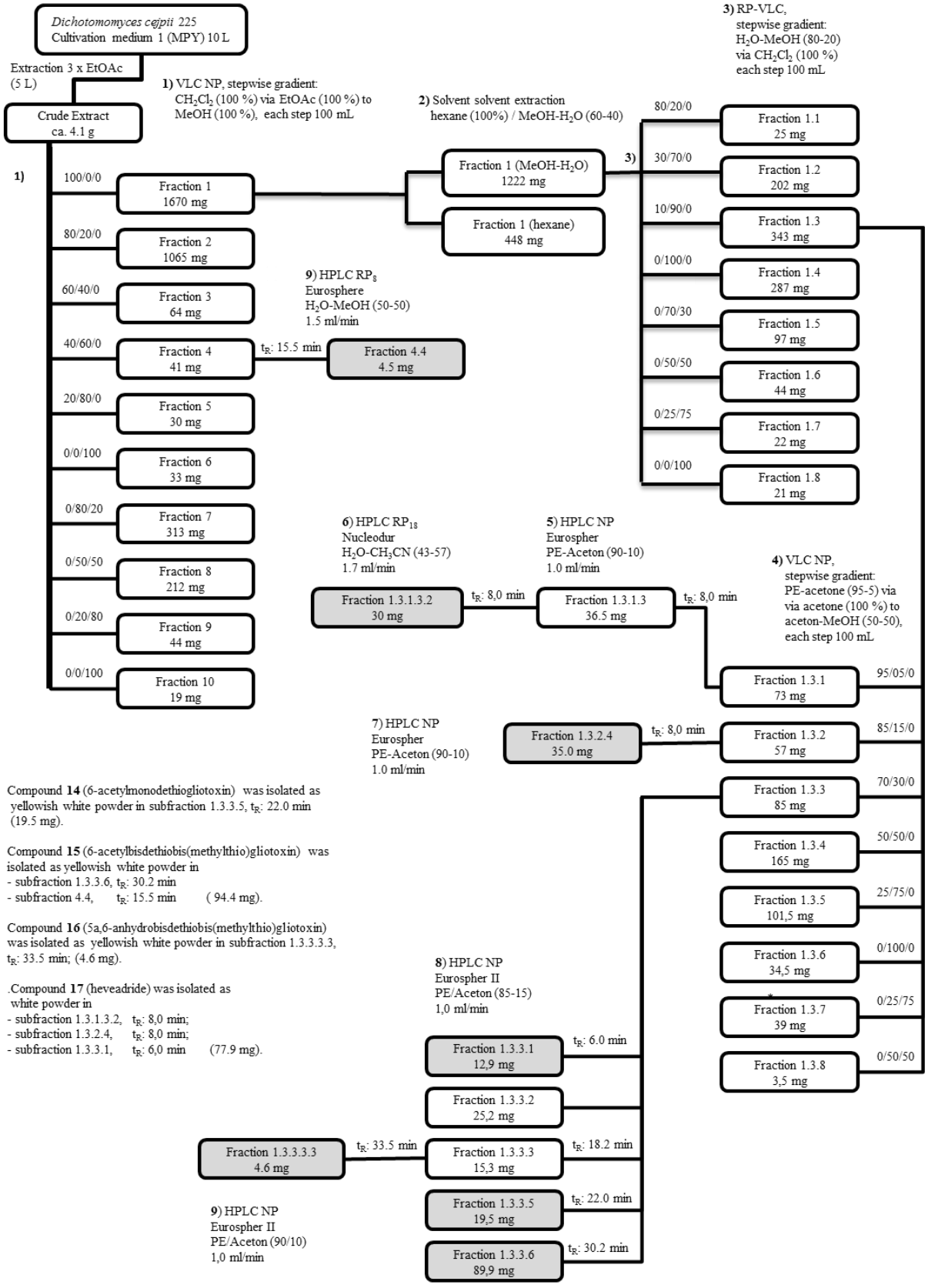

Figure 4-33: Isolation scheme for compounds **14–17**. For reasons of clarity only the most important fractions are listed.

4.4.3 Structure elucidation of isolated thiodiketopiperazines and heveadride

Compound **14** was obtained from the marine sponge-derived fungus *D. cejpii* and its structure was elucidated via intensive analysis of spectroscopic data. A UV maximum at 262 nm evidenced the presence of a conjugated $\pi \rightarrow \pi^*$ system. A broad IR absorption at 3425 cm^{-1} pointed toward a hydroxyl group, while a strong IR absorption at 1722 cm^{-1}, arising from C=O stretching frequencies, indicated an ester moiety. The molecular formula of compound **14** was deduced from the results of an accurate mass measurement (HRESIMS, *m/z* = 359.0672 $(M+Na)^+$ as $C_{15}H_{16}N_2O_5S$, implying ten degrees of unsaturation. The ^{13}C NMR and DEPT135 spectra denoted the presence of 15 resonances for two methyl groups, two sp^3 methylene groups, three sp^2 methine, two sp^3 methine, and six quaternary carbons in the molecule (Table 4-15).

The first substructure was deciphered as a cyclohexadiene by interpreting ^1H-^1H COSY correlations from H-5a through to H-9, and HMBC cross peaks between the resonances for H-9 and C-9a, C-5a, C-6, C-7 and C-8. The two conjugated carbon-carbon double bounds within this substructure could be assigned as $\Delta^{7,8}$ and $\Delta^{9,9a}$ due to the ^{13}C NMR chemical shifts of the respective carbon atoms (127.1/125.7, 119.5/137.4 ppm). The methine group CH-6 resonated at δ_H 5.87 and δ_C 74.9, indicating a substitution with oxygen at this site. Due to the ^{13}C NMR chemical shift 172.1 ppm, C-12 was assigned to be part of a carbonyl group. HMBC correlations arising from the resonance of CH_3-13 to C-12, as well as to CH-6 established that an acetyl group was linked via the oxygen atom at CH-6.

An extension of this first substructure was possible taking HMBC cross peaks between the resonances for the methylene group CH_2-10 to C-9a on one side, and to C-10a and C-1 on the other side into account. The ^{13}C NMR chemical shifts of C-10a (δ_C 82.5) and of the protons and carbon atoms of the methine group CH-5a (δ_H 4.60, δ_C 61.6), indicated a substitution with a heteroatom at these sites, whereas C-1 was a carbonyl (δ_C 174.2). CH_3-11 resonating at 3.02 and 27.8 ppm, respectively had to be linked to nitrogen. HMBC cross peaks between the resonances for this methyl group to the carbonyl carbon atoms C-1 thus revealed an amide bond. A second amide was obvious when considering the ^{13}C NMR chemical shift (δ_C 170.5) for C-4. ^1H NMR chemical shifts of δ_H 4.30 and 4.17 for the geminal methylene protons 3a' and 3a'' indicated the presence of a $-CH_2OH$ moiety. Regarding HMBC cross peaks between the resonances for these methylene group protons CH_2-3a to carbon C-3 and C-4, and of CH_3-11 to C-1 and C-3, the second substructure from C-1 through to C-4 (including C-11) could

be deduced, which was linked via N-5 to the first substructure. Compound **14** thus is a diketopiperazine with a dihydro-indoline moiety.

The molecular formula indicated the presence of one single sulphur atom within the molecule, and also two double bond equivalents were still to be accounted for. The sulphur atom was assigned to form a sulphur bridge between carbon C-10a and C-3, due to the ^{13}C NMR chemical shift of the respective carbons (C-3: 80.4 ppm, C-10a: 82.5 ppm). This is comparable to the disulfide bridge in the related compound gliotoxin (C-10a and C-3: δ_C 77.3 and 77.5, respectively).[152–154] Overall, this structural arrangement of **14** is consistent with the established structures of gliotoxin-type metabolites and with recent biosynthetic evidence for this class of compounds.[155,156]

The relative configuration was deduced on the basis of a NOESY experiment and the magnitude of significant ^{1}H-^{1}H coupling constants. The coupling constant of $J_{H\text{-}5a/H\text{-}6}$ = 13.2 Hz indicated that both protons are orientated 180 ° to each other, i.e. H-6 is axial and α-orientated whereas the axial H-5 is β-orientated. NOESY correlations between H-3a'', H-5a and H-10' indicated that these protons are located on the same side, of the molecule, whereas NOESY correlations between H-3a', H-6 and H-10'' proved the opposite orientation for these substituents. This again confirmed that proton H-5a and H-6 are trans orientated to each other. The configuration at the quaternary carbon C-10a could not be determined. We assume it to be as that of the co-occurring 6-acetylbisdethiobis(methylthio)gliotoxin (**2**) with the same basic structural arrangement.[23,24] Furthermore the fungus *D. cejpii* is a known producer of gliotoxin for which the absolute configuration had been determined and confirmed by biosynthetic evidence, the latter demonstrating the necessity of this configuration.[153,154,156,157] The fungal metabolite **14** is thus a naturally occurring gliotoxin derivative with the untypical feature of a single sulphur atom bridge. We suggest the trivial name 6-acetylmondodethiogliotoxin for **14**.

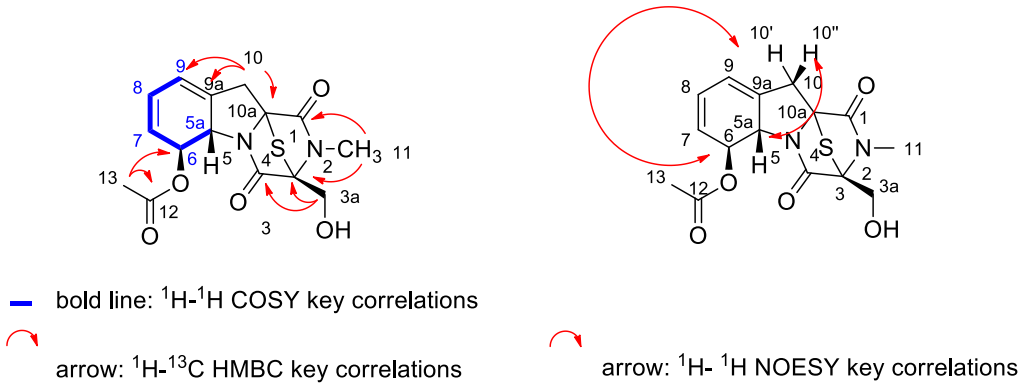

Figure **4-34**: NMR key correlations of compound **14**

Aside from **14**, a further gliotoxin derivative, an acetylated dithiodiketopiperazine with two methylthio substituents, i.e. 6-acetylbisdethiobis(methylthio)gliotoxin (**15**) was isolated for the first time as a natural product. The structure of **15** was elucidated on the basis of detailed ^{1}H and ^{13}C NMR data (Table 4-16) and comparison with literature values of the semi-synthetically obtained compound.[158] ^{1}H NMR values of **15** match very well with literature data. There were slight differences, however between the here observed ^{13}C NMR resonances for carbon C-3 and literature values (+3.6 ppm). These differences may be explained by the fact that reported literature ^{13}C NMR data had been determined only indirectly via HMBC correlations. Furthermore, it is known that NMR data of gliotoxin and its derivatives are strongly influenced by temperature and solvent.[154] Mass spectral data are according to the here shown structure and literature data.

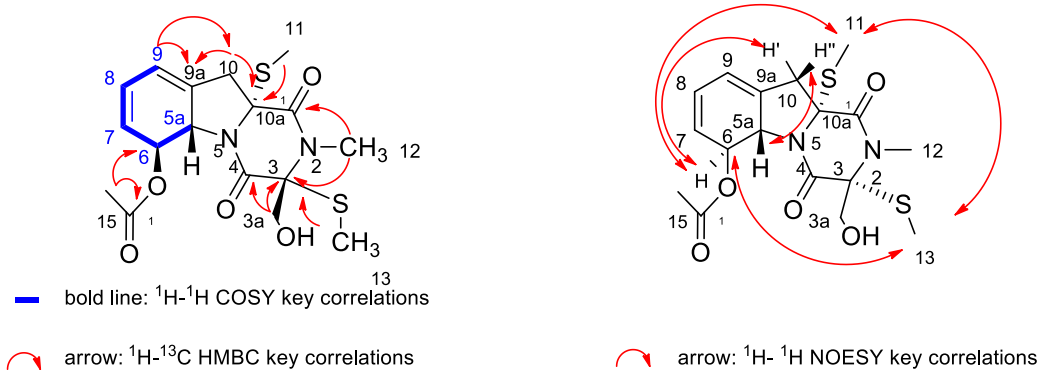

Figure **4-35:** NMR key correlations of compound **15**

5a,6-anhydrobisdethiobis(methylthio)gliotoxin (**16**) an aromatic gliotoxin derivative similar to compound **15** could also be isolated for the first time as a natural product during this study. The structure of **16** was elucidated on the basis of detailed ^{1}H and ^{13}C NMR data (Table 4-17) and comparison with literature values for the formerly semi-synthetically produced compound.[159,160]

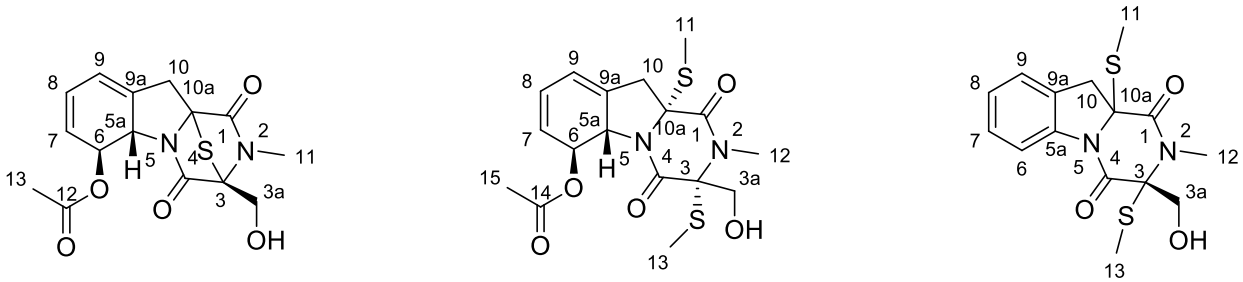

6-acetylmonodethiogliotoxin (**14**) 6-acetylbisdethiobis(methylthio)gliotoxin (**15**) 5a,6-anhydrobisdethiobis (methylthio)gliotoxin (**16**)

Figure **4-36**: Structure of isolated thiodiketopiperazines (**14**–**16**)

Table **4-15**: NMR Spectroscopic Data (300 MHz, methanol-d_4) for 6-acetylmonodethiogliotoxin (**14**)

Position	δ_C , mult	δ_H (J in Hz)	^{1}H -^{1}H COSY	^{1}H-^{13}C HMBC	^{1}H -^{1}H NOESY
1	174.2, C	-	-	-	-
2	N	-	-	-	-
3	80.4 , C	-	-	-	-
3a	58.0, CH_2	3a': 4.30, d (13.2)	3a''	3,4	3a'',5a
		3a'': 4.17, d (13.2)	3a'	3,4	3a',6
4	170.5, C	-	-	-	-
5	N	-	-	-	-
5a	61.6, CH	4.60, d (13.2)	6,7,8,9,10',10''	6,9a	3a',7,8,9,10',13
6	74.9, CH	5.87, d (13.2)	5a 7,8,9	5a,7, 8,9,9a, 10	3a'',7,8,9,10'',13
7	127.1, CH	5.57, dd (5.9, 13.2)	5a,6,8,9	5a,6,8,9	5a,6,8,9
8	125.7, CH	6.05, m	5a,6,7	5a,6,7,9,9a,	5a,6,7,11
9	119.5, CH	6.03, m	5a,6,7,10',10''	5a,6,7,8,9a,10	5a,6,7,11
9a	137.4, C	-	-	-	-
10	29.5, CH_2	10': 3.52, d (18.3)	5a, 9,10''	5a,1,9,9a,10a	5a,10''
		10'':2.98 br d	5a,9,10'	5a,1,9,9a,10a	6,10'
10a	82.5, C	-	-	-	-
11	27.8, CH_3	3.02, s	-	1,3	8,9
12	171.3, C	-	-	-	-
13	21.2, CH_3	2.16, s	-	3,6	5a,13

Table **4-16**: NMR Spectroscopic Data (300 MHz, methanol-*d4*) for 6-acetylbisdethiobis(methylthio)gliotoxin (**15**)

Position	δ_C , mult	δ_H (J in Hz)	^1H -^1H COSY	^1H-^{13}C HMBC	^1H -^1H NOESY
1	168.6, C	-	-	-	-
2	N	-	-	-	-
3	75.4, C	-			
3a	64.6, CH_2	3a' : 4.17, d (11.3)	3a''	3,4	3a'',12,13
		3a'' : 3.76, d (11.3)	3a'	3,4	3a',10',12
4	166.1, C	-	-	-	-
5	N	-	-	-	-
5a	67.1, CH	5.21, d (13.9)	6,7,10',10''	9a	7,8,9,10''
6	76.6, CH	6.28, d (13.9)	5a,7,8	5a,7, 9,10,14,15	7,8,9,10',11,13,15
7	128.4, CH	5.58, m	6,7,9,10''	6,9	5a,6,7,9,10',15
8	126.7, CH	6.07, m	5a,6,8,10''	9	5a,6,8,11,13
9	120.6, CH	6.04, m	5a,6,7,8,10',10''	5a,6,7,8,9a,10'	5a,6, 10',11,13
9a	135.9, C	-	-	-	-
10	40.9, CH_2	10': 3.13, d (15.4)	5a,10''	5a, 9a, 10a, 10''	6, 7, 8, 9, 10'', 11
		10'': 2.91, d	5a,7,9,10'	5a, 9, 9a, 10a, 10'	5a, 10'
10a	74.4, C	-	-	-	-
11	15.0, CH_3	2.33, s	-	10a	6,7,9,10',13
12	29.2, CH3	3.09, s	-	1,3,3a	3a',3a'',13
13	12.9, CH_3	2.24, s	-	3	6,7, 9,10',11,12
14	172.6, C	-	-	-	-
15	21.4, CH_3	2.13, s	-	6,14	6,8

Table **4-17**: NMR Spectroscopic Data (300 MHz, acetone-*d6*) for 5a,6-anhydrobisdethiobis(methylthio)gliotoxin (**16**)

Position	δ_C , mult	δ_H (J in Hz)	^1H -^1H COSY	^1H-^{13}C HMBC	^1H -^1H NOESY
1	166.3, C	-	-	-	-
2	N	-	-	-	-
3	73.2, C	-			
3a	64.8, CH_2	3a' : 4.42, dd (4.0, 12.1)	3a''	-	3a'',13
		3a'' : 3.95, dd (4.0, 12.1)	3a'	3,4	3a',12
4	162.9, C	-	-	-	-
5	N	-	-	-	-
5a	142.4, C	-	-	-	-'
6	118.3, CH	8.02, d (7.3)	7	5a,8	7
7	128.3, CH	7.30, dd (7.3, 7.7)	6,8,9	5a,9a,8,9	8, 9
8	126.3, CH	7.19, dd (7.3, 7.7)	6,7,9	5a,6,7,9,9a	7,9
9	126.4, CH	7.39, d (7.3)	8,10	5a,10	8,10
9a	130.3, C	-	-	-	-
10	40.0, CH_2	3.55, d (5.5)	9	1,5a,9,9a,10a,	9,11
10a	71.6, C	-	-	-	-
11	14.4, CH_3	2.22, s	-	10a	10,13
12	28.9, CH3	3.15, s	-	1,3,3a	3a',13
13	13.5, CH_3	2.32, s	-	3	11,12,

Additionally heveadride (**17**), a nonadride, formerly obtained from strains of *Helminthosporium heveae* [161], could be re-isolated by us. The structure of **17** was elucidated on the basis of detailed ^1H and ^{13}C NMR and $[\alpha]_D^{25}$ data comparison with literature values.[161,162] (Table 4-18)

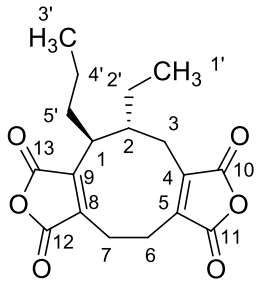

Figure **4-37:** Structure of isolated heveadride (**17**)

Table **4-18**: NMR Spectroscopic Data (300 MHz, acetone-d_6) for hevadride (**17**)

Position	δ_C , mult	δ_H (J in Hz)	^{1}H -^{1}H COSY	^{1}H-^{13}C HMBC
1	40.6, CH	2.94, m (4.4, 9.2, 18.7)	2,5'a,5'b	3a,3',4',5'a,5'b
2	48.9, CH	2.07, m	1,3a,3b,1',4',5'a,5'b	1,3a,3b,5'a,5'b
3	27.7, CH_2	3a: 2.74, dd (2.9, 13.2)	2,3b	1,2,6b
		3b: 2.26 t (13.2)	2,3a	1,2,6b
4	145.3, C	-	-	-
5	145.5, C	-	-	-
6	21.4, CH_2	6a: 2.97, m	2,6a,6b,7b	3,6a,6b
		6b: 2.49, m	2,6a,6b,7a	3,6a,6b
7	22.1, CH_2	7a. 3.03, dd (4.4, 12.8)	3a,3b,6b,7a,7b	6b,7a,7b
		7b:.2.55, m	3a,3b,6a,7a,7b	6a,7a,7b
8	146.0, C	-	-	-
9	148.0, C	-	-	-
10	166.8, C	-	-	-
11	166.6, C	-	-	-
12	166.7, C	-	-	-
13	166.2, C	-	-	-
1'	13.25, CH_3	1.03, d (6.2)	2,3,2'	2,2'a,2'b
2'	23.97, CH_2	2'a: 2.02, m	1',2'b	1,1',3a,3b
		2'b: 1.05, m	1,3,3',	1,1',3a,3b
3'	14.4, CH_3	0.80, t (7.3)	4',5'a,5'b	4',5'a,5'b
4'	21.9, CH_2	1.15, m	3',5'a,5'b	1,3',5'a,5'b,
5'	32.6, CH_2	5'a: 2.09 m	1,2,4'	1,3b,3',4'
		5'b: 1.58 m (5.5, 10.6)		

6-Acetylmonodethiogliotoxin (**14**): yellowish white amorphous compound (19.5 mg; 2.0 mg/L); $[\alpha]_D^{25}$ -4.9 (c 0.34, MeOH); UV (MeOH), λ_{max} (log ε) 203 (3.62), 262 (3.28) nm; IR (ATR) ν_{max} 3425, 2922, 1722, 1368, 1234, 1047, 877, 719,668, 628 cm^{-1}; ^{1}H and ^{13}C NMR data (see Table 4-15); ESI-MS *m/z* 337 $[M+H]^+$, 354 $[M+NH_4]^+$; HRESI-MS *m/z* 359.0672 $[M+Na]^+$ (calcd. for $C_{15}H_{16}N_2O_5SNa$, *m/z* 359.0678).

6-Acetylbisdethiobis(methylthio)gliotoxin (**15**): yellowish white amorphous compound (94.4 mg; 9.4 mg/L); $[\alpha]_D^{25}$ - 62.9 (c 0.28, MeOH); UV (MeOH), λmax (log ε) 203 (3.95), 269 nm (3.42) nm; IR (ATR) ν_{max} 3425, 2922, 1734, 1648, 1418, 1386, 1237, 1189, 1142, 1051, 979, 878, 668, 600, 534 cm-1; 1H and 13C NMR data (see Table 4-16); ESI-MS m/z 416 $[M+NH_4]^+$, 421 $[M+Na]^+$, 819 $[2*M+Na]^+$; HRESI-MS m/z 421.0801 $[M+Na]^+$ (calcd. for $C_{17}H_{22}N_2O_5S_2Na$, 421.0868).

5a,6-Anhydrobisdethiobis(methylthio)gliotoxin (**16**): yellowish white amorphous compound (4.6 mg; 0.5 mg/L). $[\alpha]_D^{25}$ -65.1 (c 0.36, MeOH); ^{1}H and ^{13}C NMR data (see Table 4-17); ESI-MS *m/z* 361 $[M+Na]^+$, 700 $[2*M+Na]^+$; HRESI-MS m/z 361.0662 $[M+Na]^+$ (calcd. for $C_{15}H_{18}N_2O_3S_2Na$, 361.0651).

Heveadride (**17**): white crystalline compound (77.9 mg; 7.8 mg/L). $[\alpha]_D^{25}$ + 20.9 (c 2.22, MeOH) [lit value $[\alpha]_D^{25}$ + 63 (c 1.19, CH_2Cl_2[161]]; ^{1}H and ^{13}C NMR data (see Table 4-18); ESI-MS *m/z* 333 $[M+H]^+$, 331 $[M-H]^-$.

4.4.4 Biological activities of isolated thiodiketopiperazines and hevadride

We evaluated the gliotoxin derivatives 6-acetylmonodethiogliotoxin (**14**) and 6-acetylbisdethiobis(methylthio)gliotoxin (**15**) as well as the nonadride derivative heveadride (**17**) for activity toward several nuclear receptors. None of the examined compounds displayed relevant cytotoxic effects at a concentration of 100 μM in K562 cells. (Figure 4-38) The compounds were tested for their agonistic activity towards several nuclear receptors, including PPAR subtype α, β/δ and γ as well as towards LXR subtype α and β. None of these compounds displayed agonistic activity toward PPAR subtype α, β and γ or LXRβ at or up to

a concentration of 125 µM or 80 µM respectively in comparison to known agonists (Table 4-19 and appendix).

In contrast, compound **14** demonstrated selective agonist activity toward LXRα. 40 µM of compound **14** were capable to activate the reporter system of LXRα. (Table 4-19 and Figure 4-39) This activity has to be judged as moderate, but is selective without relevant cytotoxic effects.

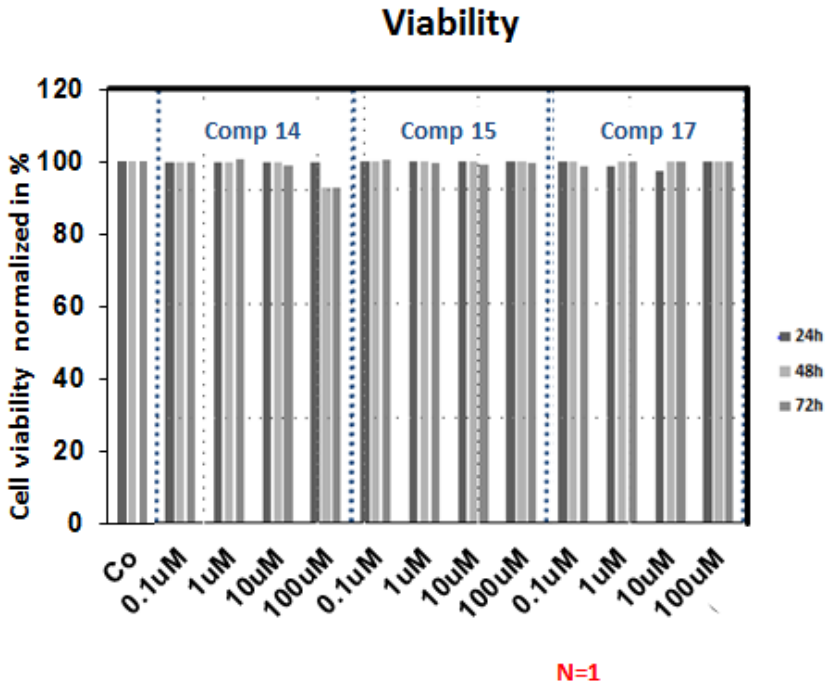

Figure **4-38:** Effect of fungal products on K562 cell viability (see 3.6.7.3)

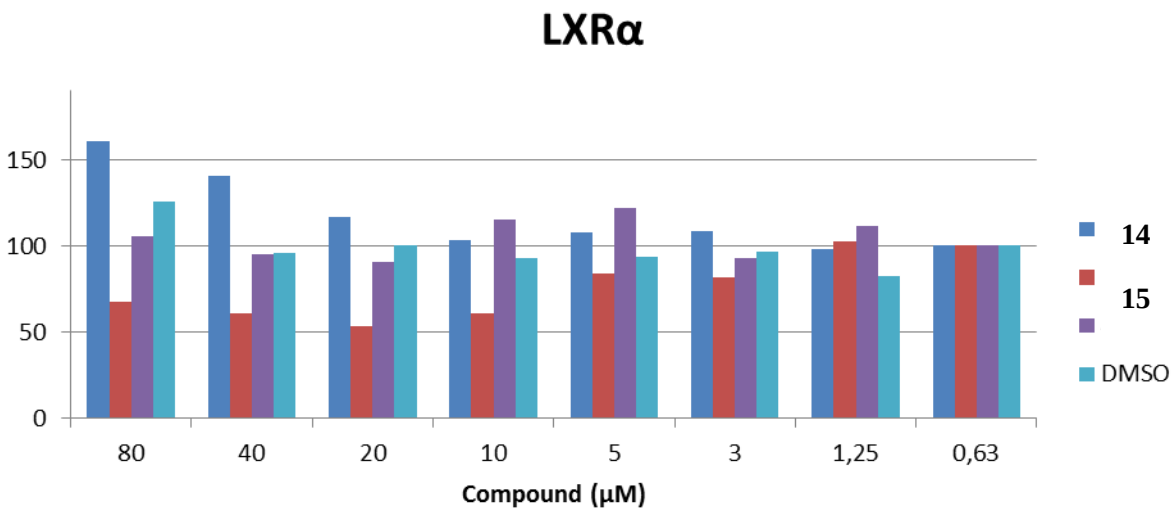

Figure **4-39:** Evaluation of Compounds **14**, **15** and **17** for LXRα agonist activity

Table **4-19**: Summary of compounds **14**, **15** and **17** for nuclear receptor agonist activity

	Activity and concentration (µM)			
Compound	PPARα	PPARβ/δ	LXRα	LXRβ
6-acetylmonodethiogliotoxin (**14**)	n.d.	n.d	**40**	n.d
6-acetylbisdethiobis(methylthio) gliotoxin (**15**)	n.d.	n.d.	n.d	n.d
heveadride (**17**)	n.d.	n.d.	n.d	n.d

4.4.5 Discussion of isolated epithiodiketopiperazine

Structural features

It is interesting to note, that monosulphides of gliotoxin derivatives have been obtained semi-synthetically from disulfid gliotoxin derivatives by reaction with tervalent phosphorus compounds, *e.g.* triphenylphosphine.[163] But up to our knowledge there is only the one example of emestrin-G, isolated from the fungus *Armillaria tabescens*, where such a bridged monosulphid was obtained directly by isolation as a natural product.[164]However 6-acetylmonodethiogliotoxin (**14**) has been isolated directly, without chemically treatment and reveals a new biosynthetic source for monosulphid gliotoxin derivatives.

Biological activity

Compound **14** demonstrated selective agonist activities toward LXRα and 40 μM of this compound were capable to activate the reporter system of LXRα.

A transannular sulphur bridge as present in compound **14** seems to be essential for this activity, as the related compound **15** without this feature did not display any activity. The finding of 6-acetylmonodethiogliotoxin with a monosulphide bridge is of importance, as this compound may serve as lead for the development of more potent and selective ligands for this therapeutically interesting nuclear receptor.

4.5 Overview of further bioactivity tests performed with isolated compounds

4.5.1 Antibiotic activities of pure compounds

11 out of 16 isolated secondary metabolites were evaluated for their antimicrobial activities in agar diffusion assays; the observed activities are summarized in Table 4-20 and 4-21. Two compounds were isolated with prominent activity against the Gram-negative bacterium *Eschericha coli*. Xanthocillin X monomethylether (**13**) exhibited explicit antibiotic activities against gram negative bacteria. The antibiotic activitiy of asporyzin C (**6**) was not determined in our institute, but was described in the literature by Qiao et al., 2010 where 30 µg/disk of asporyzin C displayed an inhibition diameter of 8.3 mm against *E. coli*.[102] Both compounds may explain the antibiotic activities of the crude extracts against *E. coli*. The two known isocyanide bearing compounds xanthocilin X mono- and dimethylether (**12** and **13**) demonstrated clear antibiotic activities against gram positive bacteria in form of *Bacillus megaterium* and the examined test fungi strains (Table 4-20). However the antibiotic activity of xanthocillin X monomethylether is according to literature data based on general unselective protein biosynthesis inhibition, that is accompanied by cytostatic or even cytotoxic effects which limit its therapeutical use as an antibiotical agent.[129,165] All examined indoloditerpenenes (**1**–**5**), including the newly isolated compounds **1**–**3**, display moderate activities against gram positive bacteria, like *Bacillus megaterium* and *Staphylococcus* spp.

The nonadride heveadride displays neglible antifungal activities against *Eurotium rubrum* whereat minor antifungal effects had been described before by Hosoe et al., 2004.[160]

According to literature other strains of *Dichotomomyces cejpii* have the ability to produce gliotoxin, a potent mycotoxin which displays antibacterial, antifungal but also cytotoxic effects.[152,155,166] This fungal strain did not produce detectable amounts of gliotoxin. The isolated gliotoxin derivatives **14** and **15** did not show any antibiotic activity. Probably, because they lack the characteristic disulfide bridge of gliotoxin, which is considered as the toxicophore of gliotoxin.[155]

Table **4-20**: Agar diffusion assay of isolated compounds in WG König (3.6.1)

sample concentration: 1 mg/mL (at 50 µg/disk level)[1]					
growth inhibition (GI) and total inhibition (T) zones against test organisms [mm]					
Compound	***Escherichia coli***	***Bacillus megaterium***	***Microbotryum violaceum***	***Eurotium rubrum***	***Mycotypha microspora***
1					
2					
3	0	3.5 (T)	0	0	0
4	0	2.5 (T)	0	2.5 (GI)	0
5	0	5.0 (T)	0	2.5 (GI)	0
6					
7					
9	0	0	0	0	0
10					
11					
12	7.0 (T)	7.0 (T)	6.0 (T)	3.5 (T)	12 (T)
13	0	2.0 (T)	3.5 (GI)	2.5 (GI)	2.5 (T)
14	0	0	0	0	0
15	0	0	0	0	0
16					
17	0	0	0	2.5 (GI)	0

Table **4-21**: Agar diffusion assay of isolated compounds in AG Sahl (3.6.2)

sample concentration: 1 mg/mL (at 3 µg[a] and 5 µg[b])			
growth inhibition (GI) and total inhibition (T) zones against test organisms [mm]			
test organism	**1**[b]	**2**[a]	**13**[a]
Staphylococcus aureus (MSSA)	0	7.0 (GI)	4.0 (GI)
Staphylococcus aureus (MRSA)	4.0 (GI)	7.0 (GI)	5.0 (GI)
Staphylococcus simulans	0	0	2.0 (T)
Staphylococcus epidermidis (MRSE)	0	/	/
Enterococcus faecium	0	4 (GI)	0
Bacillus subtilis	0	9 (T)	3 (GI)
Bacillus megaterium	/	0	/
Listeria welchimeri	4 (GI)	0	0
Corynebacterium xerosis	0	0	4 (GI)
Mycobacterium smegmatis	0	0	4 (GI)
Echerichia coli	0	0	0
Citrobacter freundii	0	5.0 (GI)	0
Klebsiella pneumoniae subsp. Ozeanae	0	0	0
Arthrobacter crystallopoietes	0	9.0 (T)	3 (T)
Candida albicans	/	/	5 (GI)
Candida glabrata	/	0	/
Micrococcus luteus	3.0 (GI)	9.0 (GI)	3 (T)
Bacillus cereus	/	9.0 (GI)	/
Pseudomonas aeruginosa	0	4.0 (GI)	0

4.5.2 Further activity tests with isolated pure compounds

Table **4-22**: Performed bioactivity tests of isolated pure compounds

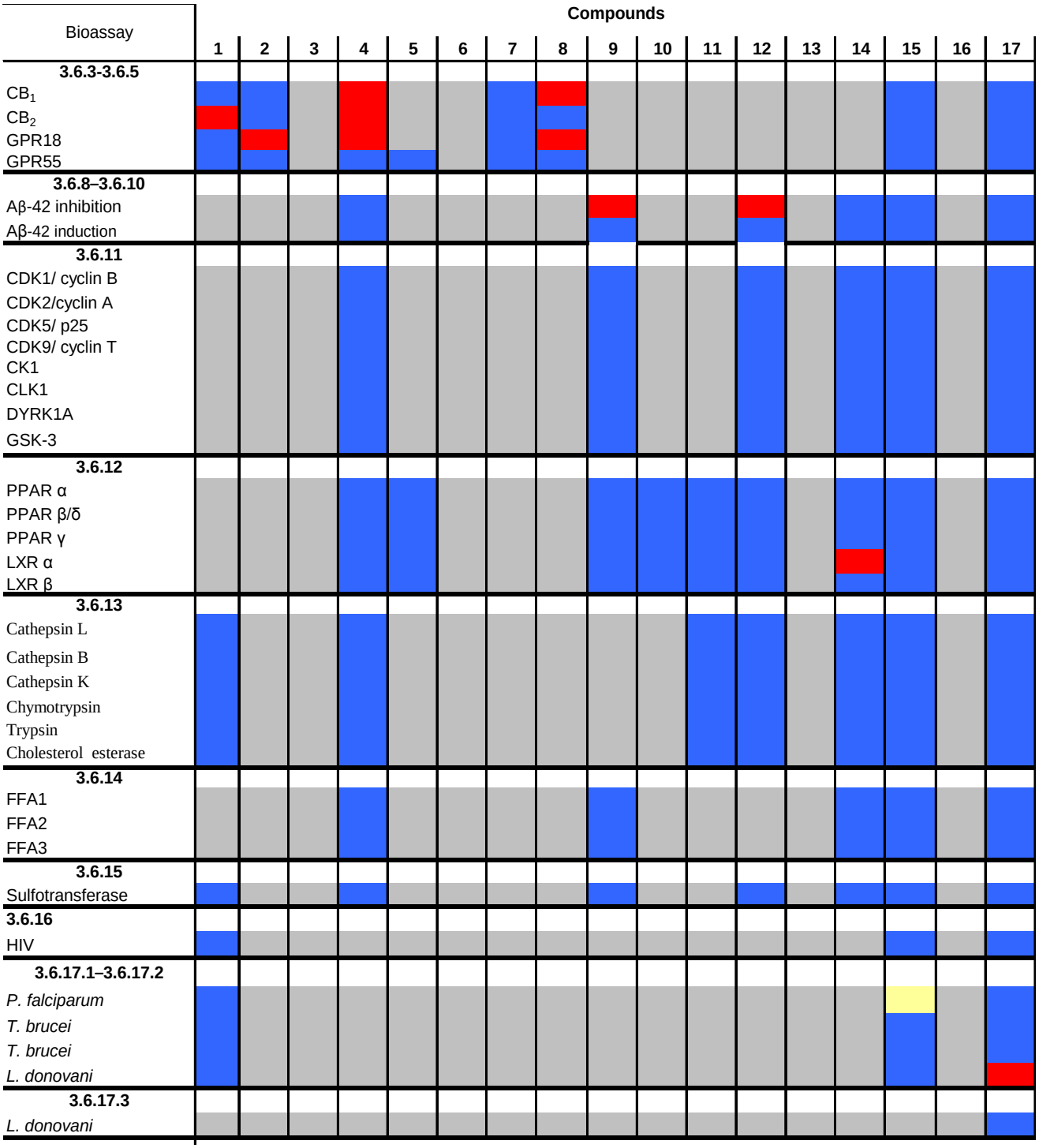

Overview of performed bioactivity tests (for details about assay and sample preaparation see chapter 3.6.3–3.6.17) red: activity in performed assay; yellow: minor activity in performed assay; blue: no activity in performed assay; grey: not tested. For details about active substances see chapter 4.2.2–4.4.4.5

4.5.3 Antiparasitic activites of isolated pure compounds

Table **4-23**: Antiparasitic activity tests of isolated pure compounds

Target: parasite/cell:	***strain:***	***stage:***		***reference drug:***		All values as:
T. b. rhodesiense	STIB 900	trypomastigotes		Melarsoprol		mg / mL
T. cruzi	Tulahuen C4	amastigotes		Benznidazole		
L. donovani	MHOM-ET-67/L82	amastigotes		Miltefosine		
P. falciparum	NF54	IEF		Chloroquine		
mammalian cell line	L6			Podophyllotoxin		
	T.b.rhodesiense	*T. cruzi*	*L. donovani.* axenic	*L. donovani* M.A	*P. falciparum* NF54	Cytotox. L6
Compound	IC-50	IC-50	IC-50	IC-50	IC-50	IC-50
Melarsoprol	0.003					
Benznidazole		0.571				
Miltefosine			0.221	1.54		
Chloroquine					0.002	
Podophyllotoxin						0.007
emindole SB-beta-mannoside (**1**)	58.2	70.1	38.1		7.03	32.8
6-acetylbisdethiobis(metylthio)gliotoxin (**15**)	18.2	62.8	19.8		5.21	>100
heveadride (**17**)	63.7	80.7	0.883	>30	31	76.5

Leishmania spp are parasites which are responsible for the disease leishmaniasis. They are transmitted through sandflies and their primary hosts are vertebrates. During their life cycle stage in mammalian hosts, *Leishmania* spp. are housed within phagolysosomes of macrophages.[167]

Compound heveadride (**17**) displays prominent antiparastic effects against axenic *Leishmania donovani* in assay 3.6.14.2, but no antiparasitic activity was detected against *Leishmania donovani* in *L. donovani* Macrophage assay (3.6.14.3). The obtained results indicate that heaveadrid possesses desirable selective toxic effects against isolated *Leishmania donovani*. Unfortunately heveadride is unable to effect *Leishmania donovani* within macrophages which limits its therapeutical use.[167] Therefore, heveadride derivatives with the ability to reach and effect *Leishmania* spec. within macrophages could be an interesting approach for antiparasitic drug development against Leishmania parasites.

5 General discussion

5.1 Classification and structural evaluation of isolated compounds

The main goal of this study was the in-depth chemical examination of a marine derived fungal strain of *Dichotomomyces cejpii* and the secondary metabolites produced by this microorganism. Therefore, the isolation, identification and biological evaluation of preferably such new natural products was intended, which might be used as potential drug leads.

Fifteen complex natural products were obtained, of which seven possess new structures, and two had been obtained semisynthethically before. Altogether, these compounds revealed the astonishing biosynthetic potential of the investigated fungal strain and its remarkable utilization of multiple biosynthetic pathways. In the following these biosynthetic pathways will be briefly described.

The six isolated indoloditerpene alkaloids (**1–6**) represent hybrid molecules, produced by a combination of two biosynthetic pathways. The indoloditerpene biosynthesis was investigated by Tagami et al., 2013 for paxilline by *Penicillium paxilli*.[168] According to their results a biosynthesis for the indoloditerpenes in *Dichotomomyces cejpii* can be assumed as shown in Figure 5.3. Thus, the indoloditerpene core structure consists of a cyclic diterpene skeleton derived from geranylgeranyldiphosphat (GGPP) and an indole nucleus. The isoprene units may be derived via the mevalonate or the methylerythritol phosphate (MEP) pathway, which uses mevalonic acid or rather deoxyxylulose phosphate as precursors. The indole substructure is derived from indole-3-glycerolphosphate (IGP), which has its origin in the shikimate pathway. The shikimate pathyway starts with a coupling of phosphoenolpyruvat (PEP) and D-erythrose-4-phosphate. Via shikimic and chorismic acid, anthranilic acid is formed. The phosphoribosylation and decarboxylation of anthranilic acid leads to indole-3-glycerolphosphate, which is a precursor of the aminoacid L-tryptophan.[169,170] (figure 5-1)

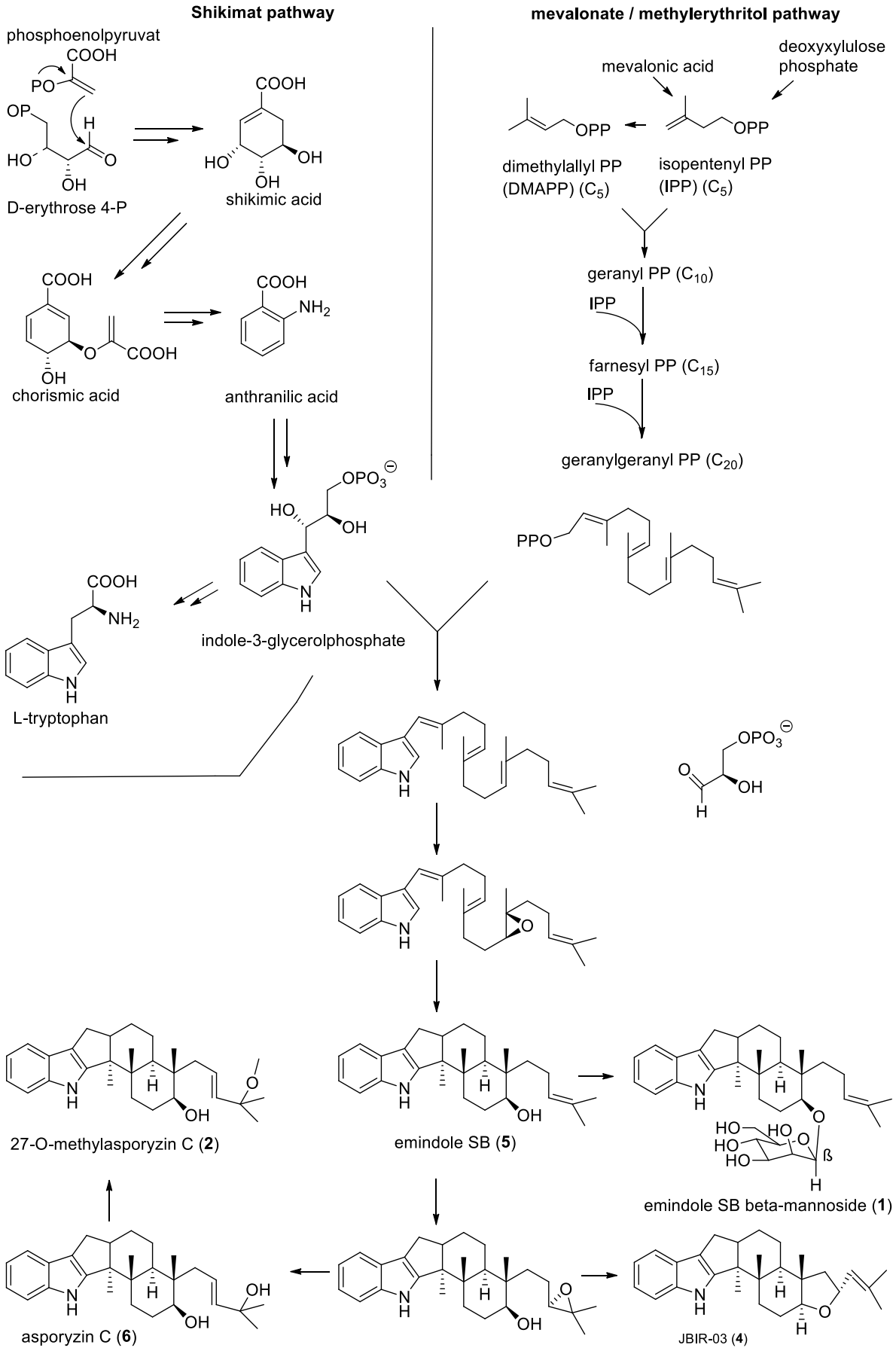

Figure 5-1: Putative indoloditerpene biosynthesis in *Dichotomomyces cejpii*

Three uncommon steroids (**9**–**11**) can be seen as examples of modified triterpenoids. Triterpenoids generally consist of six C_5 isoprene units. For triterpenoid synthesis in fungi two molecules of C_{15} farnesyl PP are head to head joined to yield the intermediate squalene. Oxidation and multiple cyclization steps lead to lanosterol which already shows the tetracyclic core structure of the steroids. Further structural modifications lead to the different types of steroids, whose nomenclature is based on a series of parent hydrocarbons.

Due to their basic chemical structure the isolated sterols (**9**–**11**) can be assigned to the 'ergostane' or rather 'campestane' type of steroids, depending on the absolute configuration at C-24.[169] Analogous conclusions to this general steroid formation led to the proposed biosynthesis as given in figure 5-2.

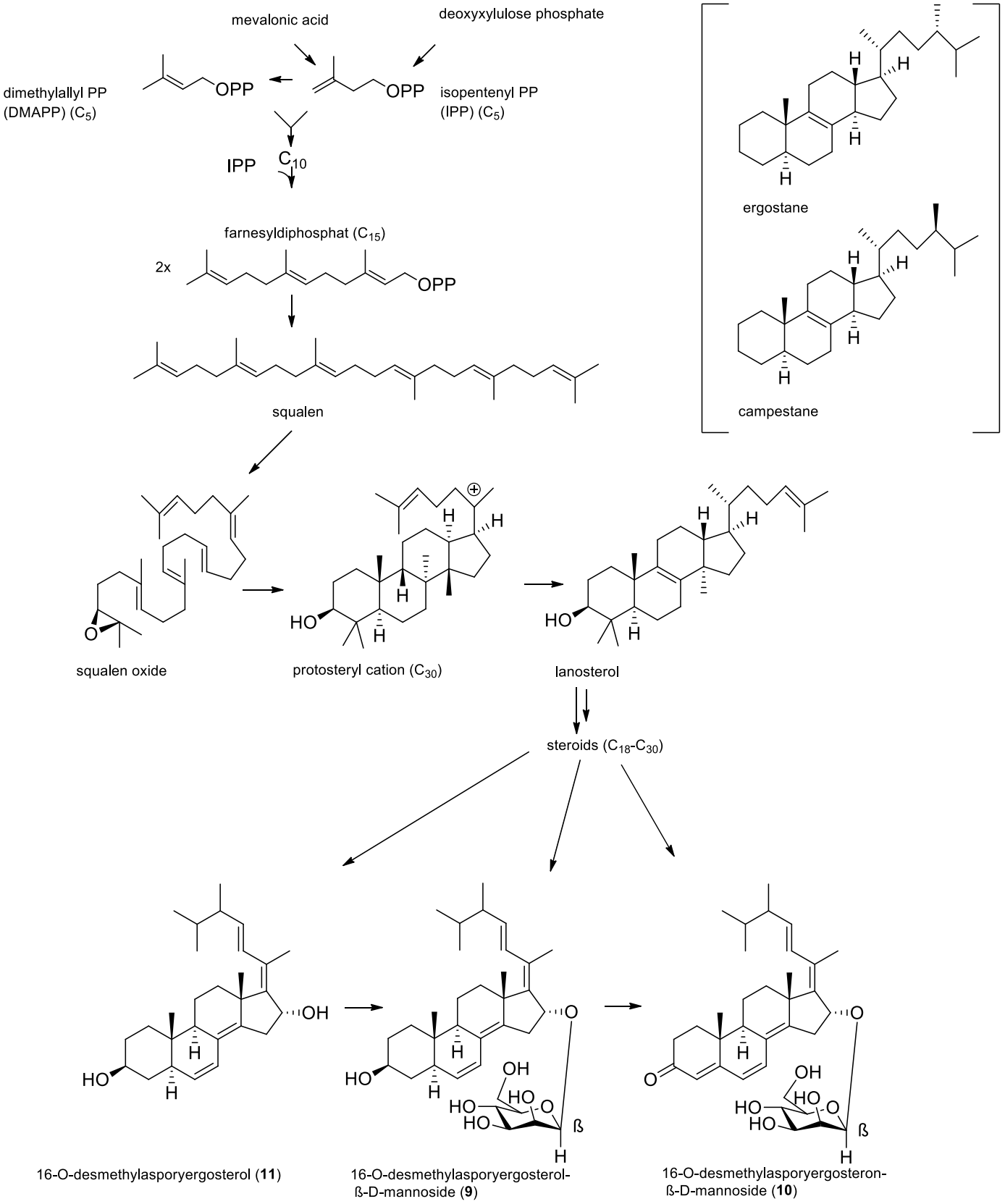

Figure 5-2: Putative sterol biosynthesis in *Dichotomomyces cejpii*.

The two isocyanide containing xanthocillin derivatives, xanthocillin X dimethylether (**12**) and xanthocillin monomethylether (**13**), are derived from the shikimate pathway as well.[171] However, their biosynthesis does not follow the route via trypthophan and its precursors but it is supposed to proceed via prephenic acid and the aromatic amino acid L-tyrosine. Several feeding experiments with labelled precursors in strains of *Dichotomomyces cejpii* and *Aspergillus* spec. indicated that a dimerization of L-tyrosine derivatives leds to xanthocillin X formation.[172,173] The formation of the prominent isocyanide group, however is not clarified yet. The nitrogen originates apparently from L-tyrosine, but the origin of the isocyanide carbon remains uncertain.[171,174]

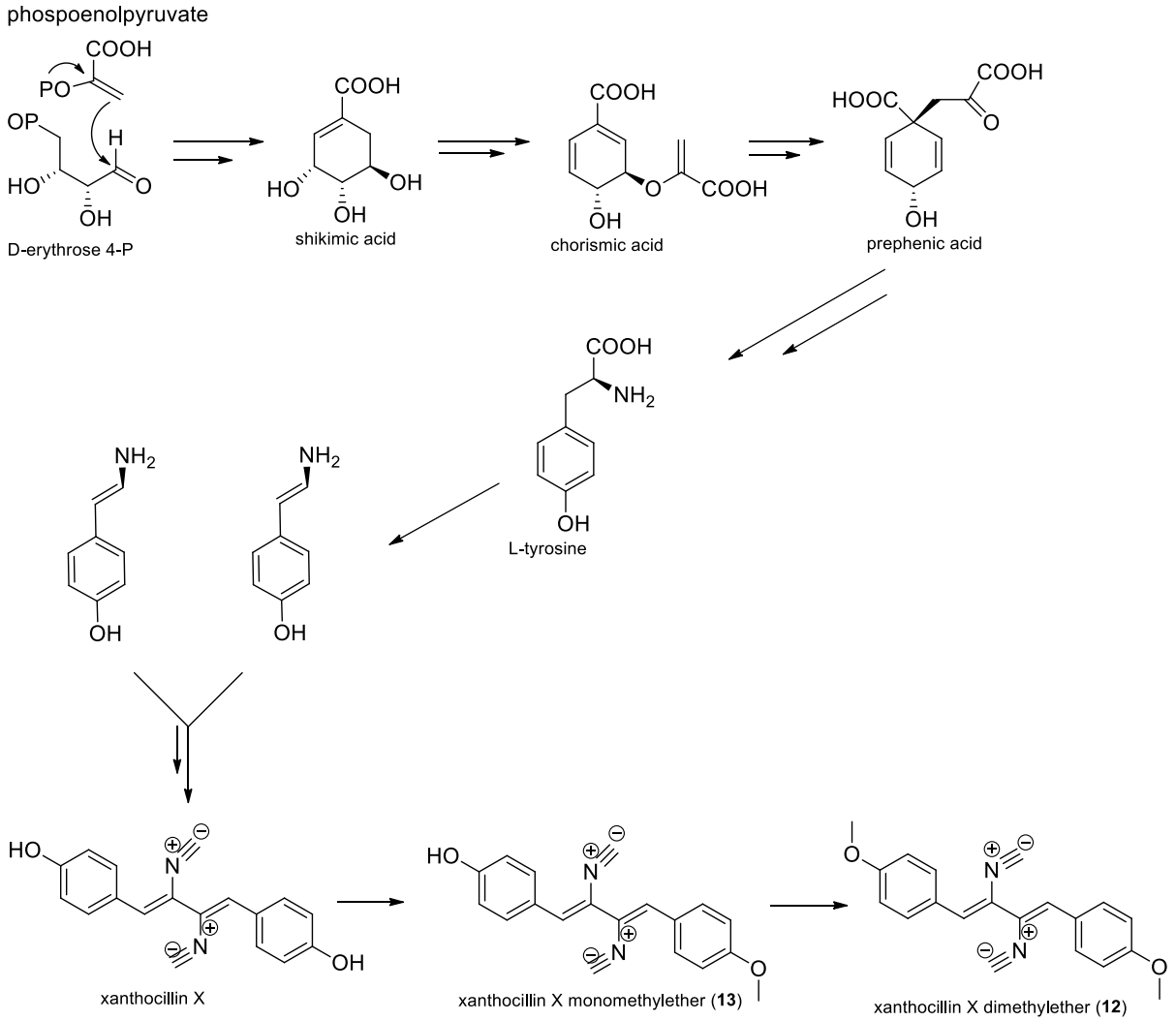

Figure 5-4: Putative xanthocillin X derivative biosynthesis in *Dichotomomyces cejpii*

Implying the same biosynthesis as for the parent substance gliotoxin in *Aspergillus fumigatus*, a non-ribosomal peptide synthase (NRPS) is responsible for the construction of the three here isolated sulphur containing gliotoxin derivatives (**14**–**16**). Their diketopiperazine basic structure is formed by L-phenylalanine and L-serine via a cyclo-L-phenylalanyl-L-seryl intermediate. [156,175–178] A complex reaction cascade, utilizing a glutathione-S-transferase, establishes the functional thiol group, which can be further processed to a transannular sulfid bridge. (see figure 5-4 for details)

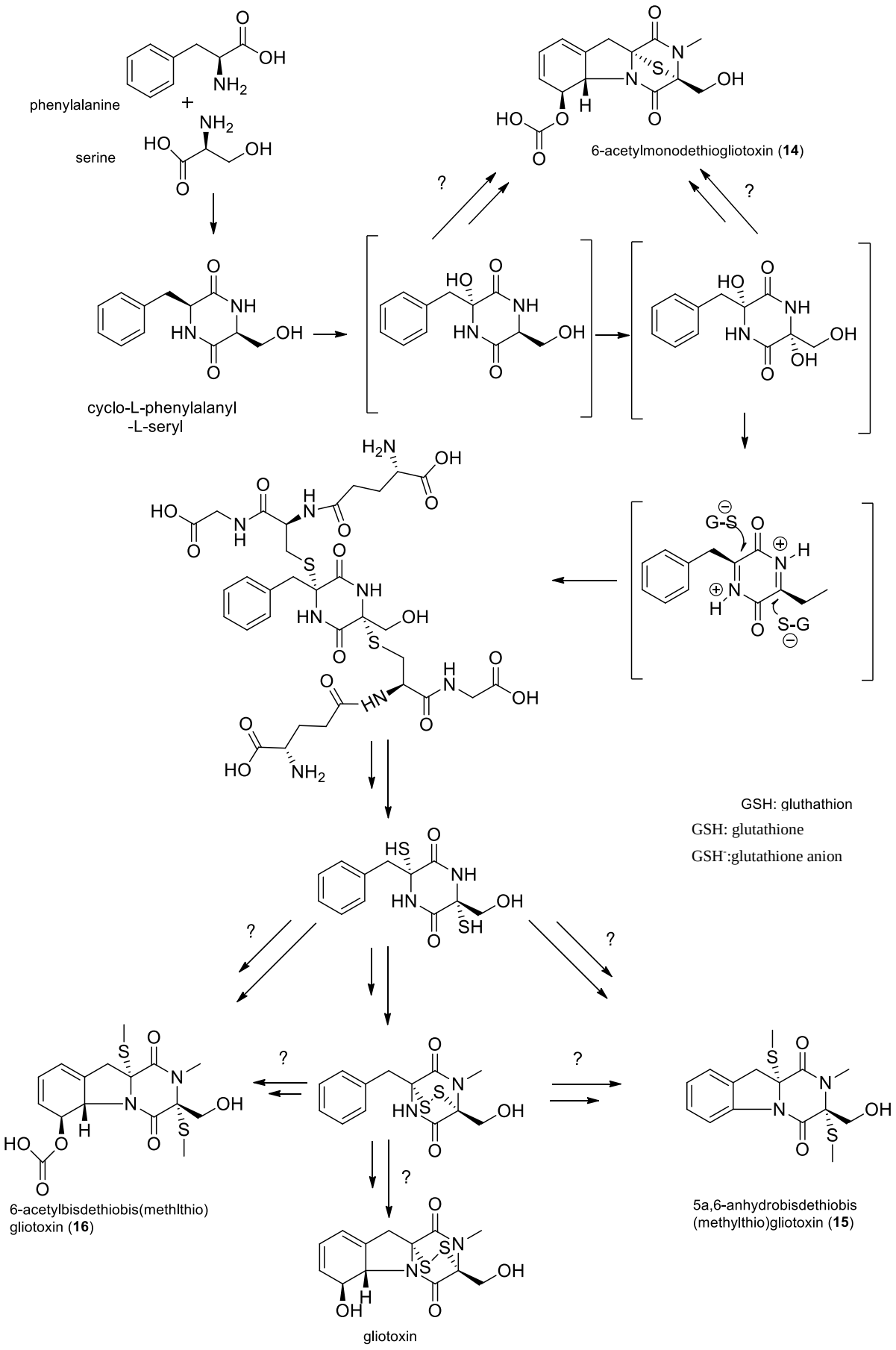

Figure 5-4: Putative biosynthesis of gliotoxin and its derivatives in *Dichotomomyces cejpii*

Finally heveadride (**17**) represents a nonadride which are chemically characterized by the presence of a nine-membered alicyclic ring and two five-ring anhydride functions. These are supposed to originate from the acetate pathway, i.e. to be a polyketide. The biosynthesis of glauconic acid, the infamous rubratoxin and related nonadrides have been investigated using feeding experiments.[179–182] Taking the results of these investigations into account leads to the suggestion that heveadride is the head-to-head dimerization product of two identical unsaturated anhydrides. These moieties are in turn produced by the condensation of oxaloacetyl-CoA and an unspecified C_6 polyketide, which could be an unsaturated hexanoyl-CoA or a ß-ketothioester. The oxaloacetyl moiety appears to be particularly derived from succinat via the citric acid cycle, whereat also other sources, e.g. via aspartate transamination, may contribute as well. The production of the C_6 polyketide instead can be achieved by either a fatty acid or a polyketide synthesis pathway utilizing acetyl-CoA and malonyl-CoA as precursors. (see figure 5-5)

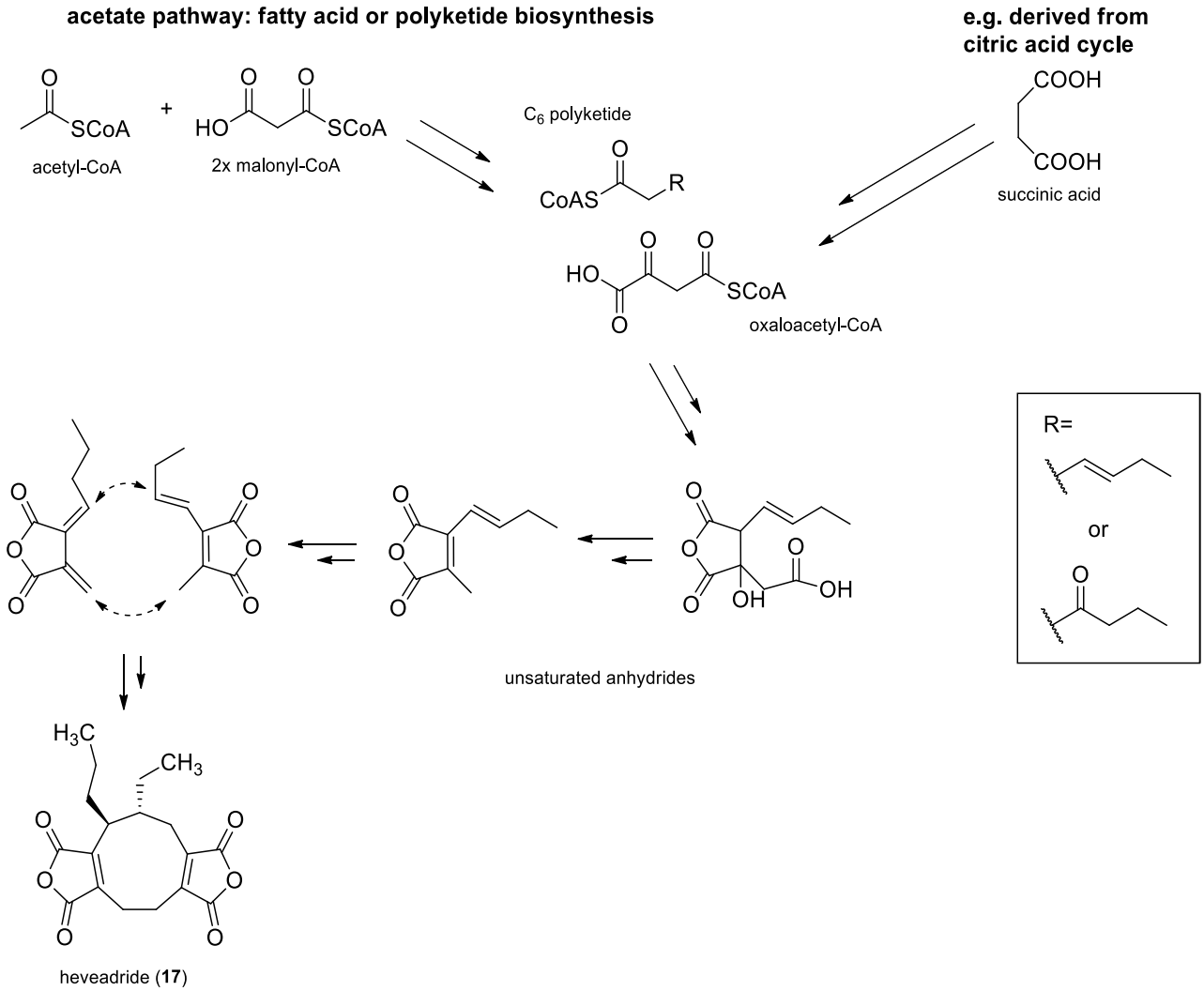

Figure 5-5: Putative nonadride biosynthesis in *Dichotomomyces cejpii*

5.2 Biological evaluation of isolated compounds

It is of major interest to investigate the obtained molecules for their biological activities. Their potential to interact with biological targets can be regarded as high due to their origin as natural products. Depending on structural features and the available quantities of the respective compounds, they were subjected to diverse, pharmacologically highly relevant bioassays. By collaboration with many working groups a wide array of activities could be examined. These included activities toward several receptors, like cannabinoid (CB), fatty acid and diverse nuclear receptors. Antibiotic effects against several bacteria, fungi and parasites were examined as well. Furthermore, inhibitory effects toward several enzymes like e.g. cerebrosid-sulfotransferase were investigated. The majority of the examined compounds indeed displayed any bioactivity in the examined assays (see table 4-23). Among these there

are three compounds that display selective activity towards one specific receptor subtype. A selective CB_2 or rather GPR18 receptor blocking activity was found for the indoloditerpenes **1** and **2**, respectively. While, a selective LXRα agonistic effect was observed for the epimonothiodiketopiperazine **14** (see chapter 4.2-4.5 for details). Furthermore compound **1** and **14** were tested for effects toward mammalian cells and none of these compounds displayed relevant cytotoxicity. Thus, these compounds form a good starting point for further investigations and compound development.

The antibiotic activities of the fungal extracts were assigned to several clearly defined compounds. These include the known xanthocillin X mono- and dimethylether (**12** and **13**) and the indoloditerpenes JBIR-03 (**4**) and asporyzin C (**6**), [101,102,183] but also the structurally new indoloditerpenes **1–3**. With the exception of the potent compound **13** all of these compounds displayed moderate antibiotic activites (Table 4-21–4-22). In an ecological sense this may indicate effective chemical defense of *D. cejpii* against competitors and predators.

5.3 New approaches for natural product research

New approaches to facilitate sample separation and compound isolation for natural product research, in consideration of the applied methodology in this study

Within the scope of this study, a classical approach for natural product research was used, which was in case of antibiotic activity, supported by bioactivity-guided fractionation.This time and resources consuming compound isolation process, starting from complex crude extracts, is often considered as an inherent and major disadvantage of natural product drug research.[184] Moreover, classical bioassay-guided fractionation allows physicochemical profiling only after accomplished compound isolation. This means that selection of lead- and drug-like compounds can usually be applied for the first time after the long isolation process has been accomplished. This might lead in unfavorable cases to bioactive, but for example not bioavailable compounds, which severely restricts their therapeutical usability.[184]

Nowadays many pharmaceutical companies base their screening libraries on the so called Lipinski ‘Rule of five’ to preselect compounds due to their drug like properties.[184] The generally accepted Lipinski ‘Rule of five’ (Ro5) describes four simple physicochemical key properties for bioavailable, orally administrable drugs, i.e. molecular weight (MW) < 500, H-

bond donors (HBD) < 5, H-bond acceptors < 10 and calculated log P (clogP) < 5.[185] Among these log P, an indicator for drug lipophilicity and solubility, is considered to be the most important parameter.[184,186] There are approaches to improve natural product research in that respect and thus to facilitate their use in HTS screening approaches. [184] In so called lead-like enhanced (LLE) extracts.[184] the relationship between log P and retention time on C_{18} chromatography columns is used to enrich compounds with desirable physicochemical properties. An optimized solid phase extraction (SPE) protocol can be used as a primary filter on log P. Log P as a primary filter can optionally be supplemented by further filters like the consequent use of MS techniques in order to establish molecular weight (MW) as a second filter. Further fractionations can be used to establish HTS friendly LLE fractions of reduced complexity, but retained chemical diversity space. Compared to classical NP drug discovery, this procedure could allow the acceleration of the process to afford natural product leads with lead like properties.

On the other hand there are voices which criticize the limitations of the Ro5 and emphasize that especially the first four rules do not apply for natural products and molecules recognized by an active transport mechanism.[3,187,188] Furthermore history has shown that many natural products with insufficient properties, which restricted their therapeutical use, have been great starting points for drug optimization on the way to therapeutically usable drugs. A range of examples for this are given in the introduction (1.1). Therefore one should perhaps also take into consideration that, following this LLE approach too strictly, we might lose powerful lead structures with insufficient physicochemical key properties, which however could have been further modified to obtain active and bioavailable drugs. Within the scope of this study, which dealed with the in-depth analysis of one single fungal strain, the application of the LLE approach, would have been an option to accelerate the separation process. However this option was rejected in favor of a more exhaustive analysis of the secondary metabolites produced by *D. cejpii* on the examined media.

Certainly the LLE approach has its potential however, especially for researchers working with very large sample amounts, which do not allow a complete exhaustive separation of all samples and require a stronger preselection. In addition, the progressive improvement of analytical methodologies provides new opportunities for natural drug research. Of particular interest in this area are analytical techniques which facilitate bioactive hit assessment in semi-purified fractions, containing only minute concentrations of each individual compound.

A combination of techniques that may also include LLE extract fractionation and improved analytical methodologies, therefore, have the potential to enhance and accelerate natural product research and make it more competitive to chemical synthesized single compound HTS.[7,184,189]

Future strategies to reveal and explore the full potential of fungal secondary metabolite production

As illustrated during this study and by viewing fungi-derived drugs, these microorganisms are capable to produce an amazing range of pharmaceutically interesting secondary metabolites.[7,8] Obviously, many of these compounds are already known today, but many more can be expected. Thus the question arises how we can induce the production and facilitate the identification of these secondary metabolites?

The increased availability of genome sequences for ever more fungal species and the improved recognition of fungal biosynthetic gene clusters provide detailed insight into fungal secondary metabolite production. The latter revealing that under routine laboratory conditions the harbored biosynthetic genes are apparently only in part transcribed into fungal products.[9,190]

In their natural environment fungi are generally growing in close neighborhood to other microorganisms, competing for living space and nutrients. These interactions are supposed to induce secondary metabolite production to asserten the specific fungus in its ecological niche (see 1.2). [9,190] Under laboratory conditions, growing free of annoying competitors and with an abundance of nutrients, secondary metabolite production may be regarded by the producer strain as a waste of its resources, and can be downregulated or even arrested. Co-cultivation studies with other fungi or bacteria have demonstrated the great potential of a well considered co-cultivation approach in order to obtain new unpredicted metabolites.[9,190] As an example the cocultivation of a marine-derived mangrove fungal strain led e.g. to the production of the new antibacterial compound aspergicin.[191] Future research activities regarding our fungal strain of *D. cejpii* could potentially pursue this option, as well. As described in chapter 4.2.2 first cultivation experiments with minimal agar media in comparison to nutrient rich agar media, revealed an increased antibiotic activity for some of the hydrophilic fractions. In the scope of this study, further investigations of this phenomenon have not been possible, but

these results indicate an enhanced secondary metabolite production triggered due to external influences.

Induction of fungal secondary metabolite production may also be achieved on the genomic level. The identification of gene clusters typically involved in secondary metabolite production by genome sequencing provides the opportunity to influence their transcription. Different strategies have been pursued, like the utilization of a) cluster-specific activation on the one hand, b) global regulators on the other hand as well as c) histone modifications.[192]

Concerning approach a), Zn(II)2Cys6 proteins which are a group of transcription factors generally activating gene clusters may be addressed to produce the encoded metabolites. This group of transcription factors share a common protein sequence motif, the 'Zn(II)2Cys6 binuclear cluster' DNA binding motif , which can be used for recognition. Recognition and targeted induction of cluster-embeded Zn(II)2Cys6 genes can be used to activate the according gene cluster.[192] This method was already utilized to activate otherwise silent gene clusters, which led to the production of new metabolites, like asperfuranone which displays anti-proliferative effects in human cancer cell lines. [192–195]

Approach b) is similar but uses global regulators of secondary metabolism like LeA and its homologs. Introduction and overexpression of LeA genes have been applied to awaken silent secondary metabolite clusters and to enhance general productivity of secondary metabolites.[192,196]

Finally, strategy c) involves histone modifications like acetylation or methylation, which have been associated with effects on global gene expression due to epigenetic effects. Genetic deletion of histone methylation complexes, which normally induce gene silencing or the application of histone deacetylase inhibitors, have for example demonstrated to be capable to induce the production of secondary metabolites and can be valuable tools to induce the expression of silent gene clusters.[192,197,198]

Taken all together, natural products will keep on playing a major role in drug discovery in the future. Natural products derived from fungal sources, like investigated in this study, will thereby continue to provide new lead compounds. Innovative techniques and approaches will facilitate the identification of chemically novel structures from known and new sources. The recognition and manipulation of silent or cryptic biosynthesis genes furthermore will increase the wide spectrum of available chemical diverse secondary metabolites, thus providing a resource for future discoveries.

6 Summary

Natural products display an astonishing diversity of bioactive structures. These compounds play a prominent role in the drug development process for a wide array of therapeutic indications. This eminent position may be explained due to the circumstance that natural products, as well as their biological targets (e.g. receptors/proteins), are produced by the interaction with biosynthetic enzymes. Due to this 'biosynthetic imprint' or shared 'protein fold topology' (PFT) they exhibit 'natural product binding motifs', which facilitate interactions with their biological targets.

Among natural products, fungal metabolites have turned out to be very valuable as lead structures, i.e. many antibiotics and immunomodulatory agents are derived from fungal metabolites. The secondary metabolite production in fungi is strongly affected by environmental influences and the isolation of fungal strains from uncommon, less investigated habitats is considered as promising approach for the discovery of novel bioactive compounds. Therefore, investigation of marine-derived fungi was targeted in the current study.

The main goal of this investigation was the isolation, identification and biological evaluation of secondary metabolites from the marine-derived fungus *Dichotomomyces cejpii* with emphasis on compounds exhibiting activities toward cannabinoid and type II nuclear receptors. Aβ-42 lowering activity potentially useful to treat Alzheimer dementia was also assayed. Of further interest were secondary metabolites with antibiotic activities.

For initial bioassays four different agar-based media were chosen for small scale cultivation, following the idea of the so-called OSMAC (One Strain Many Compounds) approach. On the basis of the chemical and biological results obtained with these extracts, two cultivation methods which differed greatly in their nitrogen and carbohydrate supply sources were selected for large scale cultivation.

Detailed chemical investigation of the resulting two extracts provided in total fifteen complex natural products. Seven of these have new structures (**1**–**3**, **9**–**11** and **14**) and two had only been obtained semi-synthethically before (**15**–**16**).

The new emindole SB beta-mannoside (**1**) and 27-O-methylasporyzin C (**2**) belong to the class of indoloditerpenes. They were obtained together with another new indoloditerpene, referred to as emindole SB-formate (**3**) and three further structurally related metabolites (**4**–**6**).

All investigated indoloditerpenes display activities toward cannabinoid and related receptors, whereat compound **1** shows selective antagonistic activity toward cannabinoid receptor subtype 2 ($CB_{2:}$ K_i 10.6 µM), while compound **2** has selective antagonistic activity toward the cannabinoid related receptor GPR18 (IC_{50} 13.4 µM). Due to the potent physiological responses, such as, e.g. immunomodulatory effects, both receptors are targets for drug development. The new natural indole derivatives **1** and **2** may thus serve as lead structures for the development of potent and selective CB_2 or GPR18 receptor-blocking drugs, respectively.

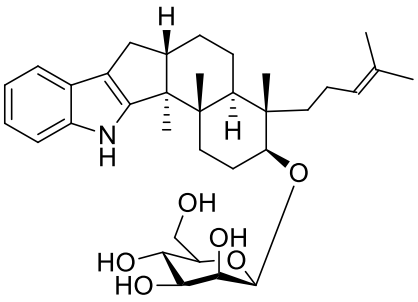

emindole SB beta-mannoside (**1**)

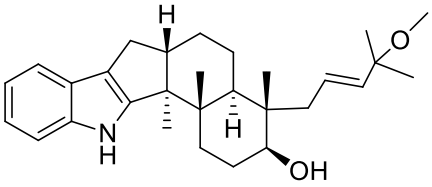

27-O-methylasporyzin C (**2**)

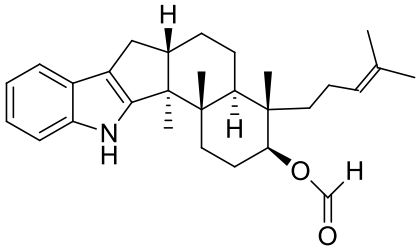

emindole SB-formate (**3**)

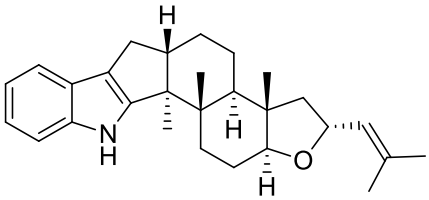

JBIR-03 (**4**)

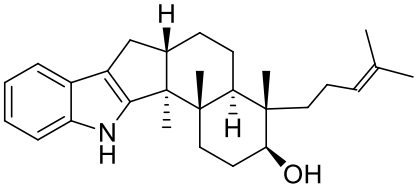

emindole SB (**5**)

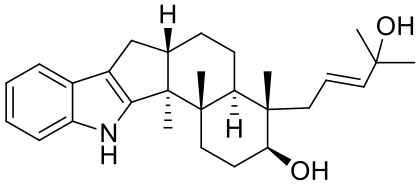

asporyzin C (**6**)

Further, we identified three new sterols with an untypical pattern of carbon-carbon double bounds (**9**–**11**) and reisolated the isocyanid xanthocillin X dimethylether (**12**). The new sterol 16-O-desmethylasporyergosterol-ß-D-mannoside (**9**) and xanthocillin X dimethylether (**12**) display moderate Aβ-42 lowering activity. Given that Aβ-42 lowering agents are, inter alia, considered as therapeutics for Alzheimer disease, these results suggest further investigations.

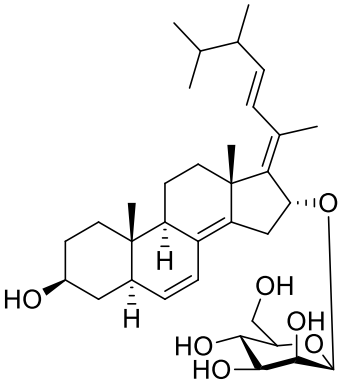

16-O-desmethylasporyergosterol-ß-D-mannoside (**9**)

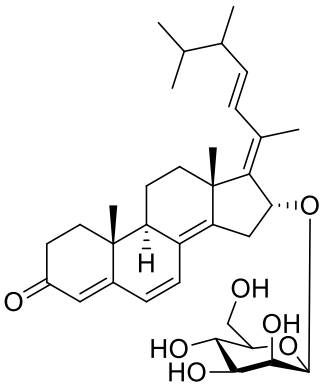

16-O-desmethylasporyergosteron-ß-D-mannoside (**10**)

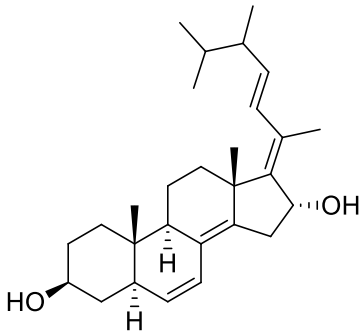

16-O-desmethylasporyergosterol (**11**)

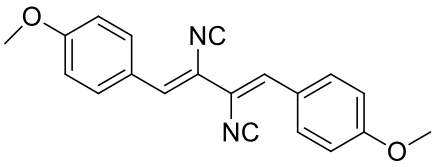

xanthocillin X dimethylether (**12**)

Additionally, three non-cytotoxic gliotoxin derivatives were isolated (**14**–**16**). The new 6-acetylmonodethiogliotoxin (**14**) is characterized by a naturally occurring very rare transannulated monosulfide bridge. This characteristic moiety seems to be essential for the observed selective agonistic activity toward nuclear liver X receptor α (LXRα). Targeting LXR has demonstrated to possess therapeutic potential in the treatment of atherosclerosis, diabetes, cancer, cardiovascular diseases, autoimmune disorders, and Alzheimer disease, whereat LXR α/β subtype selective ligands are desired. Therefore compound **14** may serve as lead for the development of more potent and selective ligands which interact with this therapeutically interesting receptor.

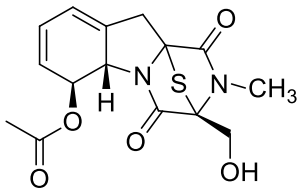

6-acetylmonodethiogliotoxin (**14**)

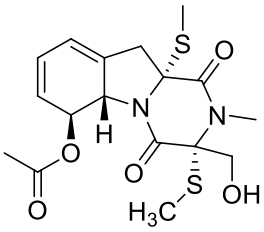

6-acetylbisdethiobis(methylthio)gliotoxin (**15**)

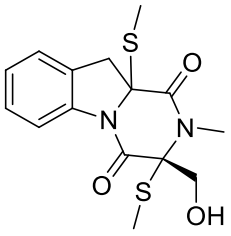

5a,6-anhydrobisdethiobis (methylthio)gliotoxin (**16**)

In conclusion the marine-derived strain of *Dichotomomyces cejpii* has been identified as powerful producer of highly diverse and bioactive secondary metabolites.

References

(1) Macarron, R.; Banks, M. N.; Bojanic, D.; Burns, D. J.; Cirovic, D. A.; Garyantes, T.; Green, D. V. S.; Hertzberg, R. P.; Janzen, W. P.; Paslay, J. W.; Schopfer, U.; Sittampalam, G. S. *Nat. Rev. Drug Discov.* **2011**, *10*, 188–195.

(2) Hert, J.; Irwin, J. J.; Laggner, C.; Keiser, M. J.; Shoichet, B. K. *Nat. Chem. Biol.* **2009**, *5*, 479–483.

(3) Newman, D. J.; Cragg, G. M. *J. Nat. Prod.* **2012**, *75*, 311–335.

(4) Kellenberger, E.; Hofmann, A.; Quinn, R. J. *Nat. Prod. Rep.* **2011**, *28*, 1483–1492.

(5) McArdle, B. M.; Campitelli, M. R.; Quinn, R. J. *J. Nat. Prod.* **2006**, *69*, 14–17.

(6) Wess, G.; Urmann, M.; Sickenberger, B. *Angew. Chem. Int. Ed.* **2001**, *40*, 3341–3350.

(7) Cragg, G. M.; Newman, D. J. *Biochim. Biophys. Acta BBA - Gen. Subj.* **2013**, *1830*, 3670–3695.

(8) Keller, N. P.; Turner, G.; Bennett, J. W. *Nat. Rev. Microbiol.* **2005**, *3*, 937–947.

(9) Losada, L.; Ajayi, O.; Frisvad, J. C.; Yu, J.; Nierman, W. C. *Med. Mycol.* **2009**, *47*, S88–S96.

(10) Ben-Ami, R.; Lewis, R. E.; Kontoyiannis, D. P. *Br. J. Haematol.* **2010**, *150*, 406–417.

(11) Survase, S. A.; Kagliwal, L. D.; Annapure, U. S.; Singhal, R. S. *Biotechnol. Adv.* **2011**, *29*, 418–435.

(12) Borel, J. F.; Feurer, C.; Gubler, H. U.; Stähelin, H. *Agents Actions* **1976**, *6*, 468–475.

(13) Lee, W. A.; Gu, L.; Miksztal, A. R.; Chu, N.; Leung, K.; Nelson, P. H. *Pharm. Res.* **1990**, *7*, 161–166.

(14) Brinkmann, V.; Billich, A.; Baumruker, T.; Heining, P.; Schmouder, R.; Francis, G.; Aradhye, S.; Burtin, P. *Nat. Rev. Drug Discov.* **2010**, *9*, 883–897.

(15) Kluepfel, D.; Bagli, J.; Baker, H.; Charest, M.-P.; Kudelski, A.; Sehgal, S. N.; VéZina, C. *J. Antibiot. (Tokyo)* **1972**, *25*, 109–115.

(16) Benz, F.; Knuesel, F.; Nueesch, J.; Treichler, H.; Voser, W.; Nyfeler, R.; Keller-Schierlein, W. *Helv. Chim. Acta* **1974**, *57*, 2459–2477.

(17) Balkovec, J. M.; Hughes, D. L.; Masurekar, P. S.; Sable, C. A.; Schwartz, R. E.; Singh, S. B. *Nat. Prod. Rep.* **2014**, *31*, 15.

(18) Vazquez, J. A.; Sobel, J. D. *Clin. Infect. Dis.* **2006**, *43*, 215–222.

(19) Baguley, B. C.; Römmele, G.; Gruner, J.; Wehrli, W. *Eur. J. Biochem.* **1979**, *97*, 345–351.

(20) Van der Kaaden, M.; Breukink, E.; Pieters, R. J. *Beilstein J. Org. Chem.* **2012**, *8*, 732–737.

(21) Abraham, E. P. *Nat. Prod. Rep.* **1987**, *4*, 41–46.

(22) Samson, R. A.; Hadlok, R.; Stolk, A. C. *Antonie Van Leeuwenhoek* **1977**, *43*, 169–175.

(23) Endo, A. *J. Antibiot. (Tokyo)* **1979**, *32*, 852–854.

(24) Alberts, A. W.; Chen, J.; Kuron, G.; Hunt, V.; Huff, J.; Hoffman, C.; Rothrock, J.; Lopez, M.; Joshua, H.; Harris, E.; Patchett, A.; Monaghan, R.; Currie, S.; Stapley, E.; Albers-Schonberg, G.; Hensens, O.; Hirshfield, J.; Hoogsteen, K.; Liesch, J.; Springer, J. *Proc. Natl. Acad. Sci.* **1980**, *77*, 3957–3961.

(25) Amarenco, P.; Labreuche, J.; Lavallée, P.; Touboul, P.-J. *Stroke* **2004**, *35*, 2902–2909.

(26) König, G. M.; Kehraus, S.; Seibert, S. F.; Abdel-Lateff, A.; Müller, D. *ChemBioChem* **2006**, *7*, 229–238.

(27) Newman, D. J.; Cragg, G. M.; Battershill, C. N. *Diving Hyperb. Med.* **2009**, *39*, 216–225.

(28) Mayer, A. M. S.; Glaser, K. B.; Cuevas, C.; Jacobs, R. S.; Kem, W.; Little, R. D.; McIntosh, J. M.; Newman, D. J.; Potts, B. C.; Shuster, D. E. *Trends Pharmacol. Sci.* **2010**, *31*, 255–265.

(29) Coll, J. C.; La Barre, S.; Sammarco, P. W.; Williams, W. T.; Bakus, G. J. *Mar. Ecol. Prog. Ser.* **1982**, *8*, 271–278.

(30) Rohde, S.; Schupp, P. J. *J. Exp. Mar. Biol. Ecol.* **2011**, *399*, 76–83.

(31) Putz, A.; König, G. M.; Wägele, H. *Nat. Prod. Rep.* **2010**, *27*, 1386–1402.

(32) Lopanik, N.; Lindquist, N.; Targett, N. *Oecologia* **2004**, *139*, 131–139.

(33) Johnson, D. B.; Hallberg, K. B. *Res. Microbiol.* **2003**, *154*, 466–473.

(34) Stock, C.; Brückner, R. *Synlett* **2010**, *2010*, 2429–2434.

(35) Rempel, V.; Volz, N.; Gläser, F.; Nieger, M.; Bräse, S.; Müller, C. E. *J. Med. Chem.* **2013**, *56*, 4798–4810.

(36) Rempel, V.; Volz, N.; Hinz, S.; Karcz, T.; Meliciani, I.; Nieger, M.; Wenzel, W.; Bräse, S.; Müller, C. E. *J. Med. Chem.* **2012**, *55*, 7967–7977.

(37) Page, B.; Page, M.; Noel, C. *Int. J. Oncol.* **1993**, *3*, 473–476.

(38) Huber, W.; Koella, J. C. *Acta Trop.* **1993**, *55*, 257–261.

(39) Mehta, P. D.; Pirttila, T. *Neurodegener. Dis.* **2005**, *2*, 242–245.

(40) Hochard, A.; Oumata, N.; Bettayeb, K.; Gloulou, O.; Fant, X.; Durieu, E.; Buron, N.; Porceddu, M.; Borgne-Sanchez, A.; Galons, H.; Flajolet, M.; Meijer, L. *J. Alzheimers Dis. JAD* **2013**, *35*, 107–120.

(41) Tahtouh, T.; Elkins, J. M.; Filippakopoulos, P.; Soundararajan, M.; Burgy, G.; Durieu, E.; Cochet, C.; Schmid, R. S.; Lo, D. C.; Delhommel, F.; Oberholzer, A. E.; Pearl, L. H.; Carreaux, F.; Bazureau, J.-P.; Knapp, S.; Meijer, L. *J. Med. Chem.* **2012**, *55*, 9312–9330.

(42) Leclerc, S.; Garnier, M.; Hoessel, R.; Marko, D.; Bibb, J. A.; Snyder, G. L.; Greengard, P.; Biernat, J.; Wu, Y.-Z.; Mandelkow, E.-M.; Eisenbrand, G.; Meijer, L. *J. Biol. Chem.* **2001**, *276*, 251–260.

(43) Ciocoiu, C. C.; Nikolić, N.; Nguyen, H. H.; Thoresen, G. H.; Aasen, A. J.; Hansen, T. V. *Eur. J. Med. Chem.* **2010**, *45*, 3047–3055.

(44) Tzameli, I.; Fang, H.; Ollero, M.; Shi, H.; Hamm, J. K.; Kievit, P.; Hollenberg, A. N.; Flier, J. S. *J. Biol. Chem.* **2004**, *279*, 36093–36102.

(45) Frizler, M.; Lohr, F.; Furtmann, N.; Kläs, J.; Gütschow, M. *J. Med. Chem.* **2011**, *54*, 396–400.

(46) Gütschow, M.; Pietsch, M.; Themann, A.; Fahrig, J.; Schulze, B. *J. Enzyme Inhib. Med. Chem.* **2005**, *20*, 341–347.

(47) Pietsch, M.; Gütschow, M. *J. Med. Chem.* **2005**, *48*, 8270–8288.

(48) Schröder, R.; Janssen, N.; Schmidt, J.; Kebig, A.; Merten, N.; Hennen, S.; Müller, A.; Blättermann, S.; Mohr-Andrä, M.; Zahn, S.; Wenzel, J.; Smith, N. J.; Gomeza, J.; Drewke, C.; Milligan, G.; Mohr, K.; Kostenis, E. *Nat. Biotechnol.* **2010**, *28*, 943–949.

(49) Schröder, R.; Schmidt, J.; Blättermann, S.; Peters, L.; Janssen, N.; Grundmann, M.; Seemann, W.; Kaufel, D.; Merten, N.; Drewke, C.; Gomeza, J.; Milligan, G.; Mohr, K.; Kostenis, E. *Nat. Protoc.* **2011**, *6*, 1748–1760.

(50) Jungalwala, F. B.; Natowicz, M. R.; Chaturvedi, P.; Newburg, D. S. In *Methods in Enzymology*; Alfred H. Merrill, J., Yusuf A. Hannun, Ed.; Sphingolipid Metabolism and Cell Signaling Part A; Academic Press, 2000; Vol. Volume 311, pp. 94–105.

(51) Kremb, S.; Helfer, M.; Heller, W.; Hoffmann, D.; Wolff, H.; Kleinschmidt, A.; Cepok, S.; Hemmer, B.; Durner, J.; Brack-Werner, R. *Antimicrob. Agents Chemother.* **2010**, *54*, 5257–5268.

(52) Trager, W.; Jensen, J. B. *Science* **1976**, *193*, 673–675.

(53) Desjardins, R. E.; Canfield, C. J.; Haynes, J. D.; Chulay, J. D. *Antimicrob. Agents Chemother.* **1979**, *16*, 710–718.

(54) Hofer, S.; Brun, R.; Maerki, S.; Matile, H.; Scheurer, C.; Wittlin, S. *J. Antimicrob. Chemother.* **2008**, *62*, 1061–1064.

(55) Regalado, E. L.; Tasdemir, D.; Kaiser, M.; Cachet, N.; Amade, P.; Thomas, O. P. *J. Nat. Prod.* **2010**, *73*, 1404–1410.

(56) Ganapaty, S.; Steve Thomas, P.; Karagianis, G.; Waterman, P. G.; Brun, R. *Phytochemistry* **2006**, *67*, 1950–1956.

(57) Bode, H. B.; Bethe, B.; Höfs, R.; Zeeck, A. *ChemBioChem* **2002**, *3*, 619–627.

(58) Graham, E. S.; Ashton, J. C.; Glass, M. *Front. Biosci. J. Virtual Libr.* **2009**, *14*, 944–957.

(59) Matsuda, L. A.; Lolait, S. J.; Brownstein, M. J.; Young, A. C.; Bonner, T. I. *Nature* **1990**, *346*, 561–564.

(60) Demuth, D. G.; Molleman, A. *Life Sci.* **2006**, *78*, 549–563.

(61) Pacher, P.; Bátkai, S.; Kunos, G. *Pharmacol. Rev.* **2006**, *58*, 389–462.

(62) Galiègue, S.; Mary, S.; Marchand, J.; Dussossoy, D.; Carrière, D.; Carayon, P.; Bouaboula, M.; Shire, D.; Le Fur, G.; Casellas, P. *Eur. J. Biochem. FEBS* **1995**, *232*, 54–61.

(63) Racz, I.; Nadal, X.; Alferink, J.; Banos, J. E.; Rehnelt, J.; Martin, M.; Pintado, B.; Gutierrez-Adan, A.; Sanguino, E.; Manzanares, J.; Zimmer, A.; Maldonado, R. *J. Neurosci.* **2008**, *28*, 12125–12135.

(64) Pertwee, R. G. *Curr. Med. Chem.* **2010**, *17*, 1360–1381.

(65) Maccarrone, M.; Gasperi, V.; Catani, M. V.; Diep, T. A.; Dainese, E.; Hansen, H. S.; Avigliano, L. *Annu. Rev. Nutr.* **2010**, *30*, 423–440.

(66) Scheen, A. J. *J. Neuroendocrinol.* **2008**, *20 Suppl 1*, 139–146.

(67) Le Foll, B.; Gorelick, D. A.; Goldberg, S. R. *Psychopharmacology (Berl.)* **2009**, *205*, 171–174.

(68) Chorvat, R. J. *Bioorg. Med. Chem. Lett.* **2013**, *23*, 4751–4760.

(69) Fulp, A.; Bortoff, K.; Zhang, Y.; Seltzman, H.; Snyder, R.; Maitra, R. *Bioorg. Med. Chem. Lett.* **2011**, *21*, 5711–5714.

(70) Dow, R. L.; Carpino, P. A.; Gautreau, D.; Hadcock, J. R.; Iredale, P. A.; Kelly-Sullivan, D.; Lizano, J. S.; O'Connor, R. E.; Schneider, S. R.; Scott, D. O.; Ward, K. M. *ACS Med. Chem. Lett.* **2012**, *3*, 397–401.

(71) Chorvat, R. J.; Berbaum, J.; Seriacki, K.; McElroy, J. F. *Bioorg. Med. Chem. Lett.* **2012**, *22*, 6173–6180.

(72) Fulp, A.; Bortoff, K.; Seltzman, H.; Zhang, Y.; Mathews, J.; Snyder, R.; Fennell, T.; Maitra, R. *J. Med. Chem.* **2012**, *55*, 2820–2834.

(73) Pacher, P. *Pharmacol. Rev.* **2006**, *58*, 389–462.

(74) Geng, D. C.; Xu, Y. Z.; Yang, H. L.; Zhu, X. S.; Zhu, G. M.; Wang, X. B. *J. Biomed. Mater. Res. A* **2010**, *95A*, 321–326.

(75) Pacher, P.; Mechoulam, R. *Prog. Lipid Res.* **2011**, *50*, 193–211.

(76) Alexander, S. *Br. J. Pharmacol.* **2012**, *165*, 2411–2413.

(77) Ryberg, E.; Larsson, N.; Sjogren, S.; Hjorth, S.; Hermansson, N.-O.; Leonova, J.; Elebring, T.; Nilsson, K.; Drmota, T.; Greasley, P. J. *Br. J. Pharmacol.* **2007**, *152*, 1092–1101.

(78) Pertwee, R. G.; Howlett, A. C.; Abood, M. E.; Alexander, S. P. H.; Di Marzo, V.; Elphick, M. R.; Greasley, P. J.; Hansen, H. S.; Kunos, G.; Mackie, K.; Mechoulam, R.; Ross, R. A. *Pharmacol. Rev.* **2010**, *62*, 588–631.

(79) McHugh, D.; Page, J.; Dunn, E.; Bradshaw, H. B. *Br. J. Pharmacol.* **2012**, *165*, 2414–2424.

(80) Sharir, H.; Abood, M. E. *Pharmacol. Ther.* **2010**, *126*, 301–313.

(81) Anavi-Goffer, S.; Baillie, G.; Irving, A. J.; Gertsch, J.; Greig, I. R.; Pertwee, R. G.; Ross, R. A. *J. Biol. Chem.* **2011**, *287*, 91–104.

(82) Brown, A. J.; Daniels, D. A.; Kassim, M.; Brown, S.; Haslam, C. P.; Terrell, V. R.; Brown, J.; Nichols, P. L.; Staton, P. C.; Wise, A.; Dowell, S. J. *J. Pharmacol. Exp. Ther.* **2011**, *337*, 236–246.

(83) McHugh, D. *Br. J. Pharmacol.* **2012**, *167*, 1575–1582.

(84) Kohno, M.; Hasegawa, H.; Inoue, A.; Muraoka, M.; Miyazaki, T.; Oka, K.; Yasukawa, M. *Biochem. Biophys. Res. Commun.* **2006**, *347*, 827–832.

(85) Bradshaw, H. B.; Rimmerman, N.; Hu, S.; Benton, V. M.; Stuart, J. M.; Masuda, K.; Cravatt, B. F.; O'Dell, D. K.; Walker, J. M. *BMC Biochem.* **2009**, *10*, 14.

(86) McHugh, D.; Hu, S. S.; Rimmerman, N.; Juknat, A.; Vogel, Z.; Walker, J. M.; Bradshaw, H. B. *BMC Neurosci.* **2010**, *11*, 44.

(87) Takenouchi, R.; Inoue, K.; Kambe, Y.; Miyata, A. *Biochem. Biophys. Res. Commun.* **2012**, *418*, 366–371.

(88) Lu, V. B.; Puhl, H. L.; Ikeda, S. R. *Mol. Pharmacol.* **2013**, *83*, 267–282.

(89) Yin, H.; Chu, A.; Li, W.; Wang, B.; Shelton, F.; Otero, F.; Nguyen, D. G.; Caldwell, J. S.; Chen, Y. A. *J. Biol. Chem.* **2009**, *284*, 12328–12338.

(90) Caldwell, M. D.; Hu, S. S.-J.; Viswanathan, S.; Bradshaw, H.; Kelly, M. E.; Straiker, A. *Br. J. Pharmacol.* **2013**, *169*, 834–843.

(91) McHugh, D.; Wager-Miller, J.; Page, J.; Bradshaw, H. B. *J. Mol. Signal.* **2012**, *7*, 10.

(92) Henstridge, C. M.; Balenga, N. A. B.; Ford, L. A.; Ross, R. A.; Waldhoer, M.; Irving, A. J. *FASEB J.* **2009**, *23*, 183–193.

(93) Obara, Y.; Ueno, S.; Yanagihata, Y.; Nakahata, N. *PLoS ONE* **2011**, *6*, e24284.

(94) Whyte, L. S.; Ryberg, E.; Sims, N. A.; Ridge, S. A.; Mackie, K.; Greasley, P. J.; Ross, R. A.; Rogers, M. J. *Proc. Natl. Acad. Sci.* **2009**, *106*, 16511–16516.

(95) Piñeiro, R.; Maffucci, T.; Falasca, M. *Oncogene* **2011**, *30*, 142–152.

(96) Ross, R. A. *Trends Pharmacol. Sci.* **2011**, *32*, 265–269.

(97) Henstridge, C. M. *Pharmacology* **2012**, *89*, 179–187.

(98) Oka, S.; Nakajima, K.; Yamashita, A.; Kishimoto, S.; Sugiura, T. *Biochem. Biophys. Res. Commun.* **2007**, *362*, 928–934.

(99) Houlihan, W. J. *The Chemistry of Heterocyclic Compounds*, *Indoles*; John Wiley & Sons: published simultaneously in Canada, 1972.

(100) Nozawa, K.; Nakajima, S.; Kawai, K.; Udagawa, S. *J. Chem. Soc. [Perkin 1]* **1988**, 2607–2610.

(101) Ogata, M.; Ueda, J.; Hoshi, M.; Hashimoto, J.; Nakashima, T.; Anzai, K.; Takagi, M.; Shin-ya, K. *J. Antibiot. (Tokyo)* **2007**, *60*, 645–648.

(102) Qiao, M.-F.; Ji, N.-Y.; Liu, X.-H.; Li, K.; Zhu, Q.-M.; Xue, Q.-Z. *Bioorg. Med. Chem. Lett.* **2010**, *20*, 5677–5680.

(103) Fan, Y.; Wang, Y.; Liu, P.; Fu, P.; Zhu, T.; Wang, W.; Zhu, W. *J. Nat. Prod.* **2013**, *76*, 1328–1336.

(104) Altona, C.; Haasnoot, C. A. G. *Org. Magn. Reson.* **1980**, *13*, 417–429.

(105) Bock, K.; Pedersen, C. *J. Chem. Soc. Perkin Trans. 2* **1974**, 293–297.

(106) Okabe, H.; Miyahara, Y.; Yamauchi, T. *Chem. Pharm. Bull. (Tokyo)* **1982**, *30*, 4334–4340.

(107) Gohbara, M.; Kosuge, Y.; Yamasaki, S.; Kimura, Y.; Suzuki, A.; Tamura, S. *Agric. Biol. Chem.* **1978**, *42*, 1037–1043.

(108) Qiao, M.-F.; Ji, N.-Y.; Liu, X.-H.; Li, F.; Xue, Q.-Z. *YIC-IR* **2010**, *5*.

(109) Pertwee, R. G. *Pharmacol. Ther.* **1997**, *74*, 129–180.

(110) Pertwee, R.; Griffin, G.; Fernando, S.; Li, X.; Hill, A.; Makriyannis, A. *Life Sci.* **1995**, *56*, 1949–1955.

(111) Elsebai, M. F.; Rempel, V.; Schnakenburg, G.; Kehraus, S.; Müller, C. E.; König, G. M. *ACS Med. Chem. Lett.* **2011**, *2*, 866–869.

(112) Rempel, V.; Fuchs, A.; Hinz, S.; Karcz, T.; Lehr, M.; Koetter, U.; Müller, C. E. *ACS Med. Chem. Lett.* **2013**, *4*, 41–45.

(113) Felder, C. C.; Joyce, K. E.; Briley, E. M.; Mansouri, J.; Mackie, K.; Blond, O.; Lai, Y.; Ma, A. L.; Mitchell, R. L. *Mol. Pharmacol.* **1995**, *48*, 443–450.

(114) Thomas, A.; Stevenson, L. A.; Wease, K. N.; Price, M. R.; Baillie, G.; Ross, R. A.; Pertwee, R. G. *Br. J. Pharmacol.* **2005**, *146*, 917–926.

(115) Gao, J.; León, F.; Radwan, M. M.; Dale, O. R.; Husni, A. S.; Manly, S. P.; Lupien, S.; Wang, X.; Hill, R. A.; Dugan, F. M.; Cutler, H. G.; Cutler, S. J. *J. Nat. Prod.* **2011**, *74*, 1636–1639.

(116) Kitajima, M.; Iwai, M.; Kikura-Hanajiri, R.; Goda, Y.; Iida, M.; Yabushita, H.; Takayama, H. *Bioorg. Med. Chem. Lett.* **2011**, *21*, 1962–1964.

(117) Dalziel, J.; Dunlop, J.; Finch, S.; Wong, S. Immune Response Inhibition Using Indole Diterpene Compound WO 2006/115423, **2006**.

(118) Ahluwalia, J.; Tinker, A.; Clapp, L. H.; Duchen, M. R.; Abramov, A. Y.; Pope, S.; Nobles, M.; Segal, A. W. *Nature* **2004**, *427*, 853–858.

(119) Zhou, F.; Lu, J.; Zhu, X.; Mao, H.; Yang, H.; Geng, D.; Xu, Y. *J. Int. Med. Res.* **2010**, *38*, 2023–2032.

(120) Ansar Ahmed, S.; Gogal Jr., R. M.; Walsh, J. E. *J. Immunol. Methods* **1994**, *170*, 211–224.

(121) Qin, Y.; Verdegaal, E. M. E.; Siderius, M.; Bebelman, J. P.; Smit, M. J.; Leurs, R.; Willemze, R.; Tensen, C. P.; Osanto, S. *Pigment Cell Melanoma Res.* **2011**, *24*, 207–218.

(122) Hardy, J.; Higgins, G. *Science* **1992**, *256*, 184–185.

(123) Bettayeb, K.; Oumata, N.; Zhang, Y.; Luo, W.; Bustos, V.; Galons, H.; Greengard, P.; Meijer, L.; Flajolet, M. *FASEB J.* **2012**, *26*, 5115–5123.

(124) Selkoe, D. J. *Ann. Neurol.* **2013**, *74*, 328–336.

(125) Golde, T. E.; Koo, E. H.; Felsenstein, K. M.; Osborne, B. A.; Miele, L. *Biochim. Biophys. Acta BBA - Biomembr.* **2013**, *1828*, 2898–2907.

(126) Ghosh, A. K.; Brindisi, M.; Tang, J. *J. Neurochem.* **2012**, *120*, 71–83.

(127) Holland, H. L.; Chenchaiah, P. C.; Thomas, E. M.; Mader, B.; Dennis, M. J. *Can. J. Chem.* **1984**, *62*, 2740–2747.

(128) Gan, K.-H.; Kuo, S.-H.; Lin, C.-N. *J. Nat. Prod.* **1998**, *61*, 1421–1422.

(129) Takatsuki, A.; Suzuki, S.; Ando, K.; Tamura, G.; Arima, K. *J. Antibiot. (Tokyo)* **1968**, *21*, 671–675.

(130) Ando, K. *J. Antibiot. (Tokyo)* **1968**, *21*, 587–591.

(131) Morino, T.; Nishimoto, M.; Itou, N.; Nishikiori, T. *J. Antibiot. (Tokyo)* **1994**, *47*, 1546–1548.

(132) Tatsuta, K.; Yamaguchi, T. *Tetrahedron Lett.* **2005**, *46*, 5017–5020.

(133) Sakai, R.; Nakamura, T.; Nishino, T.; Yamamoto, M.; Miyamura, A.; Miyamoto, H.; Ishiwata, N.; Komatsu, N.; Kamiya, H.; Tsuruzoe, N. *Bioorg. Med. Chem.* **2005**, *13*, 6388–6393.

(134) Hubbs, J. L.; Fuller, N. O.; Austin, W. F.; Shen, R.; Creaser, S. P.; McKee, T. D.; Loureiro, R. M. B.; Tate, B.; Xia, W.; Ives, J.; Bronk, B. S. *J. Med. Chem.* **2012**, *55*, 9270–9282.

(135) Findeis, M. A.; Schroeder, F.; McKee, T. D.; Yager, D.; Fraering, P. C.; Creaser, S. P.; Austin, W. F.; Clardy, J.; Wang, R.; Selkoe, D.; Eckman, C. B. *ACS Chem. Neurosci.* **2012**, *3*, 941–951.

(136) Burris, T. P.; Solt, L. A.; Wang, Y.; Crumbley, C.; Banerjee, S.; Griffett, K.; Lundasen, T.; Hughes, T.; Kojetin, D. J. *Pharmacol. Rev.* **2013**, *65*, 710–778.

(137) Sever, R.; Glass, C. K. *Cold Spring Harb. Perspect. Biol.* **2013**, *5*, a016709.

(138) Burris, T. P.; Busby, S. A.; Griffin, P. R. *Chem. Biol.* **2012**, *19*, 51–59.

(139) Michalik, L.; Auwerx, J.; Berger, J. P.; Chatterjee, V. K.; Glass, C. K.; Gonzalez, F. J.; Grimaldi, P. A.; Kadowaki, T.; Lazar, M. A.; O'Rahilly, S.; Palmer, C. N. A.; Plutzky, J.; Reddy, J. K.; Spiegelman, B. M.; Staels, B.; Wahli, W. *Pharmacol. Rev.* **2006**, *58*, 726–741.

(140) Kersten, S.; Desvergne, B.; Wahli, W. *Nature* **2000**, *405*, 421–424.

(141) Nissen SE; Nicholls SJ; Wolski K; et al *JAMA* **2007**, *297*, 1362–1373.

(142) Dhoke, G. V.; Gangwal, R. P.; Sangamwar, A. T. *J. Mol. Struct.* **2012**, *1028*, 22–30.

(143) Wagner, K.-D.; Wagner, N. *Pharmacol. Ther.* **2010**, *125*, 423–435.

(144) Repa, J. J.; Mangelsdorf, D. J. *Annu. Rev. Cell Dev. Biol.* **2000**, *16*, 459–481.

(145) Laffitte, B. A.; Chao, L. C.; Li, J.; Walczak, R.; Hummasti, S.; Joseph, S. B.; Castrillo, A.; Wilpitz, D. C.; Mangelsdorf, D. J.; Collins, J. L.; Saez, E.; Tontonoz, P. *Proc. Natl. Acad. Sci.* **2003**, *100*, 5419–5424.

(146) Joseph, S. B.; McKilligin, E.; Pei, L.; Watson, M. A.; Collins, A. R.; Laffitte, B. A.; Chen, M.; Noh, G.; Goodman, J.; Hagger, G. N.; Tran, J.; Tippin, T. K.; Wang, X.; Lusis, A. J.; Hsueh, W. A.; Law, R. E.; Collins, J. L.; Willson, T. M.; Tontonoz, P. *Proc. Natl. Acad. Sci.* **2002**, *99*, 7604–7609.

(147) Cao, G.; Liang, Y.; Broderick, C. L.; Oldham, B. A.; Beyer, T. P.; Schmidt, R. J.; Zhang, Y.; Stayrook, K. R.; Suen, C.; Otto, K. A.; Miller, A. R.; Dai, J.; Foxworthy, P.; Gao, H.; Ryan, T. P.; Jiang, X.-C.; Burris, T. P.; Eacho, P. I.; Etgen, G. J. *J. Biol. Chem.* **2003**, *278*, 1131–1136.

(148) Koldamova, R.; Lefterov, I. *Curr. Alzheimer Res.* **2007**, *4*, 171–178.

(149) Nomiyama, T.; Bruemmer, D. *Curr. Atheroscler. Rep.* **2008**, *10*, 88–95.

(150) Xu, J.; Wagoner, G.; Douglas, J. C.; Drew, P. D. *J. Leukoc. Biol.* **2009**, *86*, 401–409.

(151) Chuu, C.-P. *Med. Hypotheses* **2011**, *76*, 697–699.

(152) Johnson, J. R.; Bruce, W. F.; Dutcher, J. D. *J. Am. Chem. Soc.* **1943**, *65*, 2005–2009.

(153) Fukuyama, T.; Nakatsuka, S.-I.; Kishi, Y. *Tetrahedron* **1981**, *37*, 2045–2078.

(154) Kaouadji, M.; Steiman, R.; Seigle-Murandi, F.; Krivobok, S.; Sage, L. *J. Nat. Prod.* **1990**, *53*, 717–719.

(155) Gardiner, D. M.; Waring, P.; Howlett, B. J. *Microbiology* **2005**, *151*, 1021–1032.

(156) Scharf, D. H.; Chankhamjon, P.; Scherlach, K.; Heinekamp, T.; Roth, M.; Brakhage, A. A.; Hertweck, C. *Angew. Chem.* **2012**, *124*, 10211–10215.

(157) Beecham, A. F.; Fridrichsons, J.; Mathieson, A. M. *Tetrahedron Lett.* **1966**, *7*, 3131–3138.

(158) Watts, K. R.; Ratnam, J.; Ang, K.-H.; Tenney, K.; Compton, J. E.; McKerrow, J.; Crews, P. *Bioorg. Med. Chem.* **2010**, *18*, 2566–2574.

(159) Okamoto, M.; Yoshida, K.; Uchida, I.; Nishikawa, M.; Kohsaka, M.; Aoki, H. *Chem. Pharm. Bull. (Tokyo)* **1986**, *34*, 340–344.

(160) Hosoe, T.; Fukushima, K.; Itabashi, T.; Nozawa, K.; Takizawa, K. *Heterocycles* **2004**, *63*, 2581–2589.

(161) Crane, R. I.; Hedden, P.; MacMillan, J.; Turner, W. B. *J. Chem. Soc. [Perkin 1]* **1973**, 194–200.

(162) Nieminen, S.; Tamm, C. *Helv. Chim. Acta* **1981**, *64*, 2791–2801.

(163) Safe, S.; Taylor, A. *J. Chem. Soc. C Org.* **1971**, 1189–1192.

(164) Herath, H. M. T. B.; Jacob, M.; Wilson, A. D.; Abbas, H. K.; Nanayakkara, N. P. D. *Nat. Prod. Res.* **2013**, *27*, 1562–1568.

(165) Ando, K.; Suzuki, S.; Takatsuk.a; Arima, K.; Tamura, G. *J. Antibiot. (Tokyo)* **1968**, *21*, 582–&.

(166) Varga, J.; Due, M.; Frisvad, J. C.; Samson, R. A. *Stud. Mycol.* **2007**, *59*, 89–106.

(167) McGwire, B. S.; Satoskar, A. R. *QJM* **2014**, *107*, 7–14.

(168) Tagami, K.; Liu, C.; Minami, A.; Noike, M.; Isaka, T.; Fueki, S.; Shichijo, Y.; Toshima, H.; Gomi, K.; Dairi, T.; Oikawa, H. *J. Am. Chem. Soc.* **2013**, *135*, 1260–1263.

(169) Dewick, P. M. *Medicinal natural products: a biosynthetic approach*; 2nd ed.; Wiley: Chichester, West Sussex, England ; New York, NY, USA, 2002.

(170) Herrmann, K. M.; Weaver, L. M. *Annu. Rev. Plant Physiol. Plant Mol. Biol.* **1999**, *50*, 473–503.

(171) Cable, K. M.; Herbert, R. B.; Knaggs, A. R.; Mann, J. *J. Chem. Soc. [Perkin 1]* **1991**, 595.

(172) Herbert, R. B.; Mann, J. *Tetrahedron Lett.* **1984**, *25*, 4263–4266.

(173) Herbert, R. B.; Mann, J. *J. Chem. Soc. Chem. Commun.* **1984**, 1474–1475.

(174) Cable, K. M.; Herbert, R. B.; Mann, J. *Tetrahedron Lett.* **1987**, *28*, 3159–3162.

(175) Balibar, C. J.; Walsh, C. T. *Biochemistry (Mosc.)* **2006**, *45*, 15029–15038.

(176) Chang, S.-L.; Chiang, Y.-M.; Yeh, H.-H.; Wu, T.-K.; Wang, C. C. C. *Bioorg. Med. Chem. Lett.* **2013**, *23*, 2155–2157.

(177) Scharf, D. H.; Chankhamjon, P.; Scherlach, K.; Heinekamp, T.; Willing, K.; Brakhage, A. A.; Hertweck, C. *Angew. Chem.* **2013**, *125*, 11298–11301.

(178) Amatov, T.; Jahn, U. *Angew. Chem.* **2014**, *126*, 3378–3380.

(179) Cox, R. E.; Holker, J. S. E. *J. Chem. Soc. Chem. Commun.* **1976**, 583–584.

(180) Bloomer, J. L.; Moppett, C. E.; Sutherland, J. K. *J. Chem. Soc. C Org.* **1968**, 588.

(181) Nieminen, S.; Payne, T. G.; Senn, P.; Tamm, C. *Helv. Chim. Acta* **1981**, *64*, 2162–2174.

(182) Sulikowski, G. A.; Pongdee, R. *Synlett* **2006**, 0354–0363.

(183) Takatsuki, A.; Takatsuki, G. A.; Tamura, K.; Arima, A. *J. Antibiot. (Tokyo)* **1968**, *21*, 676–680.

(184) Camp, D.; Camp, D.; Campitelli, M.; Carroll, A. R.; Davis, R. A.; Quinn, R. J. *Chem. Biodivers.* **2013**, *10*, 524–537.

(185) Lipinski, C. A.; Lombardo, F.; Dominy, B. W.; Feeney, P. J. *Adv. Drug Deliv. Rev.* **1997**, *23*, 3–25.

(186) Leeson, P. D.; Davis, A. M. *J. Med. Chem.* **2004**, *47*, 6338–6348.

(187) Thomas; Keller, T. H.; Pichota, A.; Yin, Z. *Curr. Opin. Chem. Biol.* **2006**, *10*, 357–361.

(188) Macarron, R. *Drug Discov. Today* **2006**, *11*, 277–279.

(189) David; Camp, D.; Davis, R. A.; Evans Illidge, E. A.; Quinn, R. J. *Future Med. Chem.* **2012**, *4*, 1067–1084.

(190) Marmann, A.; Aly, A.; Lin, W.; Wang, B.; Proksch, P. *Mar. Drugs* **2014**, *12*, 1043–1065.

(191) Zhu, F.; Chen, G.; Chen, X.; Huang, M.; Wan, X. *Chem. Nat. Compd.* **2011**, *47*, 767–769.

(192) Wiemann, P.; Keller, N. P. *J. Ind. Microbiol. Biotechnol.* **2014**, *41*, 301–313.

(193) Bergmann, S.; Schümann, J.; Scherlach, K.; Lange, C.; Brakhage, A. A.; Hertweck, C. *Nat. Chem. Biol.* **2007**, *3*, 213–217.

(194) Chiang, Y.-M.; Szewczyk, E.; Davidson, A. D.; Keller, N.; Oakley, B. R.; Wang, C. C. C. *J. Am. Chem. Soc.* **2009**, *131*, 2965–2970.

(195) Wang, C. C. C.; Chiang, Y.-M.; Praseuth, M. B.; Kuo, P.-L.; Liang, H.-L.; Hsu, Y.-L. *Basic Clin. Pharmacol. Toxicol.* **2010**, *107*, 583–589.

(196) Jain, S.; Keller, N. *Fungal Biol. Rev.* **2013**, *27*, 51–59.

(197) Chiang, Y.-M.; Szewczyk, E.; Davidson, A. D.; Entwistle, R.; Keller, N. P.; Wang, C. C. C.; Oakley, B. R. *Appl. Environ. Microbiol.* **2010**, *76*, 2067–2074.

(198) Henrikson, J. C.; Hoover, A. R.; Joyner, P. M.; Cichewicz, R. H. *Org. Biomol. Chem.* **2009**, *7*, 435–438.

8 Appendix

8.1 Metabolites isolated during this study

Compound no.	trivial name
1	emindole SB beta-mannoside
2	27-O-methylasporyzin
3	emindole SB beta-formate
4	JBIR-03
5	emindole SB
6	asporyzin C
7	emindole SB-N-propylcarbamate (semisynthetic derived from emindole SB)
8	amauramin (isolated by Mahmoud Fahmi Elsebai)
9	16-O-desmethylasporyergosterol-ß-D-mannoside
10	16-O-desmethylasporyergosteron-ß-D-mannoside
11	16-O-desmethylasporyergosterol
12	xanthocillin X dimethylether
13	xanthocillin X monomethylether
14	6-acetylmonodethiogliotoxin
15	6-acetylbisdethiobis(methylthio)gliotoxin
16	5a,6-anhydrobisdethiobis(methylthio)gliotoxin
17	heveadride

8.2 Spectroscopic data of isolated compounds

^{1}H NMR spectrum (300 MHz in acetone-d_6) of compound emindole SB beta-mannoside (**1**).

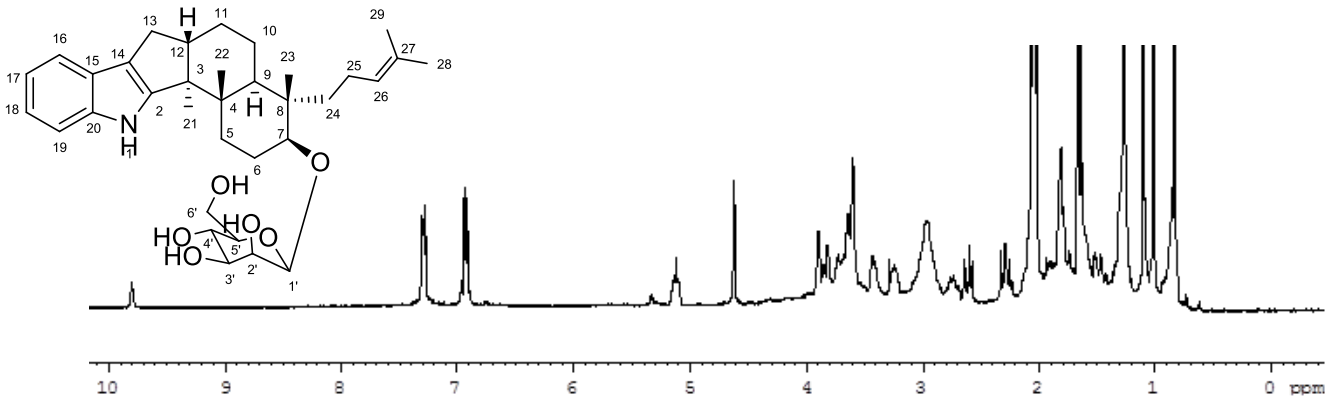

^{13}C NMR spectrum (75.5 MHz in acetone-d_6) of compound emindole SB beta-mannoside (**1**).

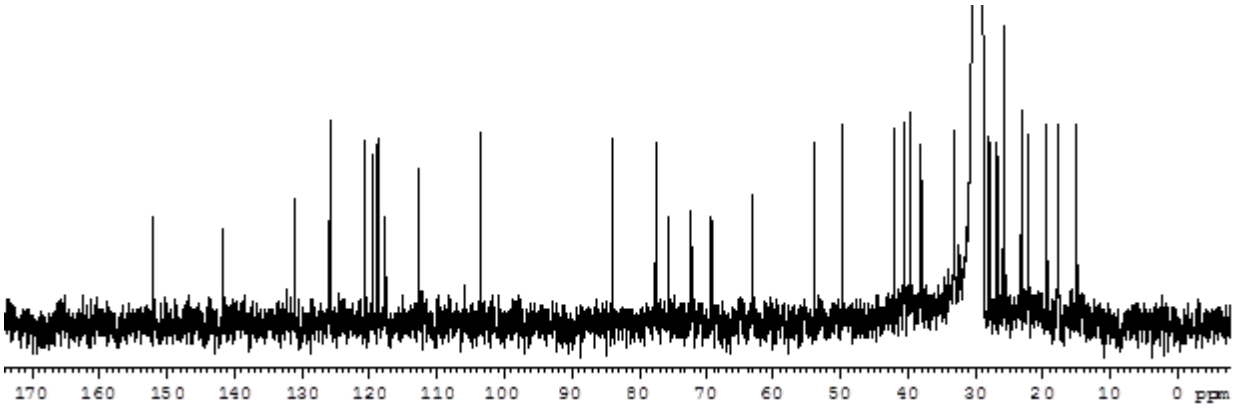

Dept 135 NMR (75.5 MHz in acetone-d_6) of compound emindole SB beta-mannoside (**1**).

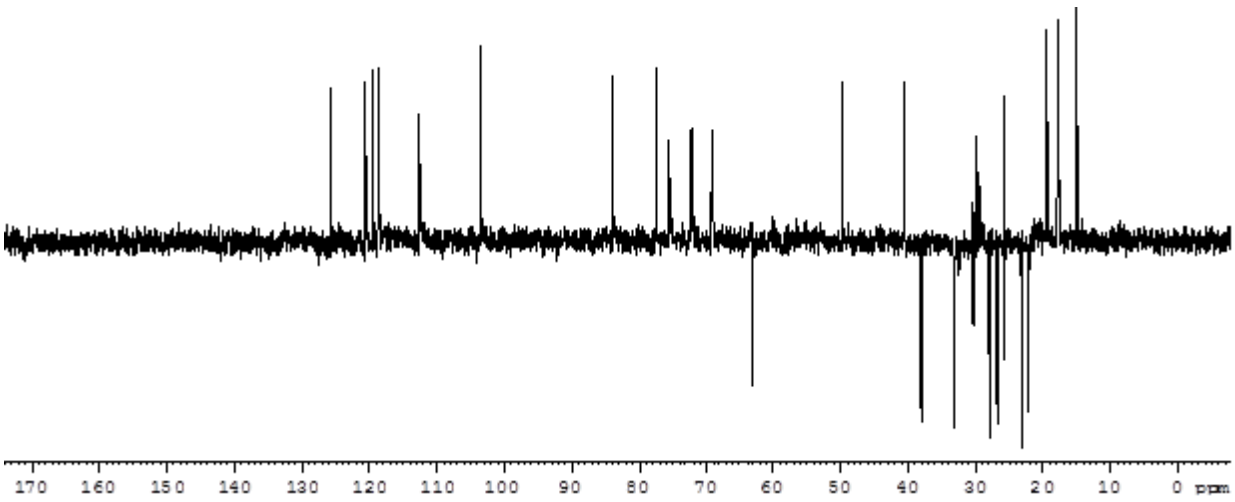

IR spectrum of compound emindole SB beta-mannoside (**1**).

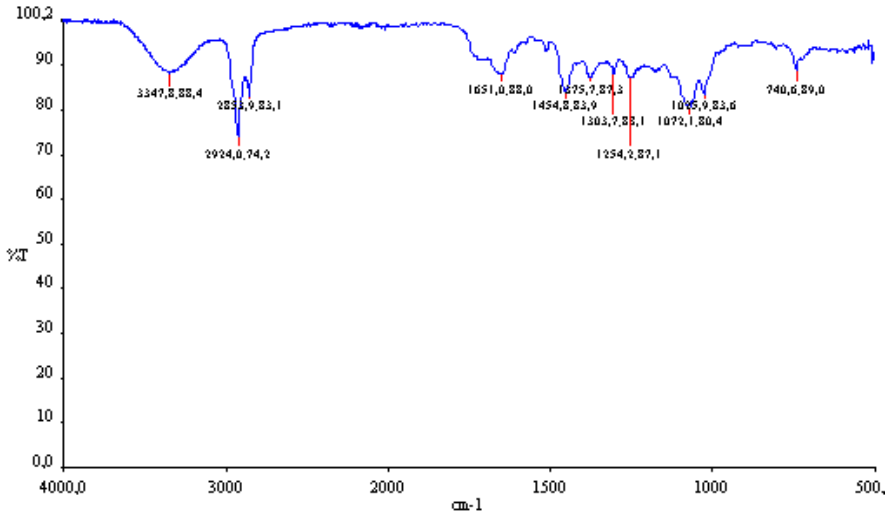

^{1}H-^{13}C HMBC 2D-NMR spectrum of compound **1** in acetone-d_6.

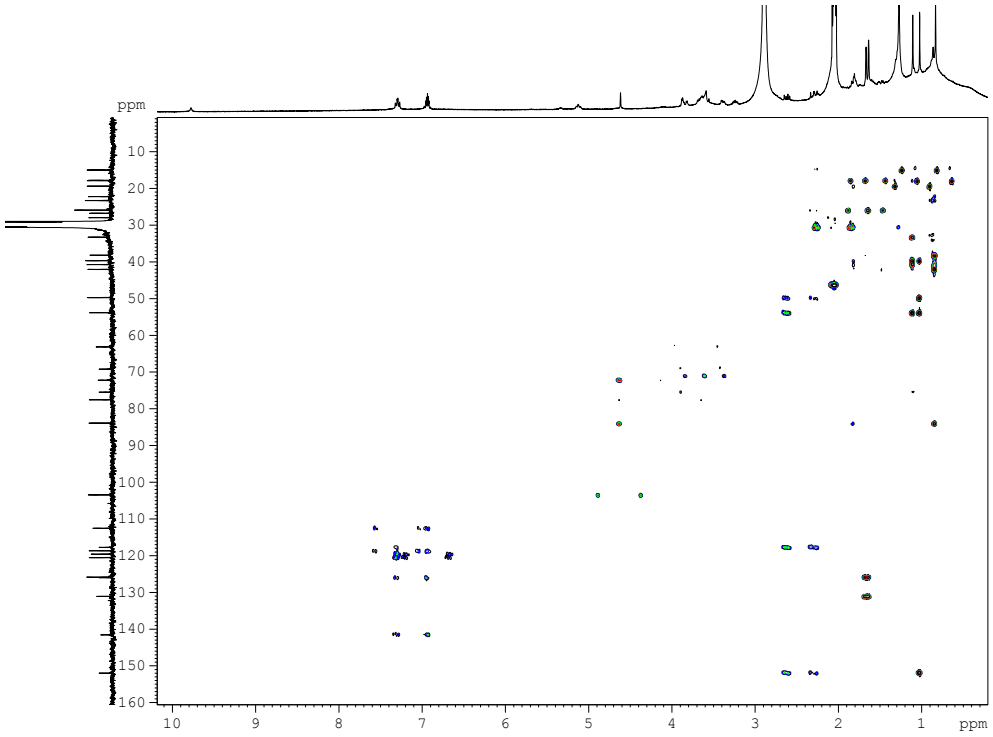

^{1}H NMR spectrum (300 MHz in acetone-d_6) of compound 27-O-methylasporyzin C (**2**).

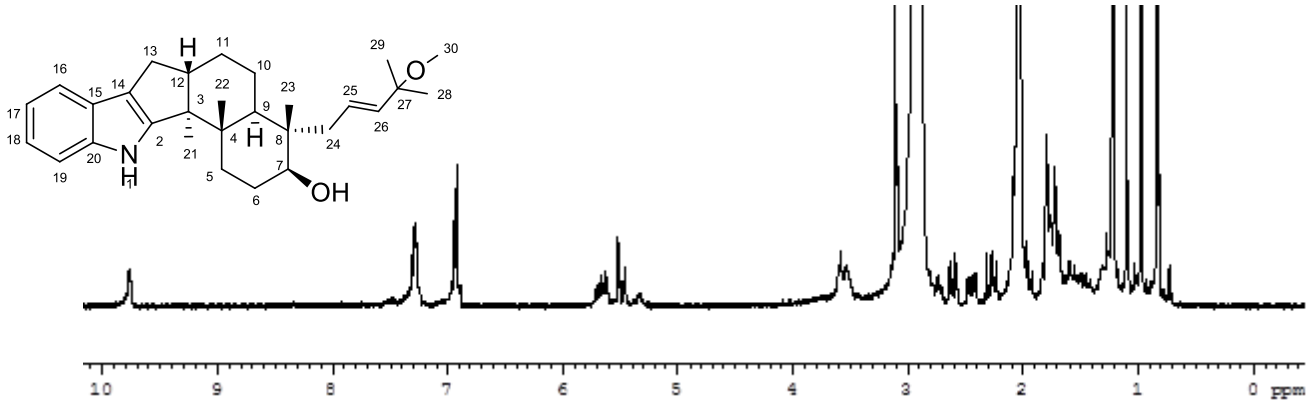

^{13}C NMR spectrum (75.5 MHz in acetone-d_6) of compound 27-O-methylasporyzin C (**2**).

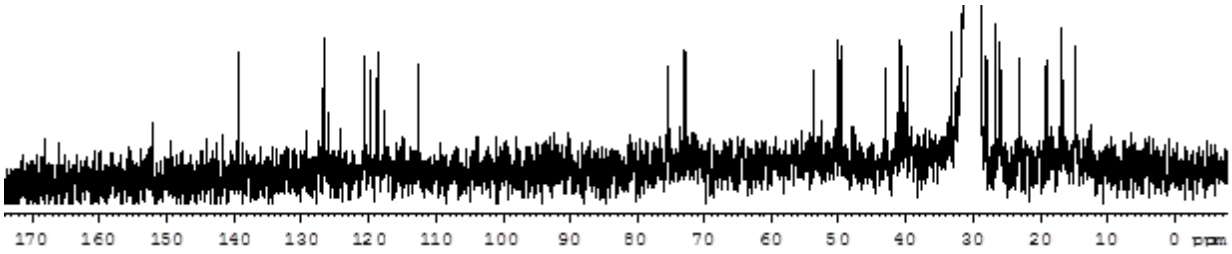

Dept135 NMR spectrum of (75.5 MHz in acetone-d6) of compound 27-O-methylasporyzin C (**2**).

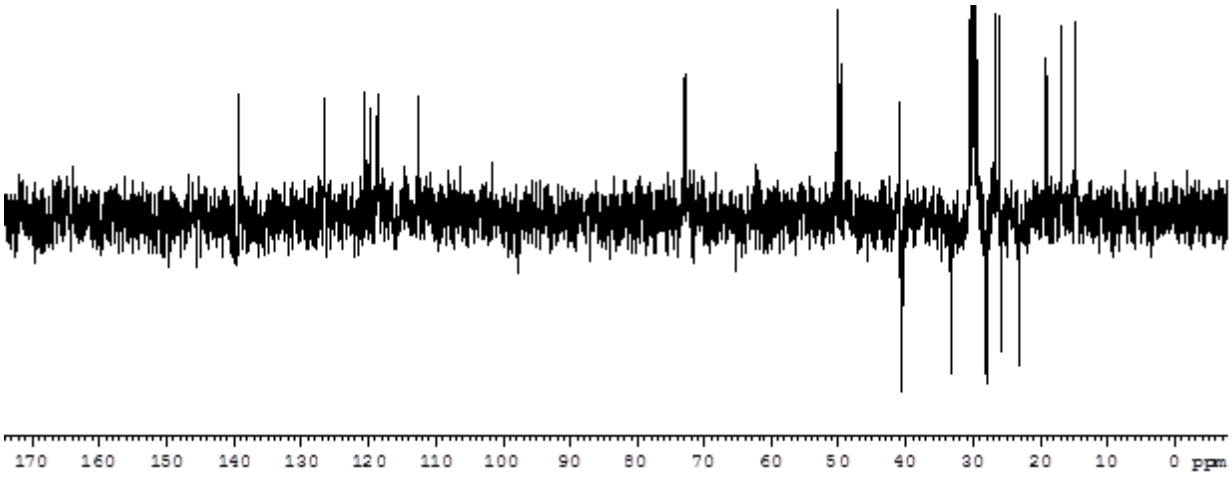

IR spectrum of compound 27-O-methylasporyzin C (**2**).

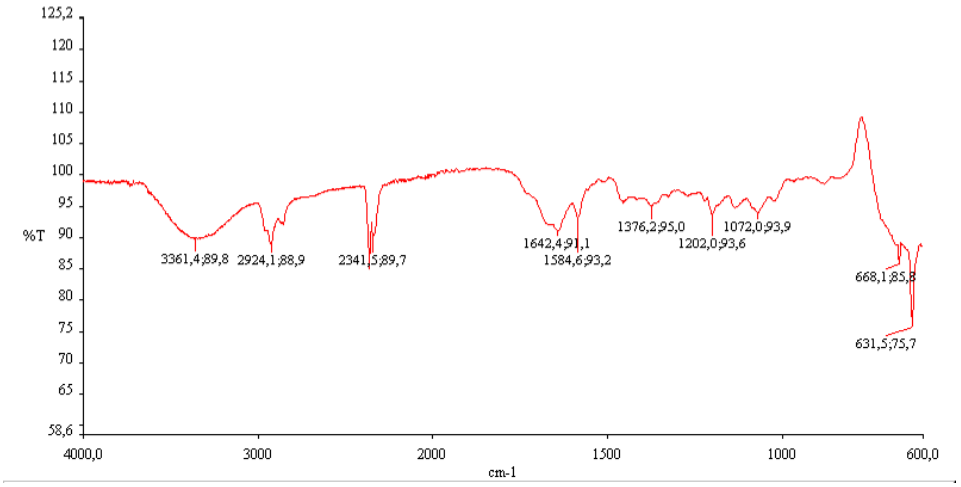

^{1}H NMR spectrum (300 MHz in acetone-d_6) of compound emindole SB beta-formate (**3**).

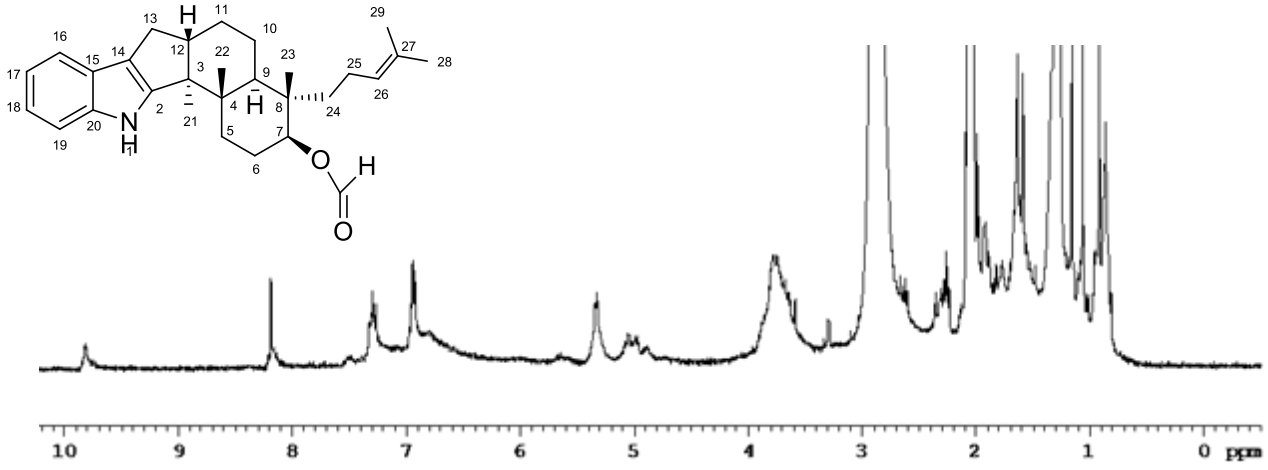

^{13}C NMR spectrum (300 MHz in acetone-d_6) of compound emindole SB beta-formate (**3**).

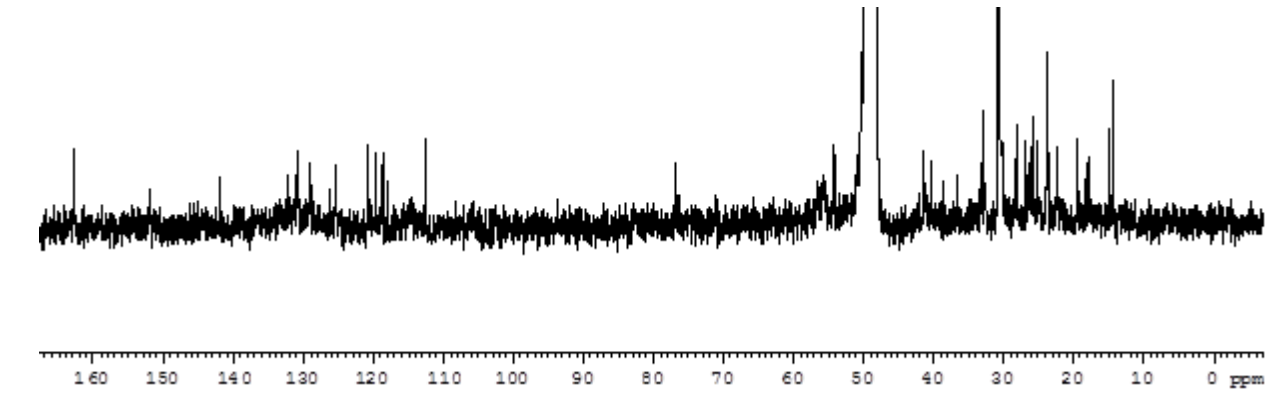

^{13}C DEPT NMR spectrum (75.5 in acetone-d_6) of compound emindole SB beta-formate (**3**).

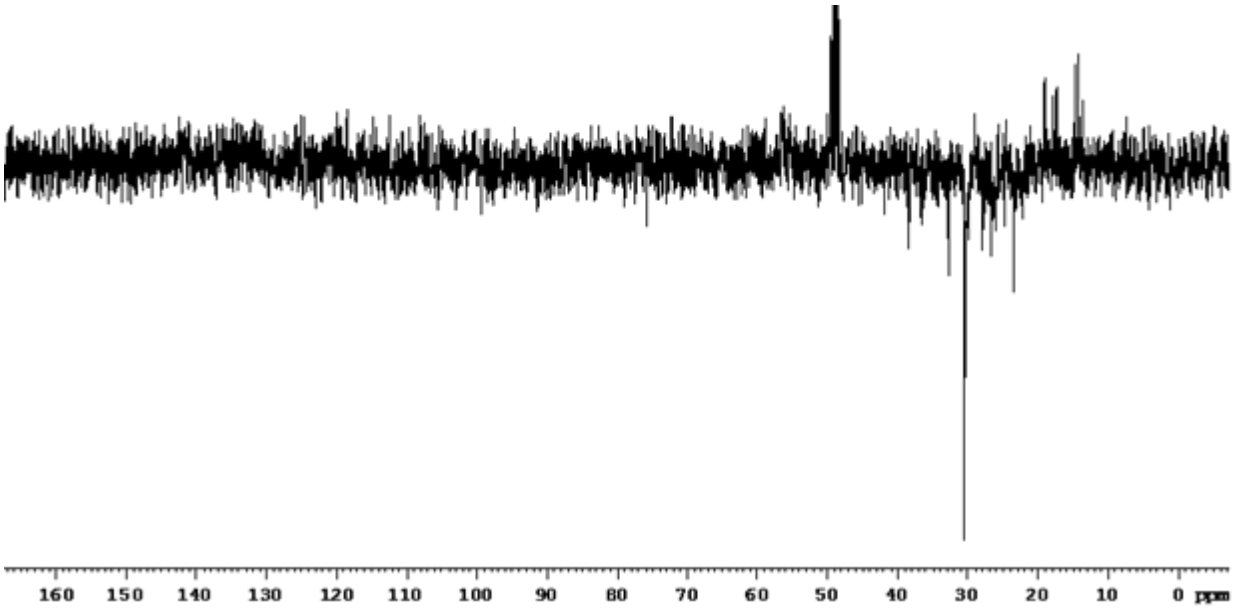

IR spectrum of compound emindole SB-formate (**3**).

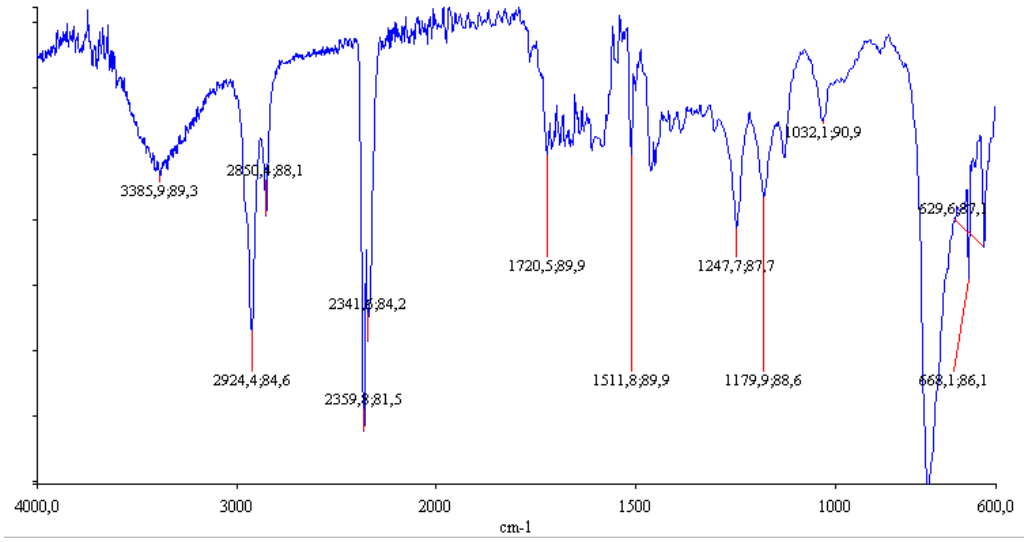

^{1}H NMR spectrum (300 MHz in methanol-d_4) of compound JBIR-03 (**4**).

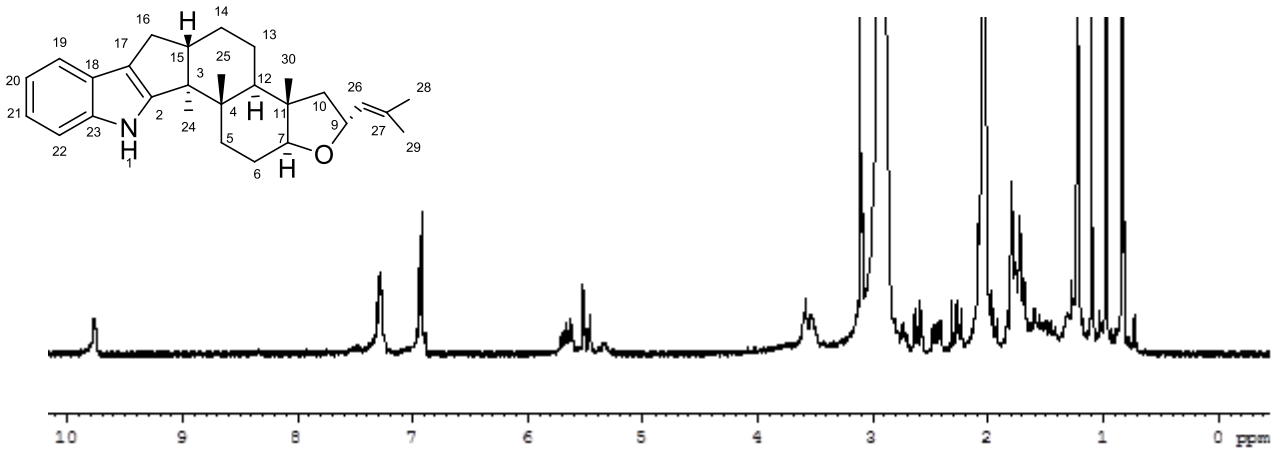

^{13}C NMR spectrum (75.5 MHz in methanol-d_4) of compound JBIR-03 (**4**).

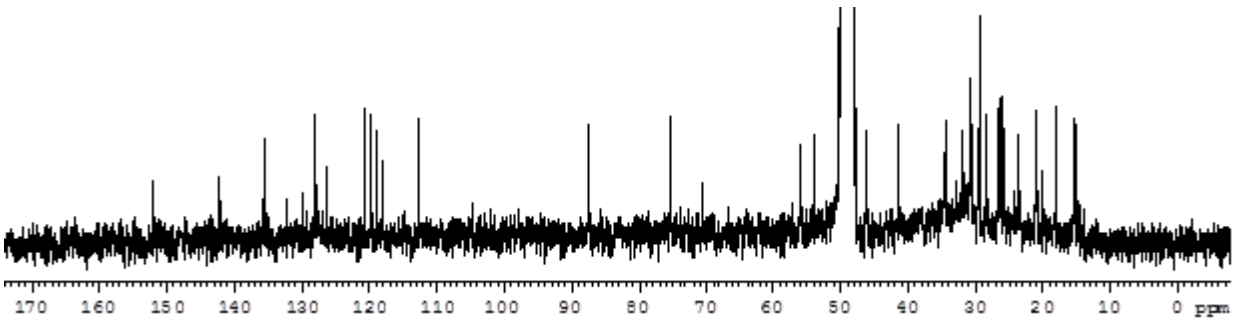

Dept 135 NMR spectrum (75.5 MHz in methanol-d_4) of compound JBIR-03 (**4**).

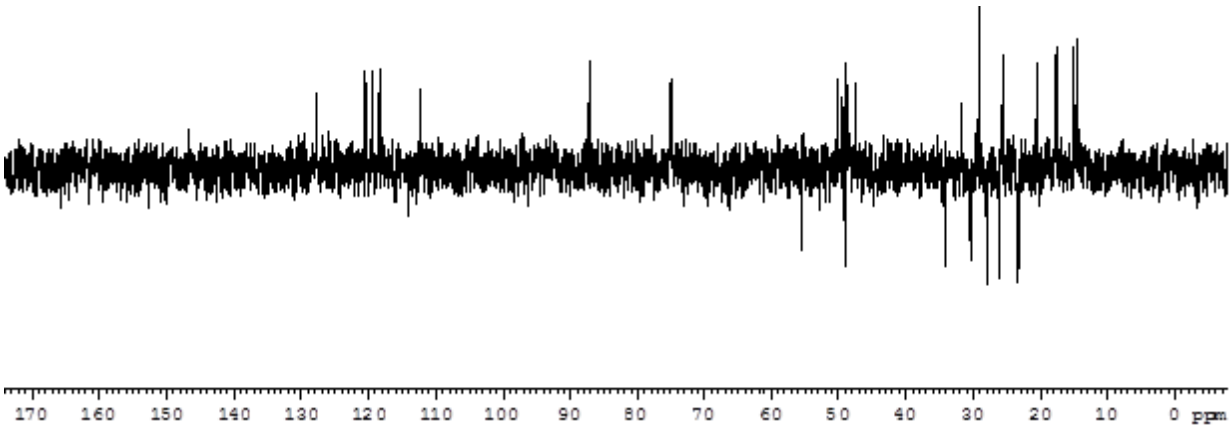

^{1}H NMR spectrum (300 MHz in acetone-d_6) of compound emindole SB (**5**)**.**

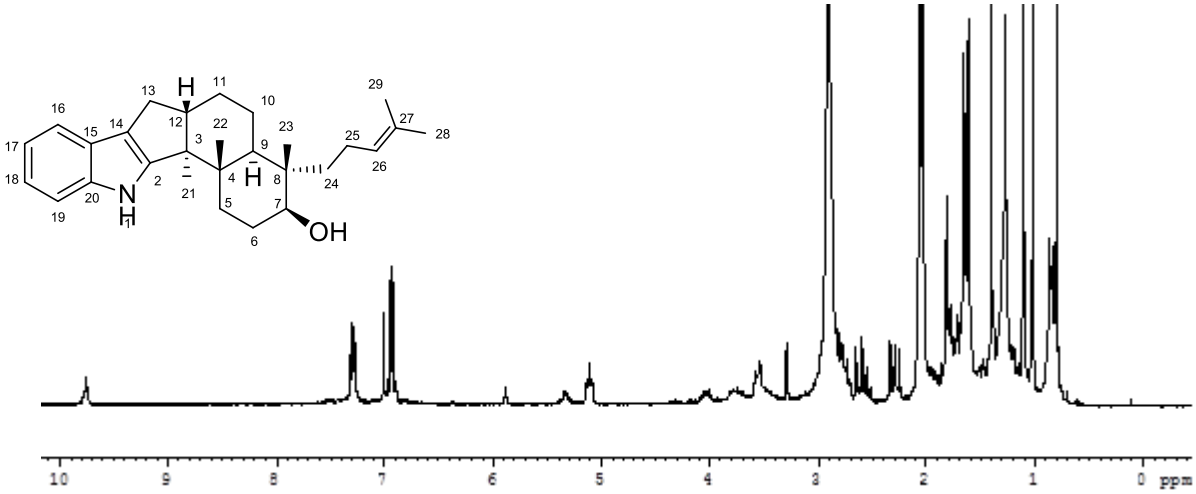

^{13}C NMR spectrum (75.5 MHz in acetone-d_6) of compound emindole SB (**5**).

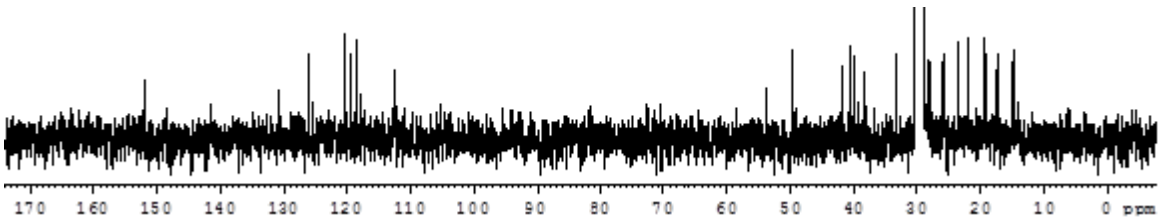

Dept 135 NMR spectrum (75.5 MHz in acetone-d_6) of compound emindole SB (**5)**.

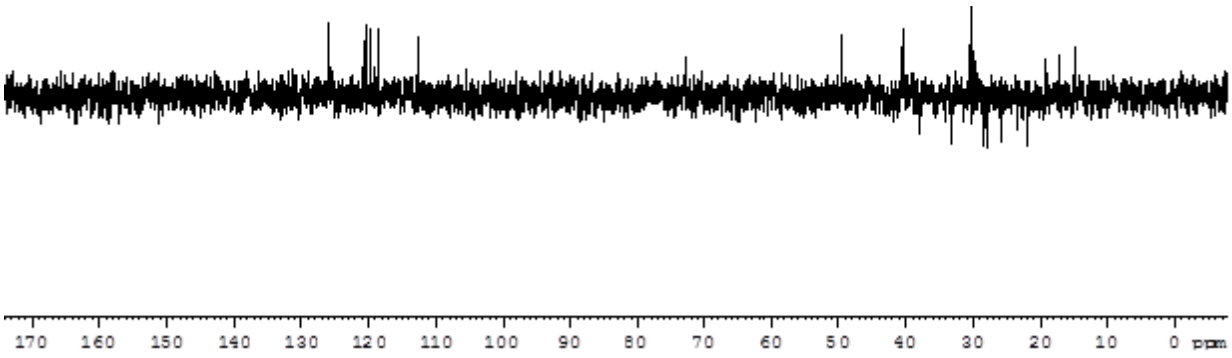

^{1}H NMR spectrum (500 MHz in methanol-d_4) of compound asporyzin C (**6**).

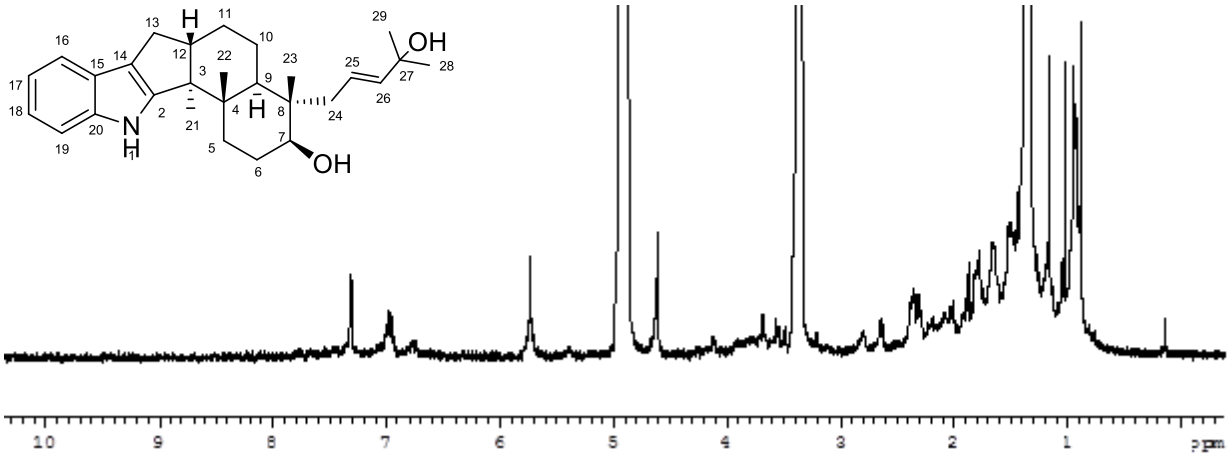

^{1}H NMR spectrum (300 MHz in methanol-*d4*) of compound emindole SB-N-propylcarbamate (**7**).

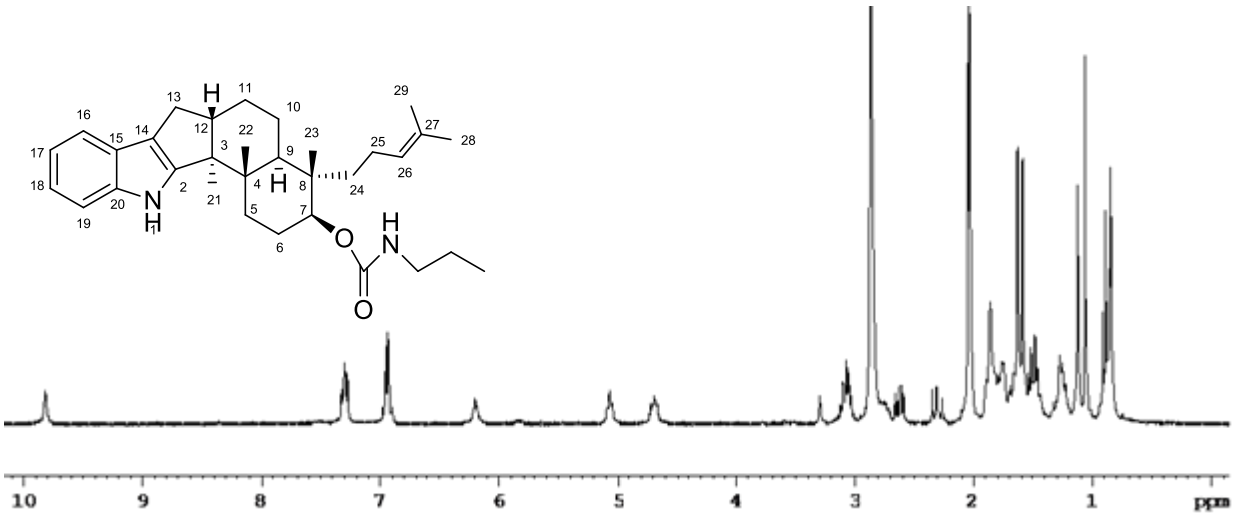

^{13}C NMR spectrum (300 MHz in methanol-*d4*) of compound emindole SB-N-propylcarbamate (**7**).

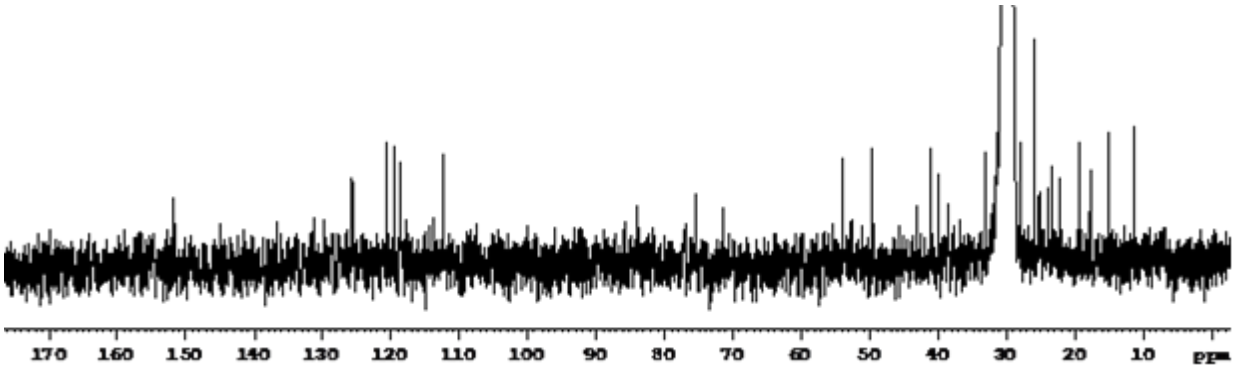

Dept 135 NMR spectrum (300 MHz in methanol-*d4*) of compound emindole SB-N-propylcarbamate (**7**).

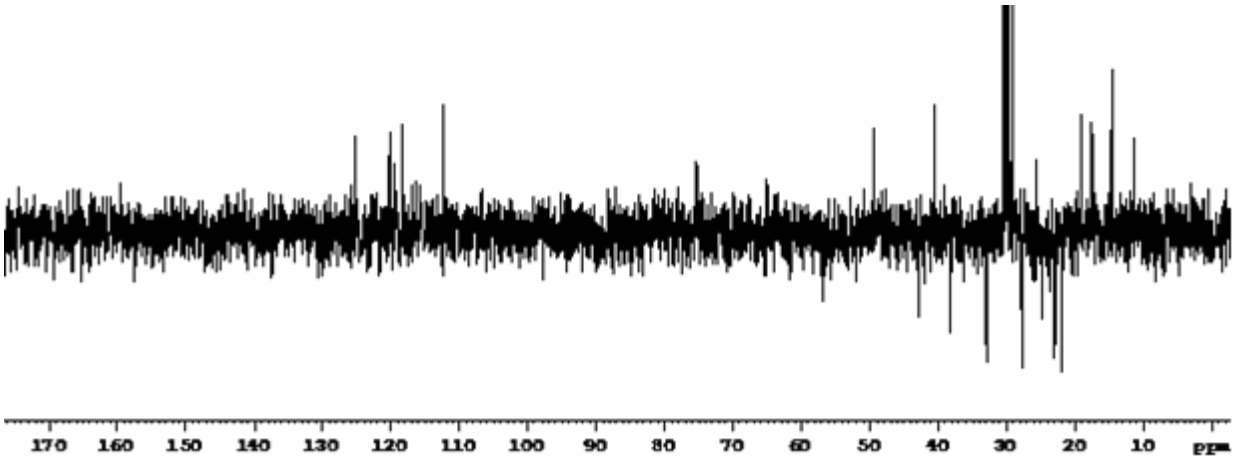

^{1}H NMR spectrum (300 MHz in methanol-*d4*) of compound 16-O-desmethylasporyergosterol-ß-D-mannoside (**9**).

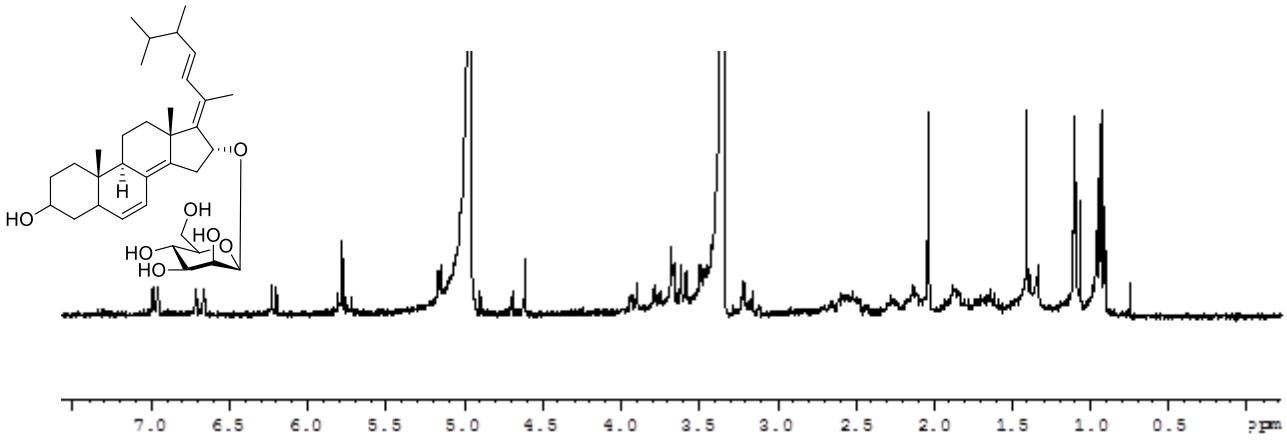

^{13}C NMR spectrum (75.5 MHz in methanol-*d4*) of compound 16-O-desmethylasporyergosterol-ß-D-mannoside (**9**).

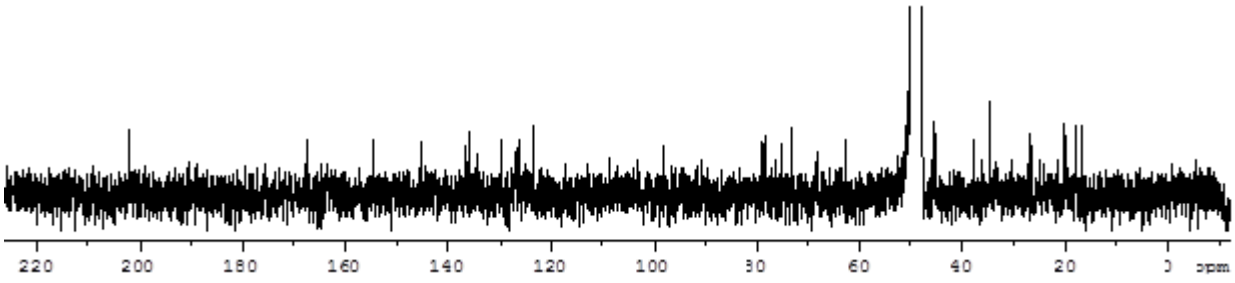

Dept 135 NMR spectrum (75.5 MHz in methanol-*d4*) of compound 16-O-desmethylasporyergosterol-ß-D-mannoside (**9**)

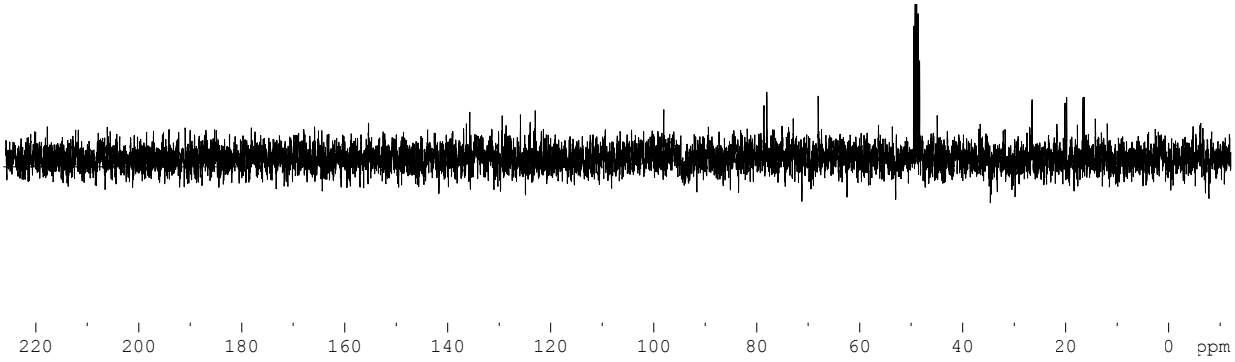

IR spectrum of compound 16-O-desmethylasporyergosterol-ß-D-mannoside (**9**).

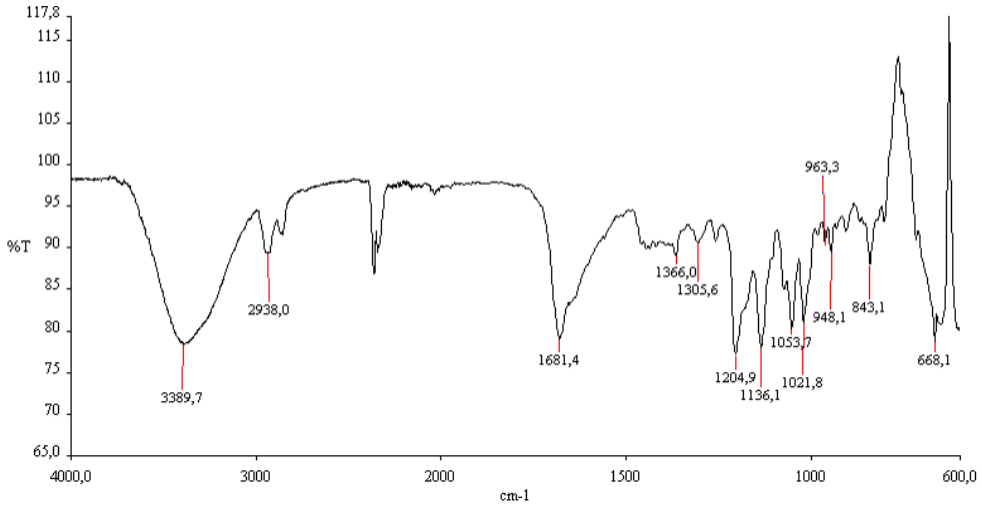

^{1}H-^{13}C HMBC 2D-NMR spectrum of compound **9** in methanol-d_4.

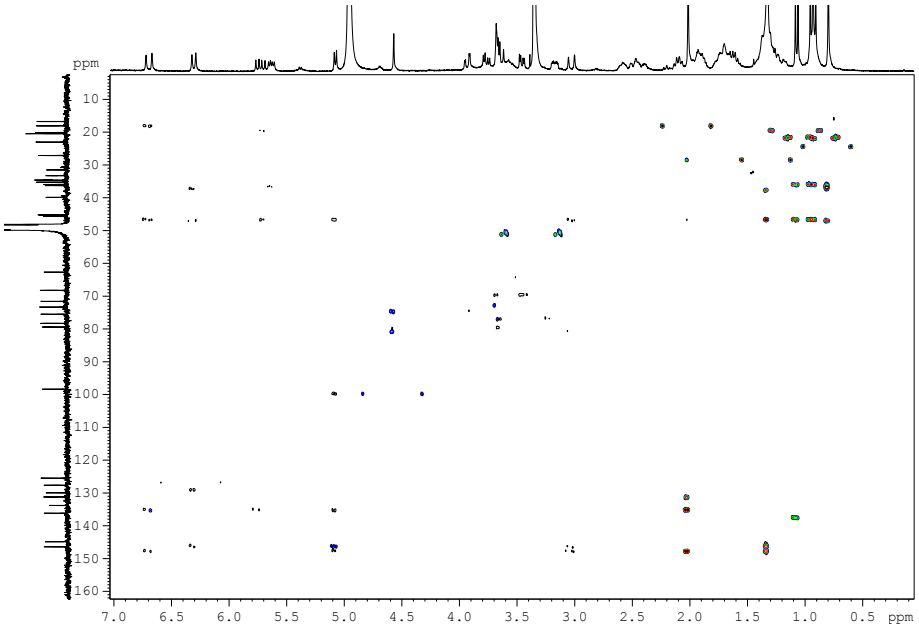

^{1}H NMR spectrum (500 MHz in methanol-*d4)* of compound of 16-O-desmethylasporyergosteron-ß-D-mannoside (**10**).

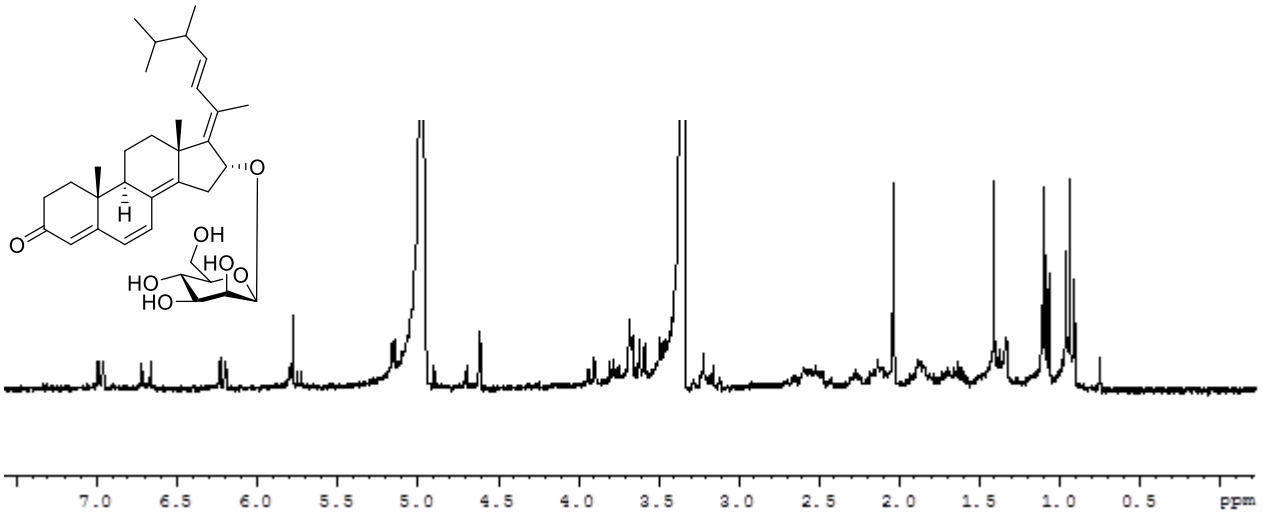

^{13}C NMR spectrum (75.5 MHz in methanol-d_4) of compound desmethylasporyergosteron-ß-D-mannoside (**10**).

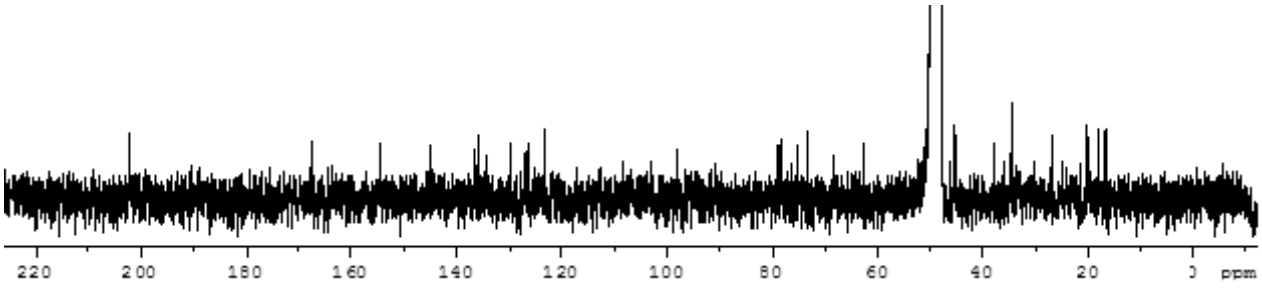

Dept 135 NMR spectrum (75.5 MHzin methanol d_4) of compound desmethylasporyergosteron-ß-D-mannoside (**10**).

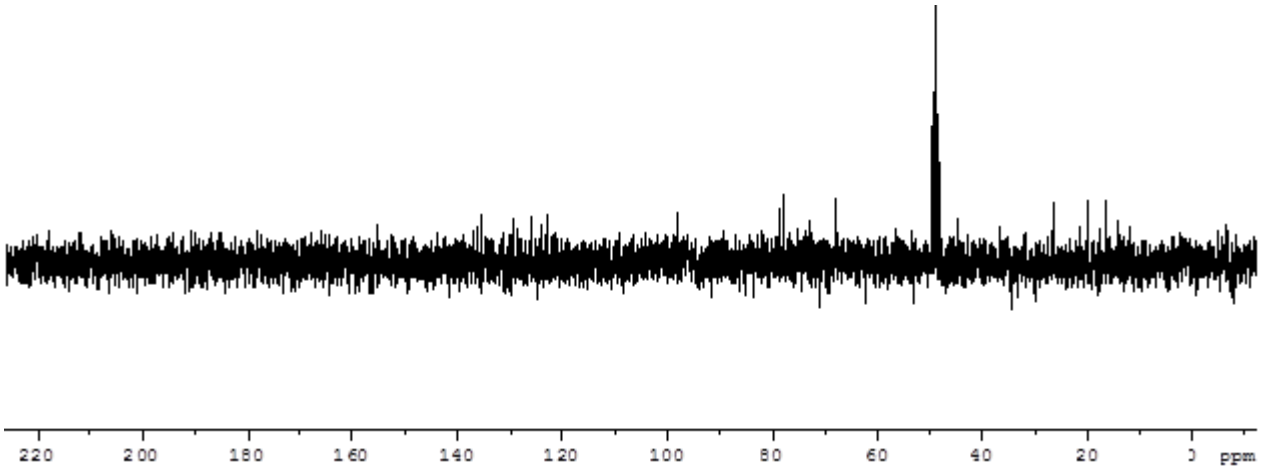

IR spectrum of compound desmethylasporyergosteron-ß-D-mannoside (**10**).

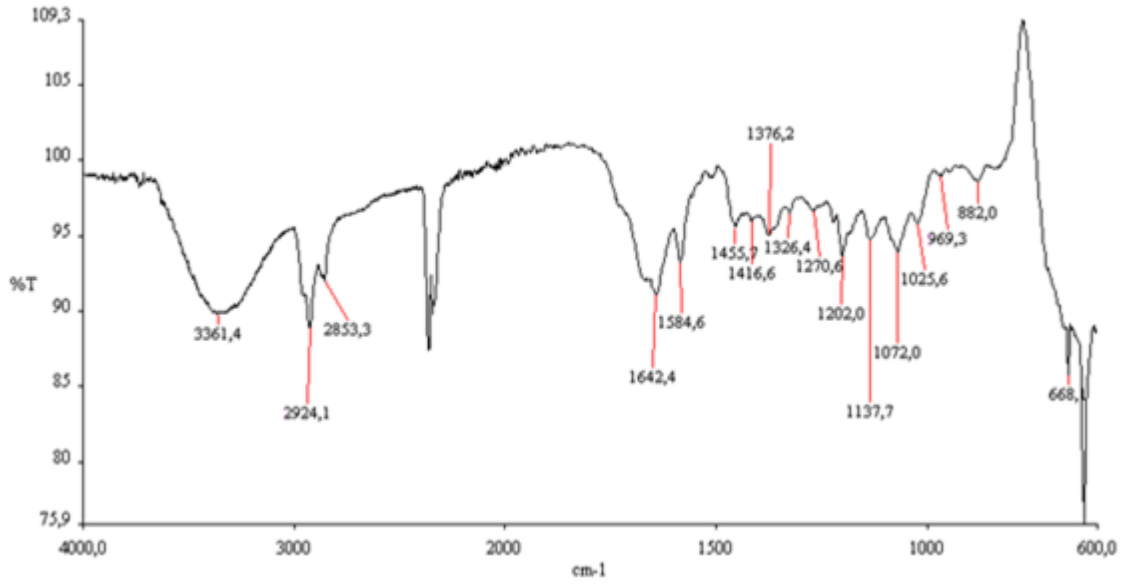

^{1}H-^{13}C HMBC 2D-NMR spectrum of compound **10** in methanol-d_4**.**

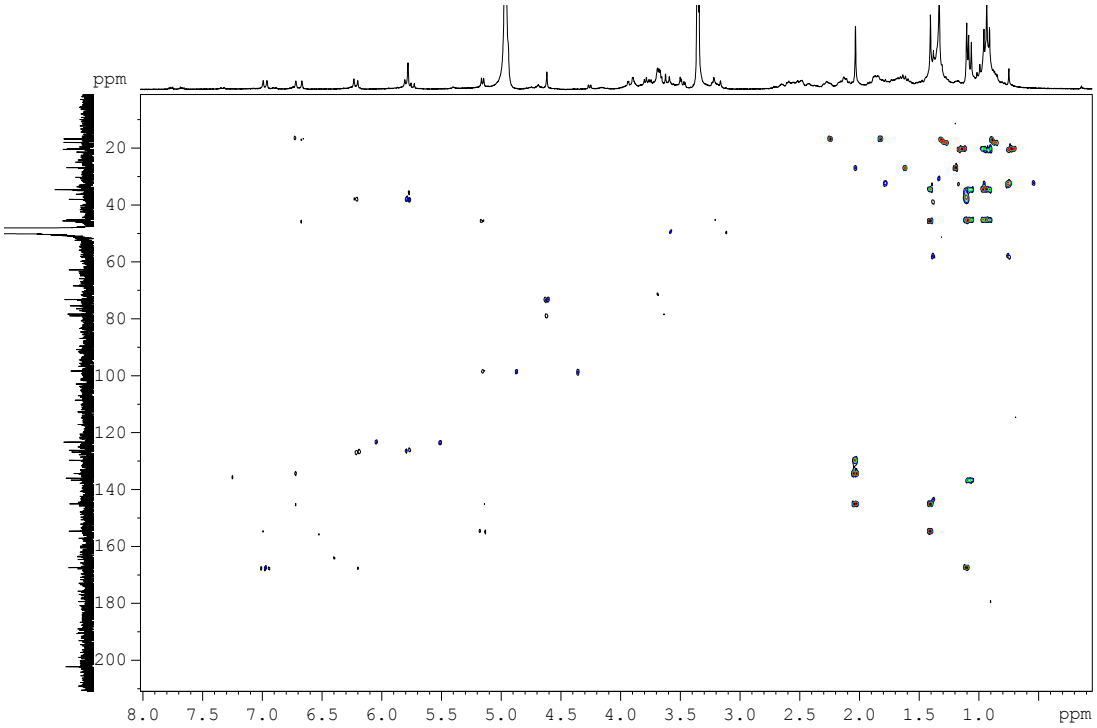

^{1}H NMR spectrum (300 MHz in acetone-d_6) of compound 16-O-desmethylasporyergosterol (**11**)

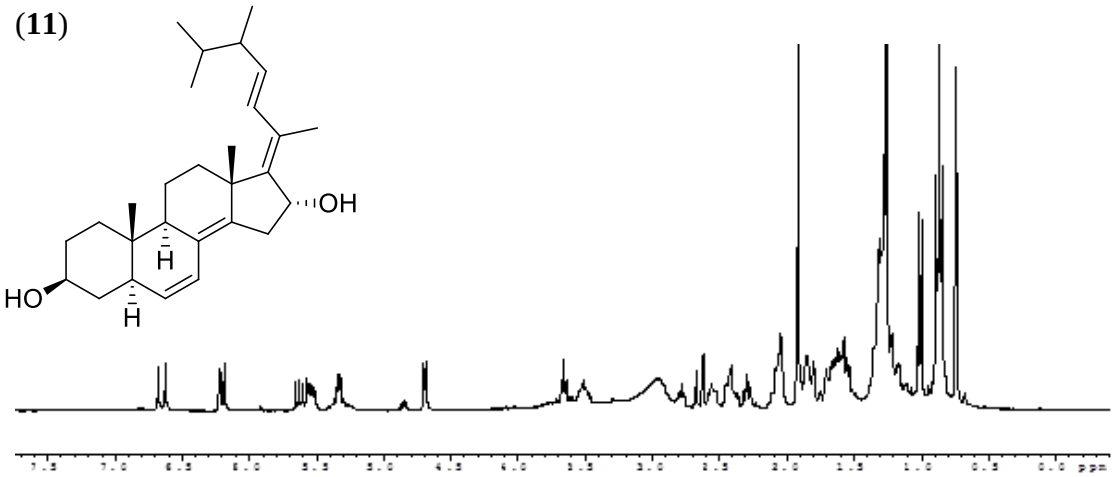

^{13}C NMR spectrum (75.5 MHz in acetone-d_6) of compound 16-O-desmethylasporyergosterol (**11**).

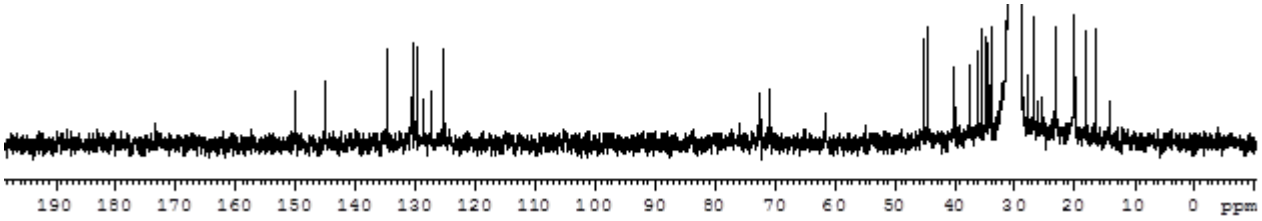

135 NMR spectrum (75.5 MHz in acetone-d_6) of compound 16-O-desmethylasporyergosterol (**11**).

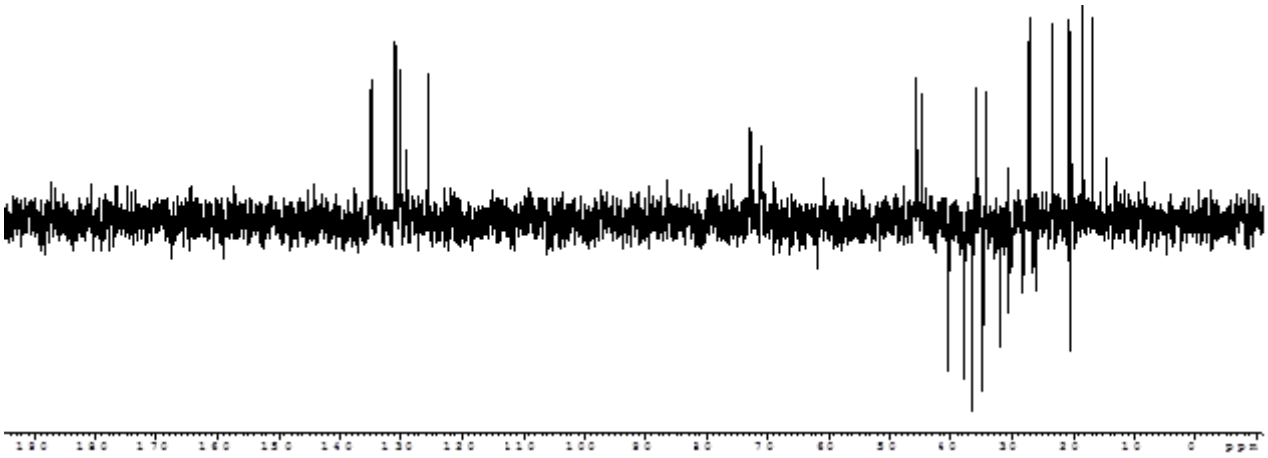

IR spectrum of compound 16-O-desmethylasporyergosterol (**11**).

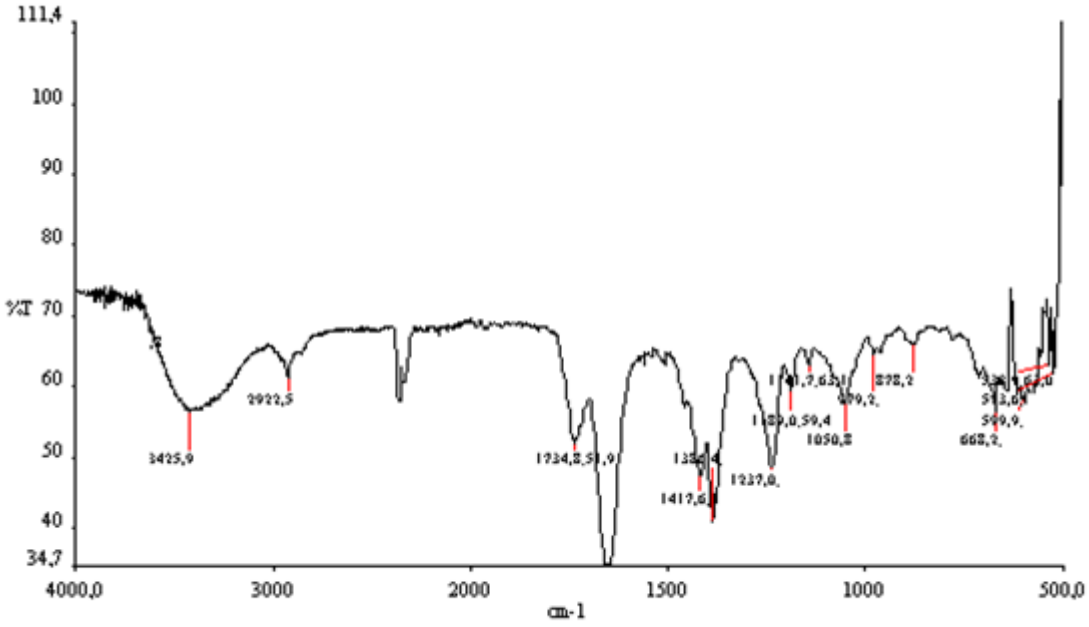

^{1}H NMR spectrum (300 MHz in chloroform-d_1) of compound xanthocillin X dimethylether (**12**).

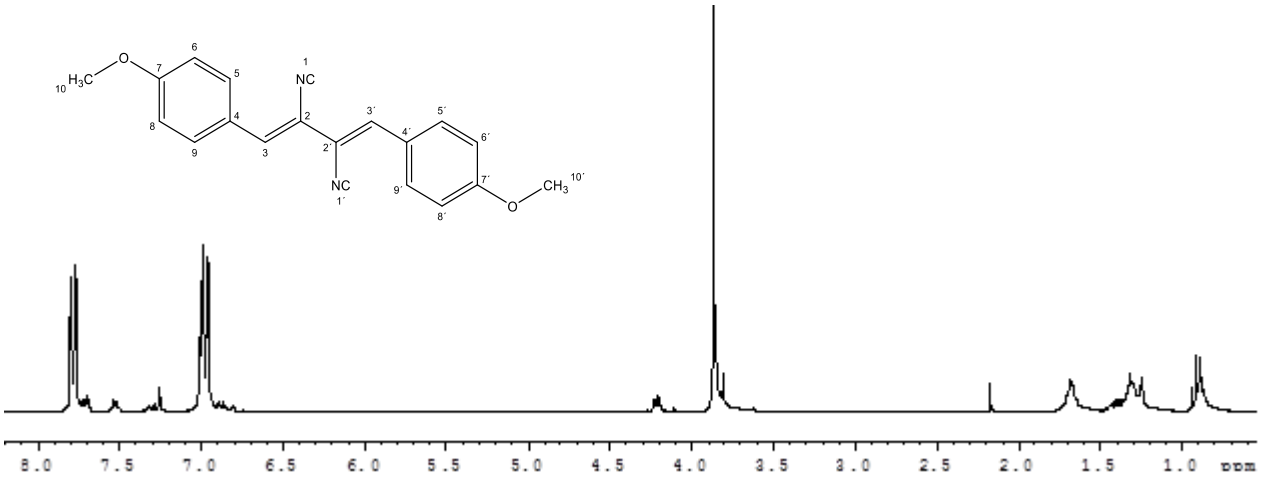

^{13}C NMR spectrum (75.5 MHz in chloroform-d_1) of compound xanthocillin X dimethylether (**12**).

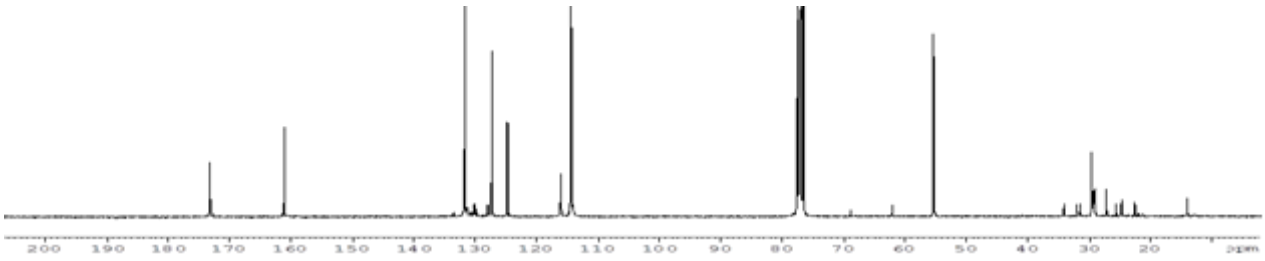

Dept 135 NMR spectrum (75.5 MHz in chloroform-d_1) of compound xanthocillin X dimethylether (**12**).

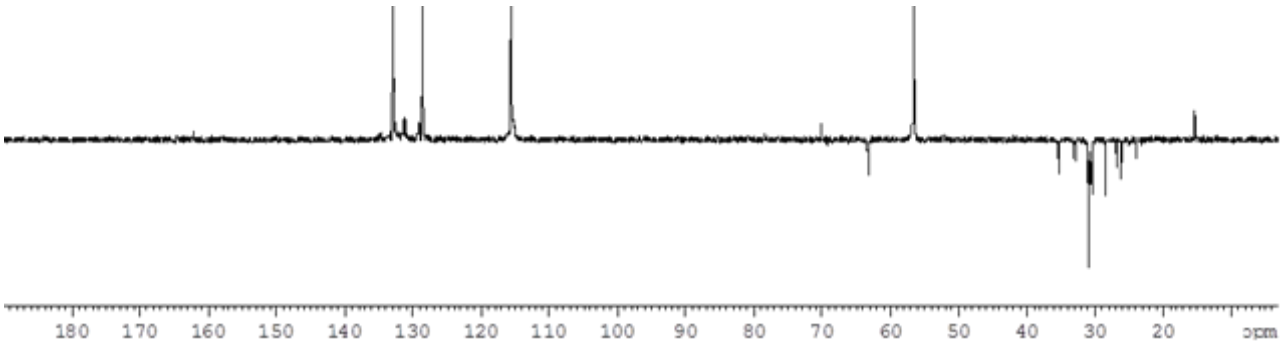

^{1}H NMR spectrum (500 MHz in chloroform-d_1) of compound xanthocillin X monomethylether (**13**).

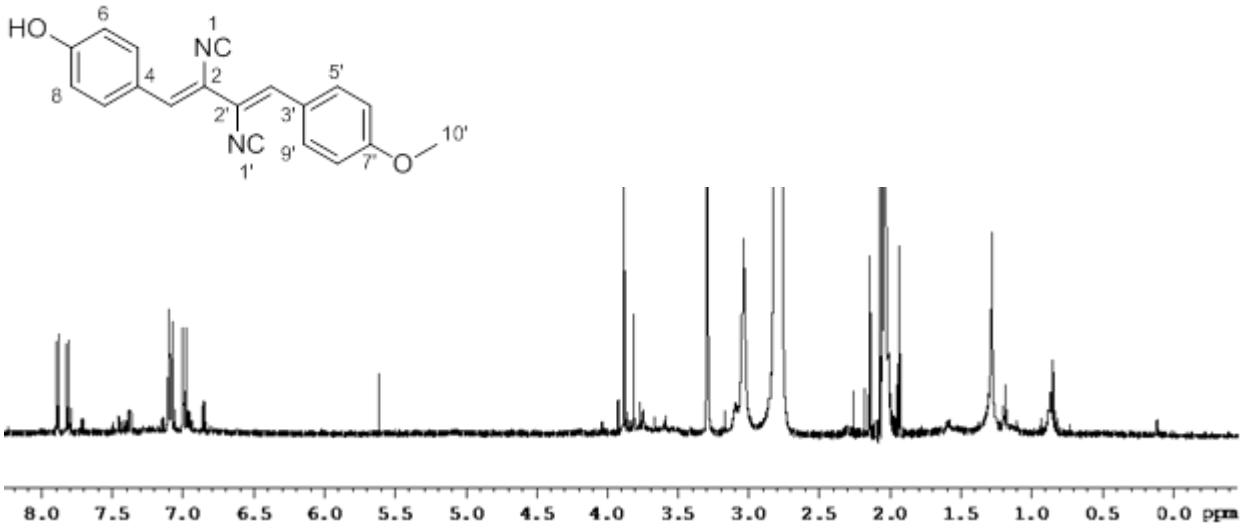

^{13}C NMR spectrum (75.5 MHz in chloroform-d_1) of compound xanthocillin X monomethylether (**13**).

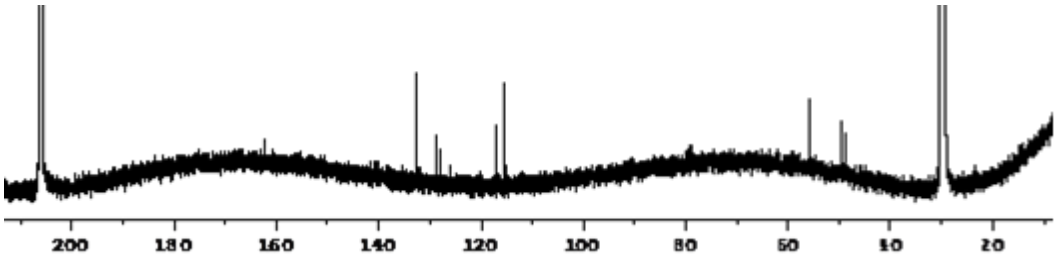

^{1}H NMR spectrum (300 MHz in acetone-d_6) of compound 6-acetylmonodethiogliotoxin (**14**).

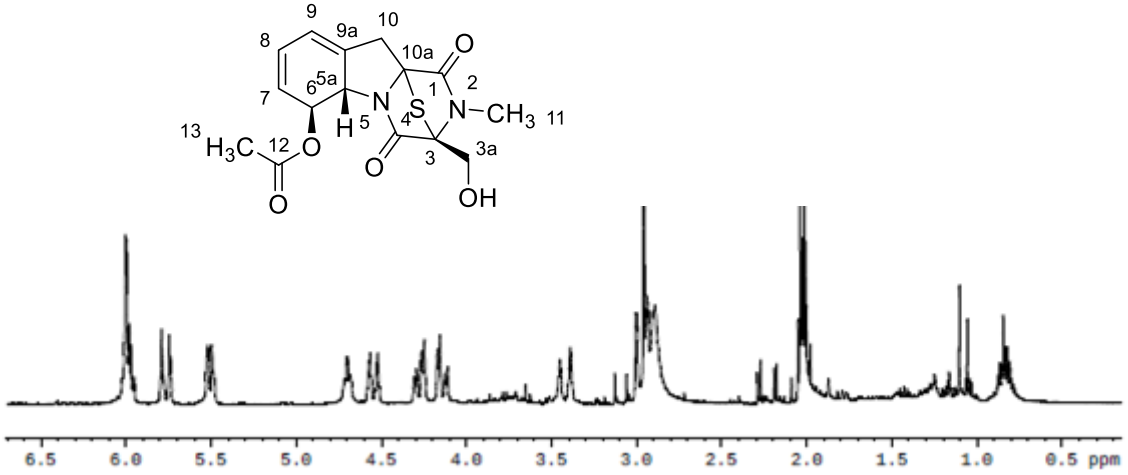

^{13}C NMR spectrum (300 MHz in acetone-d_6) of compound 6-acetylmonodethiogliotoxin (**14**).

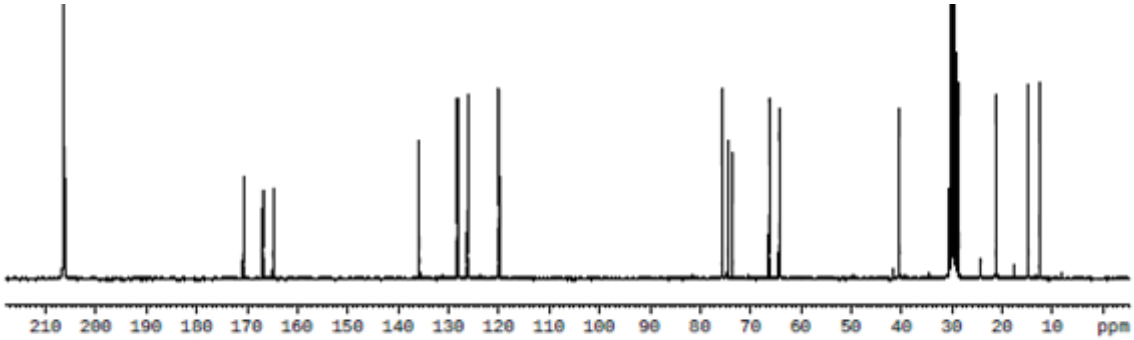

Dept 135 NMR spectrum (300 MHz in acetone-d_6) of compound 6-acetylmonodethiogliotoxin (**14**).

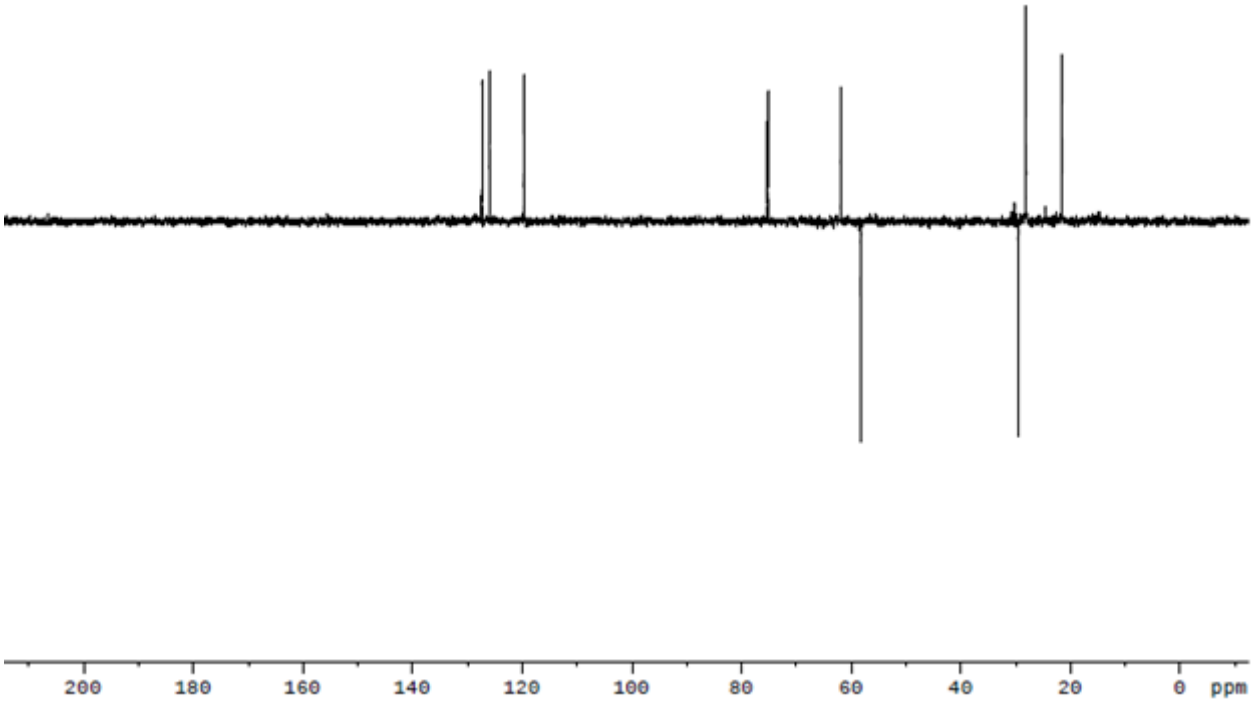

IR spectrum of compound 6-acetylmonodethiogliotoxin (**14**).

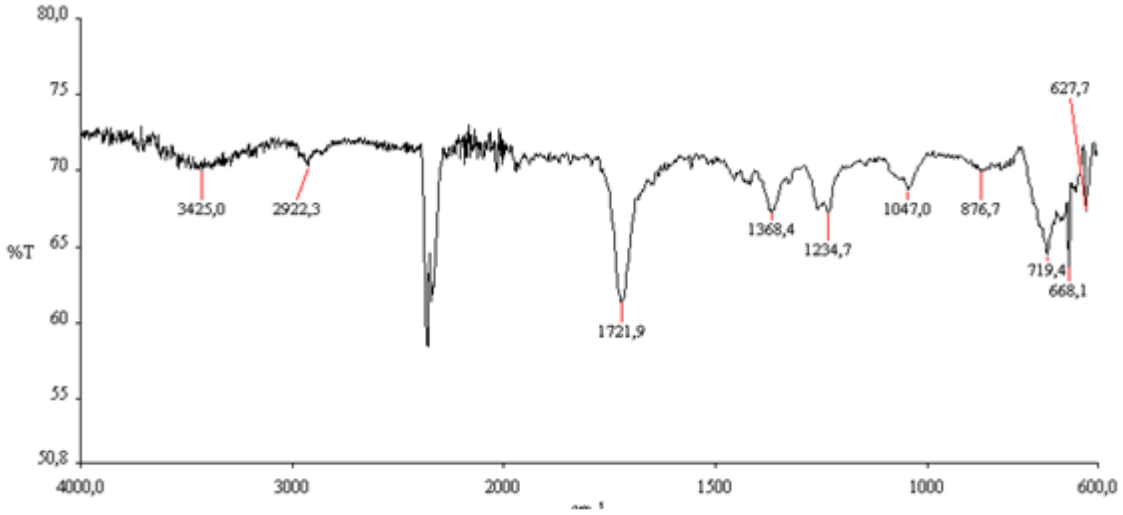

^{1}H NMR spectrum (300 MHz in acetone-d_6) of compound 6-acetylbisdethiobis (methylthio)gliotoxin (**15**).

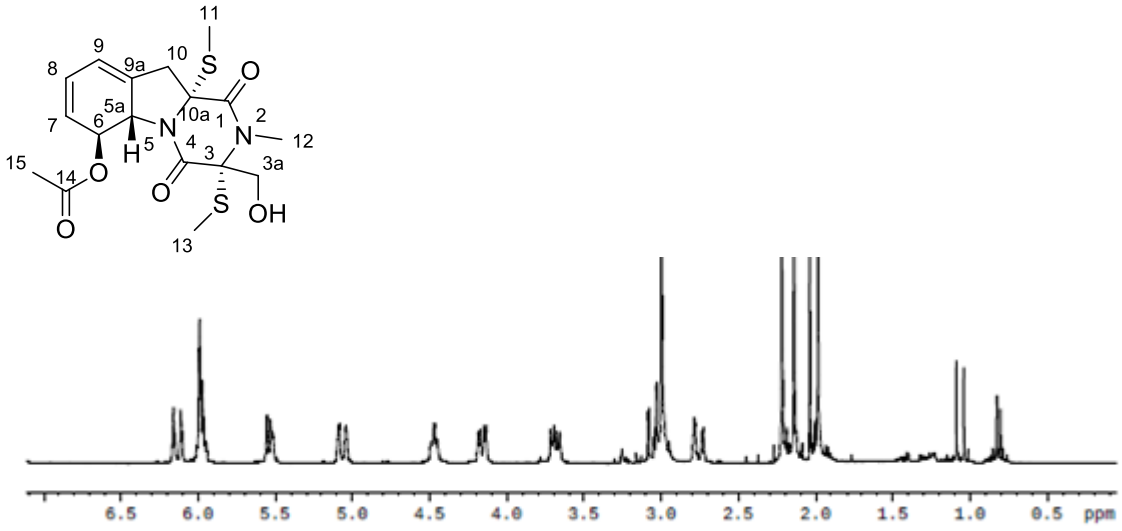

^{13}C NMR spectrum (300 MHz in acetone-d_6) of compound 6-acetylbisdethiobis (methylthio)gliotoxin (**15**).

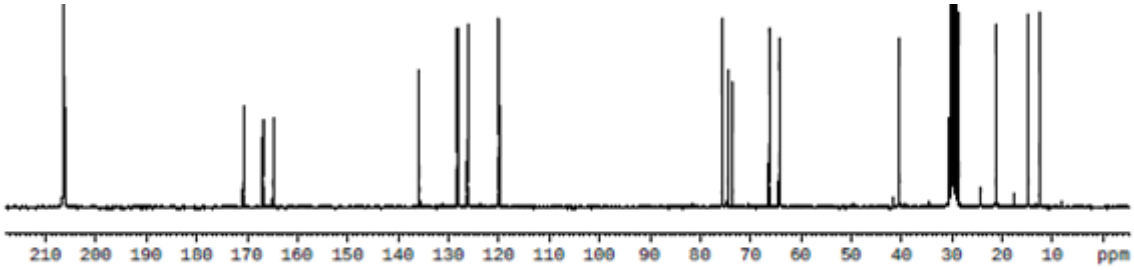

Dept 135 NMR (75.5 MHz in acetone-d_6) of compound 6-acetylbisdethiobis(methylthio)gliotoxin (**15**).

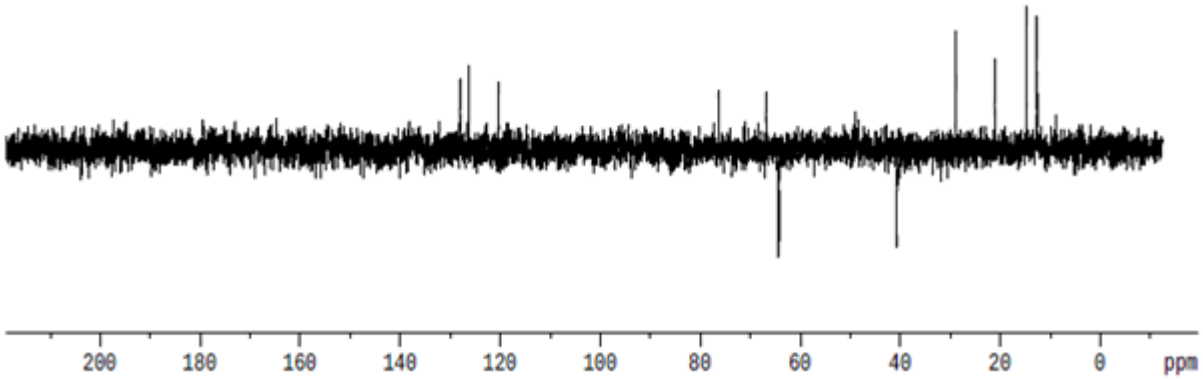

^{1}H NMR spectrum (300 MHz acetone-d_6) of compound 5a,6-anhydrobisdethiobis(methylthio)gliotoxin (**16**).

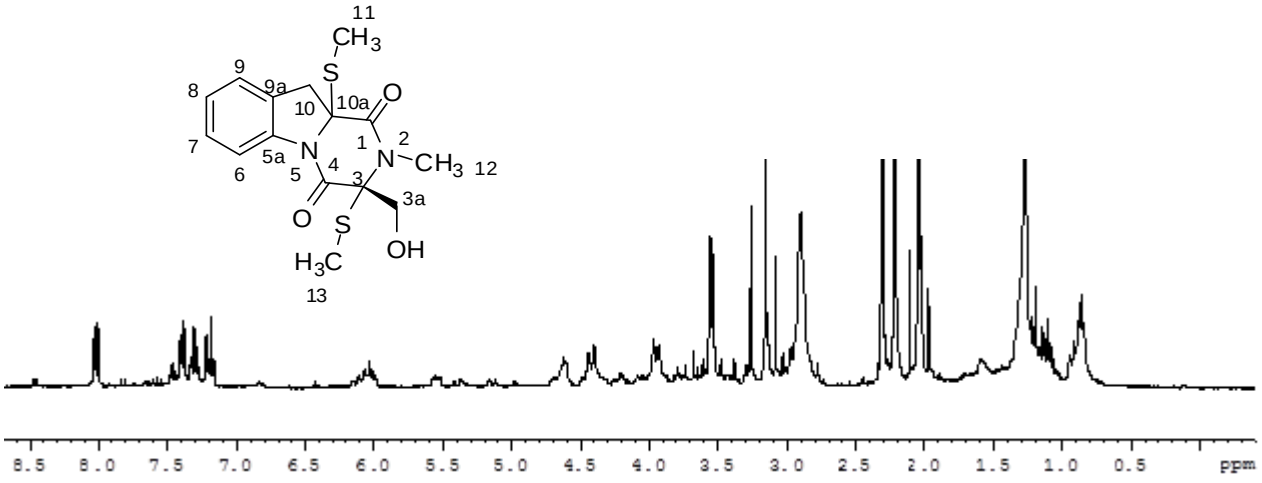

^{13}C NMR spectrum (300 MHz acetone-d_6) of compound 5a,6-anhydrobisdethiobis(methylthio)gliotoxin (**16**).

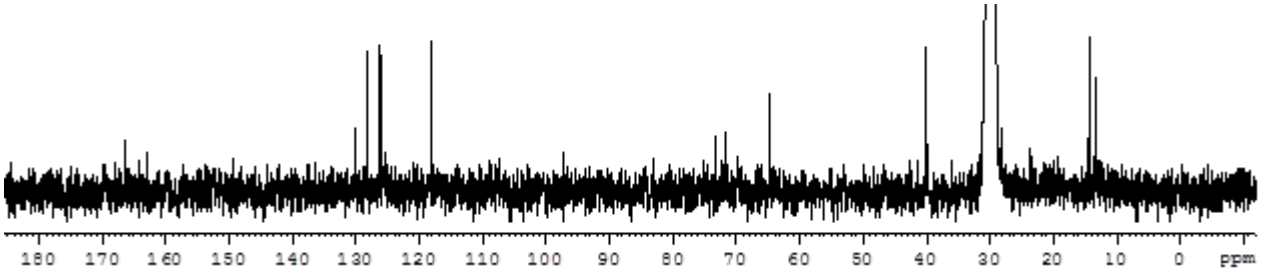

Dept 135 NMR spectrum (300 MHz acetone-d_6) of compound 5a,6-anhydrobisdethiobis(methylthio)gliotoxin (**16**).

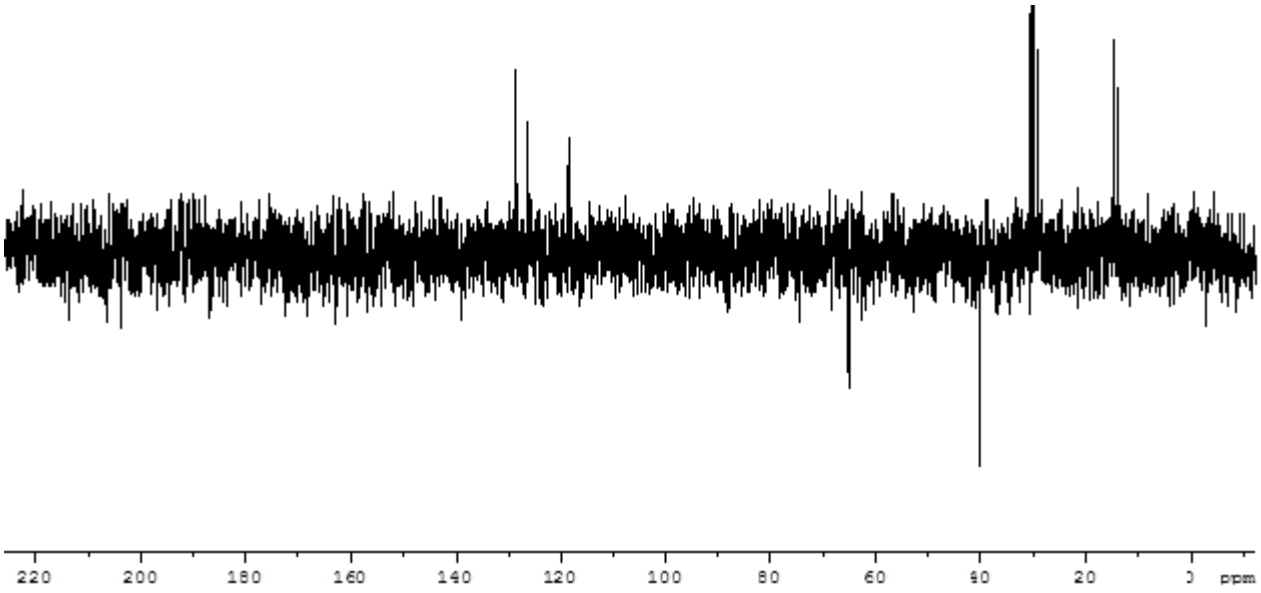

^{1}H NMR spectrum (300 MHz in acetone-d_6) of compound heveadride (**17**)

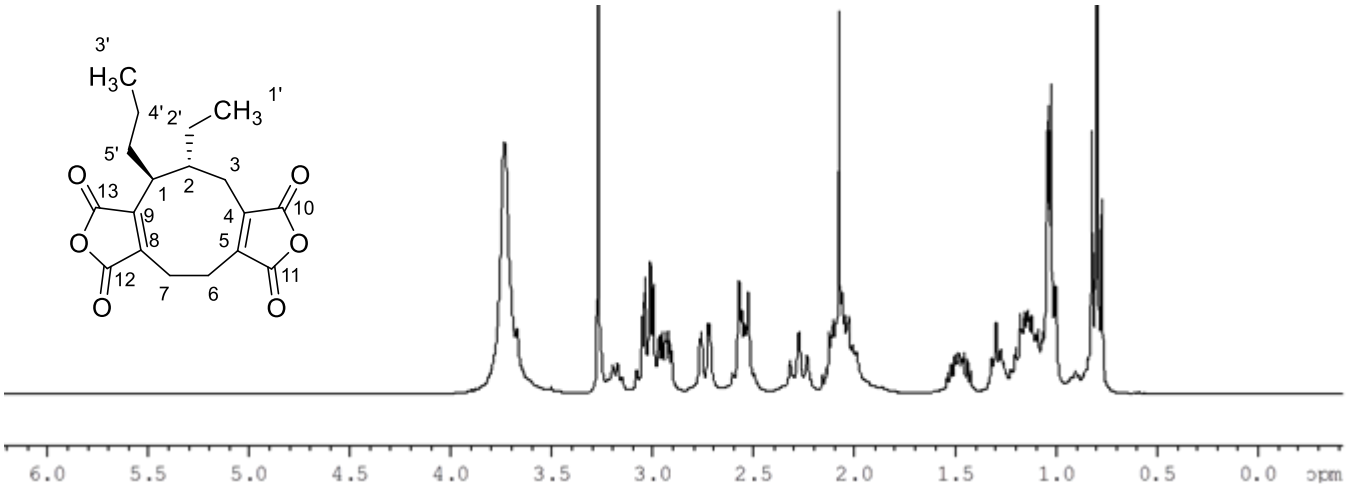

^{13}C NMR spectrum (75.5 MHz in acetone-d_6) of compound heveadride (**17**)

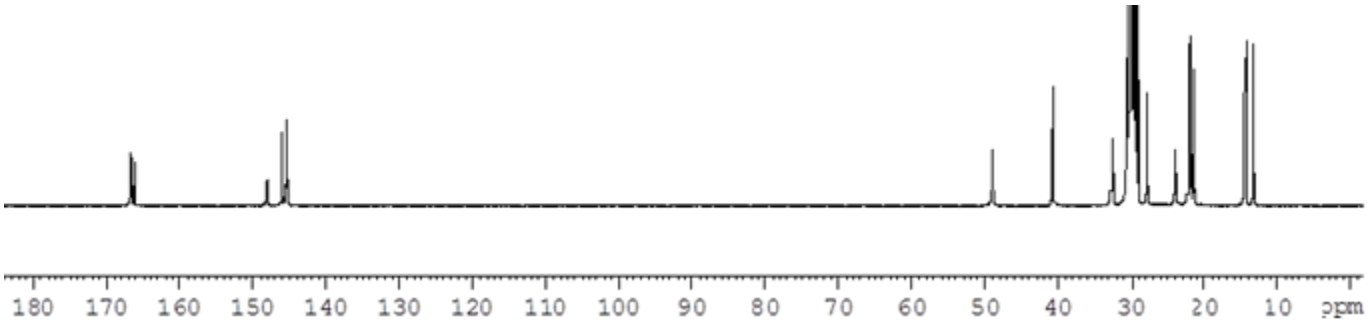

Dept 135 NMR spectrum (75.5 MHz in acetone-d_6) of compound heveadride (**17**)

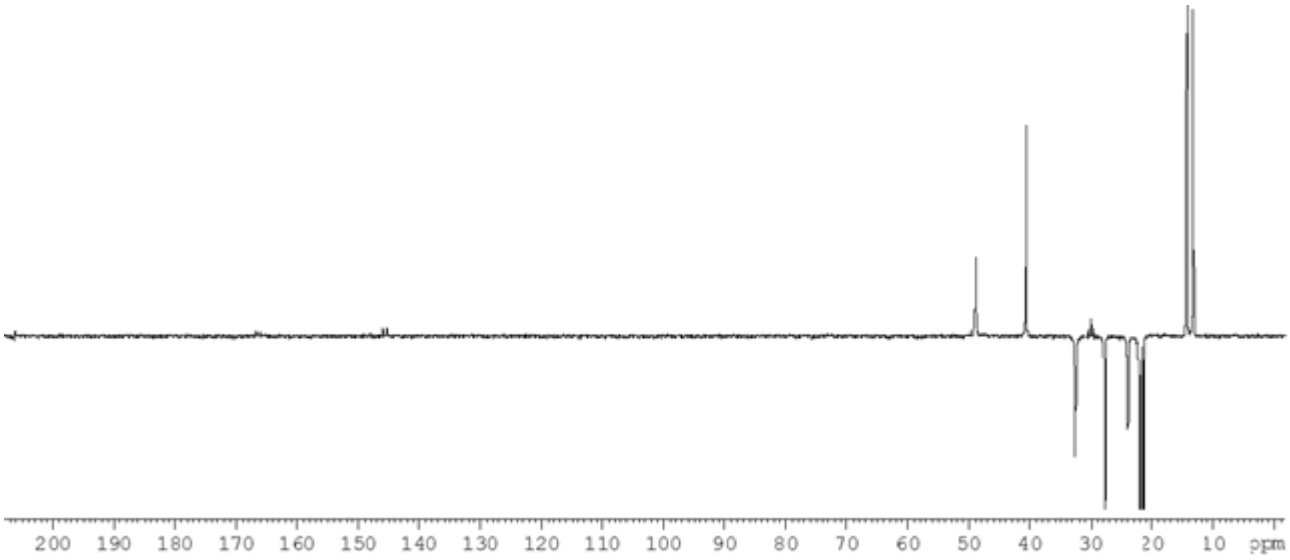

8.3 Activities of isolated thiodiketopiperazines and nonadride toward nuclear receptors

Evaluation of Compounds **14, 15** and **17** for PPARβ/δ agonist activity

AC	**14**		**15**		**17**		**DMSO**
µM	average	activity	average	activity	average	activity	average
125	400	-40	287.093	-1	289.427	-1	297.760
41.67	41.760	-21	228.480	5	212.640	2	194.500
13.89	112.693	-10	255.507	10	195.453	1	191.820
4.63	162.840	-3	234.067	7	217.253	4	177.500
1.54	183.387	0	216.160	4	191.467	1	177.820
0.514	212.133	4	241.200	8	199.000	2	186.840
0.171	257.573	10	257.573	10	203.973	3	177.160
0.057	268.320	11	268.320	11	204.360	3	197.640

Values relative to luciferase activity obtained by activating the reporter gene system with the known agonist GW 501516

Data value represent means ±SEM of three independent experiments

Evaluation of Compound **14, 15** and **17** for PPARγ agonist activity

AC	**14**		**15**		**17**		**DMSO**	
µM	average	activity	average	activity	average	activity	average	activity
125	1.373	-72	194.440	63	126.813	16	104.500	111
41.67	25.920	-30	125.467	40	94.760	19	68.300	38
13.89	63.040	5	98.587	30	73.293	12	61.060	23
4.63	85.960	21	112.320	39	70.000	10	62.980	27
1.54	84.013	20	108.213	36	78.200	15	61.700	24
0.514	95.000	27	109.720	37	61.413	4	47.940	-3
0.171	102.613	33	101.027	31	80.187	17	52.100	5
0.057	88.640	23	112.227	39	72.387	11	50.980	3

Values relative to luciferase activity obtained by activating the reporter gene system with the known agonist rosiglitazone (BRL)

Data value represent means ±SEM of three independent experiments

Table 4-25: Evaluation of Compounds 14, 15 and 17 for LXRα agonist activity

AC	14		15		17		DMSO	
µM	average	activity	average	activity		activity	average	activity
80	63,280	161	29,560	68	4,900	13	45,827	126
40	55,340	140	26,480	61	23,680	65	34,973	96
20	46,000	117	23,260	53	31,640	87	36,507	100
10	40,860	104	26,720	61	31,920	88	33,933	93
5	42,420	108	36,700	84	36,100	99	34,227	94
3	42,840	109	35,620	81	34,000	93	35,307	97
1.25	38,660	98	44,920	103	36,020	99	30,000	82
0.63	39,400	100	43,760	100	36,380	100	36,480	100

Values relative to luciferase activity obtained by activating the reporter gene system with the known agonist T0901317,

Data value represent means ±SEM of three independent experiments

Table **4-26:** Evaluation of Compounds **1, 2** and **4** for LXRβ agonist activity

AC	**1**		**2**		**4**		**DMSO**	
µM	average	activity		activity		activity	average	activity
80	23.460	98	5.880	24	1.160	6	23.747	84
40	19.940	83	6.040	25	8.100	39	22.000	78
20	19.920	83	9.760	41	14.080	68	21.653	77
10	21.720	91	9.460	39	17.480	85	22.840	81
5	20.000	83	14.960	62	18.960	92	22.600	80
3	22.760	95	13.940	58	23.000	112	22.960	81
1	21.760	91	21.480	89	20.180	98	27.413	97
1	23.980	100	24.040	100	20.560	100	28.280	100

Values relative to luciferase activity obtained by activating the reporter gene system with the known agonist T0901317

Data value represent means ±SEM of three independent experiments